


# 國立交通大學

## 生化工程研究所

### 博士論文

決定牛乳  $\beta$ -lactoglobulin-vitamin D complex 之結晶結構並利用胺  
基酸定點突變及生物資訊探討其生理與物理生化功能

Physiological and physico-biochemical function of bovine milk  
 $\beta$ -lactoglobulin as probed by site-directed mutagenesis, bioinformatics  
and its crystal structure complexed with vitamin D



研究生：楊明誌

指導教授：毛仁淡 講座教授

中華民國九十八年四月

決定牛乳  $\beta$ -lactoglobulin-vitamin D complex 之結晶結構並利用胺

基酸定點突變及生物資訊探討其生理與物理生化功能

Physiological and physico-biochemical function of bovine milk

$\beta$ -lactoglobulin as probed by site-directed mutagenesis, bioinformatics

and its crystal structure complexed with vitamin D

研究生：楊明誌

Student : Ming Chi Yang

指導教授：毛仁淡 講座教授

Advisor : Chair Prof. Simon JT Mao



A Thesis

Submitted to Institute of Biochemical Engineering

College of Biological Science and Technology

National Chiao Tung University

in partial Fulfillment of the Requirements

for the Degree of PhD

in

Biological Science and Technology

April 2009

Hsinchu, Taiwan, Republic of China

中華民國九十八年四月

# 決定牛乳 $\beta$ -lactoglobulin-vitamin D complex 之結晶結構並利用胺 基酸定點突變及生物資訊探討其生理與物理生化功能

研究生：楊明誌

指導教授：毛仁淡 講座教授

國立交通大學 生化工程研究所 博士班

## 摘要

$\beta$ -Lactoglobulin (LG) 為牛乳中主要乳清蛋白之一，calyx 公認為維生素 D 的主要結合區，而第二個維生素 D 結合區之存在仍受到許多爭論。在本研究中，利用螢光光譜分析，得知維生素 D 與 LG 結合比例為 2，表示 LG 可能具有兩個維生素 D 結合區。藉由降低 pH 值及加熱破壞 calyx 結合疏水性分子之能力，LG 仍具有結合維生素 D 之能力，其結合比例為 1，此結果證實 LG 除 calyx 以外具有第二個維生素 D 結合區。運用生物資訊程式 (Insight II、Q-SiteFinder、GEMDOCK) 發現有兩個區域可能為第二個維生素 D 結合區，且 GEMDOCK 幫助我們在具有潛力的第二維生素 D 結合區上尋找額外電子雲密度。藉由改變製備共同結晶的 pH 值及起始維生素 D/LG 之比率來優化 ligand 佔有率及增加複合體中維生素 D 的電子雲密度。在 pH 8 及起始維生素 D/LG 之比率為 3 的條件下，製備 LG 與維生素 D 複合體 (complex) 結晶，進行同步輻射光束繞射確切得知 LG 上第二個維生素 D 結合區所在區域。第二維生素 D 結合區位於 LG 分子之 C 端表

面，此結合區具有約 17.91 Å 之長度，而維生素 D 分子約為 12.51 Å，代表此結合區足以容納維生素 D 分子。第二維生素 D 結合區由 $\alpha$ -helix 提供非極性胺基酸 Phe136、Ala139、Leu140 與 $\beta$ -strand I 提供非極性胺基酸 Ile147，經由疏水性 loop (Ala142、Leu143、Pro144、Met145)連接形成一個疏水性結合區，促進維生素 D 結合。另一方面，利用定點突變進行系統化分析發現 $\gamma$ -trun loop 上 Leu143、Pro144、Met145 為 LG 第二維生素 D 結合區上參與結合之重要胺基酸。更進一步支持證據為維生素 D 抑制專一性辨識 $\gamma$ -trun loop 之單株抗體的免疫反應。眾所皆知，LG 具有中心 calyx 及第二維生素 D 結合區，然而生理上 LG 能攜帶維生素 D 通過腸胃道，增加維生素 D 吸收之能力至今尚未證實。利用小鼠作為動物模式，起初證實 LG 為牛乳中攜帶維生素 D 及增加維生素 D 吸收之主要蛋白質。深入探討加熱對於 LG 增加維生素 D 吸收之影響，發現 LG 具有兩個維生素 D 結合區，餵食老鼠添加維生素 D 之 LG，其血液中維生素 D 濃度於維生素 D/LG 比率 2 時達到飽和，而 heated LG 只具有第二維生素結合區，餵食老鼠添加維生素 D 之 heated LG，其血液中維生素 D 濃度於維生素 D/LG 比率 1 時就已達到飽和。因 LG 第二維生素結合區不受加熱破壞，其具有攜帶維生素 D 及增加維生素 D 吸收之優勢。本研究總結發現於牛乳中添加維生素 D 將能有效增加維生素 D 為人體吸收。



Physiological and physico-biochemical function of bovine milk  
 $\beta$ -lactoglobulin as probed by site-directed mutagenesis,  
bioinformatics and its crystal structure complexed with vitamin D

Student: : Ming Chi Yang

Advisor: Chair Prof. Simon JT Mao

Institute of Biochemical Engineering  
National Chiao Tung University

**Abstract**

$\beta$ -Lactoglobulin (LG) is a major milk whey protein containing primarily a calyx for vitamin D<sub>3</sub> binding, although the existence of another site beyond the calyx is controversial. In this study, using fluorescence spectral analyses, we showed the binding ratio for vitamin D<sub>3</sub> to LG to be 2:1 and a ratio of 1:1 when the calyx was “disrupted” by manipulating the pH and temperature, suggesting that a secondary vitamin D binding site existed. The bioinformatic programs (Insight II, Q-SiteFinder, and GEMDOCK) identified the two potential regions for this secondary vitamin D binding site. It was concluded that GEMDOCK can aid in searching for an extra density map around potential vitamin D binding sites. We then optimized the occupancy and enhanced the electron density of vitamin D<sub>3</sub> in the complex by altering the pH and initial ratios of vitamin D<sub>3</sub>/LG in the cocrystal preparation. Finally, we identified the secondary site (defined as the exosite) for vitamin D binding using a crystal prepared at pH 8 with a vitamin D<sub>3</sub>/LG ratio of 3:1. The exosite, however, is near the surface at the C-terminus (residues 136-149) containing part of an  $\alpha$ -helix and a  $\beta$ -strand I

with 17.91 Å in length, while the span of vitamin D<sub>3</sub> is about 12.51 Å. A remarkable feature of the exosite is that it combines amphipathic α-helix providing nonpolar residues (Phe136, Ala139, and Leu140) and β-strand I providing a nonpolar (Ile147), which are linked by a hydrophobic loop (Ala142, Leu143, Pro144, and Met145). Thus, the binding pocket of the exosite furnishes strong hydrophobic force to stabilize vitamin D<sub>3</sub> binding. On the other hand, using site-directed mutagenesis, we demonstrate that residues Leu143, Pro144 and Met145 in the γ-turn loop play a crucial role in the binding. Further evidence is provided by the ability of vitamin D<sub>3</sub> to block the binding of a specific mAb in the γ-turn loop. LG contains a central calyx and a second exosite beyond the calyx to bind vitamin D; however, the biological function of LG in transporting vitamin D remains elusive. Using the mouse (n=95) as an animal model, we initially demonstrated that LG is a major fraction of milk proteins responsible for uptake of vitamin D. Most interestingly, dosing mice with LG supplemented with vitamin D<sub>3</sub> revealed that native LG containing two binding sites gave a saturated concentration of plasma 25-hydroxyvitamin D at a dose ratio of 2:1 (vitamin D<sub>3</sub>/LG), whereas heated LG containing one exosite (lacking a central calyx) gave a ratio of 1:1. We have demonstrated for the first time that the exosite of LG has a functional advantage in the transport of vitamin D, indicating that supplementing milk with vitamin D effectively enhances its uptake.

## 誌 謝

在經過五年努力終於完成此博士論文，這個帶著苦楚、沮喪、歡欣、鼓舞等喜怒哀樂情緒夾雜的博士班求學過程，終於要告一段落了。在途中，曾因磨難而對於研究生涯產生困惑感，特別要感謝指導教授 毛仁淡講座教授，給予鼓勵與包容。毛講座的諄諄教誨及日夜叮嚀，在生活、實驗、論文撰寫上給予學生悉心地指導，明誌都將謹記在心，並獻上最誠摯地感謝。

在博士研究中，誠摯地感謝同步輻射中心生命科學組 陳俊榮教授引領我一窺蛋白質晶體結構的奧秘，不厭其煩教導我這個門外漢，給予支持令我由衷感激。與此同時，感謝生物資訊所 楊進木教授引領我進入生物資訊領域，不時地討論以化解彼此研究領域上的鴻溝，常常激發出非常驚奇、偉大之想法。此論文之英文文法上承蒙核能研究所 劉明毅教授不吝斧正，使學生許多期刊論文得以發表。除此以外，感謝中央研究院分子生物所 蕭傳鐙教授於口試及論文撰寫上的建議與指正，許多寶貴意見使我獲益良多。另感謝清華大學生物資訊與結構生物所 管泓翔學長在蛋白質晶體結構修正上給予許多協助。同時感謝生物資訊所 葛振寧同學在生物資訊預測方面給予許多幫忙。

這些日子以來，實驗室如同是我的家，學長姊、同學及學弟妹陪我度過這酸甜苦辣的五年光陰。首先感謝文亮學長製作許多單株抗體供我實驗上所需、俊瑩學長與我高談闊論許多偉大的研究方向及學弟妹乃齊、沁紘、

佶穎實驗上的幫忙。另感謝財木、文亮、繼鋒、以祥、怡荏、彰威、宏輝、俊瑩、珮真等學長姊在我沮喪時給予鼓勵及幫忙，文昭、立品同學在生活及實驗上的同甘共苦，靜怡、善琦小秘書給予許多的協助，中曦、冠佑、乃齊、小涵、威延、佩宇、詩璇、佶穎、巾涵、沁紘、俐穎、柏如、宛伶、伊玟等學弟妹帶來眾多的歡樂。在未來的日子裡，回味起這段充滿喜怒哀樂的記憶時，仍是充滿感激。

最後，最必須感謝的是雙親(金圳及玉美)及知己朋友(志宏、俊杰、逸宏、老顧、韶康、詩玉、孟璇、筱婷、小寶貝)，謝謝你們在背後默默地支持我，當我的避風港。每當遇到困難及鬱悶時，替我排憂解難，讓我不斷地鼓起勇氣，去克服接踵而來的挑戰，如果沒有你們，我將無法順利完成博士學位。前方的道路雖有荊棘、磨難，有你們的陪伴將使我更有毅力往前邁進。謹以此論文獻給你們，此為我們共同的榮耀。

# Dissertation index

<b>Abstract in Chinese</b> .....	I
<b>Abstract in English</b> .....	III
<b>Acknowledgements</b> .....	V
<b>Index</b> .....	VII
<b>Overview</b> .....	1
Overall experimental design.....	8
References .....	9
<b>Section 1: The existence and location of secondary vitamin D binding site of LG (Proteins: Structure, Function, and Bioinformatics)</b> .....	16
Abstract .....	17
Introduction.....	18
Materials and Methods.....	21
Results.....	26
Discussion .....	34
Acknowledgments .....	42
References .....	42
Figure Legends.....	51
Tables.....	55
Figures .....	58
<b>Section 2: Rational design for crystallization of LG-vitamin D complex (Crystal Growth &amp; Design)</b> .....	68
Abstract .....	69
Introduction.....	69
Materials and Methods.....	73
Results and Discussion.....	76
Conclusion.....	86
Acknowledgments .....	87
References .....	87
Figure Legends.....	94
Tables.....	97
Figures .....	100
<b>Section 3: Evidence for LG involvement in vitamin D transport <i>in vivo</i> (FEBS Journal)</b> .....	106

Abstract -----	107
Introduction-----	108
Results-----	109
Discussion -----	117
Materials and Methods-----	122
Acknowledgments -----	129
References -----	129
Figure Legends-----	135
Tables-----	139
Figures -----	141
<b>Appendix</b> -----	149
Curriculum vitae -----	150
Publications-----	158
Deposited Structure-----	230



## Overview

Bovine  $\beta$ -lactoglobulin (LG) is a major whey protein consisting about 10-15% of total proteins in milk.<sup>1</sup> Due to its thermally unstable and molten-globule nature, LG has been studied extensively for its physical and biochemical properties in the past 40 years.<sup>2-8</sup> The overall folding of LG is remarkably similar to that of the human plasma retinol binding protein<sup>9-12</sup> and human tear lipocalin<sup>13</sup>, known as members of the lipocalin superfamily. LG comprises of 162 amino-acid residues with two disulfide linkages and one free cysteine. It has predominantly a  $\beta$ -sheet configuration containing nine anti-parallel  $\beta$ -strands from A to I.<sup>14-16</sup> Topographically,  $\beta$ -strands A-D form one surface of the barrel (calyx), whereas strands E-H form the other.<sup>17-19</sup> The only  $\alpha$ -helical structure with three turns is at the COOH-terminus (residues 130-141), which is followed by a  $\beta$ -strand I lying on the outer surface of the calyx.<sup>20</sup> The structural and functional relationship of this helical region is not yet clearly defined. The calyx has a remarkable ability to bind hydrophobic molecules such as retinol, fatty acids and vitamin D.<sup>21-24</sup> It seems clear that the binding of fatty acid, retinol, and vitamin D is within the central calyx of the protein; however, the existence of a second ligand binding site beyond the calyx is a matter of controversy.<sup>17</sup>

LG is quite sensitive to thermal denaturation, the secondary structure is altered upon heating with a transition temperature at 70-80 °C. Recently, it has shown that the conformational changes of LG are rapid and extensive at temperatures above the transition,<sup>5-8</sup>

and  $\beta$ -strand D of the calyx is directly involved in the unfolding during the thermal denaturation.<sup>8</sup> As a result, the binding of palmitate or retinol to the central calyx is diminished.<sup>8</sup> The EF loop of LG is known to act as a gate over the calyx;<sup>14</sup> at pH values lower than 6 the loop is in a “closed” position. We manipulated the binding capability by switching off the gate of calyx at low pH or denaturing the conformation of the calyx by heat treatment to further substantiate the “two site hypothesis”.

Although the biological functions of LG still remain elusive, some essential functions of LG, such as cholesterol lowering,<sup>7</sup> modulation of immune system,<sup>3,17</sup> binding of retinol, fatty acid, and vitamin D,<sup>21-24</sup> and prevention of oxidative stress,<sup>26,27</sup> have been reported. Biological function of LG in terms of the transport role of LG for retinol, fatty acids, and vitamin D is still unproven. Intact LG has been demonstrated to resist acid and to be superpermeable to cross the epithelium cells of the gastrointestinal tract via a receptor.<sup>28</sup> The LG therefore may be an effective vehicle in transporting the hydrophobic ligands.

Vitamin D (cholecalciferol), a hormone that regulates bone development, metabolism, calcium homeostasis, cell growth and cell differentiation, can be obtained through endogenous pathways (photolysis of vitamin D precursors in the skin).<sup>29-31</sup> Other major sources of vitamin D include fortified milk, fish and vitamin D-containing supplements.<sup>29-31</sup> Latitude, season, age, skin color, and skin coverage can all potentially influence the amount of circulating 25-hydroxyvitamin D.<sup>32</sup> There are accumulating evidences indicating that



increased plasma vitamin D concentration is associated with decreased incidence of colon, prostate, and breast cancers, osteoarthritis, autoimmune diseases, and diabetes.<sup>33-37</sup>

Increased mean 25-hydroxyvitamin D was significantly related to increasing milk consumption in the summer and winter ( $P = 0.02$  and  $P = 0.01$ ).<sup>38</sup> Because the binding of vitamin D to milk LG is well known, we can test the hypothesis questioning whether LG enhances the transport of vitamin D of milk.

The present dissertation is divided as three sections:

1. The existence and location of secondary vitamin D binding site of LG
2. Rational design for crystallization of LG-vitamin D complex
3. Evidence for LG involvement in vitamin D transport *in vivo*

### **Section 1: The existence and location of secondary vitamin D binding site of LG**

The existence of a second vitamin D binding site beyond the calyx is controversial.<sup>17</sup> It has been postulated that there are two binding sites for vitamin D based on the work of Swaisgood and de Wolf<sup>39-43</sup> using fluorescence binding assays. Nevertheless, the location of the secondary binding site remote from the calyx has been implicated,<sup>9,10</sup> but has not yet been identified by the crystal structure of bovine LG with vitamin D<sub>2</sub>.<sup>17</sup> We first conducted a ligand binding assay using the fluorescence changes by retinol, palmitic acid, and vitamin D<sub>3</sub> to address the existence of another site for vitamin D binding. This data demonstrated that

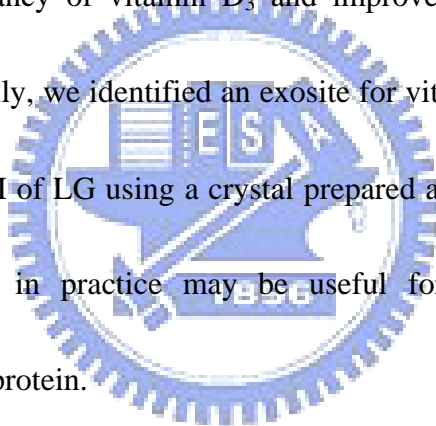
the maximal binding stoichiometry of vitamin D<sub>3</sub> with LG was 2:1, whereas that of retinol or palmitic acid was 1:1, suggesting that there was another binding site for the vitamin D<sub>3</sub> molecule. Second, we manipulated the binding capability by switching off the gate of calyx at low pH (2-6)<sup>14</sup> to further substantiate the “two site hypothesis”. As expected, the binding capability of retinol and palmitic acid diminished under this condition, but it retained the vitamin D binding (30% of the maximal binding) with a vitamin D<sub>3</sub> to LG stoichiometry of 1:1. We also used a strategy to denature the conformation of the calyx by heat treatment and conducted the binding assay after the calyx was thermally “disrupted”. Under this condition, heated LG retained 40% of the vitamin D<sub>3</sub> binding even at 100 °C heating for 16 min and its vitamin D<sub>3</sub> binding stoichiometry was found to be 1:1. These binding experiments suggest that there is a secondary site for vitamin D<sub>3</sub> binding, which is thermally resistant and distinct from the calyx. To confirm the hypothesis that a second vitamin D<sub>3</sub> binding site exists, we determined the crystal structure of LG-vitamin D<sub>3</sub> complex and attempted to identify, localize, and characterize such a site. In this section of the thesis, we report a second vitamin D<sub>3</sub> binding site identified by synchrotron X-ray diffraction (at 2.4 Å resolution). The second binding site (defined as an exosite) is near the surface at the C-terminus (residues 136-149) containing part of an α-helix and a β-strand I with 17.91 Å in length, while the span of vitamin D<sub>3</sub> is about 12.51 Å. A remarkable feature of the exosite is that it combines an amphipathic α-helix providing nonpolar residues (Phe136, Ala139, and Leu140) and a

$\beta$ -strand I providing another nonpolar residue (Ile147). They are linked by a hydrophobic loop (Ala142, Leu143, Pro144, and Met145). Thus, the binding pocket furnishes strong hydrophobic force to stabilize vitamin D<sub>3</sub> binding. This finding provides a new insight into the exosite may provide another route for the transport of vitamin D in vitamin D fortified dairy products.

## **Section 2: Rational design for crystallization of LG-vitamin D complex**

Based on vitamin D<sub>3</sub> binding assay of LG treated at various pH and temperature, we concluded that a thermally stable exosite beyond the calyx exists for vitamin D binding. We attempted to identify the regions of LG that might be available for the interaction with vitamin D using well-known bioinformatics programs (Insight II,<sup>44</sup> Q-SiteFinder,<sup>45</sup> and GEMDOCK<sup>46</sup>). The Insight II<sup>44</sup> is based on the size of surface cavities of a given protein without a specified ligand; it searches for the location and extent of the pocket according to the geometric criteria. The Q-SiteFinder,<sup>45</sup> however, defines a binding pocket only by energy calculations using a methyl probe for van der Waals interactions with a given protein. The GEMDOCK<sup>46</sup> is a more accurate docking program to dock a specific ligand with a given protein based on a nonbiased search for their interactions. Following the analyses of Insight II, Q-SiteFinder, and GEMDOCK cross-docking, we were able to narrow the region of potential binding sites to two sites which were located near the C-terminal  $\alpha$ -helical region. This led us to determine the crystal structure of LG-vitamin D<sub>3</sub> complex to further identify the

secondary vitamin D binding site. Furthermore, we cocrystallized the LG-vitamin D<sub>3</sub> complex which was prepared at pH 7 with a vitamin D<sub>3</sub>/LG ratio of 2 according to the previous crystallographic study.<sup>47</sup> We found a weak extra electron density that was located near the C-terminal  $\alpha$ -helical region. With respect to cocrystallization, the maximum occupancy of the ligand should provide a better opportunity in growing high-quality crystals of the ligand-protein complex. In this section of thesis, we reported a rationally designed approach for preparing the complex of LG and vitamin D<sub>3</sub> at various pH and vitamin D<sub>3</sub>/LG ratios to optimize the occupancy of vitamin D<sub>3</sub> and improve the electron density of the secondary binding site. Finally, we identified an exosite for vitamin D binding to be located near the  $\alpha$ -helix and  $\beta$ -strand I of LG using a crystal prepared at pH 8 with a vitamin D<sub>3</sub>/LG ratio of 3:1. The strategy in practice may be useful for future identification of a ligand-binding site in a given protein.

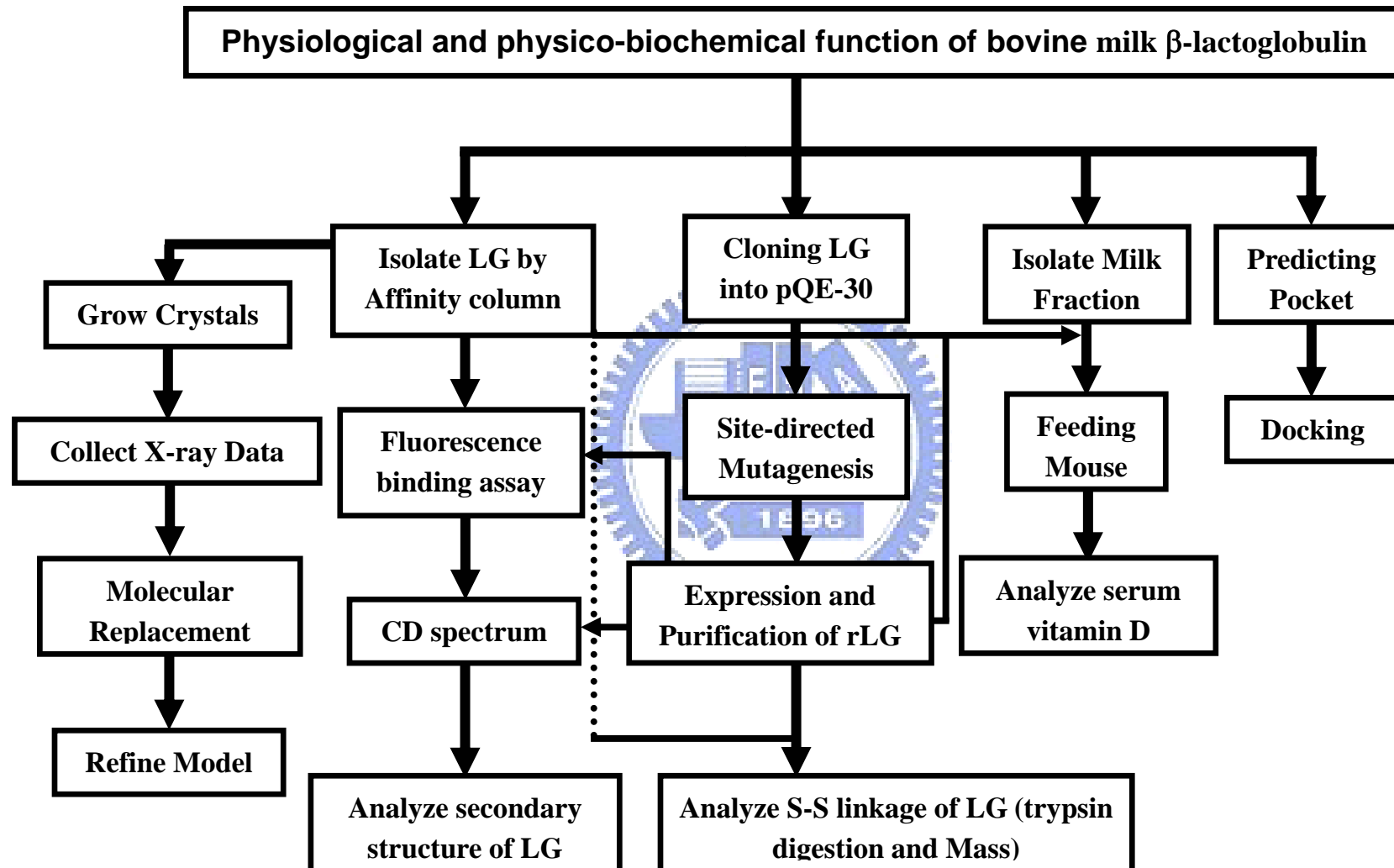


### **Section 3: Evidence for LG involvement in vitamin D transport *in vivo***

In the previous section, we proposed that this exosite contains a unique inverse  $\gamma$ -turn loop (residues 143-145 or Leu-Pro-Met), located between the  $\alpha$ -helix and  $\beta$ -strand I, that is essential in forming a pocket to bind vitamin D according to the crystal structure of LG-vitamin D<sub>3</sub> complex. In the present section, we expressed recombinant LG (rLG) in *Escherichia coli*, and used site-directed mutagenesis to produce a set of mutants to test the hypothesis that this  $\gamma$ -turn plays an essential role in the interaction between LG and vitamin D.

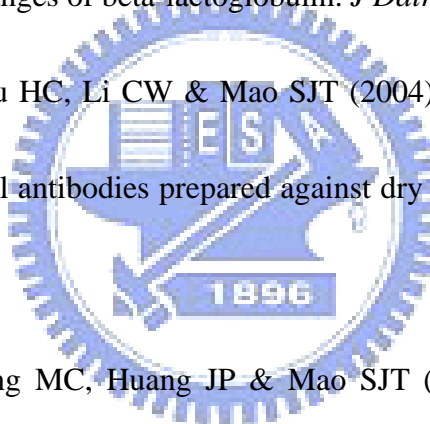
We further tested this hypothesis using a mAb specific for this  $\gamma$ -turn region (selected from a battery containing 900 mAbs) as a probe, and then determined whether vitamin D might interfere with the binding between LG and the mAb. We provide several observations that might support the idea that the  $\gamma$ -turn loop plays a role in the interaction between the exosite and vitamin D. First, substituting each Leu143 and Met145 with charged amino acids resulted in a substantially decreased binding affinity of vitamin D<sub>3</sub> (4.7-fold to 8.1-fold, which is consistent with our previous crystallographic study showing the side chains of these two residues to be directly involved in vitamin D binding. Second, substituting centered Pro144 by Ala also significantly attenuated the binding affinity (4.6-fold). Because Pro144 has no direct contact with vitamin D<sub>3</sub>, we suggest that it might be essential to maintain the conformation of the loop structure. Third, binding of vitamin D<sub>3</sub> to LG attenuated the recognition of a  $\gamma$ -turn loop specific mAb (1D8F8). Although the binding of vitamin D to milk LG is well known,<sup>17,39,42</sup> whether it enhances the transport of vitamin D of milk is still unproven. We have demonstrated for the first time that LG is a fraction responsible for the uptake of vitamin D<sub>3</sub> from milk, using the mouse (n=95) as an animal model. Most interestingly, we showed that native LG containing both the calyx and exosite had an efficacy in vitamin D<sub>3</sub> uptake almost twice that of heated LG containing a single exosite. Our study therefore provides new insights concerning the value of supplementing dairy products with vitamin D.

## Overall experimental design



## References

1. Hambling SG, MacAlpine AS & Sawyer L (1992) Beta-lactoglobulin. In *Advanced Dairy Chemistry I* (Fox PF eds) pp. 141-190. Elsevier, Amsterdam.
2. Sawyer L & Kontopidis G (2000) The core lipocalin, bovine beta-lactoglobulin. *Biochim Biophys Acta* **1482**, 136-148.
3. Marshall K (2004) Therapeutic applications of whey protein. *Altern Med Rev* **9**, 136-156.
4. Sava N, Van der Plancken I, Claeys W & Hendrickx M (2005) The kinetics of heat-induced structural changes of beta-lactoglobulin. *J Dairy Sci* **88**, 1646-1653.
5. Chen WL, Huang MT, Liu HC, Li CW & Mao SJT (2004) Distinction between dry and raw milk using monoclonal antibodies prepared against dry milk proteins. *J Dairy Sci* **87**, 2720-2729.
6. Song CY, Chen WL, Yang MC, Huang JP & Mao SJT (2005) Epitope mapping of a monoclonal antibody specific to bovine dry milk: involvement of residues 66-76 of strand D in thermal denatured beta-lactoglobulin. *J Biol Chem* **280**, 3574-3582.
7. Chen WL, Hwang MT, Liao CY, Ho JC, Hong KC & Mao SJT (2005)  $\beta$ -Lactoglobulin is a Thermal Marker in Processed Milk as Studied by Electrophoresis and Circular Dichroic Spectra. *J Dairy Sci* **88**, 1618-1630.

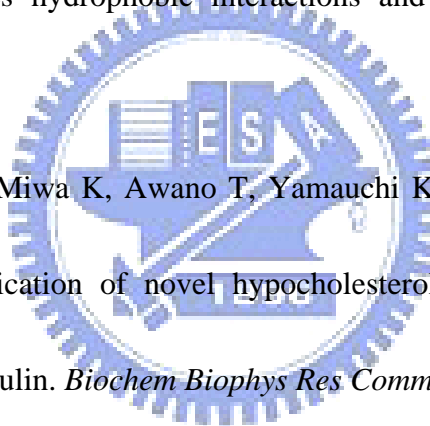


8. Chen WL, Liu WT, Yang MC, Hwang MT, Tsao JH & Mao SJT (2006) A novel conformation-dependent monoclonal antibody specific to the native structure of beta-lactoglobulin and its application. *J Dairy Sci* **89**, 912-921.
9. Papiz MZ, Sawyer L, Eliopoulos EE, North AC, Findlay JB, Sivaprasadarao R, Jones TA, Newcomer ME & Kraulis PJ (1986) The structure of beta-lactoglobulin and its similarity to plasma retinol-binding protein. *Nature* **324**, 383-385.
10. Monaco HL, Zanotti G, Spadon P, Bolognesi M, Sawyer L & Eliopoulos EE (1987) Crystal structure of the trigonal form of bovine beta-lactoglobulin and of its complex with retinol at 2.5 Å resolution. *J Mol Biol* **197**, 695-706.
11. Sawyer L, Papiz MZ, North ACT & Eliopoulos EE (1985) Structure and function of bovine β-lactoglobulin. *Biochem Soc Trans* **13**, 265-266.
12. Newcomer ME, Jones TA, Aqvist J, Sundelin J, Eriksson U, Rask L & Peterson PA (1984) The three-dimensional structure of retinol-binding protein. *EMBO J* **3**, 1451-1454.
13. Redl B (2000) Human tear lipocalin. *Biochim Biophys Acta* **1482**, 241-248.
14. Qin BY, Bewley MC, Creamer LK, Baker HM, Baker EN & Jameson GB (1998) Structural basis of the Tanford transition of bovine beta-lactoglobulin. *Biochemistry* **37**, 14014-14023.

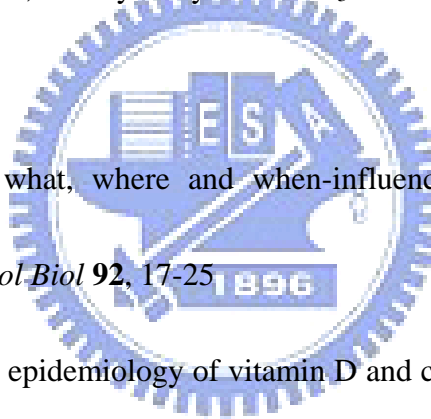


15. Qin BY, Bewley MC, Creamer LK, Baker EN & Jameson GB (1999) Functional implications of structural differences between variants A and B of bovine beta-lactoglobulin. *Protein Sci* **8**, 75-83.
16. Kuwata K, Hoshino M, Forge V, Era S, Batt CA & Goto Y (1999) Solution structure and dynamics of bovine beta-lactoglobulin A. *Protein Sci* **8**, 2541-2545.
17. Kontopidis G, Holt C & Sawyer L (2004) Invited review: beta-lactoglobulin: binding properties, structure, and function. *J Dairy Sci* **87**, 785-796.
18. Adams JJ, Anderson BF, Norris GE, Creamer LK & Jameson GB (2006) Structure of bovine beta-lactoglobulin (variant A) at very low ionic strength. *J Struct Biol* **154**, 246-254.
19. Bello M, Pérez-Hernández G, Fernández-Velasco DA, Arreguín-Espinosa R & García-Hernández E (2008) Energetics of protein homodimerization: effects of water sequestering on the formation of beta-lactoglobulin dimer. *Proteins* **70**, 1475-1487.
20. Uhrinova S, Smith MH, Jameson GB, Uhrin D, Sawyer L & Barlow PN (2000) Structural changes accompanying pH-induced dissociation of the beta-lactoglobulin dimer. *Biochemistry* **39**, 3565-3574.
21. Wu SY, Perez MD, Puyol P & Sawyer L (1999) beta-lactoglobulin binds palmitate within its central cavity. *J Biol Chem* **274**, 170-174.

22. Kontopidis G, Holt C & Sawyer L (2002) The ligand-binding site of bovine beta-lactoglobulin: evidence for a function? *J Mol Biol* **318**, 1043-1055.
23. Considine T, Singh H, Patel HA & Creamer LK (2005) Influence of binding of sodium dodecyl sulfate, all-trans-retinol, and 8-anilino-1-naphthalenesulfonate on the high-pressure-induced unfolding and aggregation of beta-lactoglobulin B. *J Agric Food Chem* **53**, 8010-8018.
24. Konuma T, Sakurai K & Goto Y (2007) Promiscuous binding of ligands by beta-lactoglobulin involves hydrophobic interactions and plasticity. *J Mol Biol* **368**, 209-218.
25. Nagaoka S, Futamura Y, Miwa K, Awano T, Yamauchi K, Kanamaru Y, Tadashi K & Kuwata T (2001) Identification of novel hypocholesterolemic peptides derived from bovine milk beta-lactoglobulin. *Biochem Biophys Res Commun* **281**, 11-17.
26. Chevalier F, Chobert JM, Genot C & Haertle T (2001) Scavenging of free radicals, antimicrobial, and cytotoxic activities of the Maillard reaction products of beta-lactoglobulin glycosylated with several sugars. *J Agric Food Chem* **49**, 5031-5038.
27. Liu HC, Chen WL & Mao SJT (2007) Antioxidant nature of bovine milk beta-lactoglobulin. *J Dairy Sci* **90**, 547-555.



28. Fluckinger M, Merschak P, Hermann M, Haertlé T & Redl B (2008) Lipocalin-interacting-membrane-receptor (LIMR) mediates cellular internalization of beta-lactoglobulin. *Biochim Biophys Acta* **1778**, 342-347.
29. Holick MF (2003) Vitamin D: A millenium perspective. *J Cell Biochem* **88**, 296-307.
30. Vieth R (2005) The pharmacology of vitamin D, including fortification strategies. In *Vitamin D vol. 2* (Feldman D, Pike JW & Glorieux FH, eds), pp. 995–1015. Elsevier.
31. Bortman P, Folgueira MA, Katayama ML, Snitcovsky IM & Brentani MM (2002) Antiproliferative effects of 1,25-dihydroxyvitamin D<sub>3</sub> on breast cells: a mini review. *Braz J Med Biol Res* **35**, 1-9.
32. Webb AR (2006) Who, what, where and when-influences on cutaneous vitamin D synthesis. *Prog Biophys Mol Biol* **92**, 17-25
33. Giovannucci E (2005) The epidemiology of vitamin D and cancer incidence and mortality: a review (United States). *Cancer Causes Control* **16**, 83-95.
34. Cui Y & Rohan TE (2006) Vitamin D, calcium, and breast cancer risk: a review. *Cancer Epidemiol Biomarkers Prev* **15**, 1427-1437.
35. Knight JA, Lesosky M, Barnett H, Raboud JM & Vieth R (2007) Vitamin D and reduced risk of breast cancer: a population-based case-control study. *Cancer Epidemiol Biomarkers Prev* **16**, 422-429.

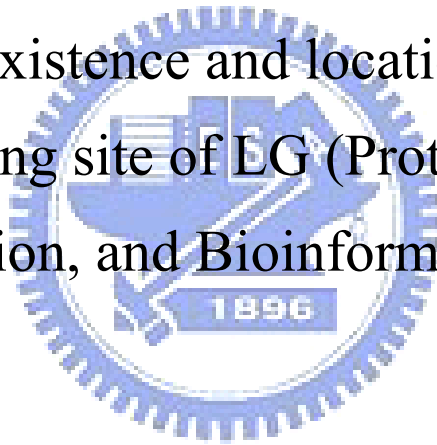


36. Lappe JM, Travers-Gustafson D, Davies KM, Recker RR & Heaney RP (2007) Vitamin D and calcium supplementation reduces cancer risk: results of a randomized trial. *Am J Clin Nutr* **85**, 1586-1591.
37. Holick MF (2007) Vitamin D deficiency. *N Engl J Med* **357**, 266-281.
38. Sahota H, Barnett H, Lesosky M, Raboud JM, Vieth R & Knight JA (2008) Association of vitamin D related information from a telephone interview with 25-hydroxyvitamin D. *Cancer Epidemiol Biomarkers Prev* **17**, 232-238.
39. Wang Q, Allen JC & Swaisgood HE (1997) Binding of vitamin D and cholesterol to beta-lactoglobulin. *J Dairy Sci* **80**, 1054-1059.
40. Wang Q, Allen JC & Swaisgood HE (1997) Binding of retinoids to beta-lactoglobulin isolated by bioselective adsorption. *J Dairy Sci* **80**, 1047-1053.
41. Wang Q, Allen JC & Swaisgood HE (1998) Protein concentration dependence of palmitate binding to beta-lactoglobulin. *J Dairy Sci* **81**, 76-81.
42. Wang Q, Allen JC & Swaisgood HE (1999) Binding of lipophilic nutrients to beta-lactoglobulin prepared by bioselective adsorption. *J Dairy Sci* **82**, 257-264.
43. Muresan S, van der Bent A & de Wolf FA (2001) Interaction of beta-lactoglobulin with small hydrophobic ligands as monitored by fluorometry and equilibrium dialysis: nonlinear quenching effects related to protein--protein association. *J Agric Food Chem* **49**, 2609-2618.

44. Xiao L, Cui X, Madison V, White RE & Cheng KC (2002) Insights from a three-dimensional model into ligand binding to constitutive active receptor. *Drug Metab Dispos* **30**, 951-956.
45. Laurie AT & Jackson RM (2005) Q-SiteFinder: an energy-based method for the prediction of protein-ligand binding sites. *Bioinformatics* **21**, 1908-1916.
46. Yang JM & Chen CC (2004) GEMDOCK: a generic evolutionary method for molecular docking. *Proteins* **55**, 288-304.
47. Qin BY, Creamer LK, Baker EN & Jameson GB (1998) 12-Bromododecanoic acid binds inside the calyx of bovine beta-lactoglobulin. *FEBS Lett* **438**, 272-278.



Section 1: The existence and location of secondary  
vitamin D binding site of LG (Proteins: Structure,  
Function, and Bioinformatics)



## Abstract

$\beta$ -lactoglobulin (LG), one of the most investigated proteins, is a major bovine milk protein with a predominantly  $\beta$  structure. The structural function of the only  $\alpha$ -helix with three turns at the C-terminus is unknown. Vitamin D<sub>3</sub> binds to the central calyx formed by the  $\beta$ -strands. Whether there are two vitamin D binding-sites in each LG molecule has been a subject of controversy. Here, we report a second vitamin D<sub>3</sub> binding site identified by synchrotron X-ray diffraction (at 2.4 Å resolution). In the central calyx binding mode, the aliphatic tail of vitamin D<sub>3</sub> clearly inserts into the binding cavity, where the 3-OH group of vitamin D<sub>3</sub> binds externally. The electron density map suggests that the 3-OH group interacts with the carbonyl of Lys60 forming a hydrogen bond (2.97 Å). The second binding site, however, is near the surface at the C-terminus (residues 136-149) containing part of an  $\alpha$ -helix and a  $\beta$ -strand I with 17.91 Å in length, while the span of vitamin D<sub>3</sub> is about 12.51 Å. A remarkable feature of the second exosite is that it combines an amphipathic  $\alpha$ -helix providing nonpolar residues (Phe136, Ala139, and Leu140) and a  $\beta$ -strand providing a nonpolar (Ile147) and a buried polar residue (Arg148). They are linked by a hydrophobic loop (Ala142, Leu143, Pro144, and Met145). Thus, the binding pocket furnishes strong hydrophobic force to stabilize vitamin D<sub>3</sub> binding. This finding provides a new insight into the interaction between vitamin D<sub>3</sub> and LG, in which the exosite may provide another route for the transport of vitamin D<sub>3</sub> in vitamin D<sub>3</sub> fortified dairy products. Atomic coordinates

for the crystal structure of LG-vitamin D<sub>3</sub> complex described in this work have been deposited in the PDB (access code 2GJ5).

**(Keywords:** fluorescence ligand binding assay, crystallography, localized alternative vitamin D binding site, thermal denaturation, amphipathic helix)

## Introduction

Bovine  $\beta$ -lactoglobulin (LG) is a major whey protein in milk to an extent of about 50%.<sup>1</sup> Because of its thermally unstable and molten-globule nature, LG has been studied extensively for its physical and biochemical properties in the past 40 years.<sup>2-6</sup> Although the biological functions of the protein still remain elusive, some essential functions of LG, such as cholesterol lowering, modulation of immune system, transport of retinol, fatty acid, and vitamin D,<sup>7-9</sup> and prevention of oxidative stress,<sup>10,11</sup> have been reported.

Several crystal forms of bovine LG have been described.<sup>12-21</sup> Of these, lattices X and Z (Space group *P*1 and *P*3<sub>2</sub>21) have been investigated at a low resolution.<sup>14</sup> A high resolution study of another crystal form, lattice Y, has yielded a chain trace and a preliminary model.<sup>14</sup> The overall folding turns out to be remarkably similar to that of the human plasma retinol binding protein<sup>15,16,22,23</sup> and human tear lipocalin,<sup>24</sup> known as members of the lipocalin superfamily. As shown in Figure 1A, LG comprises of 162 amino acid residues with two disulfide linkages and one free cysteine. It has predominantly a  $\beta$ -sheet configuration



containing nine antiparallel  $\beta$ -strands from A to I.<sup>18,19,25</sup> Topographically,  $\beta$ -strands A-D form one surface of the barrel (calyx), whereas  $\beta$ -strands E-H form the other.

The only  $\alpha$ -helical structure with three turns is at the COOH-terminus (residues 130-141), which is followed by a  $\beta$ -strand I lying on the outer surface of the calyx.<sup>26</sup> The structural and functional relationship of this helical region is not yet clearly defined. Studies on the crystal structure of LG-retinol complex at 2.5 Å resolution by Monaco *et al.* have pointed out that there is a surface pocket consisting of almost completely hydrophobic residues near the helical region.<sup>16</sup>

The remarkable ability of the calyx to bind hydrophobic molecules, such as retinol, fatty acids, and vitamin D (Figure 1B),<sup>27-29</sup> has recently been reviewed by Kontopidis *et al.*<sup>9</sup> It seems clear that the binding of fatty acid, retinol, and vitamin D is within the central calyx of the protein; however, the existence of a second ligand binding site beyond the calyx is a matter of controversy.<sup>9</sup> Interestingly, an early study has suggested that a hydrophobic pocket, formed by the  $\alpha$ -helix and the surface of the barrel, also exists.<sup>16</sup> This surface pocket, limited by Phe136 and followed by residues 139-143 (Ala-Leu-Lys-Ala-Leu), has been suspected to potentially bind retinol;<sup>16</sup> however, later studies by X-ray diffraction did not reveal that retinol could occupy this site.<sup>9,29</sup> Using *cis*-parinaric acid as a ligand, Dufour *et al.*<sup>30</sup> have suggested that this ligand is bound in this hydrophobic pocket. It remains unclear what type of ligands may interact with this surface site. The binding of vitamin D to LG is

also controversial.<sup>9,31</sup> It has been postulated that there is another binding site, in addition to the calyx, for vitamin D based on the work of Swaisgood and de Wolf<sup>31-35</sup> by using biochemical binding assays. Subsequently, they also suggested that one vitamin D is bound in that hydrophobic site. Nevertheless, the location of the secondary binding site remote from the calyx has been implicated,<sup>15,16</sup> but has not yet been identified by the crystal structure of bovine LG with vitamin D<sub>2</sub>.<sup>9</sup>

Spectroscopic studies and thermodynamic analysis of the calorimetric signal have demonstrated that irreversible unfolding of the LG structure occurs upon thermal treatment above its transition temperature, 65-70 °C.<sup>36</sup> Recently, we have shown that the conformational changes of LG are rapid and extensive at temperatures above the transition,<sup>5</sup> and  $\beta$ -strand D of the calyx is directly involved in the unfolding during the thermal denaturation.<sup>4</sup> As a result, the binding of palmitate or retinol to the central calyx is diminished. In the present study, we also demonstrated that the maximal binding ratios of vitamin D<sub>3</sub> to LG were 2:1, similar to that established by Wang *et al.*<sup>31</sup> Our next strategy was to denature the conformation of the calyx by heating at 100 °C for 16 min; under this condition the calyx pocket was thermally “removed”. We then tested whether the thermally denatured LG was able to bind vitamin D<sub>3</sub>, palmitate, and retinol. Interestingly, only vitamin D<sub>3</sub> bound the heated LG and the binding ratio of vitamin D<sub>3</sub> to the heated LG was found to be 1:1. Thus, it suggests that there is a secondary site for vitamin D<sub>3</sub> binding,

which is thermally independent. To confirm the hypothesis that a second vitamin D<sub>3</sub> binding site exists, we determined the crystal structure of LG-vitamin D<sub>3</sub> complex and attempted to identify, localize, and characterize such a site.

## Materials and methods

### Materials

LG was purified from raw milk using saturated ammonium sulfate (40%) followed by a G-150 column chromatography of the upper fraction as described previously.<sup>3</sup> All-*trans* retinol, palmitic acid, vitamin D<sub>3</sub> (cholecalciferol), and N-acetyl-L-tryptophanamide were purchased from Sigma-Aldrich (St. Louis, MO).

### Ligand binding to LG

LG stock solution was prepared in 0.01M phosphate buffered solution, pH 8.0 (PB). Retinol, palmitate, and vitamin D<sub>3</sub> were prepared using absolute ethanol and purged with nitrogen and stored at -80 °C in the dark. All the binding assays described below were conducted at 24 °C. The ligand binding assay of LG was measured by fluorescence emission techniques similar to that previously described.<sup>4,31,32</sup> In general, the binding of retinol to LG was measured by extrinsic fluorescence emission of a retinol molecule at 470 nm using excitation at 287 nm, whereas binding of palmitate or vitamin D<sub>3</sub> to LG was measured by the fluorescence enhancement or quenching of Trp19 of LG at 332 nm using excitation at 287 nm.

Fluorescence spectra were recorded with a fluorescence spectrophotometer (Hitachi F-4500; Tokyo, Japan). For the titration experiment, 5  $\mu\text{M}$  of native LG was instantly incubated with various proportions of retinol or vitamin D<sub>3</sub> (0.625-25  $\mu\text{M}$ ) at pH 8.0. For palmitate (2.5-100  $\mu\text{M}$ ), 20  $\mu\text{M}$  of native LG was used. A solution of N-acetyl-L-tryptophanamide with an absorbance at 287 nm - equal to that of the protein - served as a blank. The change in fluorescence of this solution with titration caused by an inner filter effect was corrected as described by Cogan *et al.*<sup>37</sup> The change in fluorescence intensity at 332 nm or 470 nm was assumed to depend on the amount of protein-ligand complex, which allowed the calculation of  $a$ , the fraction of unoccupied ligand-binding sites on the protein:  $a = (F - F_{\text{sat}})/(F_0 - F_{\text{sat}})$ . Here  $F$  is the fluorescence intensity at a certain titration ratio,  $F_{\text{sat}}$  is the corrected fluorescence intensity of LG solution with its sites saturated, and  $F_0$  is the initial corrected fluorescence intensity. These data were then used to construct a plot of  $P_{\text{T}}a$  versus  $R_{\text{T}}a/(1 - a)$  according to the equation:  $P_{\text{T}}a = (1/n)[R_{\text{T}}a/(1 - a)] - K_d^{\text{app}}/n$ , where  $P_{\text{T}}$  is the total protein concentration,  $n$  is the number of binding sites per molecule,  $R_{\text{T}}$  is the total ligand concentration, and  $K_d^{\text{app}}$  is the apparent dissociation constant.

To study the effect of pH on the binding capacity, native LG between 5 and 20  $\mu\text{M}$  was instantly incubated with retinol, vitamin D<sub>3</sub>, or palmitate between 5 and 20  $\mu\text{M}$ . To determine the effect of heat on the binding ability, LG was preheated at between 50 and 100  $^{\circ}\text{C}$  for 15 s to 16 min and stopped using a 20  $^{\circ}\text{C}$  water bath. The preheated LG was then

incubated with retinol, palmitate, or vitamin D<sub>3</sub> at pH 8.0. The final concentration of ethanol in the reaction mixture was kept less than 3% (vol/vol) for all the experiments mentioned above. The ligand binding ability of LG was calculated as described previously.<sup>4,31</sup> For the titration curve experiment, the data were expressed as the percentage of emission of LG that had the maximal binding ratio. For the heat denaturation experiment, the data were expressed as the percentage relative to native LG. All the data were collected in triplicate determinations.

### **Circular dichroism spectrum**

For the circular dichroism (CD) spectral measurements, each sample (0.5 mg/mL) was heated in 20 mM Tris, pH 8.0.<sup>4,38</sup> The CD spectra were recorded on a spectropolarimeter (Jasco-J715; Tokyo, Japan) at 24 °C over wavelength ranges from 200 to 250 nm, and recorded at a scan speed of 20 nm/min. All spectra were measured twenty times in a cuvette with a path length of 1.0 mm. Each LG sample (100 µL) was preheated at 50, 60, 70, 80, 90, and 100 °C for 16 min and instantly stopped in a 20 °C water bath before an immediate measurement.

### **Crystallization**

Purified LG was concentrated to 20 mg/mL in 20 mM Tris, pH 8.0. Vitamin D<sub>3</sub> stock solution made up as 50 mM in ethanol was added to LG solution to give a molar ratio of 3:1 and incubated for 3 h at 37 °C. Precipitation immediately occurred when LG and vitamin D<sub>3</sub>

were mixed, and the solution drops became clear on the slides after 3-4 days. Crystallization of the LG-vitamin D<sub>3</sub> complex was achieved using the hanging-drop vapor-diffusion method at 18 °C with 2 μL hanging drops containing equal amounts of LG-vitamin D<sub>3</sub> complex and a reservoir solution (0.1M HEPES containing 1.4M trisodium citrate dehydrate, pH 7.5). Crystals 0.1-0.2 mm long grew after 7 days.

### **Crystallographic data collection and processing**

The crystals were mounted on a Cryoloop (0.1-0.2 mm), dipped briefly in 20% glycerol as a cryoprotectant solution, and frozen in liquid nitrogen. X-ray diffraction data at 2.4 Å resolution were collected at 110 K using the synchrotron radiation on the beamlines BL12B2 at SPring-8 (Harima, Japan) and BL13B at NSRRC (Hsinchu, Taiwan). The data were processed using the *HKL2000* program.<sup>39</sup> The crystals belong to the space group *P*3<sub>2</sub>21 with unit cell dimensions of  $a = b = 53.78$  Å and  $c = 111.573$  Å. There is one molecule per asymmetric unit according to an estimated solvent content in a reasonable region. Details of the data statistics are given in a table in the text.

### **Crystal structure determination and refinement**

The structure of the LG-vitamin D<sub>3</sub> was determined by molecular replacement<sup>40</sup> as implemented in *CNS v1.1*<sup>41</sup> using the crystal structure of bovine LG (PDB code 2BLG)<sup>18</sup> as a search model. The LG molecule was located in the asymmetric unit after rotation and translation function searches. All refinement procedures were performed using *CNS v1.1*.

The composite omitted electron density maps with coefficients  $|2F_o - F_c|$  were calculated and visualized using *O v7.0*,<sup>42</sup> and the model was rebuilt and adjusted iteratively as required. Throughout the refinement, a random selection (8%) of the data was placed aside as a “free data set”, and the model was refined against the rest of the data with  $F \geq 0$  as a working set.<sup>43-45</sup> The monomer protein model was initially refined by rigid-body refinement using the data from 15.0 to 3.0 Å resolution, for which the group temperature *B* values were first restrained at 20 Å<sup>2</sup>. This refinement was followed by simulated annealing using a slow cooling protocol with a starting temperature of 2500 K, provided in *CNS*, applied to all data between 15.0 and 2.4 Å. The bulk solvent correction was then applied, and group *B* factors were adjusted. After several cycles of positional and grouped *B* factor refinement interspersed with interactive modeling, the *R*-factor for the LG-vitamin D<sub>3</sub> complex decreased to about 28% with the *R*<sub>free</sub> around 36%. Two elongated extra electron densities with one LG molecule were clearly visible and recognized as the vitamin D<sub>3</sub> in  $\sigma_A$ -weighted  $|F_o - F_c|$  difference maps. Two vitamin D<sub>3</sub> molecules were then adjusted and well fitted into the density map. The refinement then proceeded with another cycle of simulated annealing with a slow cooling, starting at a temperature of 1000 K. The vitamin D<sub>3</sub> molecules were adjusted iteratively according to the omitted electron density maps. Finally, water molecules were added using the program *CNS v1.1*.

### **Model validation**

The final model of LG and vitamin D<sub>3</sub> complex contains 1272 nonhydrogen protein atoms for the monomer LG, 28 atoms for one vitamin D<sub>3</sub> molecule, and 38 water molecules. The refinement statistics are given in the text. The correctness of stereochemistry of the model was verified using *PROCHECK*.<sup>46</sup> The calculations of r.m.s. deviations from ideality<sup>47</sup> for bonds, angles, and dihedral and improper angles performed in *CNS* showed satisfactory stereochemistry. In a Ramachandran plot,<sup>48</sup> all main chain dihedral angles were in the most favored and additionally allowed regions except for Tyr99.

### Coordinates

Atomic coordinates for the crystal structure of LG-vitamin D<sub>3</sub> complex described in this work have been deposited in the PDB (access code 2GJ5).



### Results

#### Binding of LG to retinol, palmitate, and vitamin D<sub>3</sub>

Using the titration method previously established by Wang *et al.*,<sup>31,32</sup> we show that the maximal binding of vitamin D<sub>3</sub> with LG was achieved at a 2:1 ratio; whereas the binding for retinol or palmitate remained to be 1:1 (Figure 2). This result is similar to that reported previously by Wang *et al.*<sup>31,32</sup> and tends to support a notion that LG binds two vitamin D<sub>3</sub> molecules. The two possibilities for this result are either that LG has the same binding site for two vitamin D<sub>3</sub> molecules or it possesses two independent vitamin D<sub>3</sub> binding sites.



### **Effect of pH on LG binding to retinol, palmitate, and vitamin D<sub>3</sub>**

It has been postulated that pH plays a crucial role in controlling the opening of the calyx to allow the entrance of LG ligands. At low pH or below the Tanford transition (about pH 6), the EF loop (the calyx cap) is closed, disallowing the binding of the ligands. To explore whether there is another vitamin D<sub>3</sub> binding site that may not be affected by the Tanford transition, we monitored the binding of vitamin D<sub>3</sub> at various pH while using retinol or palmitate as a reference. A notable transition of vitamin D<sub>3</sub> binding to LG was found to occur between pH 6.0 and 8.0 (Figure 3), similar to that of retinol and palmitate. The binding to vitamin D<sub>3</sub> or palmitate was decreased to some extent at pH 9-10 (Figure 3). This could be due to the protonated state of Lys69 inside the calyx being neutralized at a high pH as suggested previously.<sup>4,29</sup> It is of interest to note that unlike retinol and palmitate; LG at a pH between 2 and 6 still retains about 35% of the maximal binding for vitamin D<sub>3</sub> (Figure 3C). The data imply that there is a possible secondary binding site for vitamin D<sub>3</sub> that is independent of the calyx.

### **Effect of heating on LG binding to retinol, palmitate, and vitamin D<sub>3</sub>**

The pH titration experiment described above was unable to yield an accurate explanation of the existence of another binding site for vitamin D<sub>3</sub>. Our previous work showed that thermally denatured LG (heated to 100 °C for 5 min) was unable to bind to retinol and palmitate because of the unfolding of the calyx.<sup>4</sup> In the next experiment, our strategy was to

thermally “remove” the calyx and then test whether heated LG retained an activity allowing vitamin D<sub>3</sub> binding. Figure 4 shows a notable and sharp decrease in retinol, palmitate, and vitamin D<sub>3</sub> binding to LG heated between 70 °C and 80 °C over time. The change of binding is consistent to the molten-globule nature of LG, which correlates to its transition temperature.<sup>4</sup> At temperatures above 80 °C, the protein lost its binding ability to retinol and palmitate in a time-dependent fashion, but it still retained 40% of the binding to vitamin D<sub>3</sub> even after being heated at 100 °C for 16 min (Figure 4C). The heated LG (100 °C for 16 min) was further titrated with the binding of vitamin D<sub>3</sub> in excess. Figure 4D reveals that there was about 42% of maximal binding of vitamin D<sub>3</sub> relative to that using native LG. There was no fluorescence change while titrating with retinol or palmate (data not shown). Remarkably, a maximal stoichiometry of 1:1 was observed between the denatured LG and vitamin D<sub>3</sub>. Thus, it suggests that a thermally stable site exists in LG to bind vitamin D<sub>3</sub>.

### **Comparison of binding affinity of LG to retinol, palmitate, and vitamin D<sub>3</sub>**

We further determined the binding affinities of LG for retinol, palmitate, and vitamin D<sub>3</sub> using the method previously described by Wang *et al.*<sup>31,32</sup> The fluorescence data obtained for retinol, palmitate, and vitamin D<sub>3</sub> binding to native LG are shown in Figure 2 (right panels), while the vitamin D<sub>3</sub> binding to heated LG (100 °C for 16 min) is shown in Figure 4D (inserted panel). Yielding values for the number of binding sites per molecule and apparent dissociation constant from the slope are listed in Table 1. The binding affinity of

vitamin D<sub>3</sub> to native LG using this method was about 5 nM ( $K_d^{app} = 4.74 \pm 0.37$  nM) and appears to be 5-10 times greater than that of retinol and palmitate. On the other hand, the binding affinity of vitamin D<sub>3</sub> to heated LG was attenuated at about 45 nM ( $K_d^{app} = 45.67 \pm 3.12$  nM), but is within the same order as that between native LG and retinol or palmitate. Because heating LG also induces the aggregation of LG,<sup>5</sup> the overall attenuated binding affinity of the “secondary site” indicates a structural change in the second binding site in heated LG. Nevertheless, the data temptingly suggest that the putative second binding site is somewhat heat resistant.

#### **Overall crystal structure of LG-vitamin D<sub>3</sub> complex**

We have clarified that there are two vitamin D binding sites on LG according to ligand binding assay performed in solution. Protein crystallography was used to locate the secondary vitamin D binding site of LG. There are several crystal forms of bovine LG that have been well reported, including the triclinic (lattice X), orthorhombic (lattice Y), and trigonal (lattice Z) forms belonging to space groups  $P1$ ,  $C222_1$ , and  $P3_221$ , respectively.<sup>12-21</sup> The crystal of the LG-vitamin D<sub>3</sub> complex we obtained was found to be a trigonal (lattice Z) space group  $P3_221$  based on the data of 2.4 Å resolution. The final model comprised of 161 residues and its refinement statistics of the complex are given in Table 2. The discrepancy indices for  $R$  and  $R_{free}$  are 23.86% and 26.12%, respectively. The LG-vitamin D<sub>3</sub> complex possesses a well geometry similar to that reported by *CNS*<sup>27</sup> with a root-mean-square (r.m.s.)

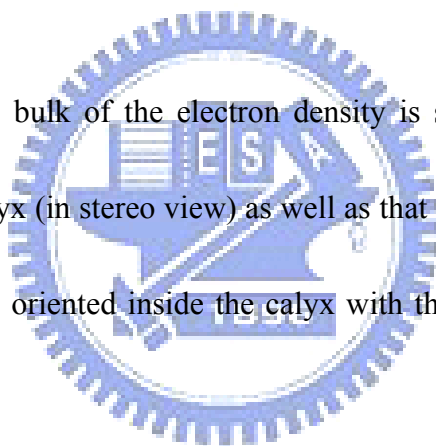
bond length and bond angle deviation from ideality 0.007 Å and 1.264° respectively (Table 2). A Ramachandran plot reveals that only one residue is in the disallowed regions (Tyr99), which arises in most of the lipocalin family as a result of the  $\gamma$ -turn associated with the sequence “TDY” (residues 97-99). The average temperature factor for all protein atoms is 55.02 Å<sup>2</sup>, which is considered to be inadequate for established crystallographic standards. This may be explained by LG having nearly 25% of the residues located around flexible surface loops and NH<sub>2</sub>- and COOH-terminal regions. Previously published statistics of LG complexes<sup>9,27,29</sup> show a *B*-factor range of 41.3-57.27 (Table 3), which accommodates for the elevated values acquired in this study that seem to deviate from the norm.

The overall topology of LG is similar to that previously described<sup>15-19</sup> with a well-defined antiparallel  $\beta$ -sheet structure and flexible loops connecting the secondary structure elements. The loops AB, CD, EF, and GH are more flexible than the others, consistent with the observations from other reported crystal structures.<sup>15-19</sup> The EF loop that acts as a flap is in the open position of the central calyx, which is expected when vitamin D<sub>3</sub> is present.

Space-filling drawings of the LG-vitamin D<sub>3</sub> complex show that there are two domains for vitamin D<sub>3</sub> binding (Figure 5). One vitamin D<sub>3</sub> molecule inserts almost perpendicularly into the calyx cavity as expected and is consistent to the previous reports.<sup>9,29</sup> The other binds to the surface near the COOH-terminus of LG (residues 136-149), including part of the

$\alpha$ -helix and  $\beta$ -strand I (Figure 1) as shown in Figure 6. The *B*-factor for the vitamin D<sub>3</sub> molecules in the calyx and the second site are 39.19 and 46.90, respectively (Table 2). Proximity of these values to the published data<sup>9,27,29</sup> reveals the rigidity of vitamin D<sub>3</sub> bound to LG (Table 3). For the second site, vitamin D<sub>3</sub> is close to the surface of LG with 17.91 Å in length, while the span of vitamin D<sub>3</sub> is about 12.51 Å. Under this orientation, the A ring or the aliphatic tail following the C/D rings of vitamin D<sub>3</sub> interacts with the  $\beta$ -strand I or the  $\alpha$ -helix of LG, respectively (Figure 6). We putatively defined this second vitamin D<sub>3</sub> binding site as an exosite.

Figure 6 depicts that the bulk of the electron density is sufficient to cover the entire extent of vitamin D<sub>3</sub> in the calyx (in stereo view) as well as that in the exosite. The aliphatic tail of vitamin D<sub>3</sub> (C17-27) is oriented inside the calyx with the 3-OH group of vitamin D<sub>3</sub> near the outside of the pocket.



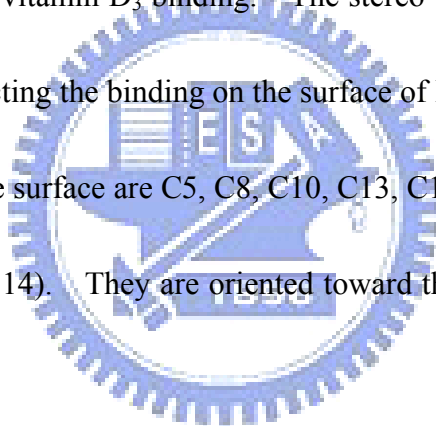
Superimposing the current LG-vitamin D<sub>3</sub> and previously described LG models (PDB codes 1BSQ) in the region of the calyx (Figure 7A) reveals that the movement of the external EF “gate loop” of LG-vitamin D<sub>3</sub> is quite similar to that of the LG-retinol complex<sup>18,29</sup> (data not shown). Some side chains, such as Lys60, Glu62, Phe105, and Met107, require significant reposition to make room for vitamin D<sub>3</sub> insertion into the calyx. The atoms of vitamin D<sub>3</sub> near or at the “mouth” of the calyx possess higher values of *B*-factors suggesting their higher mobility. Figure 7B depicts the distance of vitamin D<sub>3</sub> to the LG calyx. The

shortest interaction distance is hydrogen bonding between the 3-OH group of vitamin D<sub>3</sub> and Lys60 (2.97 Å) of LG; whereas the only hydrogen bond involving retinol binding is that to Glu62.<sup>29</sup> Hydrophobic interaction and the distances between the carbons of vitamin D<sub>3</sub> and Pro38, Leu39, Val41, Ile71, Ala86, Phe105, and Met107 of LG are also displayed.

With respect to the second binding site for vitamin D<sub>3</sub>, it appears that vitamin D<sub>3</sub> is bound to a surface pocket between the COOH-terminal  $\alpha$ -helix and  $\beta$ -strand I (residues 136-149). The current LG-vitamin D<sub>3</sub> and previously described native LG models in this region (PDB codes 1BSQ) are superimposed and shown in Figure 8A. Notably, there is not much conformational change near the exosite of LG upon the vitamin D<sub>3</sub> binding. Figure 8B shows the distance between vitamin D<sub>3</sub> and the amino acids involved (Asp137, Leu140, Lys141, Leu143, Met145, His146, Ile147, and Arg148). Although some charged residues of the exosite are involved, their interaction with vitamin D<sub>3</sub> is mainly hydrophobic with the charged groups of LG sticking out of the pocket. The data suggest that the contact is via a hydrophobic interaction. There is no evidence that the hydroxyl group of vitamin D<sub>3</sub> interacts with  $\eta$ 1 N of Arg148 as the distance (4.9 Å) is greater than that of hydrogen bonding (bond length less than 3.13 Å) (Figure 8B).

Furthermore, LG is primarily oriented as a  $\beta$  structure (50%); the only  $\alpha$ -helix region of LG consisting of three turns is located at the COOH-terminus between residues 130 and 141. Remarkably interesting, the  $\alpha$ -helix is arranged as amphipathic consisting of all the charged

residues (Asp130, Glu131, Glu134, Asp137, Lys138, and Lys141) clustered at one face with hydrophobic or noncharged residues (Ala132, Leu133, Phe136, Ala139, and Leu140) at another face without an exception (Figure 9A). A remarkable feature is that the exosite is comprised of an amphipathic  $\alpha$ -helix providing hydrophobic residues (Phe136, Ala139, and Leu140) at one side and a  $\beta$ -strand providing a hydrophobic Ile147 and a backbone His146 at the other side (Figure 9B). These two sides are linked by a loop containing hydrophobic residues Ala142, Leu143, and Pro144. Thus, the binding pocket provides a strong hydrophobic force to stabilize vitamin D<sub>3</sub> binding. The stereo view of such an interaction is also drawn in Figure 9B, depicting the binding on the surface of LG. The carbons of vitamin D<sub>3</sub> ( $n = 27$  in total) close to the surface are C5, C8, C10, C13, C14, C15, C16, C17, C18, C19, C22, C24, C25, and C26 ( $n = 14$ ). They are oriented toward the surface consistent with the analysis of Figure 5.



### **CD spectrum analysis of heated LG**

In general, the CD spectrum at 222 nm is used for the calculation of the  $\alpha$ -helical content of a given protein. Because the  $\alpha$ -helix region of LG is located in the second binding site and heating LG retains ~40% of the maximal vitamin D<sub>3</sub> binding to the whole LG molecule, we monitored whether there were spectral changes of LG at 222 nm of LG upon heating at 50, 60, 70, 80, 90, and 100 °C. Figure 10 reveals that there were no significant changes in spectra at 222 nm. As expected, the  $\beta$ -configuration was disordered at temperatures above

70 °C, consistent with our previous observation.<sup>4</sup> Thus, it temptingly offers support that the proposed exosite is somewhat thermally stable.

## Discussion

During the past 40 years, LG has been extensively studied for its biochemical properties, and an abundance of literature exists about its physicochemical nature.<sup>9</sup> Although the exact physiological functions of LG are not fully explored, one of its roles is to transport hydrophobic molecules, such as retinol, fatty acids, and vitamin D.<sup>49,50</sup> The active form of vitamin D is  $1\alpha, 25(\text{OH})_2$  vitamin  $\text{D}_3$ , which maintains calcium homeostasis and plays important roles on the immune system and prevents the growth and differentiation of cancer cells. Recent studies indicate that increased plasma vitamin  $\text{D}_3$  concentrations are associated with decreased incidence of breast, ovarian, prostate and colorectal cancers,<sup>51</sup> and osteoporotic fractures.<sup>52</sup> The concentration of vitamin  $\text{D}_3$  in plasma is about 80 nM. A double-blind placebo controlled study conducted in Europe indicated this level to be significantly reduced over the winter season (about 37%) due to the lack of exposure to sunlight.<sup>53</sup> However, drinking vitamin  $\text{D}_3$  fortified milk (312 nM) significantly compensated the seasonal loss of vitamin D by greater than 50%. For this reason, it has been recommended that milk enriched with vitamin  $\text{D}_3$  be provided in high-latitude European countries. Thus, we chose vitamin  $\text{D}_3$ , instead of vitamin  $\text{D}_2$ , to form a LG-vitamin  $\text{D}_3$



complex in this study. Structurally, the only difference of vitamin D<sub>3</sub> from D<sub>2</sub> is the latter being a double bond between the carbon positions 22 and 23 (Figure 1). Despite the minor difference, their binding characteristics to LG are similar.<sup>31</sup> One additional goal in the present study is to test the possibility of binding vitamin D<sub>3</sub> to thermally denatured milk, which is often produced in the processing of milk.

With respect to the ligand binding of LG, many research groups<sup>28,31,32</sup> have shown that the stoichiometry for binding retinol or palmitate to LG is 1:1, and most experimental evidence points to the calyx of LG as the binding site for retinol and palmitate.<sup>29</sup> However, there remains a debate about the stoichiometry for vitamin D<sub>3</sub> binding being 1 or 2. Wang *et al.*<sup>31,34</sup> proposed that LG has another binding site for vitamin D in addition to the central calyx, but doubt has been raised based on crystallographic analysis.<sup>9,29</sup> In fact, the presence of a secondary site for ligand binding has been described and proposed for some time,<sup>16</sup> but the identity of a LG-ligand complex by an X-ray crystal structure has not been elucidated.<sup>9</sup>

In the present work, using the method of extrinsic fluorescence emission and fluorescence enhancement and quenching established previously,<sup>4,31,32</sup> we show the maximal binding ratios of retinol or palmitate with LG to be 1:1, whereas it was 2:1 for that of vitamin D<sub>3</sub> (Figure 2). The latter result is consistent to that reported by Wang *et al.*<sup>31,32</sup> It is worth mentioning that using the intrinsic fluorescence of Trp can give results that indicate significantly tighter ligand binding than other methods, especially equilibrium dialysis. This

effect is particularly noticeable when the Trp fluorescence decreases with ligand addition.<sup>9,35</sup>

A recent review<sup>9</sup> suggests that a surface low-affinity binding site together with a central high-affinity binding site (calyx) would appear to satisfy most of the reported experimental observations. In brief, the diverse reports of more than a single binding site may be dependent on the method used.

In an attempt to resolve the controversy about an additional binding site for vitamin D<sub>3</sub>, we used several additional approaches involving structural change to study the interaction between vitamin D<sub>3</sub> and LG. First, it has been established that the EF loop acts as a gate over the calyx.<sup>9,18,29,54</sup> At a low pH, the loop is in a “closed” position, and the ligand binding into the calyx is inhibited. On the contrary, at a high pH above the Tanford transition, the loop is “open” allowing ligands to penetrate into the calyx.<sup>4,54,55</sup> We explored the binding ability between LG and vitamin D<sub>3</sub> at various pH. Similar to that of retinol and palmitate, the present study shows that there is a notable transition of vitamin D<sub>3</sub> binding to the calyx of LG occurring between pH 6.0 and 8.0 (Figure 3). Most interestingly, at pH between 2 and 6 we show vitamin D<sub>3</sub> interacting with LG (with about 35% of maximal binding ability), but not retinol and palmitate (Figure 3C). Because the EF loop is “closed” below the Tanford transition, such binding suggests the presence of another binding site for vitamin D<sub>3</sub>. Physiologically, such low pH binding could be essential, since LG is well known to be stable at low pH<sup>1,2</sup> and resistant to acid hydrolysis and protease digestion in the gastrointestinal

tract.<sup>56,57</sup> Notably, the binding of vitamin D<sub>3</sub> or palmitate to LG was decreased to some extent at pH 9-10 (Figure 3). One of the possible explanations is that the positively charged groups of lysine residues inside calyx are neutralized at pH above 8 resulting in a weakening of the interaction with the carboxyl group of palmitate.<sup>4</sup>

Second, we have shown that the  $\beta$ -strand D of the calyx is directly involved in the thermal denaturation.<sup>4</sup> The conformational changes of LG were rapid, extensive, and irreversible upon heating over 70-80 °C.<sup>5</sup> As a result, it completely diminishes the binding of palmitate and retinol. To test the hypothesis that there is a putative second binding site for vitamin D<sub>3</sub> located independently from the calyx, we thermally denatured the calyx (between 50 and 100 °C) and then conducted the binding for retinol, palmitate, or vitamin D<sub>3</sub> over time (Figure 4). It is of interest that only vitamin D<sub>3</sub> was able to bind to heated LG (at 100 °C for 16 min) with a stoichiometry of almost 1:1, instead of 2:1 (Figure 4D). Our data suggests that the second binding site for vitamin D<sub>3</sub> is heat stable to some extent.

Third, analysis of the binding shows that the binding affinity between native LG and vitamin D<sub>3</sub> is relatively high within a nM range, about 10 times greater than palmitate and retinol (Table 1). The result is almost the same as that of vitamin D<sub>2</sub> reported by Wang *et al.*,<sup>31</sup> but somewhat higher than the affinity reported for vitamin D<sub>3</sub>.<sup>31</sup> The reason contributing to such discrepancy remains elusive. One possibility may be due to the 5  $\mu$ M concentration (pH 8.0) of LG that we employed, while Wang *et al.* used a 20  $\mu$ M

concentration (pH 7.0) for a typical emission spectrum.<sup>34</sup> The other possibility may be due to the pH; the fluorescence of Trp may be affected by ionization of neighboring prototropic groups or by conformation changes due to the dimerization of the protein.<sup>2,34</sup> Nevertheless, the calculated affinity for vitamin D<sub>3</sub> ( $K_d^{app} = 45.67 \pm 3.12$  nM) to putative second or thermally stable binding site is about 10 times lower than that to native LG (calyx plus second site) (Table 1). Thus, it seems to be consistent with the hypothesis proposed by Kontopidis *et al.*<sup>9</sup> that the central site (calyx) is a main binding site possessing a high affinity for most of the hydrophobic ligands, whereas the affinity for the secondary site is low. Ultimately, the secondary binding may depend on the nature of the ligands, such as their size, structure, and hydrophobicity. It would be of interest to further investigate other ligand bindings to heated LG, although the calculation of binding affinity of heated LG is somewhat complicated owing to the formation of large LG polymers as mentioned (see Results).

Finally, to confirm our hypothesis that there exists a second vitamin D<sub>3</sub> binding site remote from the calyx, we used a synchrotron radiation X-ray to determine the crystal structure of the LG-vitamin D<sub>3</sub> complex. Our crystal of the complex is defined in trigonal (lattice Z) space group  $P3_221$ . This final model reveals that one vitamin D<sub>3</sub> molecule binds to the calyx (central internal binding-site) of LG and the other binds to the surface of LG between the  $\alpha$ -helix and  $\beta$ -strand I (external binding site; Figure 5).

In the electron density map at 2.4 Å resolution, vitamin D<sub>3</sub> is well fitted into the bulk of electron density around the calyx or the exosite (Figure 6). In central calyx binding mode, the aliphatic tail of vitamin D<sub>3</sub> clearly inserts into the binding cavity where the 3-OH group of vitamin D<sub>3</sub> binds externally. In an early report using vitamin D<sub>2</sub>,<sup>9</sup> the end that inserted into the calyx was not conclusively identified because the electron density was not enough to cover the entire ligand. It is not clear whether vitamin D<sub>3</sub> is superior to vitamin D<sub>2</sub> in binding to LG. The other difference is that in our study the 3-OH group of vitamin D<sub>3</sub> forms a hydrogen bond with the carbonyl of Lys60 (Figure 7B) instead of Lys69 as proposed using vitamin D<sub>2</sub>.<sup>9</sup> Again, the electron density was not strong enough for the outer extremity of vitamin D<sub>2</sub> making the exact conclusion difficult. Another explanation is that there might be a significant difference in the orientation between vitamin D<sub>2</sub> and D<sub>3</sub>, although the difference in chemical structure is subtle. Regardless, the vitamin D<sub>3</sub>-LG binding mode is quite similar to that of retinol-LG interaction over the calyx.<sup>29</sup> Pro38, Leu39, Val41, Ile71, Ala86, Phe105, and Met107 are all involved in providing hydrophobic interactions with the displayed distance of less than 3.8 Å to the carbon backbone of vitamin D<sub>3</sub> (Figure 7B).

In exosite binding mode, the vitamin D<sub>3</sub> molecule attaches at a pocket between the C-terminal α-helix and β-strand I (Figure 5). We specifically demonstrated that the exosite of LG provides a hydrophobic force to stabilize vitamin D<sub>3</sub> (Figure 8B) and concluded that the exosite is located near the surface of the C-terminal α-helix and β-strand I, where there is

no strong evidence to show that the 3-OH group of vitamin D<sub>3</sub> is capable of interacting with LG (Figure 8B). A stereo view shown in Figure 9B reveals that part of the vitamin D<sub>3</sub> molecule is exposed toward the surface, consistent to that depicted in Figure 5. Although this second binding is located near the surface of LG, our data suggest that the binding affinity of vitamin D<sub>3</sub> to exosite is reasonably high and almost equivalent to that of retinol or palmitate to calyx (Table 1). Apparently, vitamin D<sub>3</sub> interacts mostly with those hydrophobic amino acids within residues 136-149 with distances less than 3.8 Å (Figure 8B). The linking-loop residues 142-145 (Ala-Leu-Pro-Met) between the  $\alpha$ -helix and  $\beta$ -strand I are all hydrophobic. With such an orientation, a hydrophobic pocket is constructed in facilitating the binding for vitamin D<sub>3</sub>. It is worth mentioning that this exosite is very similar to the surface hydrophobic site (mentioned and discussed above) that has been described by Monaco *et al.*<sup>16</sup> and proposed by Wang *et al.*<sup>31</sup>

It is of interest that the  $\alpha$ -helix involved in the exosite is typically amphipathic. This amphipathic region could be heat resistant as suggested from our binding experiment for vitamin D<sub>3</sub> and heated LG. A similar situation is seen in a typically amphipathic apolipoprotein A-I; its conformation and lipid binding properties are completely maintained upon heating over 100 °C.<sup>58</sup> It might be worthwhile to study the crystal structure of the heated-LG-vitamin D<sub>3</sub> complex to finally prove its heat resistance. Unfortunately, we are

not able to crystallize such a complex at the present time. This could be due to the formation of multiple aggregated forms of LG upon heating.<sup>3-6</sup>

Vitamin D is found in only a few foods, such as fish oil, liver, milk, and eggs, in which milk is a major source for vitamin D in the diet. The level of vitamin D in bovine milk has been reported to be low. In many sophisticated food industries, processed milk, dry milk, margarine, and other dairy products are fortified with vitamin D<sub>3</sub> to a level of about 0.35 μM. The concentration of LG in milk is about 270 μM, providing a sufficient amount of LG to transport spiked vitamin D. It is of interest to point out that recent studies have demonstrated that intact LG is acid resistant with a super permeability to cross the epithelium cells of the gastrointestinal tract.<sup>56,57</sup> Such a unique property of LG is worthy of consideration for transporting vitamin D in the milk.

There are two advantages for the presence of vitamin D<sub>3</sub> binding exosite in LG. First, central calyx of LG is thought to be primarily occupied by the fatty acid in milk.<sup>59</sup> The available exosite may provide another route for transporting the vitamin D. Second, many dairy products today are processed under excessive heat for the purpose of sterilization. The presence of a heat stable exosite may maintain the binding for vitamin D<sub>3</sub>.

Finally, since the putative exosite is located at the surface of LG, an approach using site-directed mutagenesis may eventually be served as to probe the structural and vitamin D binding relationship. The experiment is now in progress in our laboratory.

## Acknowledgements

We are grateful to our colleagues, Dr. Yuch-Cheng Jean and Dr. Chun-Shiun Chao, and the supporting staffs for the technical assistance and discussion of the synchrotron radiation X-ray facility on data collection at BL13B1 of NSRRC, Taiwan, and Dr. Yu-San Huang and Dr. Kuan-Li Yu at BL12B2 of SPring-8, Japan. We also thank Dr. Su-Ying Wu of National Health Research Institutes (NHRI, Taiwan) for the useful discussion in preparing this manuscript.

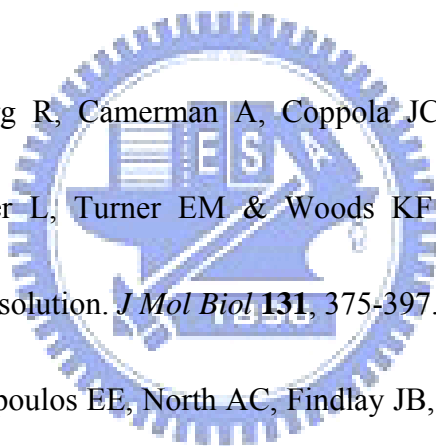


1. Hambling SG, MacAlpine AS & Sawyer L (1992) Beta-lactoglobulin. In *Advanced Dairy Chemistry I* (Fox PF eds) pp. 141-190. Elsevier, Amsterdam.
2. Sawyer L & Kontopidis G (2000) The core lipocalin, bovine beta-lactoglobulin. *Biochim Biophys Acta* **1482**, 136-148.
3. Chen WL, Huang MT, Liu HC, Li CW & Mao SJT (2004) Distinction between dry and raw milk using monoclonal antibodies prepared against dry milk proteins. *J Dairy Sci* **87**, 2720-2729.



4. Song CY, Chen WL, Yang MC, Huang JP & Mao SJT (2005) Epitope mapping of a monoclonal antibody specific to bovine dry milk: involvement of residues 66-76 of strand D in thermal denatured beta-lactoglobulin. *J Biol Chem* **280**, 3574-3582.
5. Chen WL, Hwang MT, Liao CY, Ho JC, Hong KC & Mao SJT (2005)  $\beta$ -Lactoglobulin is a Thermal Marker in Processed Milk as Studied by Electrophoresis and Circular Dichroic Spectra. *J Dairy Sci* **88**, 1618-1630.
6. Chen WL, Liu WT, Yang MC, Hwang MT, Tsao JH & Mao SJT (2006) A novel conformation-dependent monoclonal antibody specific to the native structure of beta-lactoglobulin and its application. *J Dairy Sci* **89**, 912-921.
7. Nagaoka S, Futamura Y, Miwa K, Awano T, Yamauchi K, Kanamaru Y, Tadashi K & Kuwata T (2001) Identification of novel hypocholesterolemic peptides derived from bovine milk beta-lactoglobulin. *Biochem Biophys Res Commun* **281**, 11-17.
8. Zsila F, Bikadi Z & Simonyi M (2002) Retinoic acid binding properties of the lipocalin member beta-lactoglobulin studied by circular dichroism, electronic absorption spectroscopy and molecular modeling methods. *Biochem Pharmacol* **64**, 1651-1660.
9. Kontopidis G, Holt C & Sawyer L (2004) Invited review: beta-lactoglobulin: binding properties, structure, and function. *J Dairy Sci* **87**, 785-796.

10. Chevalier F, Chobert JM, Genot C & Haertle T (2001) Scavenging of free radicals, antimicrobial, and cytotoxic activities of the Maillard reaction products of beta-lactoglobulin glycated with several sugars. *J Agric Food Chem* **49**, 5031-5038.
11. Marshall K (2004) Therapeutic applications of whey protein. *Altern Med Rev* **9**, 136-156.
12. Steinrauf LK (1959) Preliminary X-ray data for some new crystalline forms of  $\beta$ -lactoglobulin and hen-egg-white lysozyme. *Acta Cryst* **12**, 77-79.
13. Aschaffenburg R, Green DW & Simmons RM (1965) Crystal forms of Beta-lactoglobulin. *J Mol Biol* **13**, 194-201.
14. Green DW, Aschaffenburg R, Camerman A, Coppola JC, Dunnill P, Simmons RM, Komorowski E S, Sawyer L, Turner EM & Woods KF (1979) Structure of bovine beta-lactoglobulin at 6A resolution. *J Mol Biol* **131**, 375-397.
15. Papiz MZ, Sawyer L, Eliopoulos EE, North AC, Findlay JB, Sivaprasadarao R, Jones TA, Newcomer ME & Kraulis PJ (1986) The structure of beta-lactoglobulin and its similarity to plasma retinol-binding protein. *Nature* **324**, 383-385.
16. Monaco HL, Zanotti G, Spadon P, Bolognesi M, Sawyer L & Eliopoulos EE (1987) Crystal structure of the trigonal form of bovine beta-lactoglobulin and of its complex with retinol at 2.5 A resolution. *J Mol Biol* **197**, 695-706.



17. Brownlow S, Morais Cabral JH, Cooper R, Flower DR, Yewdall SJ, Polikarpov I, North AC & Sawyer L (1997) Bovine beta-lactoglobulin at 1.8 Å resolution--still an enigmatic lipocalin. *Structure* **5**, 481-495.
18. Qin BY, Bewley MC, Creamer LK, Baker HM, Baker EN & Jameson GB (1998) Structural basis of the Tanford transition of bovine beta-lactoglobulin. *Biochemistry* **37**, 14014-14023.
19. Qin BY, Bewley MC, Creamer LK, Baker EN & Jameson GB (1999) Functional implications of structural differences between variants A and B of bovine beta-lactoglobulin. *Protein Sci* **8**, 75-83.
20. Oliveira KM, Valente-Mesquita VL, Botelho MM, Sawyer L, Ferreira ST & Polikarpov I (2001) Crystal structures of bovine beta-lactoglobulin in the orthorhombic space group C222(1). Structural differences between genetic variants A and B and features of the Tanford transition. *Eur J Biochem* **268**, 477-483.
21. Adams JJ, Anderson BF, Norris GE, Creamer LK & Jameson GB (2006) Structure of bovine beta-lactoglobulin (variant A) at very low ionic strength. *J Struct Biol* **154**, 246-254.
22. Sawyer L, Papiz MZ, North ACT & Eliopoulos EE (1985) Structure and function of bovine  $\beta$ -lactoglobulin. *Biochem Soc Trans* **13**, 265-266.

23. Newcomer ME, Jones TA, Aqvist J, Sundelin J, Eriksson U, Rask L & Peterson PA (1984) The three-dimensional structure of retinol-binding protein. *EMBO J* **3**, 1451-1454.
24. Redl B (2000) Human tear lipocalin. *Biochim Biophys Acta* **1482**, 241-248.
25. Kuwata K, Hoshino M, Forge V, Era S, Batt CA & Goto Y (1999) Solution structure and dynamics of bovine beta-lactoglobulin A. *Protein Sci* **8**, 2541-2545.
26. Uhrinova S, Smith MH, Jameson GB, Uhrin D, Sawyer L & Barlow PN (2000) Structural changes accompanying pH-induced dissociation of the beta-lactoglobulin dimer. *Biochemistry* **39**, 3565-3574.
27. Qin BY, Creamer LK, Baker EN & Jameson GB (1998) 12-Bromododecanoic acid binds inside the calyx of bovine beta-lactoglobulin. *FEBS Lett* **438**, 272-278.
28. Wu SY, Perez MD, Puyol P & Sawyer L (1999) beta-lactoglobulin binds palmitate within its central cavity. *J Biol Chem* **274**, 170-174.
29. Kontopidis G, Holt C & Sawyer L (2002) The ligand-binding site of bovine beta-lactoglobulin: evidence for a function. *J Mol Biol* **318**, 1043-1055.
30. Dufour E, Genot C & Haertle T (1994) beta-Lactoglobulin binding properties during its folding changes studied by fluorescence spectroscopy. *Biochim Biophys Acta* **1205**, 105-112.
31. Wang Q, Allen JC & Swaisgood HE (1997) Binding of vitamin D and cholesterol to beta-lactoglobulin. *J Dairy Sci* **80**, 1054-1059.

32. Wang Q, Allen JC & Swaisgood HE (1997) Binding of retinoids to beta-lactoglobulin isolated by bioselective adsorption. *J Dairy Sci* **80**, 1047-1053.
33. Wang Q, Allen JC & Swaisgood HE (1998) Protein concentration dependence of palmitate binding to beta-lactoglobulin. *J Dairy Sci* **81**, 76–81.
34. Wang Q, Allen JC & Swaisgood HE (1999) Binding of lipophilic nutrients to beta-lactoglobulin prepared by bioselective adsorption. *J Dairy Sci* **82**, 257-264.
35. Muresan S, van der Bent A & de Wolf FA (2001) Interaction of beta-lactoglobulin with small hydrophobic ligands as monitored by fluorometry and equilibrium dialysis: nonlinear quenching effects related to protein--protein association. *J Agric Food Chem* **49**, 2609-2618.
36. Fessas D, Iametti S, Schiraldi A & Bonomi F (2001) Thermal unfolding of monomeric and dimeric beta-lactoglobulins. *Eur J Biochem* **268**, 5439-5448.
37. Cogan U, Kopelman M, Mokady S & Shinitzky M (1976) Binding affinities of retinol and related compounds to retinol binding proteins. *Eur J Biochem* **65**, 71-78.
38. Tseng CF, Lin CC, Huang HY, Liu HC & Mao SJT (2004) Antioxidant role of human haptoglobin. *Proteomics* **4**, 2221-2228.
39. Otwinowski Z & Minor W (1997) Processing of X-ray Diffraction Data Collected in Oscillation Mode. *Methods Enzymol* **276**, 307-326.
40. Rossmann MG (1990) The molecular replacement method. *Acta Crystallogr A* **46**, 73-82.

41. Brunger AT, Adams PD, Clore GM, DeLano WL, Gros P, Grosse-Kunstleve RW, Jiang JS, Kuszewski J, Nilges M, Pannu NS, Read RJ, Rice LM, Simonson T & Warren GL (1998) Crystallography & NMR system: A new software suite for macromolecular structure determination. *Acta Crystallogr D Biol Crystallogr* **54**, 905-921.
42. Jones TA, Zou JY, Cowan SW & Kjeldgaard M (1991) Improved methods for building protein models in electron density maps and the location of errors in these models. *Acta Crystallogr A* **47**, 110-119.
43. Lee SC, Guan HH, Wang CH, Huang WN, Tjong SC, Chen CJ & Wu WG (2005) Structural basis of citrate-dependent and heparan sulfate-mediated cell surface retention of cobra cardiotoxin A3. *J Biol Chem* **280**, 9567-9577.
44. Covarrubias AS, Bergfors T, Jones TA & Hogbom M (2006) Structural mechanics of the pH-dependent activity of beta-carbonic anhydrase from *Mycobacterium tuberculosis*, *J Biol Chem* **281**, 4993-4999.
45. Brünger AT (1992) Free *R* value: a novel statistical quantity for assessing the accuracy of crystal structures. *Nature* **355**, 472-475.
46. Laskowski RA, MacArthur MW, Moss DS & Thornton JM (1993) PROCHECK: A program to check the stereochemical quality of protein structures. *J Appl Cryst* **26**, 283-291.

47. Engh RA & Huber R (1991) Accurate bond and angle parameters for X-ray protein structure refinement. *Acta Cryst A* **47**, 392-400.
48. Ramachandran GN & Sasisekharan V (1968) Conformation of polypeptides and proteins. *Adv Protein Chem* **23**, 283-438.
49. Said HM, Ong DE & Shingleton JL (1989) Intestinal uptake of retinol: enhancement by bovine milk beta-lactoglobulin. *Am J Clin Nutr* **49**, 690-694.
50. Kushibiki S, Hodate K, Kurisaki J, Shingu H, Ueda Y, Watanabe A & Shinoda M (2001) Effect of beta-lactoglobulin on plasma retinol and triglyceride concentrations, and fatty acid composition in calves. *J Dairy Res* **68**, 579-586.
51. Vieth R (2001) Vitamin D nutrition and its potential health benefits for bone, cancer and other conditions. *J Nutr Environ Med* **11**, 275-291.
52. Chapuy MC, Arlot ME, Duboeuf F, Brun J, Crouzet B, Arnaud S, Delmas PD & Meunier PJ (1992) Vitamin D<sub>3</sub> and calcium to prevent hip fractures in the elderly women. *N Engl J Med* **327**, 1637-1642.
53. McKenna MJ, Freaney R, Byrne P, McBrinn Y, Murray B, Kelly M, Donne B & O'Brien M (1995) Safety and efficacy of increasing wintertime vitamin D and calcium intake by milk fortification. *QJM* **88**, 895-898.

54. Ragona L, Fogolari F, Catalano M, Ugolini R, Zetta L & Molinari H (2003) EF loop conformational change triggers ligand binding in beta-lactoglobulins. *J Biol Chem* **278**, 38840-38846.
55. Yang J, Powers JR, Clark S, Dunker AK & Swanson BG (2002) Hydrophobic probe binding of beta-lactoglobulin in the native and molten globule state induced by high pressure as affected by pH, KIO(3) and N-ethylmaleimide. *J Agric Food Chem* **50**, 5207-5214.
56. Makinen-Kiljunen S & Palosuo T (1992) A sensitive enzyme-linked immunosorbent assay for determination of bovine beta-lactoglobulin in infant feeding formulas and in human milk. *Allergy* **47**, 347-352.
57. Lovegrove JA, Osman DL, Morgan JB & Hampton SM (1993) Transfer of cow's milk beta-lactoglobulin to human serum after a milk load: a pilot study. *Gut* **34**, 203-207.
58. Saito H, Dhanasekaran P, Nguyen D, Holvoet P, Lund-Katz S & Phillips MC (2003) Domain structure and lipid interaction in human apolipoproteins A-I and E, a general model. *J Biol Chem* **278**, 23227-23232.
59. Perez MD, Diaz de Villegas C, Sanchez L, Aranda P, Ena JM & Calvo M (1989) Interaction of fatty acids with beta-lactoglobulin and albumin from ruminant milk. *J Biochem* **106**, 1094-1097.



## Figure legends

**Figure 1.** Amino acid sequence of LG and chemical structure of its binding ligands. (A) LG is consisted of 162 amino acids with nine  $\beta$ -sheet strands (A-I) and one  $\alpha$ -helix at the COOH-terminus. There are two disulfide linkages located between strand D and COOH-terminus (Cys66 and Cys160) and between strands G and H (Cys106 and Cys119), with a free buried thio-group at Cys121.  $\alpha$ -helix with three turns is located between residues 130 and 141 (in light gray). (B) Chemical structure of retinol, palmitic acid, and vitamin D<sub>3</sub>.

**Figure 2.** Binding ratio of LG with ligands. (A) Titration experiment for binding of LG to retinol measured at 470 nm with excitation at 287 nm (pH 8.0). Binding was determined by the enhancement of extrinsic fluorescence of retinol. (B, C) Titration experiment for binding of LG to palmitate and vitamin D<sub>3</sub> measured at 332 nm with excitation at 287 nm (pH 8.0). Binding was determined by the fluorescence enhancement (palmitate) and quenching (vitamin D<sub>3</sub>) of intrinsic fluorescence of LG. The maximal binding ratio of vitamin D<sub>3</sub> to LG is 2:1.

Right panels:  $P_T$  = Total protein concentration,  $R_T$  = Total ligand concentration, and  $a$  = Fraction of unoccupied ligand sites on the protein. Each point represents the mean of triplicate determinations with an average of standard deviation (SD) less than 5-8% of the mean.

**Figure 3.** Effect of pH (Tanford transition) on LG binding with ligands. (A) Emission fluorescence of retinol. (B) Enhanced fluorescence of LG upon the binding of palmitate.

(C) Quenched intrinsic fluorescence of LG upon the binding of vitamin D<sub>3</sub>. All the measurements are identical to that described in Figure 2. Each point represents the mean of triplicate determinations  $\pm$  SD.

**Figure 4.** Effect of heating on LG binding with ligands. (A-C) LG was heated between 50 and 100 °C for 15 s to 16 min before the addition of retinol, palmitate, and vitamin D<sub>3</sub>. (D) Titration curve of heated LG (100 °C for 16 min) with vitamin D<sub>3</sub>. Only vitamin D<sub>3</sub>, but not retinol and palmitate, was able to bind denatured LG with a molar ratio of ~1:1. The data suggest that there is another thermally independent vitamin D<sub>3</sub> binding site, which is remote from the calyx pocket. Each point in panels A-C represents the mean of triplicate determinations  $\pm$  SD. While, each point in panel D represents the mean of triplicate determinations with a SD less than 5-8% of the mean.

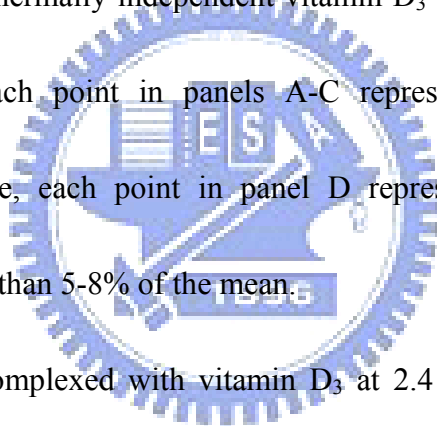


**Figure 5.** Structure of LG complexed with vitamin D<sub>3</sub> at 2.4 Å resolution. Space-filling drawing of LG-vitamin D<sub>3</sub> complex. Vitamin D<sub>3</sub> (colored in yellow) and LG are drawn based on our final refined model with carbon, oxygen, and nitrogen atoms depicted in gray, red, and blue, respectively. Sulfur molecules (in orange) are buried inside at this face. It demonstrates that there are two distinct vitamin D<sub>3</sub> binding sites on each LG molecule. One is penetrated inside the calyx (left) and the other is lying on the surface between the  $\alpha$ -helix and  $\beta$ -strand I at the COOH-terminus (residues 136-149) (right).

**Figure 6.** Electron density map around the calyx and the exosite of vitamin D<sub>3</sub>-LG complex at

2.4 Å resolution. Final refined model together with the  $2|F_{obs} - F_{calc}|$  electron density show that the bulk of the electron density is sufficient to cover a vitamin D<sub>3</sub> molecule, both in the calyx (top) and the exosite (bottom). In the central calyx binding mode, the aliphatic tail of vitamin D<sub>3</sub> clearly inserts into the binding cavity, where the 3-OH group of vitamin D<sub>3</sub> binds externally. In exosite binding mode, vitamin D<sub>3</sub> interacts mostly with the hydrophobic moiety of the pocket.

**Figure 7.** Superimposed structure of the calyx before and after binding of vitamin D<sub>3</sub> and a diagram showing their contacts less than 3.8 Å. (A) Superimposing the current model for vitamin D<sub>3</sub>-LG (colored in gray) with previously described native LG (in red) (PDB code 1BSQ) in the calyx shows that there is a significant repositioning of Glu62 and Met107 to make room for the ligand into the calyx. Notably, vitamin D<sub>3</sub> binding has resulted in a local conformational change by opening the EF loop as shown in a dotted circle (residues 85-89). Such conformational change in the loop is similar to the binding of retinol (data not shown).

(B) The calyx of LG offers mainly hydrophobic interactions to vitamin D<sub>3</sub> binding (less than 3.8 Å). The shortest distance, 2.97 Å, is the hydrogen bond between the 3-OH group of vitamin D<sub>3</sub> and Lys-60 (dotted red).

**Figure 8.** Superimposed structure of the exosite before and after binding of vitamin D<sub>3</sub> and a diagram showing their contacts of less than 3.8 Å. (A) Superimposing the current model for vitamin D<sub>3</sub>-LG (colored in gray) with previously described native LG (in red) (PDB code

1BSQ) in the exosite reveals that the overall conformation is not substantially changed upon the binding of vitamin D<sub>3</sub>. (B) The exosite is near the surface of C-terminal  $\alpha$ -helix and  $\beta$ -strand I, where the 3-OH group of vitamin D<sub>3</sub> does not apparently form hydrogen bonding with LG.

**Figure 9.** Amphipathic helix of LG and its interaction with vitamin D<sub>3</sub>. (A) The only  $\alpha$ -helix region of LG is located between residues 130 and 141 (Figure 1). Most interestingly, the  $\alpha$ -helix is oriented as amphipathic with all the charged residues clustered on one side without an exception. (B) The crystal structure reveals that the hydrophobic side of the  $\alpha$ -helix forms a stable hydrophobic pocket with  $\beta$ -strand I. They are linked by a hydrophobic loop (residues 142-145) and thus facilitate the binding to vitamin D<sub>3</sub>. The stereo view shows that part of vitamin D<sub>3</sub> is near the surface, particularly for the aliphatic tail, which is consistent with that depicted in Figure 5.

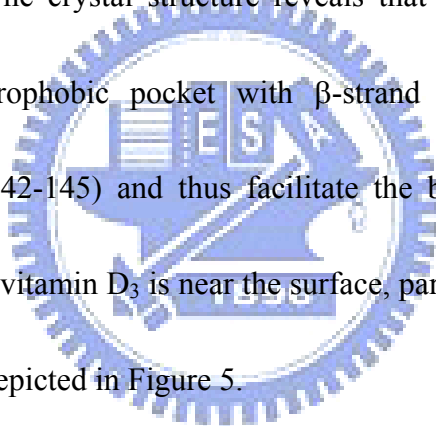


**Figure 10.** Circular dichroic spectra of native and heated LG. LG preheated between 50 and 100 °C for 16 min was recorded by circular dichroism at a final concentration of 0.2 mg/mL. The  $\beta$ -structure of LG underwent disordering upon continuous heating as significant changes of ellipticity at 205-208 nm occurred above 80 °C. The negative ellipticity at 222 nm, commonly a criterion for  $\alpha$ -helical structure, was identical between native and heated LG.

**Table 1.** Apparent dissociation constants and binding ratio for binding ligands to native or heated LG

<b>Ligand</b>	<b>Binding ratio (ligand / LG)</b>	<b><math>K_d^{app}</math></b> ( $10^{-9}$ M)
	$\bar{X} \pm SD$	$\bar{X} \pm SD$
Retinol with native LG	$0.908 \pm 0.089$	$17.28 \pm 1.62$
Palmitate with native LG	$0.801 \pm 0.072$	$44.03 \pm 4.56$
Vitamin D <sub>3</sub> with		
native LG	$1.761 \pm 0.121$	$4.74 \pm 0.37$
heated LG	$0.835 \pm 0.054$	$45.67 \pm 3.12$

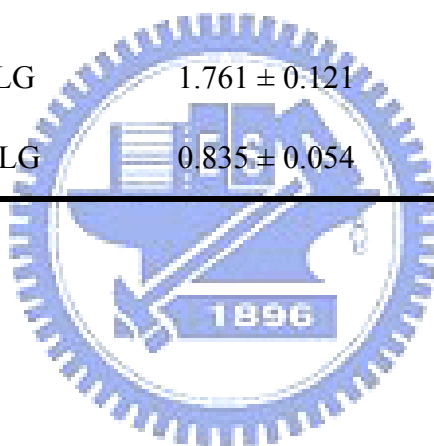


**Table 2.** Data collection and refinement statistics of LG-vitamin D<sub>3</sub> complex

<b>Data collection</b>	
Space group	<i>P</i> 3 <sub>2</sub> 21
Cell dimensions	
<i>a</i> , <i>b</i> , <i>c</i> (Å)	53.780, 53.780, 111.573
$\alpha$ , $\beta$ , $\gamma$ (°)	90, 90, 120
Resolution (Å)	30-2.4 (2.49-2.4)
<i>R</i> <sub>sym</sub>	0.034 (0.226)
$\langle I / \sigma I \rangle$	43.3 (10.3)
Completeness (%)	98.5% (99.5%)
Redundancy	7.0
<b>Refinement</b>	
Resolution (Å)	15-2.4
No. of unique reflections	7422
<i>R</i> <sub>work</sub> / <i>R</i> <sub>free</sub>	23.86% / 26.12%
No. of atoms	
Protein	1272
Ligand	56
Water	38
<i>B</i> -factors	
Protein	55.02
Ligand in calyx / exosite	39.19 / 46.90
Water	52.47
R.m.s deviations	
Bond lengths (Å)	0.007
Bond angles (°)	1.264

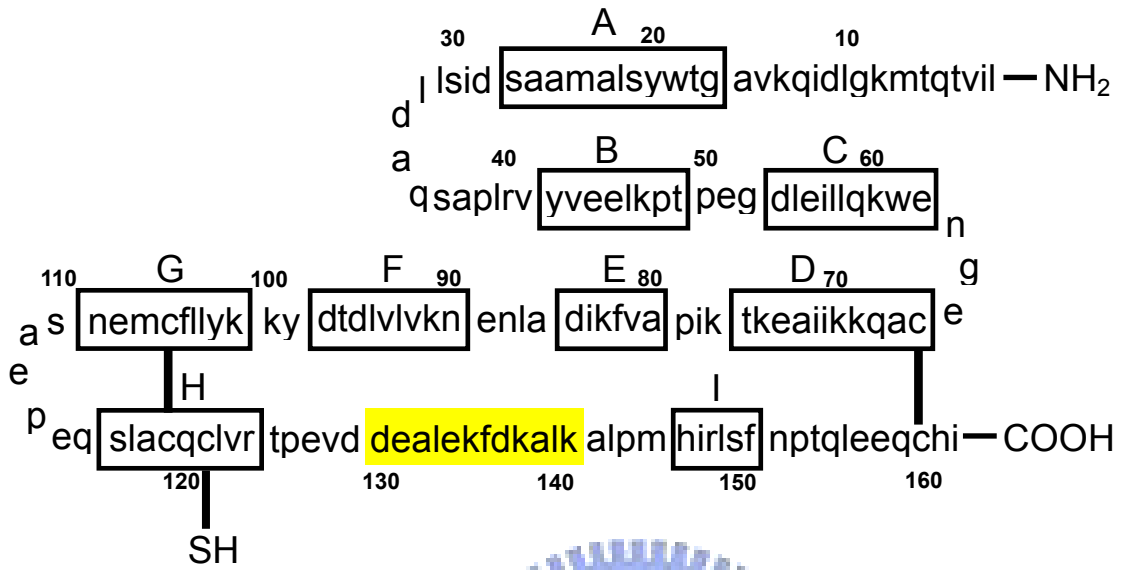
**Table 3.** Mean *B*-factor for LG complexes with ligands extracted from previously published papers.

Ligand	Retinol	Retinoic acid	Palmitate	Cholesterol	Vitamin D <sub>2</sub>	Mercury	12-Bromodecanoic acid
Mean <i>B</i> -factor for protein atoms (Å <sup>2</sup> )	56.1	48.8	54.2	44.5	57.27	50.0	41.3
Mean <i>B</i> -factor for ligand atoms (Å <sup>2</sup> )	65.0	66.8	58.4	69.9	72.6	53.5	52.1
Mean <i>B</i> -factor for water molecules (Å <sup>2</sup> )	67.4	59.0	68.1	53.0	56.9	55.9	72.6



**Figure 1**

**A**



**B**

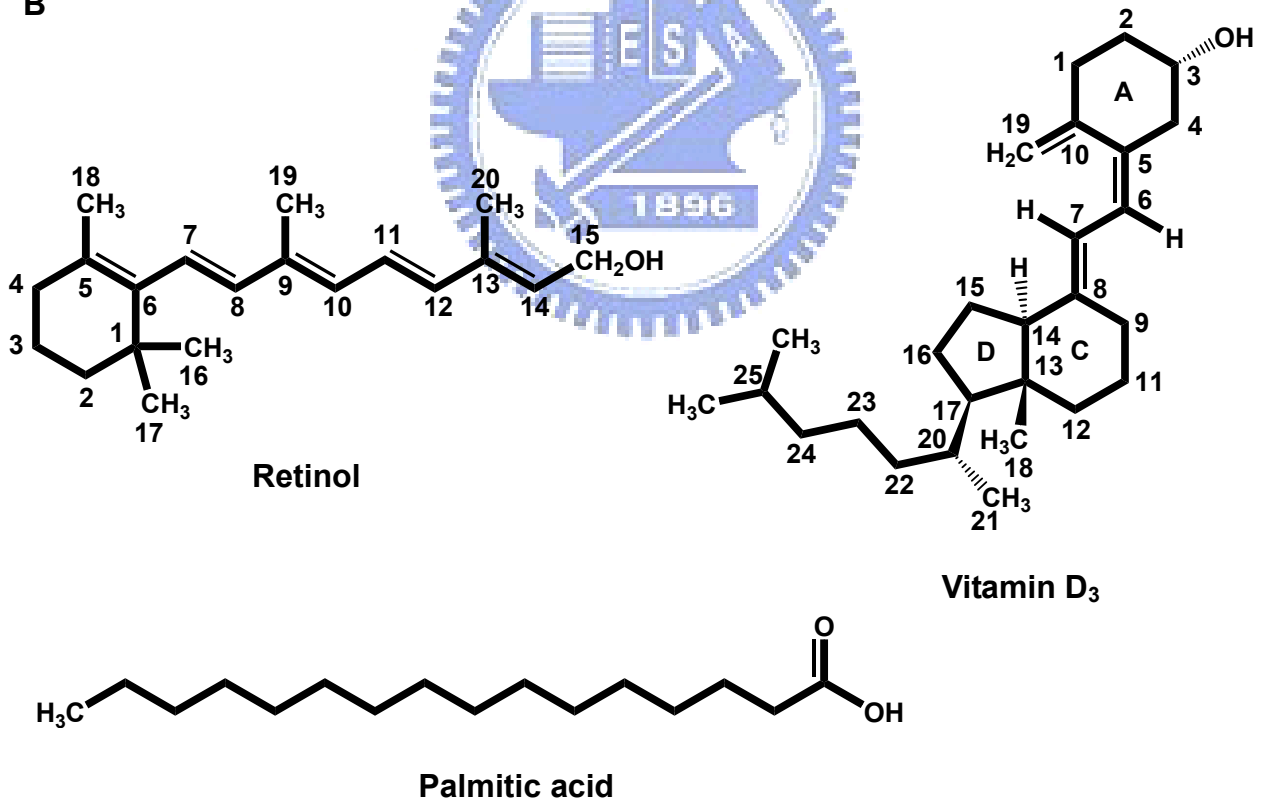




Figure 2

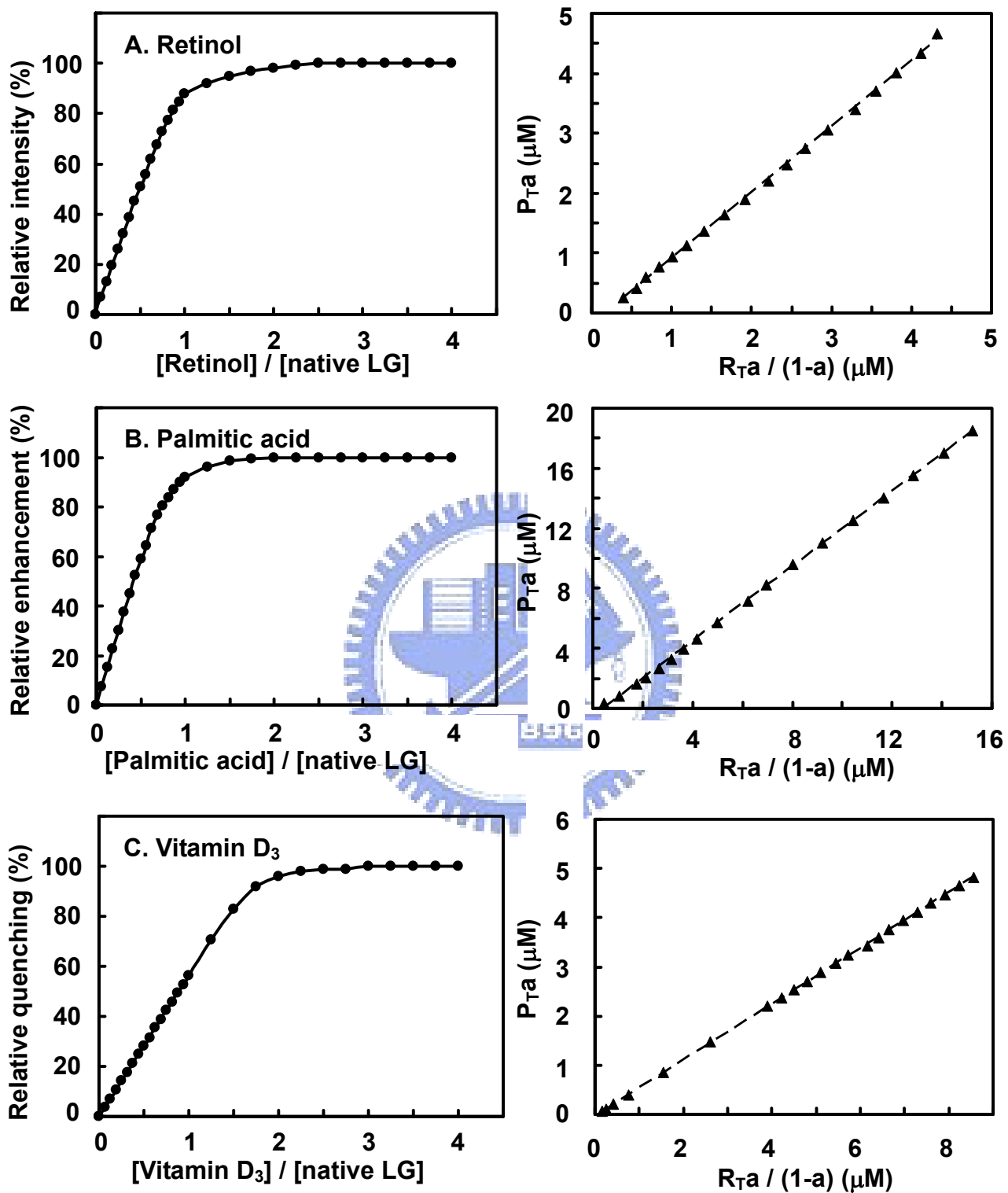


Figure 3

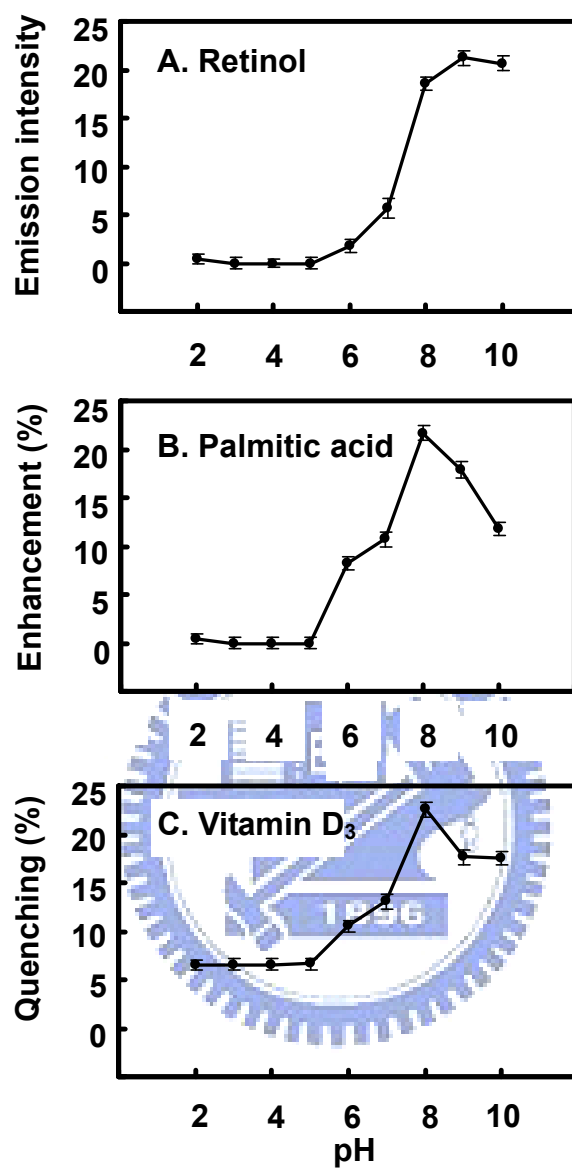
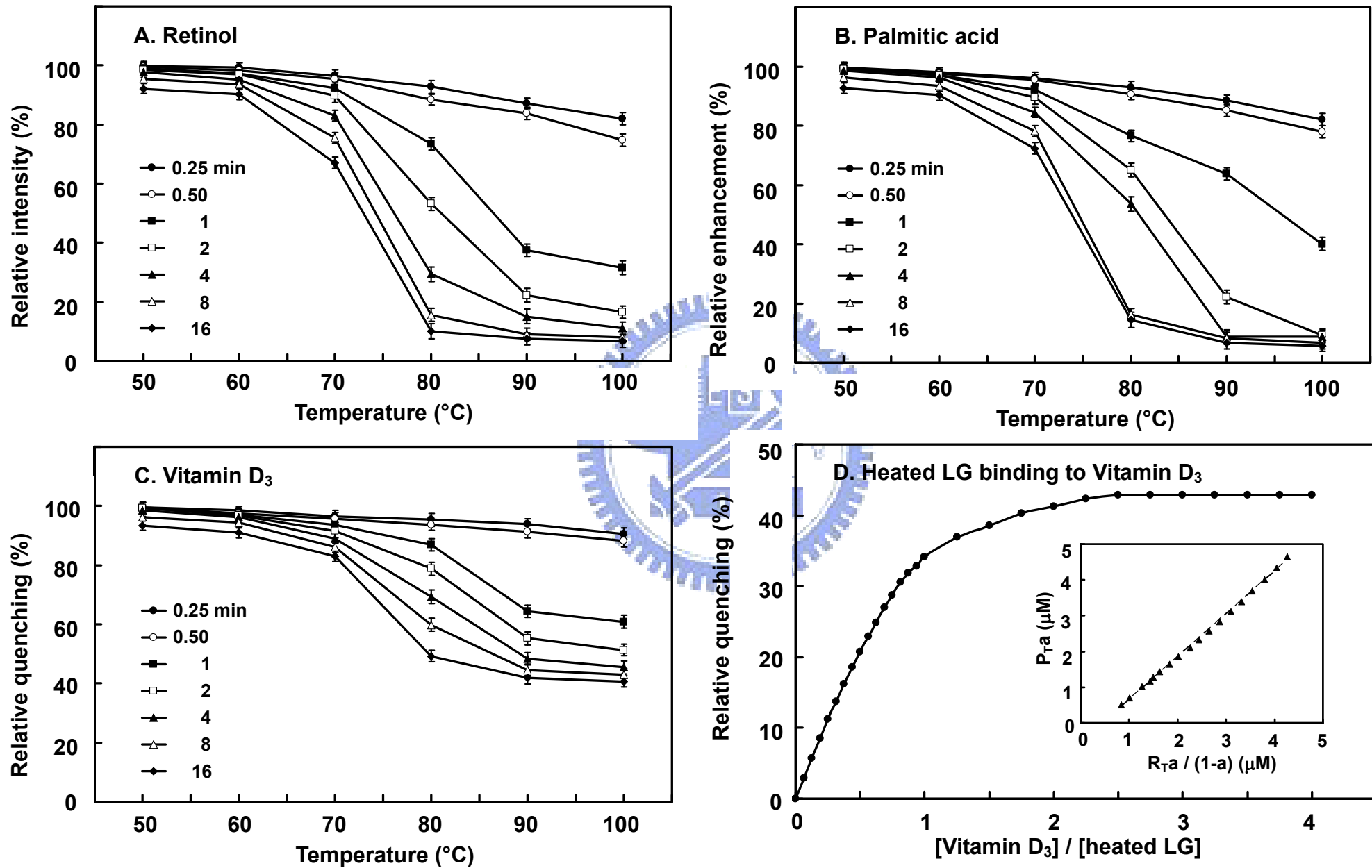


Figure 4



**Figure 5**

**Space-filling model**

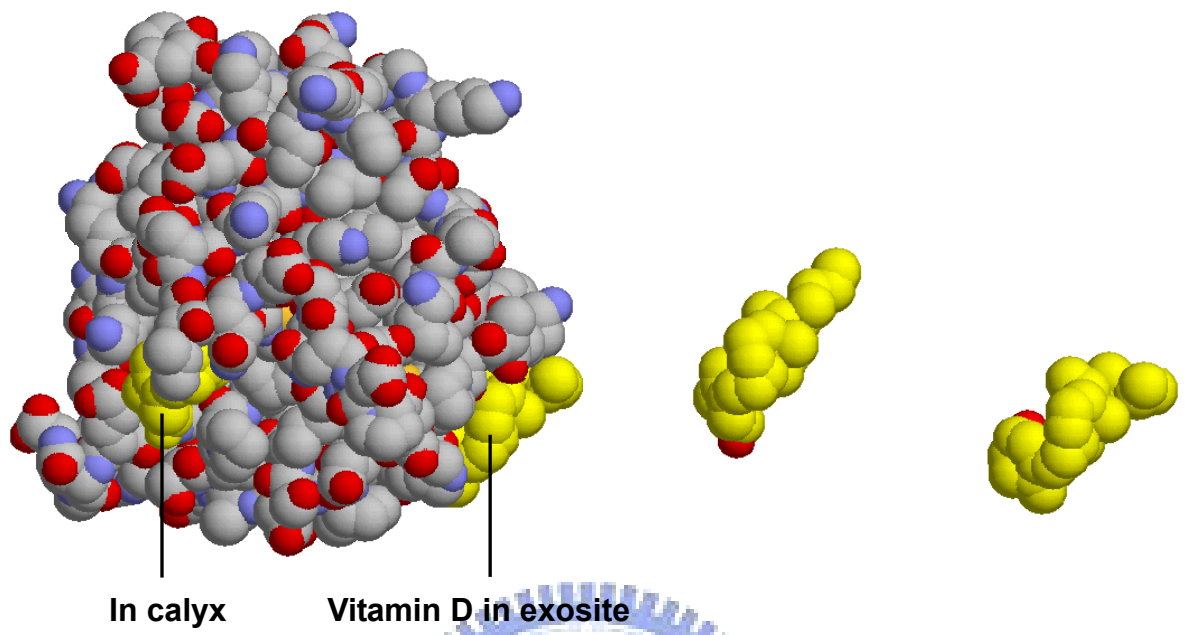


Figure 6

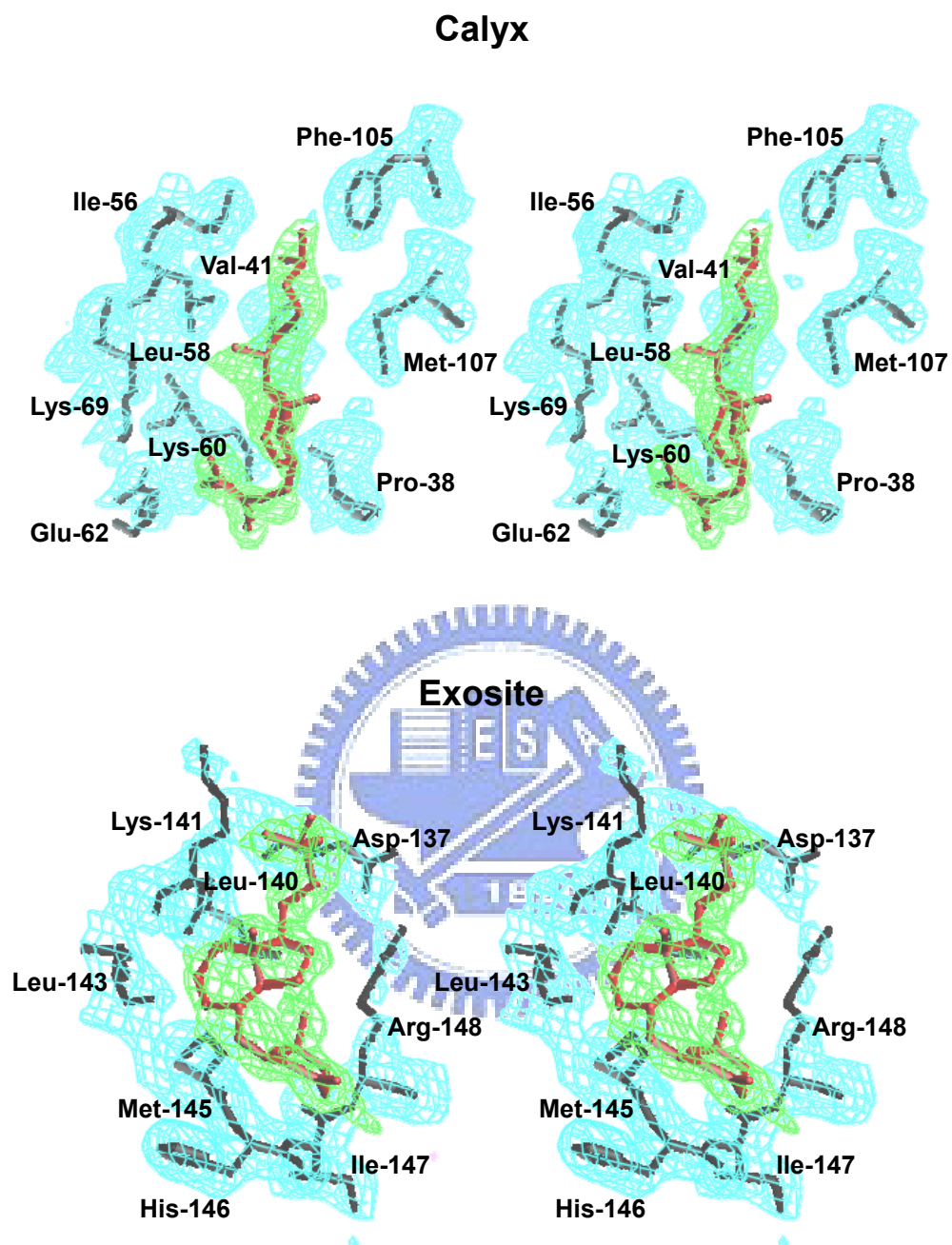
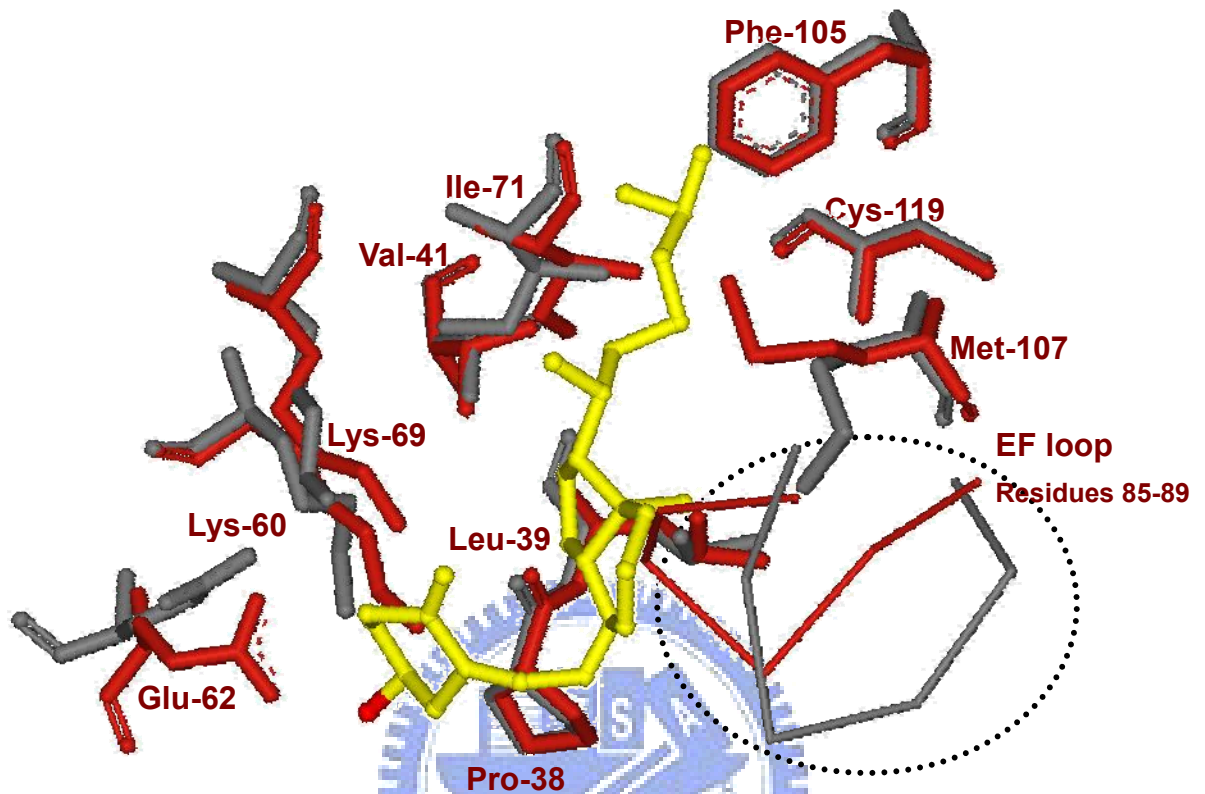


Figure 7

A. Calyx with and without vitamin D<sub>3</sub>



B. Interaction distance

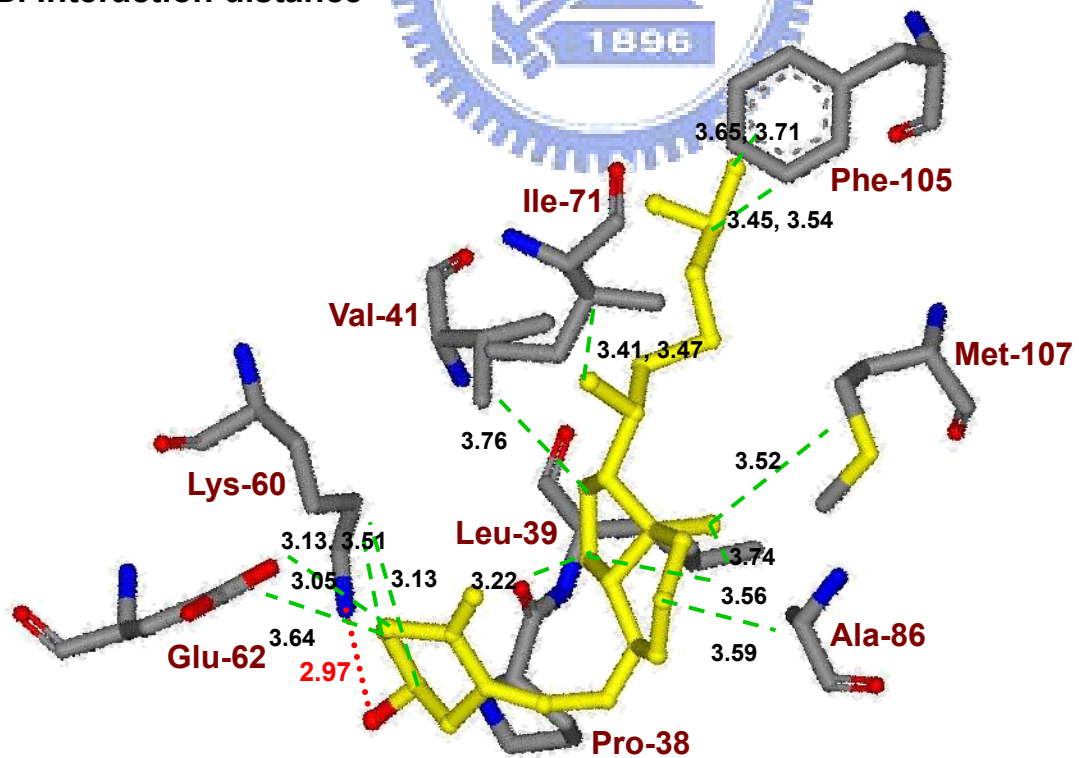
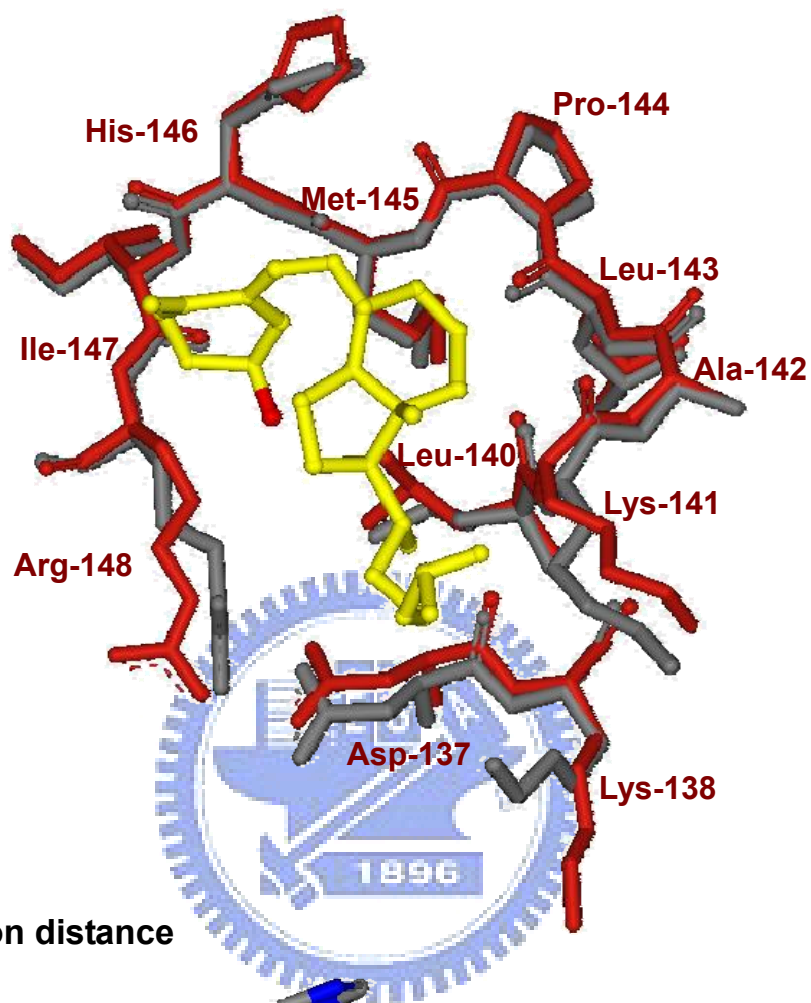


Figure 8

A. Exosite with and without vitamin D<sub>3</sub>



B. Interaction distance

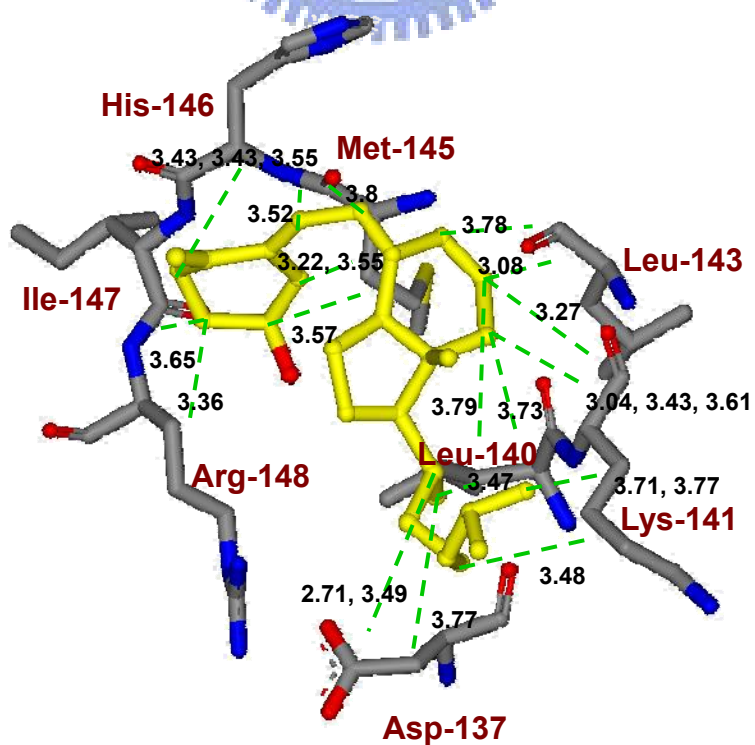
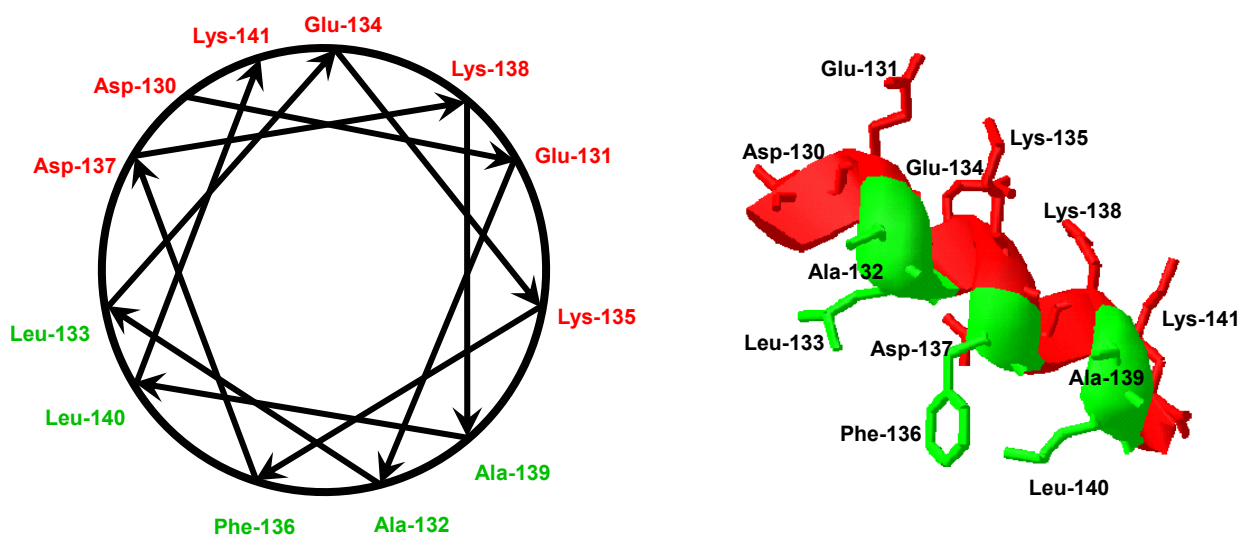




Figure 9

A. Amphipathic  $\alpha$ -helix



B. Stereo view of vitamin D<sub>3</sub>-exosite complex

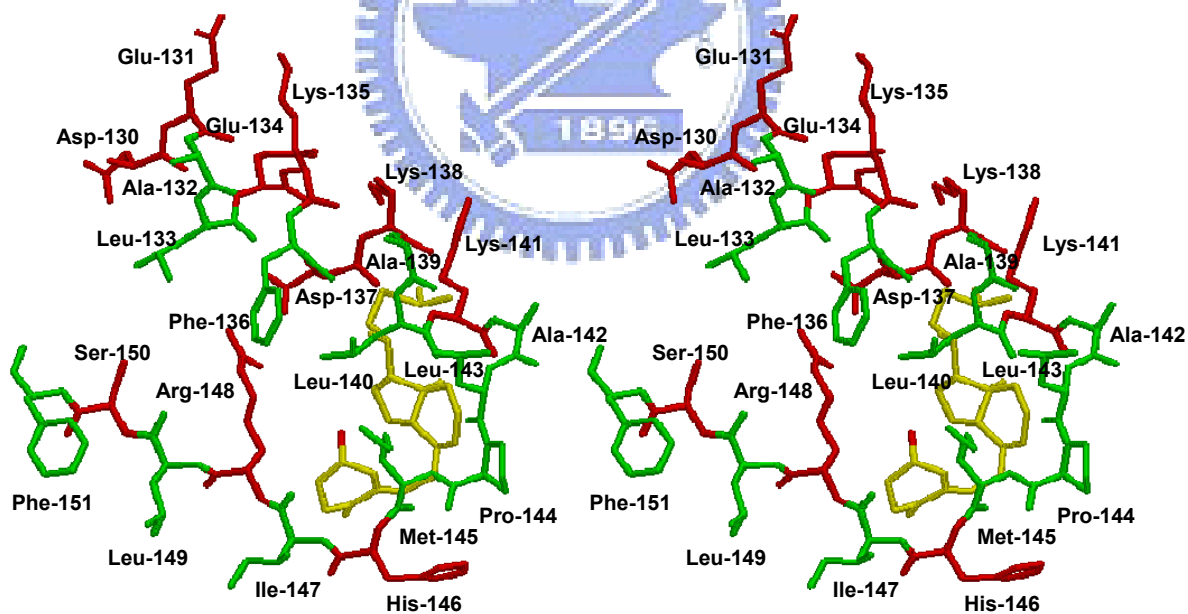
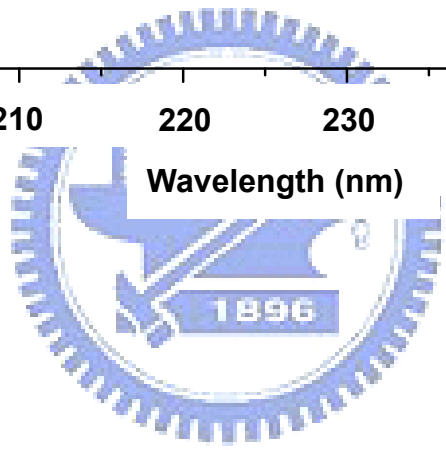
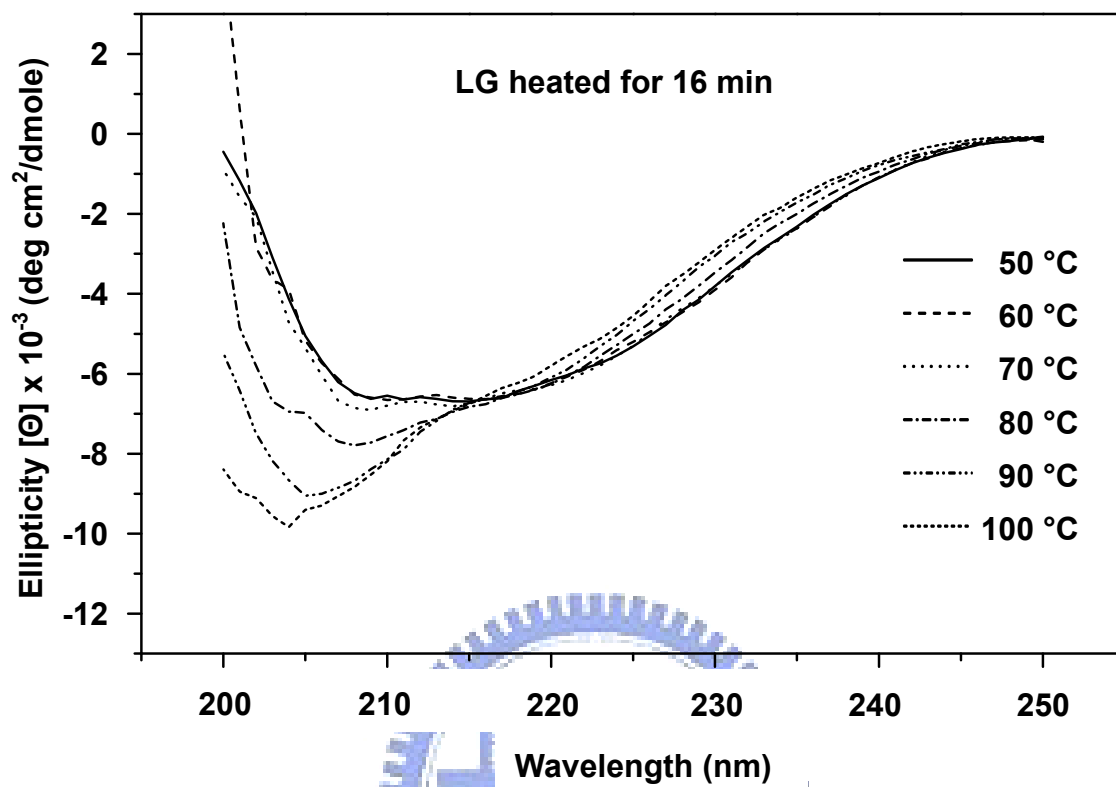




Figure 10



Section 2: Rational design for crystallization of  
LG-vitamin D complex (Crystal Growth & Design)

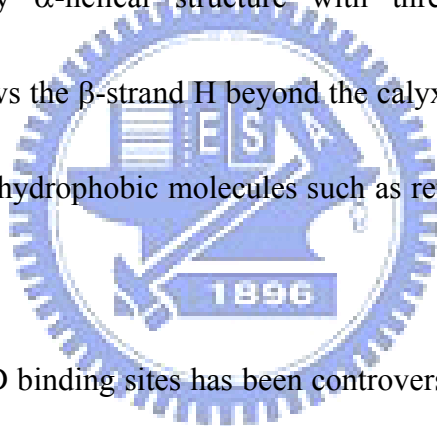


## Abstract

$\beta$ -Lactoglobulin (LG) is a major milk whey protein containing primarily a calyx for vitamin D<sub>3</sub> binding, although the existence of another site beyond the calyx is controversial. Using fluorescence spectral analyses in the previous study, we showed the binding stoichiometry for vitamin D<sub>3</sub> to LG to be 2:1 and a stoichiometry of 1:1 when the calyx was “disrupted” by manipulating the pH and temperature, suggesting that a secondary vitamin D binding site existed. To help localize this secondary site using X-ray crystallography in the present study, we used bioinformatic programs (Insight II, Q-SiteFinder, and GEMDOCK) to identify the potential location of this site. We then optimized the occupancy and enhanced the electron density of vitamin D<sub>3</sub> in the complex by altering the pH and initial ratios of vitamin D<sub>3</sub>/LG in the cocrystal preparation. We conclude that GEMDOCK can aid in searching for an extra density map around potential vitamin D binding sites. Both pH (8) and initial ratio of vitamin D<sub>3</sub>/LG (3:1) are crucial to optimize the occupancy and enhance the electron density of vitamin D<sub>3</sub> in the complex for rational-designed crystallization. The strategy in practice may be useful for future identification of a ligand-binding site in a given protein.

## Introduction

Bovine  $\beta$ -lactoglobulin (LG) is a major protein in milk comprising about 10–15%.<sup>1</sup> Because of its thermally unstable and molten-globule nature, LG has been studied extensively for its physical and biochemical properties.<sup>2-7</sup> Some essential functions of LG including hypocholesterolemic effect,<sup>8</sup> retinol transport,<sup>9,10</sup> and antioxidant activity<sup>11-14</sup> have been reported. According to the crystal structure, LG comprises predominantly a  $\beta$ -sheet configuration containing nine antiparallel  $\beta$ -strands from A to I (Figure 1A).<sup>15-17</sup> Topographically,  $\beta$ -strands A-D form one surface of the barrel (calyx), whereas  $\beta$ -strands E-H form the other. The only  $\alpha$ -helical structure with three turns is located at the COOH-terminus, which follows the  $\beta$ -strand H beyond the calyx.<sup>18</sup> A remarkable feature of the calyx is its ability to bind hydrophobic molecules such as retinol, fatty acids, and vitamin D<sub>3</sub> (Figure 1B).<sup>19-22</sup>

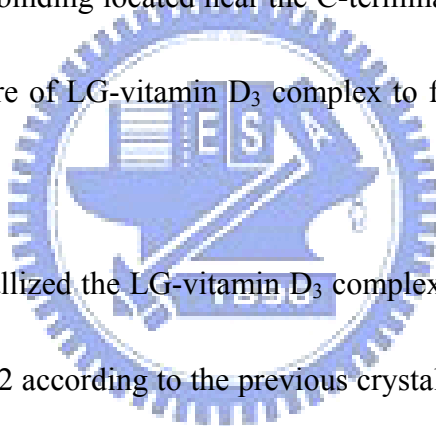


The location of vitamin D binding sites has been controversial, yet most evidence points toward the calyx. It has been postulated that another site exists,<sup>23-25</sup> but it could not be verified by the crystal structure using the vitamin D<sub>2</sub>-LG complex.<sup>10</sup> In a previous study, we first conducted a ligand binding assay using the fluorescence changes by retinol, palmitic acid, and vitamin D<sub>3</sub> to address the existence of another site for vitamin D binding. This data demonstrated that the maximal binding stoichiometry of vitamin D<sub>3</sub> with LG was 2:1, whereas that of retinol or palmitic acid was 1:1 (Table 1),<sup>26</sup> suggesting that there was another binding site for the vitamin D<sub>3</sub> molecule. Second, we manipulated the binding capability by

switching off the gate of calyx at low pH (2-6)<sup>15</sup> to further substantiate the “two site hypothesis”. As expected, the binding capability of retinol and palmitic acid diminished under this condition, but it retained the vitamin D binding with a vitamin D<sub>3</sub> to LG stoichiometry of 1:1 (Table 1).<sup>26</sup> We also used a strategy to denature the conformation of the calyx by heat treatment<sup>7</sup> and conducted the binding assay after the calyx was thermally “disrupted”. Under this condition, the binding stoichiometry of vitamin D<sub>3</sub> to heated LG (100 °C for 16 min) was found to be 1:1 (Table 1).<sup>26</sup> These previous binding experiments<sup>26</sup> suggest that there is a secondary site for vitamin D<sub>3</sub> binding distinct from the calyx.

In the present study, we located the secondary vitamin D<sub>3</sub> binding site of LG, which has been a controversy among many researchers, using bioinformatic analysis to narrow the region of potential binding sites for crystallographic verification. We first utilized well-known programs (ActiveSite\_Search Insight II and Q-SiteFinder) to predict the ligand-binding site in search of a possible location for vitamin D binding with the geometric or energetic criteria. The Insight II<sup>27</sup> is based on the size of surface cavities of a given protein without a specified ligand; it searches the location and extent of the pocket according to the geometric criteria. The Q-SiteFinder,<sup>28</sup> however, defines a binding pocket only by energy calculations using a methyl probe for van der Waals interactions with a given protein. We next used a more accurate docking program, GEMDOCK, which was developed in our laboratories,<sup>29</sup> to dock a specific ligand with a given protein based on a nonbiased search for

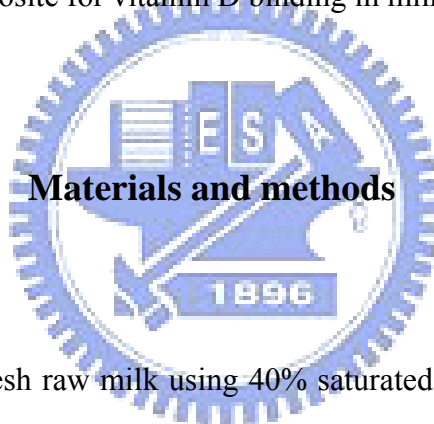
their interactions. GEMDOCK is specifically designed for a flexible ligand that may best fit into possible binding sites. Under this condition the docked ligand conformations are generated. All three programs require an established 3D structure of a given protein. We show that Insight II and Q-SiteFinder predicted three and six major potential regions, respectively, available for any nondefined ligand binding on LG. Docking using GEMDOCK predicted six possible sites for vitamin D<sub>3</sub> binding. Following the analyses of Insight II, Q-SiteFinder, and GEMDOCK cross-docking, we identified that there were two potential secondary sites for vitamin D binding located near the C-terminal  $\alpha$ -helical region. This led us to study the crystal structure of LG-vitamin D<sub>3</sub> complex to further identify the secondary vitamin D binding site, if any.



Furthermore, we cocrystallized the LG-vitamin D<sub>3</sub> complex which was prepared at pH 7 with a vitamin D<sub>3</sub>/LG ratio of 2 according to the previous crystallographic study.<sup>20</sup> A search for an extra electron density for vitamin D<sub>3</sub> around potential secondary binding sites was based on the predicted data obtained from bioinformatic analysis. We found a weak extra electron density that was located near the C-terminal  $\alpha$ -helical region. With respect to cocrystallization, the maximum occupancy of the ligand should provide a better opportunity in growing high-quality crystals of the ligand-protein complex. In general, the affinity, solubility, and concentrations of added hydrophobic ligands would influence the ligand

occupancy at equilibrium. For 90% occupancy, the amount of added ligands must be greater than the amount of protein so that the free ligands at equilibrium are not depleted.<sup>30</sup>

In this work, we reported a rationally designed approach for preparing the complex of LG and vitamin D<sub>3</sub> at various pH and vitamin D<sub>3</sub>/LG ratios to optimize the occupancy of vitamin D<sub>3</sub> and improve the electron density of the secondary binding site. Finally, we identified an exosite for vitamin D binding to be located near the  $\alpha$ -helix and  $\beta$ -strand I of LG using a crystal prepared at pH 8 with a vitamin D<sub>3</sub>/LG ratio of 3:1. The biological significance of the revealed exosite for vitamin D binding in milk LG was also discussed.



## Materials and methods

### Materials

LG was purified from fresh raw milk using 40% saturated ammonium-sulfate, followed by a G-150 column chromatography of the supernatant as described previously.<sup>4</sup> Vitamin D<sub>3</sub> (cholecalciferol) was purchased from Sigma (St. Louis, MO).

### Predicting possible binding site by ActiveSite\_Search Insight II and Q-SiteFinder

To identify the possible binding sites, the ActiveSite\_Search Insight II<sup>27</sup> and Q-SiteFinder<sup>28</sup> software were used, and the prediction was performed according to the standard protocol. For ActiveSite\_Search Insight II, we used the size within 50 Å as a cutoff site for the smallest cavity (in grid points). For Q-SiteFinder, the parameters for identified

protein residues involved in the van der Waals interactions with the methyl probe, 5.0 Å was used. The coordinates of possible sites predicted by Insight II and Q-SiteFinder were saved in PDB format and depicted using the Swiss-Pdb Viewer program.<sup>31</sup>

### **Docking analysis between ligands and LG by GEMDOCK**

We extrapolated the 3D structure of retinol (PDB ID 1GX8, LG-retinol complex), palmitic acid (1GXA, LG-palmitic acid complex), and vitamin D<sub>3</sub> (modified from 25(OH)-vitamin D<sub>3</sub>; 1MZ9, cartilage oligomeric matrix protein-vitamin D<sub>3</sub>) from the Protein Data Bank (PDB). Energy minimization of these three compounds was performed using a SYBYL program package. An established 3D structure of LG (1GX8) was used as the target for cross-docking. Since GEMDOCK is able to search the whole protein for exploring the binding site of a given ligand, we presumed those atoms near the charged surface and hydrophobic areas of LG were the potential binding sites for vitamin D<sub>3</sub>. The predicted area(s) was then compared with the established binding pocket (calyx) for palmitic acid and retinol. Following the removal of all structured water molecules in LG molecule, GEMDOCK search was then conducted according to the procedures previously described.<sup>29</sup> Using an empirical energy function which consists of the electrostatic, steric, and hydrogen bonding potentials for docking, GEMDOCK<sup>29</sup> seemed to be more accurate than some conventional approaches, such as GOLD and FlexX, based on a diverse data set of 100 protein-ligand complexes proposed by Jones *et al.*<sup>32</sup> The accuracy of GEMDOCK was



demonstrated when screening the ligand database for antagonist and agonist ligands of the estrogen receptor (ER).<sup>33</sup>

In this work, we used an empirical scoring function to estimate interaction energies between LG and ligands. The parameters used in the flexible docking included the initial step size ( $\sigma = 0.8$  and  $\psi = 0.2$ ), family competition length ( $L = 2$ ), population size ( $N = 1000$ ), and recombination probability ( $p_c = 0.3$ ). For each docked ligand, optimization was stopped when either the convergence was below a certain threshold value or the iterations exceeded the maximal preset value of 80. Therefore, GEMDOCK produced 3600 solutions in one generation and terminated when it exhausted to 324 000 solutions for each docked ligand.

### **Crystallization**

Purified LG was concentrated to 20 mg/mL in 20 mM acetate (pH 4), cacodylate (pH 6), HEPES (pH 7), or Tris buffer (pH 8). Vitamin D<sub>3</sub> stock solution prepared as 50 mM in 100% ethanol was added to LG solution to give a molar ratio of 3:1, 2:1, or 1:1 with a final ethanol concentration less than 7% and incubation for three hours at 37 °C. Crystallization of the LG-vitamin D<sub>3</sub> complex was achieved using the hanging-drop vapor-diffusion method at 18 °C with 2  $\mu$ L hanging drops containing equal amounts of LG-vitamin D<sub>3</sub> complex and a reservoir solution (0.1 M HEPES containing 1.4 M trisodium citrate dehydrate, pH 7.5).

### **Crystallographic data collection and processing**

The crystals were mounted on a Cryoloop (0.1-0.2 mm), dipped briefly in 20% glycerol as a cryoprotectant solution, and frozen in liquid nitrogen. X-ray diffraction data at 2.1-2.2 Å resolution were collected at 110 K using synchrotron radiation on the Taiwan contracted beamlines BL12B2 at SPring-8 (Harima, Japan) and BL13B at NSRRC (Hsinchu, Taiwan). The data were indexed and processed using a *HKL2000* program.<sup>34</sup>

## Results and discussion

Although a secondary vitamin D binding site of LG has been proposed from some physicochemical experiments,<sup>23-25, 35, 36</sup> its existence and location have remained elusive and controversial. Several studies have clearly demonstrated that the binding stoichiometry between retinol or palmitic acid and LG is 1 where the central calyx of LG is responsible for retinol and palmitic acid binding,<sup>21-23</sup> but whether the binding of vitamin D to LG is 1 or 2 remains uncertain. Wang *et al.* proposed that LG possesses two potential binding sites for vitamin D: one is in the calyx formed by a  $\beta$ -barrel and the other is near an external hydrophobic pocket between the  $\alpha$ -helix and the  $\beta$ -barrel.<sup>24, 25</sup> In the previous study, we first showed that the relative binding of vitamin D to LG was 56% of the maximal binding at a vitamin D<sub>3</sub>/LG ratio of 1:1 and the binding stoichiometry of vitamin D<sub>3</sub> to LG was 2:1 relative to that 1:1 of retinol or palmitic acid verified using extrinsic fluorescence emission, fluorescence enhancement and quenching methods (Table 1).<sup>26</sup> Our previous data tended to

support the view that LG comprises two vitamin D binding sites. Second, we monitored the vitamin D<sub>3</sub> binding of LG by utilizing a unique structural change property of LG at various pH to further substantiate the “two site hypothesis”. The EF loop of LG is known to act as a gate over the calyx;<sup>15</sup> at pH values lower than 6 the loop is in a “closed” position. Of remarkable interest, LG still retained about 30% of the maximal binding for vitamin D<sub>3</sub> at pH below the transition (2-6) (Table 1).<sup>26</sup> It suggested that there might be another vitamin D binding site that is independent of pH. Our previous study has shown that thermally denatured LG (heated 100 °C for 5 min) is unable to bind to retinol and palmitic acid owing to the deterioration of the calyx.<sup>7</sup> We tested the hypothesis whether the “secondary binding site” for vitamin D (if any) still existed after heating. Since LG is a molten globule with a heating transition between 70 and 80 °C,<sup>5,7</sup> we monitored the vitamin D<sub>3</sub> binding with LG preheated at different temperatures including one that could denature the calyx structure. Interestingly, it showed a dramatic and sharp decrease in retinol, palmitic acid, and vitamin D<sub>3</sub> binding near the LG transition temperature. At the temperature above 80 °C, it almost completely abolished the retinol and palmitic acid binding, while still retaining 40% of the vitamin D<sub>3</sub> binding even at 100 °C heating for 16 min (Table 1).<sup>26</sup> To confirm it further, we monitored the binding of heated LG (100 °C for 16 min) with various amounts of vitamin D<sub>3</sub>, and a stoichiometry of 1:1 was observed between heat-denatured LG and vitamin D<sub>3</sub> using the same fluorescence quenching analysis.<sup>26</sup> Taking the previous pH and thermal experiments

together (Table 1), we concluded that a thermally stable site (defined as an exosite) beyond the calyx exists for vitamin D<sub>3</sub> binding. In the present study, we located the secondary vitamin D<sub>3</sub> binding site of LG using bioinformatic analysis to narrow the region of potential binding sites, the search of extra electron density around the potential binding sites of the cocrystal prepared on previous crystallographic study,<sup>20</sup> and a rationally designed crystallographic approach for obtaining cocrystals with sufficient quality and ligand occupancy.

### **Structural analysis of the binding pockets of LG using Insight II and Q-SiteFinder**

We attempted to identify the regions of LG that might be available for the interaction with any nondefined molecules using well-known programs (Insight II<sup>27</sup> and Q-SiteFinder<sup>28</sup>), which are based on the size of the binding pocket and the binding energy between the methyl group and the pocket of a given protein, respectively, for prediction of a ligand binding site. The former and latter predicted that there were 3 and 10 possible “binding sites” for any ligand, respectively. Table 2 and Figure 2A show the ranking and the location of six major predicted sites. Essentially both programs predicted that site **1** is exactly located at the calyx with the ranking superior to any others. This site is also known for all the vitamin D, retinol, and palmitic acid binding. Location of other predicted sites **2** (among C-terminal loop,  $\beta$ -strands C and D), **3** (among the pocket C-terminal  $\alpha$ -helix,  $\beta$ -strands F, G, H, and A), **4** (at

the side  $\alpha$ -helix and  $\beta$ -strands I), **5** (near loop H), and **6** (between CD and DE loops) is depicted in Figure 2A.

### **Docking analysis of the interaction between LG and retinol or palmitic acid using GEMDOCK**

Because both Insight II and Q-SiteFinder are not able to perform the specific interaction between an assigned ligand and a given binding site, we next used a more accurate docking program, GEMDOCK,<sup>29</sup> for molecular docking to search for a possible number of vitamin D binding sites and to further assess the interaction of a specific ligand with each site.

GEMDOCK appeared to be more accurate than comparative approaches, such as GOLD and FlexX, on a diverse data set of 100 protein-ligand complexes<sup>32</sup> for docking and two cross-docking experimental sets.<sup>29</sup> The screening accuracies of GEMDOCK were also better

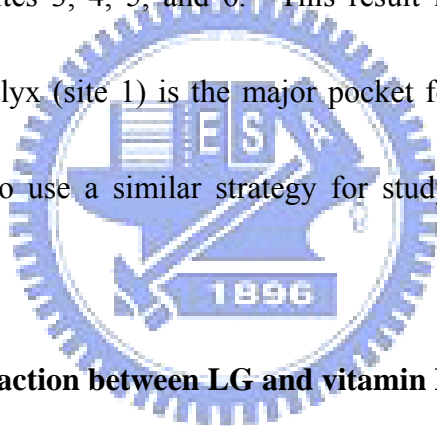
than GOLD, FlexX, and DOCK on screening the ligand database for antagonist and agonist ligands of estrogen receptor (ER).<sup>33</sup> GEMDOCK is a better docking tool for assessing the

interaction of a specific ligand with each site of LG. We generated 30 docked conformations of each retinol or palmitic acid with whole LG. Based on the docking protocol,<sup>29</sup> we

considered that a correct binding-mode was reproducible when the root-mean-square deviation (rmsd) between the best energy-scored conformation and crystal coordinates was

less than 2 Å.<sup>32</sup> In order to meet this criterion, we then evaluated the feasibility of GEMDOCK by cross-docking retinol and palmitic acid into the calyx or site 1 of LG (PDB

code: 1GX8), known to be an established site for the binding of retinol or palmitic acid. Our data reveal that these two ligands could be docked exactly into the calyx with a rmsd less than 2.0 Å. The average fitness of docked energy of retinol and palmitic acid was -86.3 and -75.7 kcal/mol (Table 3), respectively. Following the analyses of all the docking data, we found that none of the other sites 2-6 were fitted by either retinol or palmitic acid (<10% probability), except for palmitic acid interacting with site 2 (46% of total 30-docked conformations) (Table 3). For example, none of the docked conformations of retinol and palmitic acid could fit into sites 3, 4, 5, and 6. This result is almost consistent with the current knowledge that the calyx (site 1) is the major pocket for interacting with these two ligands. It is thus feasible to use a similar strategy for studying the interaction between vitamin D<sub>3</sub> and LG.



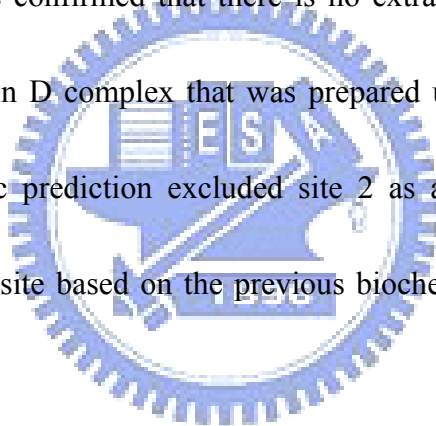
#### **Docking analysis of the interaction between LG and vitamin D<sub>3</sub> using GEMDOCK**

Each docked conformation of vitamin D<sub>3</sub> ( $n = 30$ ) obtained from GEMDOCK was then evaluated for a possible vitamin D binding ability. Table 2 shows that vitamin D<sub>3</sub> could fit into the calyx with about 50% of the probability. Interestingly, the docked energy of vitamin D<sub>3</sub> into the calyx site 1 was similar to that of retinol. The result suggests that GEMDOCK is suitable in conducting interactions between vitamin D<sub>3</sub> and LG. It also pointed out site 2 (Figure 2B) as a possible second binding site for palmitic acid (46%) and vitamin D<sub>3</sub> (20%). However, since the binding stoichiometry between palmitic acid and LG is 1 (Table 1) and

the calyx is the only available binding site for palmitic acid;<sup>21</sup> we ruled out site 2 as a particular site for palmitic acid binding. This site is located among the C-terminal loop,  $\beta$ -strand C, and  $\beta$ -strand D. Since  $\beta$ -strand D is thermally unstable,<sup>7</sup> it is not consistent to the proposed secondary vitamin D binding site that is supposed to be thermally stable in nature (Table 1). Site 2 is thus unlikely for vitamin D interaction.

In order to search for a potential secondary vitamin D<sub>3</sub> binding site location, we blocked sites 1 and 2 with the reason mentioned above and then performed GEMDOCK, while using retinol and palmitic acid as a “negative control”. Table 3 shows that, under this condition, sites 3 and 4 possessed high probability for vitamin D<sub>3</sub> interaction (40 and 20%) relative to retinol and palmitic acid. The other domains (sites 5 and 6) were considered nonsignificant due to the low probability (<3%). Notably, the docked orientation of the vitamin D<sub>3</sub> in sites 3 and 4 was distinctly different from that of other ligands (Figure 2C). Figure 2D tempted to suggest that the docked orientation of vitamin D<sub>3</sub> in site 3 is more stable (with a low rmsd) than that in site 4 due to its large pocket size that could stabilize ligand docking. On the other hand, the hydrophobicity of site 4 is high relative to site 3 based on the electrostatic potential surface model between LG and docked vitamin D<sub>3</sub> conformation (Figure 2E). The prediction of site 4 being involved in vitamin D<sub>3</sub> interaction is consistent with ranking predicted by Q-SiteFinder which is based on van der Waals interaction (Table 2). Taken together, sites 3 and 4 are the potential candidates for the secondary vitamin D binding site

and thus led us to localize it via a high-quality LG-vitamin D<sub>3</sub> crystal. We searched for an extra density around C-terminal  $\alpha$ -helix (sites 3 and 4) of LG-vitamin D<sub>3</sub> complex which was prepared at pH 7 with a vitamin D<sub>3</sub>/LG ratio of 2 according to the previous crystallographic study.<sup>20</sup> We found a weak extra electron density located near the C-terminal  $\alpha$ -helical region. Later, we used a rationally designed crystallography experiment for improving electron density of vitamin D<sub>3</sub> of the secondary binding site. In the bioinformatic prediction of the secondary vitamin D<sub>3</sub> binding site, we excluded false-positive site 2 on the previous biochemical findings. It was confirmed that there is no extra density around site 2 in the crystal structure of LG-vitamin D complex that was prepared using the previous condition. For this reason, bioinformatic prediction excluded site 2 as a potential candidate for the secondary vitamin D binding site based on the previous biochemical findings that is proper for this study.



### **Crystallization and diffraction of LG-vitamin D<sub>3</sub> complex prepared at various pH and vitamin D<sub>3</sub>/LG ratios**

In any event, starting the cocrystallization experiment with maximum ligand occupancy should provide a better opportunity in growing high-quality ligand-protein crystals. The affinity and concentrations of added ligands, as well as ligand solubility, would influence the occupancy of ligands at equilibrium. For 90% occupancy, the amount of added ligands must be greater than the amount of protein so that free ligands at equilibrium is not depleted to less



than about  $10 \times K_d$ .<sup>30</sup> In practice, ratios of ligands to a given protein up to 10:1 or more are commonly used, but large excesses should be avoided owing to the possibility of ligand binding to nonspecific sites. In the case of a weak binding affinity, the concentrations of ligands (or ligand solubility) may have to be 10 mM or higher in order to observe crystallographic occupancy.<sup>37,38</sup> We suspect that the lower occupancy of vitamin D<sub>2</sub> might explain an early study in which no electron density was found beyond the calyx using the crystal structure of LG-vitamin D<sub>2</sub> complex.<sup>10</sup> To optimize the binding and occupancy of vitamin D<sub>3</sub> to LG, we prepared this complex at various pH values ranging from 4 to 8 with a vitamin D<sub>3</sub>/LG ratio ranging from 1 to 3. Cocrystallization was conducted using the hanging-drop vapor-diffusion method in the same reservoir solution. Although the complexes were prepared at various pH, all were crystallized in the same bottom reservoir at pH 7.5. It is difficult to assess the true effect of pH on maximizing ligand occupancy, but one can prepare a LG-vitamin D<sub>3</sub> complex with the maximal ligand binding for cocrystallization, and avoid precipitation of water-insoluble vitamin D<sub>3</sub> during preparation of the LG-vitamin D<sub>3</sub> complex. The LG-vitamin D<sub>3</sub> complex crystals of rhombohedral shape appeared in 6-11 days and continued to grow slowly to a dimension of 0.2-0.4 mm in 18 days (Figure 3). In general, crystal could form except for the condition when prepared at pH 6 with a vitamin D<sub>3</sub>/LG ratio of 1. Crystals grew in larger quantity when the complex was prepared at pH 8 with a vitamin D<sub>3</sub>/LG ratio of 3 (data not shown). Although some

precipitation was observed while the ratio of vitamin D<sub>3</sub>/LG increased, this was probably due to an excess of water-insoluble vitamin D<sub>3</sub>. Analysis of the diffraction pattern indicated that the crystals exhibited trigonal symmetry and systematic absences suggested that the space group was  $P3_221$ , with unit-cell parameters  $a = b = 53.78 \text{ \AA}$  and  $c = 111.57 \text{ \AA}$ .

### **Initial electron density for secondary vitamin D<sub>3</sub> binding site**

The structures of the LG-vitamin D<sub>3</sub> complexes prepared in various conditions were determined by molecular replacement<sup>39</sup> as implemented in *CNS v1.1*<sup>40</sup> using the crystal structure of bovine LG (PDB code 2BLG)<sup>15</sup> as a search model. The LG molecule was located in the asymmetric unit after the rotation and translation function searches. The initial electron density maps of complexes prepared at various conditions were generated from the molecular-replacement phase. One elongated extra electron density in the calyx was clearly visible. We then searched the extra electron density around the  $\alpha$ -helix, which was predicted by bioinformatic programs, to explore the existence and location of the exosite. We found one extra electron density located near the  $\alpha$ -helix and  $\beta$ -strand I as “site 4” which was predicted by bioinformatic programs (Figure 4). Interestingly, the electron densities around the exosite of LG-vitamin D<sub>3</sub> crystals prepared at pH 8 were the best defined (Figure 4). Figure 4 reveals the greater the vitamin D<sub>3</sub>/LG ratio prepared for crystallization at pH 8 the more visible electron densities were around the exosite. The result indicates that the occupancy of vitamin D<sub>3</sub> in complexes is an essential requirement for exploring the location

of a secondary vitamin D binding site. Stereoviews of the  $|F_{\text{obs}} - F_{\text{calc}}|$  and  $|2F_{\text{obs}} - F_{\text{calc}}|$  electron density maps of LG-vitamin D<sub>3</sub> complex prepared at pH 8 with a vitamin D<sub>3</sub>/LG ratio 3:1 were generated by the initial model with omitted vitamin D<sub>3</sub> (Figure 5). The electron densities around vitamin D<sub>3</sub> in the exosite were all more visible in the  $|F_{\text{obs}} - F_{\text{calc}}|$  and  $|2F_{\text{obs}} - F_{\text{calc}}|$  electron density maps (Figure 5). This result supported the notion that the secondary vitamin D binding site exists and is located between  $\alpha$ -helix and  $\beta$ -strand I. The final refined structure determined using the LG-vitamin D<sub>3</sub> complex prepared at pH 8 with a vitamin D<sub>3</sub>/LG ratio of 3:1 was given in detail and discussed elsewhere.<sup>26</sup> The surface model of the LG-vitamin D<sub>3</sub> complex reveals that vitamin D<sub>3</sub> almost perpendicularly inserts into the calyx cavity, while the other vitamin D<sub>3</sub> is located near the carboxyl terminus of LG (residues 136-149 including part of the  $\alpha$ -helix and  $\beta$ -strand I) (Figure 6). It shows the exosite containing most hydrophobic residues fitted parallel with one vitamin D<sub>3</sub> molecule (Figure 6).

In the present study, with bioinformatic analysis we were able to suggest two sites (sites 3 and 4) around the C-terminal  $\alpha$ -helix as potential binding sites on LG. Subsequently, we searched for an extra density around the C-terminal  $\alpha$ -helix (sites 3 and 4) in the electron density map of the cocrystal prepared in a previous crystallographic study.<sup>20</sup> A weak electron density around site 4 (located between  $\alpha$ -helix and  $\beta$ -strand I) of LG-vitamin D<sub>3</sub> complex was found. The rationally designed crystallographic approach resulted in obtaining

cocrystals with sufficient quality and ligand occupancy so as to allow experimental validation of the second vitamin D<sub>3</sub> binding site on LG. We believe that our strategy is useful for others in the search for a ligand-binding site on a given protein.

### **Biological significance**

Recent studies indicate that increased plasma vitamin D<sub>3</sub> concentrations are associated with decreased incidence of cancer<sup>41</sup> and osteoporotic fractures.<sup>42</sup> Vitamin D is found in only a few foods, such as fish oil, liver, milk, and eggs. As the level of vitamin D in bovine milk has been reported to be low, dairy products are fortified with vitamin D<sub>3</sub> to a level of about 0.35  $\mu$ M in many sophisticated food industries.<sup>43</sup> Therefore, the vitamin D-fortified milk is a major source for vitamin D in the diet. Because intact LG is acid resistant with a superpermeability to cross the epithelium cells of the gastrointestinal tract via a receptor mediated process,<sup>44</sup> this unique property of LG is worthy of consideration for transport of vitamin D in milk. There are two advantages for the presence of an exosite for vitamin D<sub>3</sub> binding. First, the central calyx of LG is primarily occupied by the fatty acids in milk.<sup>45</sup> Second, many dairy products are currently processed under excessive heat treatment for the purpose of sterilization. The presence of a thermally stable exosite may provide another route for transporting vitamin D.

### **Conclusion**

We concluded that there is a heat-resistant exosite beyond the calyx responsible for vitamin D<sub>3</sub> binding in a previous binding study. GEMDOCK is a helpful tool to localize and search for an extra density map around a possible secondary vitamin D binding site. Both pH and the initial ratio of vitamin D<sub>3</sub>/LG are crucial to optimize the occupancy and enhance the electron density of vitamin D<sub>3</sub> in the complex for rational-designed crystallization. This strategy may be useful for future identification of a ligand-binding site in a given protein.

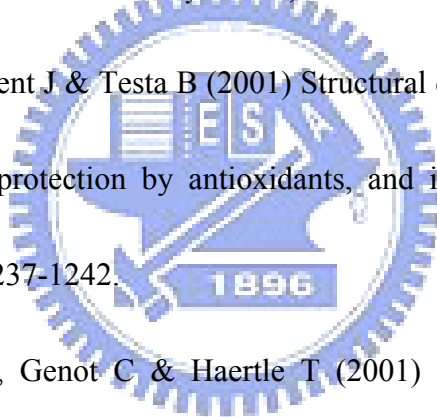
### **Acknowledgments**

We are grateful to Dr. Yuch-Cheng Jean and the supporting staff for technical assistance and the discussion of the synchrotron radiation X-ray data collected at BL13B1 of NSRRC, Taiwan, and Dr. Jeyaraman Jeyakanthan at BL12B2 of SPring-8, Japan. We also thank Mr. James Lee for the critical editing. This work was supported in part by the National Science Council NSC 92-2313-B-009-002, 93-2313-B009-002, 94-2313-B-009-001 & 95-2313-B-009-001 to S. J. T. Mao and NSC 94-2321-B-213-001, 95-2321-B-213-001-M and the National Synchrotron Radiation Research Center 944RSB02 & 954RSB02 to C.-J. Chen, Taiwan, ROC.

### **References**

1. Hambling SG, MacAlpine AS & Sawyer L (1992) Beta-lactoglobulin. In *Advanced Dairy Chemistry I* (Fox PF eds) pp. 141-190. Elsevier, Amsterdam.
2. Qi XL, Brownlow S, Holt C & Sellers P (1995) Thermal denaturation of beta-lactoglobulin: effect of protein concentration at pH 6.75 and 8.05. *Biochim Biophys Acta* **1248**, 43-49.
3. Sawyer L & Kontopidis G (2000) The core lipocalin, bovine beta-lactoglobulin. *Biochim Biophys Acta* **1482**, 136-148.
4. Chen WL, Huang MT, Liu HC, Li CW & Mao SJT (2004) Distinction between dry and raw milk using monoclonal antibodies prepared against dry milk proteins. *J Dairy Sci* **87**, 2720-2729.
5. Chen WL, Huang MT, Liao CY, Ho JC, Hong KC & Mao SJT (2005)  $\beta$ -Lactoglobulin is a Thermal Marker in Processed Milk as Studied by Electrophoresis and Circular Dichroic Spectra. *J Dairy Sci* **88**, 1618-1630.
6. Chen WL, Liu WT, Yang MC, Hwang MT, Tsao JH & Mao SJT (2006) A novel conformation-dependent monoclonal antibody specific to the native structure of beta-lactoglobulin and its application. *J Dairy Sci* **89**, 912-921.
7. Song CY, Chen WL, Yang MC, Huang JP & Mao SJT (2005) Epitope mapping of a monoclonal antibody specific to bovine dry milk: involvement of residues 66-76 of strand D in thermal denatured beta-lactoglobulin. *J Biol Chem* **280**, 3574-3582.

8. Nagaoka S, Futamura Y, Miwa K, Awano T, Yamauchi K, Kanamaru Y, Tadashi K & Kuwata T (2001) Identification of novel hypocholesterolemic peptides derived from bovine milk beta-lactoglobulin. *Biochem Biophys Res Commun* **281**, 11-17.
9. Zsila F, Bikadi Z & Simonyi M (2002) Retinoic acid binding properties of the lipocalin member beta-lactoglobulin studied by circular dichroism, electronic absorption spectroscopy and molecular modeling methods. *Biochem Pharmacol* **64**, 1651-1660.
10. Kontopidis G, Holt C & Sawyer L (2004) Invited review: beta-lactoglobulin: binding properties, structure, and function. *J Dairy Sci* **87**, 785-796.
11. Salvi A, Carrupt P, Tillement J & Testa B (2001) Structural damage to proteins caused by free radicals: assessment, protection by antioxidants, and influence of protein binding. *Biochem Pharmacol* **61**, 1237-1242.
12. Chevalier F, Chobert JM, Genot C & Haertle T (2001) Scavenging of free radicals, antimicrobial, and cytotoxic activities of the Maillard reaction products of beta-lactoglobulin glycosylated with several sugars. *J Agric Food Chem* **49**, 5031-5038.
13. Marshall K (2004) Therapeutic applications of whey protein. *Altern Med Rev* **9**, 136-156.
14. Liu HC, Chen WL & Mao SJT (2007) Antioxidant nature of bovine milk beta-lactoglobulin. *J Dairy Sci* **90**, 547-555.



15. Qin BY, Bewley MC, Creamer LK, Baker HM, Baker EN & Jameson GB (1998) Structural basis of the Tanford transition of bovine beta-lactoglobulin. *Biochemistry* **37**, 14014-14023.
16. Qin BY, Bewley MC, Creamer LK, Baker EN & Jameson GB (1999) Functional implications of structural differences between variants A and B of bovine beta-lactoglobulin. *Protein Sci* **8**, 75-83.
17. Kuwata K, Hoshino M, Forge V, Era S, Batt CA & Goto Y (1999) Solution structure and dynamics of bovine beta-lactoglobulin A. *Protein Sci* **8**, 2541-2545.
18. Uhrinova S, Smith MH, Jameson GB, Uhrin D, Sawyer L & Barlow PN (2000) Structural changes accompanying pH-induced dissociation of the beta-lactoglobulin dimer. *Biochemistry* **39**, 3565-3574.
19. Narayan M & Berliner LJ (1997) Fatty acids and retinoids bind independently and simultaneously to beta-lactoglobulin. *Biochemistry* **36**, 1906-1911.
20. Qin BY, Creamer LK, Baker EN & Jameson GB (1998) 12-Bromododecanoic acid binds inside the calyx of bovine beta-lactoglobulin. *FEBS Lett* **438**, 272-278.
21. Wu SY, Perez MD, Puyol P & Sawyer L (1999) beta-lactoglobulin binds palmitate within its central cavity. *J Biol Chem* **274**, 170-174.
22. Kontopidis G, Holt C & Sawyer L (2002) The ligand-binding site of bovine beta-lactoglobulin: evidence for a function? *J Mol Biol* **318**, 1043-1055.



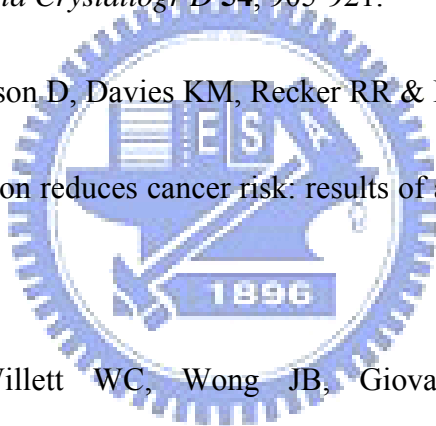
23. Wang Q, Allen JC & Swaisgood HE (1997) Binding of retinoids to beta-lactoglobulin isolated by bioselective adsorption. *J Dairy Sci* **80**, 1047-1053.
24. Wang Q, Allen JC & Swaisgood HE (1997) Binding of vitamin D and cholesterol to beta-lactoglobulin. *J Dairy Sci* **80**, 1054-1059.
25. Wang Q, Allen JC & Swaisgood HE (1999) Binding of lipophilic nutrients to beta-lactoglobulin prepared by bioselective adsorption. *J Dairy Sci* **82**, 257-264.
26. Yang MC, Guan HH, Liu MY, Lin YH, Yang JM, Chen WL, Chen CJ & Mao SJT (2008) Crystal structure of a secondary vitamin D<sub>3</sub> binding site of milk beta-lactoglobulin. *Proteins* **71**, 1197-1210.
27. Xiao L, Cui X, Madison V, White RE & Cheng KC (2002) Insights from a three-dimensional model into ligand binding to constitutive active receptor. *Drug Metab Dispos* **30**, 951-956.
28. Laurie AT & Jackson RM (2005) Q-SiteFinder: an energy-based method for the prediction of protein-ligand binding sites. *Bioinformatics* **21**, 1908-1916.
29. Yang JM & Chen CC (2004) GEMDOCK: a generic evolutionary method for molecular docking. *Proteins* **55**, 288-304.
30. Danley DE (2006) Crystallization to obtain protein-ligand complexes for structure-aided drug design. *Acta Crystallogr D* **62**, 569-575.



31. Guex N & Peitsch MC (1997) SWISS-MODEL and the Swiss-PdbViewer: an environment for comparative protein modeling. *Electrophoresis* **18**, 2714-2723.
32. Jones G, Willett P, Glen RC, Leach AR & Taylor R (1997) Development and validation of a genetic algorithm for flexible docking. *J Mol Biol* **267**, 727-748.
33. Yang JM & Shen TW (2005) A pharmacophore-based evolutionary approach for screening selective estrogen receptor modulators. *Proteins* **59**, 205-220.
34. Otwinowski Z & Minor W (1997) Processing of X-ray Diffraction Data Collected in Oscillation Mode. *Methods Enzymol* **276**, 307-326.
35. Ragona L, Fogolari F, Zetta L, Pérez DM, Puyol P, De Kruif K, Löhr F, Rüterjans H & Molinari H (2000) Bovine beta-lactoglobulin: interaction studies with palmitic acid. *Protein Sci* **9**, 1347-1356.
36. Muresan S, van der Bent A & de Wolf FA (2001) Interaction of beta-lactoglobulin with small hydrophobic ligands as monitored by fluorometry and equilibrium dialysis: nonlinear quenching effects related to protein-protein association. *J Agric Food Chem* **49**, 2609-2618.
37. Hartshorn MJ, Murray CW, Cleasby A, Frederickson M, Tickle IJ & Jhoti H (2005) Fragment-based lead discovery using X-ray crystallography. *J Med Chem* **48**, 403-413.



38. Nienaber VL, Richardson PL, Klighofer V, Bouska JJ, Giranda VL & Greer J (2000) Discovering novel ligands for macromolecules using X-ray crystallographic screening. *Nature Biotechnol* **18**, 1105-1108.
39. Rossmann MG (1990) The molecular replacement method. *Acta Crystallogr A* **46**, 73-82.
40. Brunger AT, Adams PD, Clore GM, DeLano WL, Gros P, Grosse-Kunstleve RW, Jiang JS, Kuszewski J, Nilges M, Pannu NS, Read RJ, Rice LM, Simonson T & Warren GL (1998) Crystallography & NMR system: A new software suite for macromolecular structure determination. *Acta Crystallogr D* **54**, 905-921.
41. Lappe JM, Travers-Gustafson D, Davies KM, Recker RR & Heaney RP (2007) Vitamin D and calcium supplementation reduces cancer risk: results of a randomized trial. *Am J Clin Nutr* **85**, 1586-1591.
42. Bischoff-Ferrari HA, Willett WC, Wong JB, Giovannucci E, Dietrich T & Dawson-Hughes B (2005) Fracture prevention with vitamin D supplementation: a meta-analysis of randomized controlled trials. *JAMA* **293**, 2257-2264.
43. Holick MF, Shao Q, Liu WW & Chen TC (1992) The vitamin D content of fortified milk and infant formula. *N Engl J Med* **326**, 1178-1181.
44. Fluckinger M, Merschak P, Hermann M, Haertlé T & Redl B (2008) Lipocalin-interacting-membrane-receptor (LIMR) mediates cellular internalization of beta-lactoglobulin. *Biochim Biophys Acta* **1778**, 342-347.



45. Pérez MD, Díaz de Villegas C, Sánchez L, Aranda P, Ena JM & Calvo M (1989)

Interaction of fatty acids with beta-lactoglobulin and albumin from ruminant milk. *J Biochem* **106**, 1094-1097.

46. Jones TA, Zou JY, Cowan SW & Kjeldgaard M (1991) Improved methods for building

protein models in electron density maps and the location of errors in these models. *Acta Crystallogr A* **47**, 110-119.

### Figure legends

**Figure 1.** Primary structure of LG and chemical structure of its binding ligands. (A) LG comprises 162 amino acids with nine antiparallel  $\beta$ -sheet strands (A-I) and one  $\alpha$ -helix (in gray). There are two disulfide bonds located between  $\beta$ -strand D and carboxyl-terminus (Cys-66 and Cys-160) and between  $\beta$ -strands G and H (Cys-106 and Cys-119), while a free buried thiol group is at Cys-121. (B) Chemical structure of ligands which bind to LG, such as vitamin D<sub>3</sub>, retinol, and palmitic acid.

**Figure 2.** Prediction of potential binding pockets of LG using Insight II, Q-SiteFinder, and GEMDOCK. (A) Binding pockets of LG predicted by Insight II (color in blue) and Q-SiteFinder (in black). There are three and six major binding sites predicted by Insight II or Q-SiteFinder, respectively, for any nondefined ligand. (B) There are total six potential binding sites for retinol, palmitic acid, and vitamin D<sub>3</sub> (red, black, and blue) in LG following

the GEMDOCK docking. LG structure in 3D used was based on LG-retinol complex (PDB code: 1GX8). Retinol and palmitic acid are able to dock exactly into the calyx (site 1), but not to the other sites except for palmitic acid interacting with site 2. The probability of vitamin D<sub>3</sub> fitting into the calyx is about 50% (see Table 1). It indicates that the calyx is a superior binding site for vitamin D. (C) Cross-docking of retinol, palmitic acid, and vitamin D<sub>3</sub> into the cavity of LG with sites 1 and 2 blocked. The docked orientation of the vitamin D<sub>3</sub> in sites 3 and 4 are distinctly different from retinol and palmitic acid. (D) Comparison of the docked orientation of vitamin D<sub>3</sub> between sites 3 and 4. The docked conformation of vitamin D<sub>3</sub> binding in site 3 seems to be more stable than in site 4. (E) The electrostatic surface model of LG depicting the positively charged (in blue), negatively charged (in red), and hydrophobic (white) side chains, in which the hydrophobic surface of site 4 seems to be large relative to that of site 3.

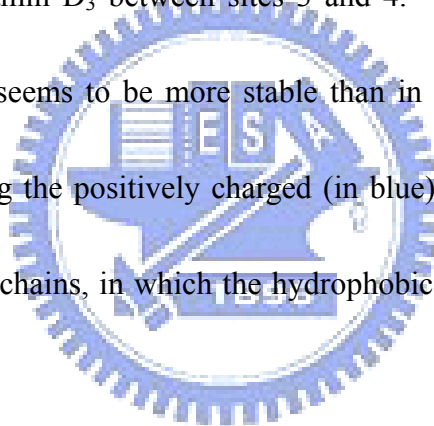


**Figure 3.** Typical example of LG-vitamin D<sub>3</sub> crystals prepared with various vitamin D<sub>3</sub>/LG ratios at pH 8. Crystals of LG-vitamin D<sub>3</sub> complexes were grown using a hanging-drop vapor-diffusion method. Complex crystals of rhombohedral shape prepared at vitamin D<sub>3</sub>/LG ratios of 1, 2, or 3 appeared at day 11, 10, or 6 with 2.1, 2.2, or 2.1 Å resolution diffraction were observed, respectively. The crystals grew slowly to a dimension of 0.2-0.4 mm in 18 days. Each bar represents 0.2 mm.

**Figure 4.** Initial electron densities map around the exosite of LG-vitamin D<sub>3</sub> complex

prepared at indicated conditions. The  $|2F_{\text{obs}} - F_{\text{calc}}|$  electron density maps generated by the initial LG model with omitted vitamin D<sub>3</sub> show that the electron density (in cyan) of vitamin D<sub>3</sub> molecule (in red) in the exosite is more visible when the complex was prepared at pH 8 with a vitamin D<sub>3</sub>/LG ratio of 3:1. The images were generated using the program *O*.<sup>46</sup>

**Figure 5.** The electron density maps around the exosite of LG-vitamin D<sub>3</sub> complex prepared at pH 8 with an initial vitamin D<sub>3</sub>/LG ratio of 3:1 in stereoview. The  $|F_{\text{obs}} - F_{\text{calc}}|$  (in blue) and  $|2F_{\text{obs}} - F_{\text{calc}}|$  (in cyan) electron density maps generated by the initial LG model with vitamin D<sub>3</sub> omitted show that the electron density of the vitamin D<sub>3</sub> molecule (in red) in the exosite is clearly visible.

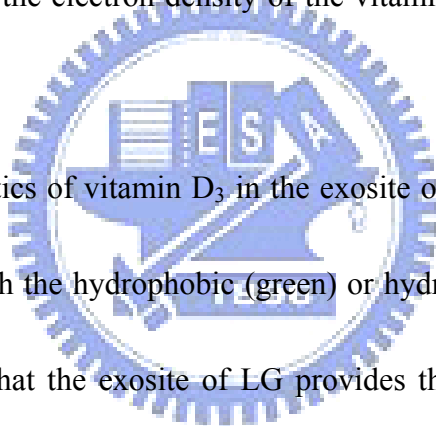


**Figure 6.** Binding characteristics of vitamin D<sub>3</sub> in the exosite of LG. The surface model of vitamin D<sub>3</sub> interacting LG with the hydrophobic (green) or hydrophilic region (red) of LG is displayed. The data reveal that the exosite of LG provides the hydrophobic force to bind vitamin D<sub>3</sub> stably. Notably, the 3-OH group (red) of vitamin D<sub>3</sub> sticks out from the pocket.

**Table 1.** Relative ligand binding ability of LG at the various pH and preheated temperatures extracted from our published paper<sup>26</sup>

Relative binding (%)											
Titration experiment				Effect of pH				Effect of heating (preheated for 16 min)			
[ligand] / [native LG]	Vitamin D <sub>3</sub>	Retinol	Palmitic acid	pH	Vitamin D <sub>3</sub>	Retinol	Palmitic acid	Temperature (°C)	Vitamin D <sub>3</sub>	Retinol	Palmitic acid
0.125	7.1	13.2	15.1	2.0	<b>29.1</b>	2.2	2.0	50	93.4	92.1	92.6
0.25	14.1	26.0	30.0	3.0	<b>29.0</b>	0	0	60	91.1	90.2	90.4
0.375	21.2	38.8	44.9	4.0	<b>29.3</b>	0	0	70	83.0	67.0	72.3
0.5	28.1	50.6	59.0	5.0	<b>29.3</b>	0	0	80	49.2	10.2	14.4
0.625	35.3	62.0	71.5	6.0	46.7	8.5	38.0	90	41.9	7.5	6.8
0.75	42.3	72.7	80.4	7.0	58.1	27.0	49.4	100	<b>40.7</b>	6.7	5.8
0.875	49.3	81.3	86.9	8.0	100	87.7	100				
1.0	<b>56.2</b>	88.0	91.9	9.0	78.2	100	82.6				
1.25	70.6	91.8	96.0	10.0	77.7	97.6	54.3				
1.5	82.9	95.0	98.5								
1.75	92.0	96.7	99.2								
2.0	96.0	98.0	99.7								

**Table 2.** Possible sites predicted by Insight II, Q-SiteFinder, and GEMDOCK

Programs Ranking Fitness (ratio)	Insight II	Q-SiteFinder	GEMDOCK	
			Vitamin D <sub>3</sub> docking for whole protein	Vitamin D <sub>3</sub> docking for other parts of protein besides sites 1 and 2
Site 1 (calyx)	1	1	-87.2 (50 %)	
Site 2	2	2	-88.4 (20 %)	
Site 3	3	8	-85.4 (6 %)	-83.9 (40 %)
Site 4		3	-82.4 (6 %)	-81.2 (20 %)
Site 5		5	-75.4 (3 %)	-80.1 (3 %)
Site 6		4	-83.4 (3 %)	-87.0 (3 %)

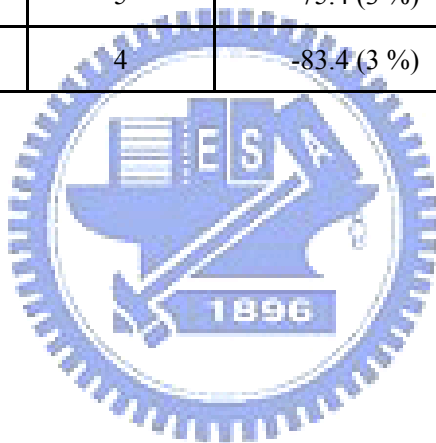


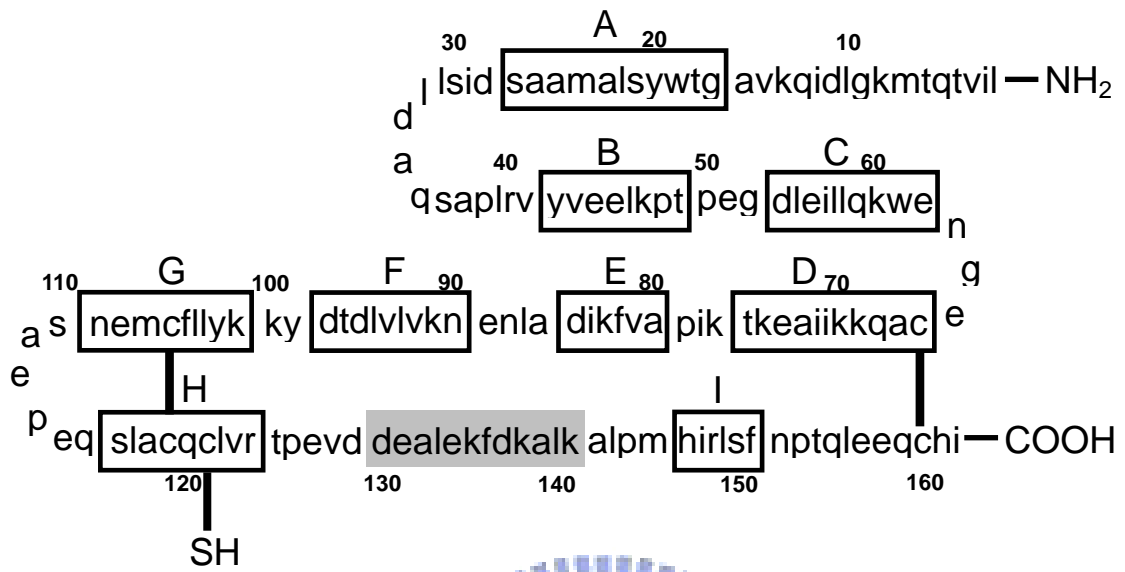


**Table 3.** Percentage probability of different ligands docking into possible sites of LG

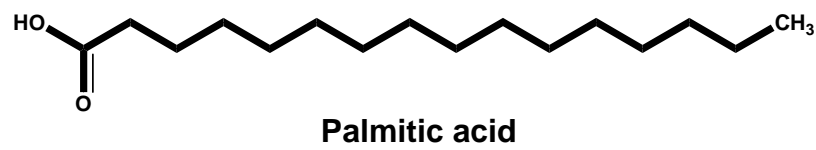
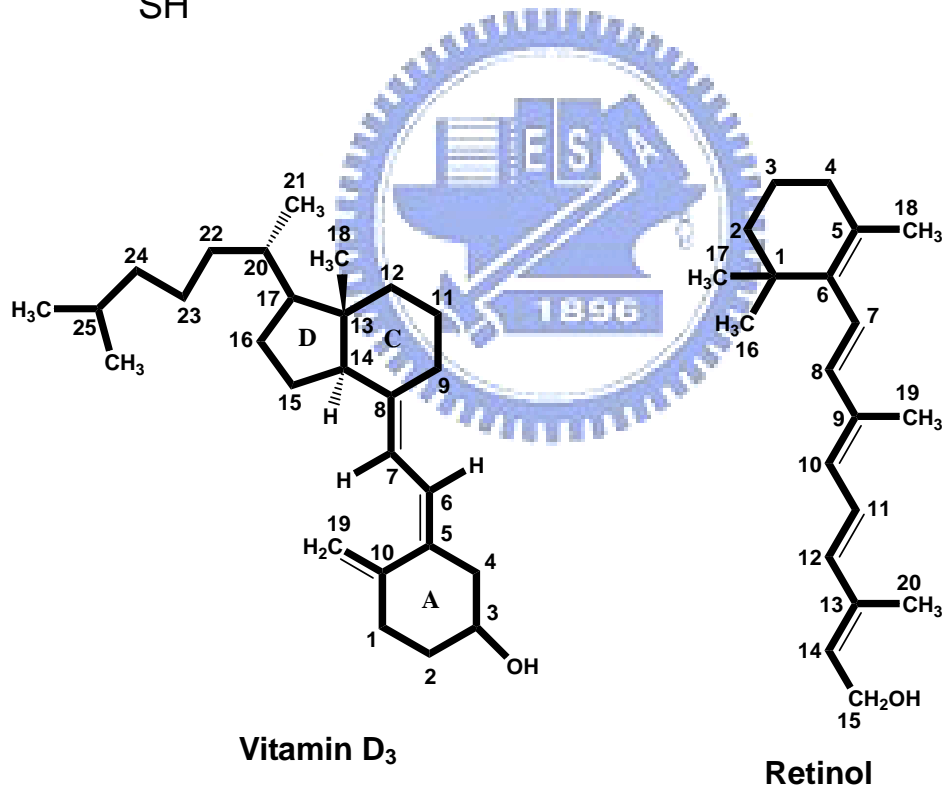
Conditions	Docking ligands into 1GX8					
	Docking search on whole protein			Docking search on other parts of protein		
Fitness (ratio)	Retinol	Palmitic acid	Vitamin D <sub>3</sub>	Retinol	Palmitic acid	Vitamin D <sub>3</sub>
Site 1 (calyx)	-86.3 (93 %)	-75.7 (43 %)	-87.2 (50 %)			
Site 2	-86.4 (6 %)	-77.6 (46 %)	-88.4 (20 %)			
Site 3			-85.4 (6 %)	-76.2 (3 %)	-69.7 (10 %)	-83.9 (40 %)
Site 4			-82.4 (6 %)	-73.3 (10 %)	-69.4 (16 %)	-81.2 (20 %)
Site 5		-76.1 (6 %)	-75.4 (3 %)	-72.9 (6 %)	-67.7 (10 %)	-80.1 (3 %)
Site 6			-83.4 (3 %)	-77.2 (43 %)	-72.5 (13 %)	-87.0 (3 %)

Figure 1

A



B



**Figure 2**

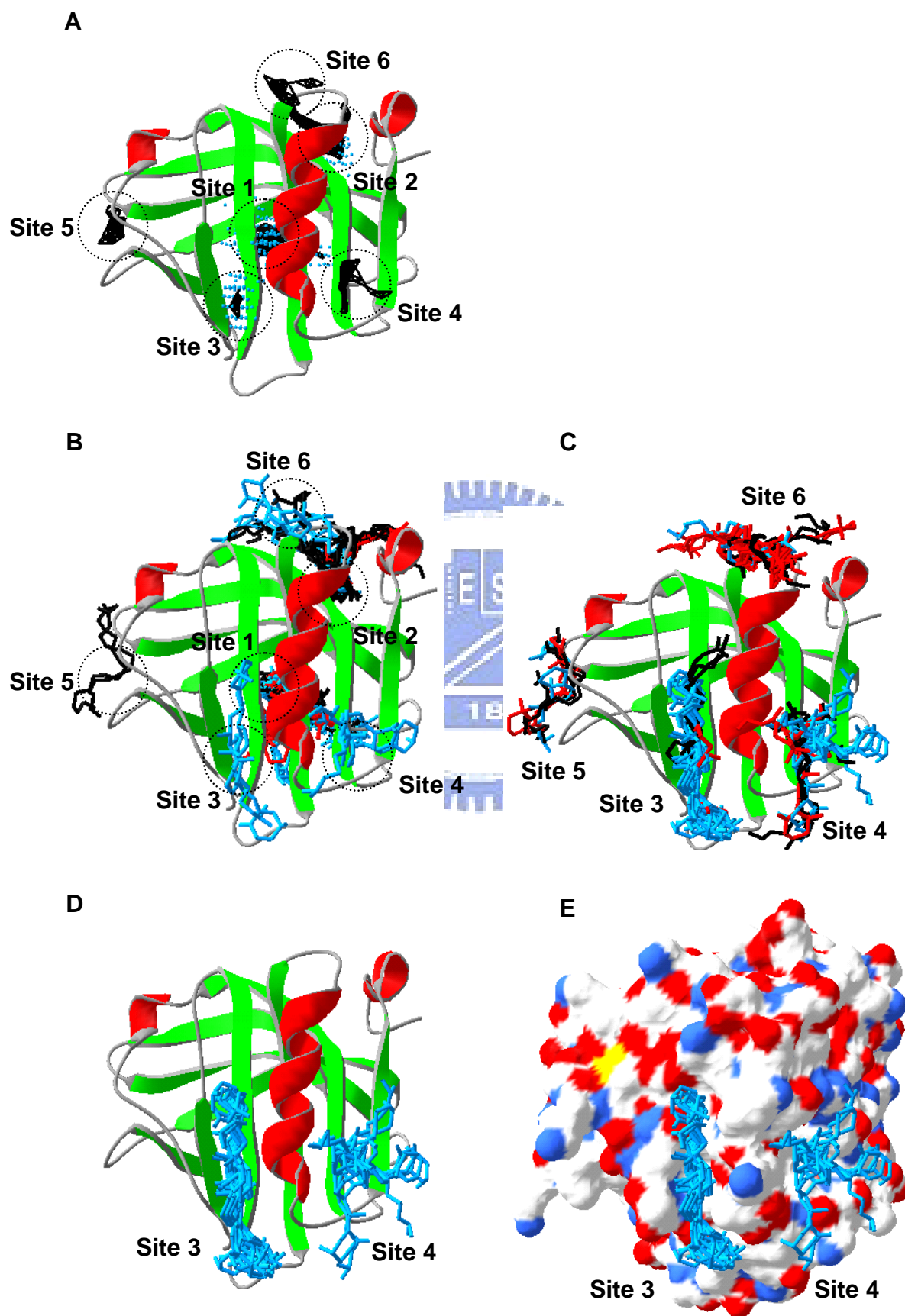
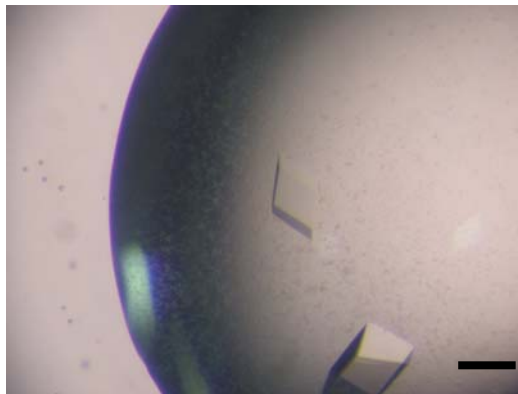
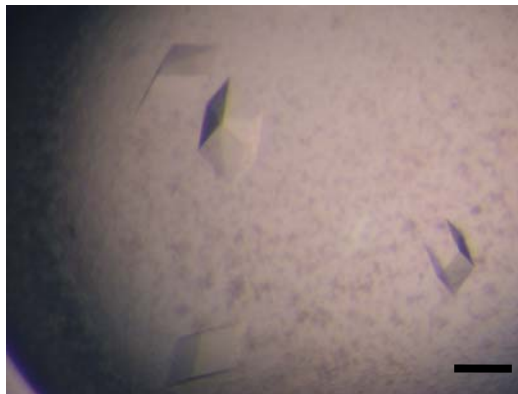


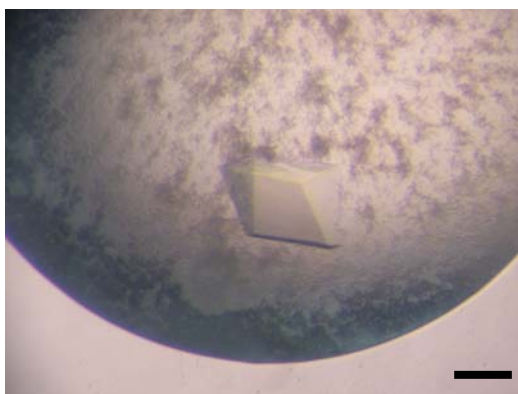
**Figure 3**



**pH 8.0, D<sub>3</sub>/LG ratio 1**  
**Resolution 2.1 Å**  
***R*<sub>sym</sub>: 4%**

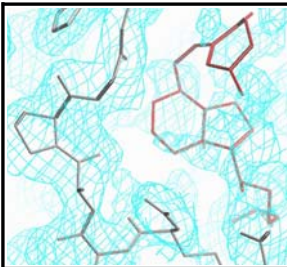
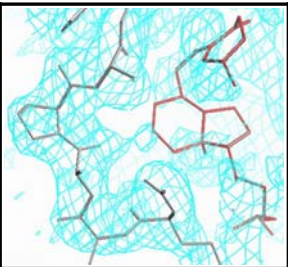
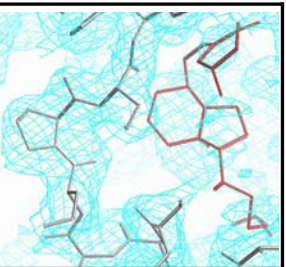
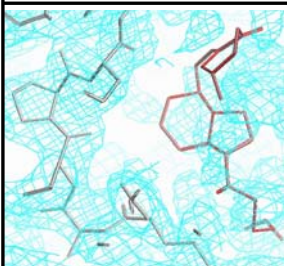
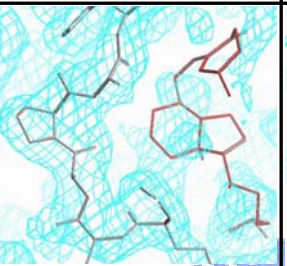
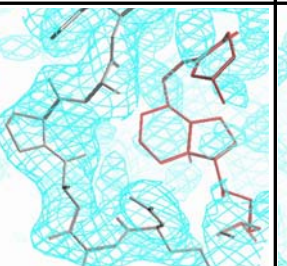
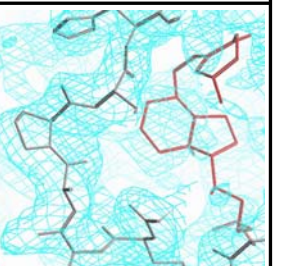
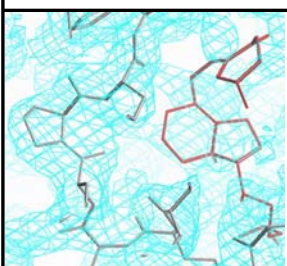
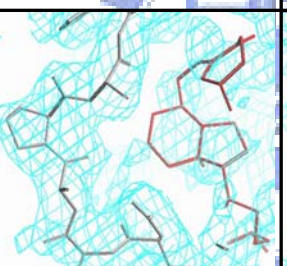
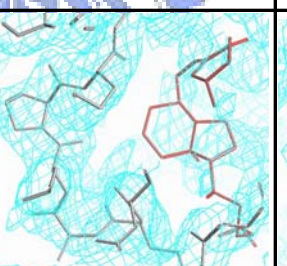
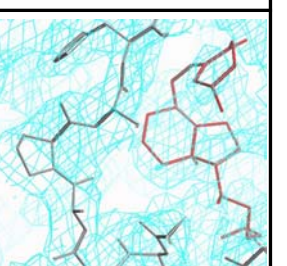


**pH 8.0, D<sub>3</sub>/LG ratio 2**  
**Resolution 2.2 Å**  
***R*<sub>sym</sub>: 5%**



**pH 8.0, D<sub>3</sub>/LG ratio 3**  
**Resolution 2.1 Å**  
***R*<sub>sym</sub>: 5.5%**

**Figure 4**

	No crystal		
pH 4.0, D <sub>3</sub> /LG ratio 1 <i>R</i> <sub>sym</sub> : 5.9%	pH 6.0, D <sub>3</sub> /LG ratio 1	pH 7.0, D <sub>3</sub> /LG ratio 1 <i>R</i> <sub>sym</sub> : 5.3%	pH 8.0, D <sub>3</sub> /LG ratio 1 <i>R</i> <sub>sym</sub> : 4%
			
pH 4.0, D <sub>3</sub> /LG ratio 2 <i>R</i> <sub>sym</sub> : 5.4%	pH 6.0, D <sub>3</sub> /LG ratio 2 <i>R</i> <sub>sym</sub> : 4.7%	pH 7.0, D <sub>3</sub> /LG ratio 2 <i>R</i> <sub>sym</sub> : 7.3%	pH 8.0, D <sub>3</sub> /LG ratio 2 <i>R</i> <sub>sym</sub> : 5%
			
pH 4.0, D <sub>3</sub> /LG ratio 3 <i>R</i> <sub>sym</sub> : 5.9%	pH 6.0, D <sub>3</sub> /LG ratio 3 <i>R</i> <sub>sym</sub> : 5.4%	pH 7.0, D <sub>3</sub> /LG ratio 3 <i>R</i> <sub>sym</sub> : 6.8%	pH 8.0, D <sub>3</sub> /LG ratio 3 <i>R</i> <sub>sym</sub> : 5.5%

**Figure 5**

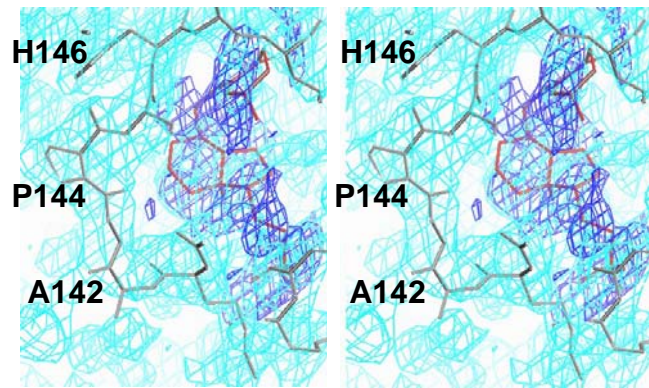
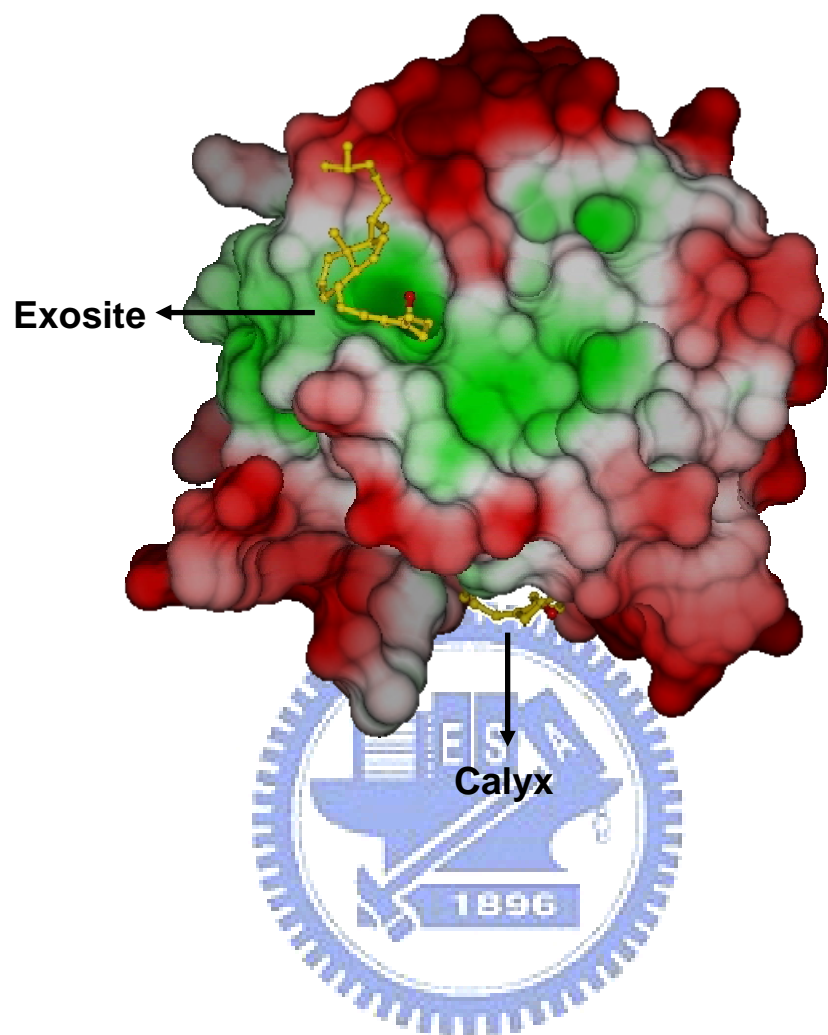




Figure 6



Section 3: Evidence for LG involvement in vitamin  
D transport *in vivo* (FEBS Journal)





## Abstract

$\beta$ -lactoglobulin (LG) is a major bovine milk protein, containing a central calyx and a second exosite beyond the calyx to bind vitamin D; however, the biological function of LG in transporting vitamin D remains elusive. Crystallographic findings from our previous study showed the exosite to be located at the pocket between the  $\alpha$ -helix and  $\beta$ -strand I. In the present study, using site-directed mutagenesis, we demonstrate that residues Leu143, Pro144 and Met145 in the  $\gamma$ -turn loop play a crucial role in the binding. Further evidence is provided by the ability of vitamin D<sub>3</sub> to block the binding of a specific mAb in the  $\gamma$ -turn loop. Using the mouse (n=95) as an animal model, we initially demonstrated that LG is a major fraction of milk proteins responsible for uptake of vitamin D. Most interestingly, dosing mice with LG supplemented with vitamin D<sub>3</sub> revealed that native LG containing two binding sites gave a saturated concentration of plasma 25-hydroxyvitamin D at a dose ratio of 2:1 (vitamin D<sub>3</sub>/LG), whereas heated LG containing one exosite (lacking a central calyx) gave a ratio of 1:1. We have demonstrated for the first time that LG has a functional advantage in the transport of vitamin D, indicating that supplementing milk with vitamin D effectively enhances its uptake.

**(Keywords:**  $\beta$ -Lactoglobulin, Monoclonal antibody, Site-directed mutagenesis, Vitamin D binding, Vitamin D transport and uptake)

### Abbreviations

LG,  $\beta$ -lactoglobulin; rLG, recombinant  $\beta$ -lactoglobulin; SD, standard deviation.

## Introduction

Bovine  $\beta$ -lactoglobulin (LG) is a major whey protein that constitutes 10-15% of the total proteins in bovine milk.<sup>1</sup> Since the 1960s, the thermally unstable and molten globule nature of LG has stimulated extensive research into its physical and biochemical properties.<sup>2-10</sup> The crystal structure of LG, which is well established,<sup>11,12</sup> has been used mostly as a benchmark to predict the secondary structure of a given protein with a known amino acid sequence.<sup>13</sup> As shown in Figure 1A, the protein has predominantly a  $\beta$ -sheet conformation containing nine antiparallel  $\beta$ -strands from A to I. Topographically,  $\beta$ -strands A-D form one surface of the barrel (calyx), and  $\beta$ -strands E-H form the other.<sup>14-16</sup> The calyx has a remarkable ability to bind hydrophobic molecules such as retinol, fatty acids and vitamin D.<sup>17-20</sup> According to a crystallographic structure of the LG-vitamin D<sub>3</sub> complex (Figure 1B),<sup>9,10</sup> the  $\alpha$ -helical region with three turns linking with  $\beta$ -strand I on the surface is involved in binding vitamin D at the secondary exosite. The conformational changes of LG upon heating are rapid and extensive above the transition temperature ( $\sim 70$  °C), at which  $\beta$ -strand D of the calyx participates in the unfolding during thermal denaturation.<sup>6</sup> As a result, thermal treatment diminishes the calyx binding site for palmitate or retinol, but does not affect the exosite for vitamin D binding.<sup>6,9,10</sup> In our previous study, we proposed that this exosite contains a unique inverse  $\gamma$ -turn loop (residues 143-145 or Leu-Pro-Met), located between the  $\alpha$ -helix and  $\beta$ -strand I, that is essential in forming a pocket to bind vitamin D.<sup>9</sup>

In the present study, we expressed recombinant LG (rLG) in *Escherichia coli*, and used site-directed mutagenesis to produce a set of mutants to test the hypothesis that this  $\gamma$ -turn plays an essential role in the interaction between LG and vitamin D. We further tested this hypothesis using a mAb specific for this  $\gamma$ -turn region (selected from a battery containing 900 mAbs) as a probe, and then determined whether vitamin D might interfere with the binding between LG and the mAb. In addition, although the binding of vitamin D to milk LG is well known,<sup>9,10,14,21,22</sup> whether it enhances the transport of vitamin D of milk is still unproven.

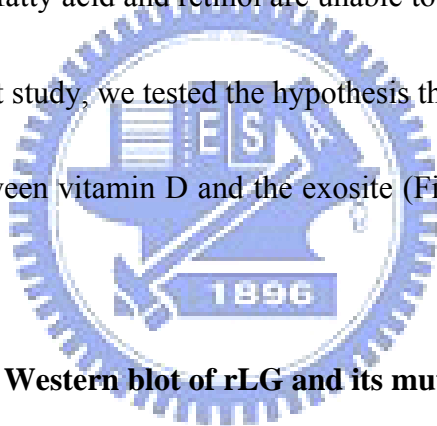
We have demonstrated for the first time that LG is a fraction responsible for the uptake of vitamin D<sub>3</sub> from milk, using the mouse (n=95) as an animal model. Most interestingly, we showed that native LG containing both the calyx and exosite had an efficacy in vitamin D<sub>3</sub> uptake almost twice that of heated LG containing a single exosite. Our study therefore provides new insights concerning the value of supplementing dairy products with vitamin D.

## Results

### Overall crystal structure of the LG-vitamin D<sub>3</sub> complex

Our space-filling drawing of the LG-vitamin D<sub>3</sub> complex at 2.4 Å resolution reveals two domains in which vitamin D<sub>3</sub> is bound (Figure 1B). One vitamin D<sub>3</sub> molecule inserts almost perpendicularly into the calyx cavity with the 3-OH near the outside similar to that of retinol binding; the other binds to the exosite near the C-terminus of LG (residues 136-149),

including a  $\gamma$ -turn loop (residues 143-145) by combining part of the  $\alpha$ -helix and  $\beta$ -strand I (Figure 1C,D). Uniquely, the  $\alpha$ -helix in the exosite is totally amphipathic, as pointed out previously,<sup>23</sup> with one face totally comprising charged amino acid residues, and another face totally comprising hydrophobic residues (Figure 2A). The A ring and the aliphatic tail of vitamin D<sub>3</sub> (following the C/D-rings) interact with  $\beta$ -strand I and the  $\alpha$ -helix of LG, respectively (Figure 1D). The crystal structure of the LG-vitamin D<sub>3</sub> complex shows clearly that the conformation of vitamin D<sub>3</sub> differs significantly between the two binding sites (Figure 1B). This fact explains why fatty acid and retinol are unable to bind at the secondary exosite. In the first phase of the present study, we tested the hypothesis that a  $\gamma$ -turn loop is essential to allow a stable interaction between vitamin D and the exosite (Figure 1D),<sup>9</sup> using LG mutants produced from *E. coli*.



### **Expression, purification and Western blot of rLG and its mutant**

Figure 3A shows that each rLG or mutant was abundantly expressed, with the average expressed levels being approximately 30% of total of total lysate proteins. As each mutant consists a 6 $\times$  His-tag, the molecular mass (~19.7 kDa) was slightly greater than that (18.4 kDa) of native LG. Each purified recombinant protein shows ~ 95% homogeneity in reducing SDS-PAGE, and this was verified with a Western blot using a LG-specific mAb (4D11) (Figure 3B).<sup>6</sup>

### **Vitamin D<sub>3</sub> binding to LG and rLG**

To determine whether rLG was capable of interacting with vitamin D in a manner similar to that of native LG, we monitored the quenching of Trp fluorescence for the binding according to an established method.<sup>6,9,10,21,22</sup> Figure 4A and Table 1 show that maximal vitamin D<sub>3</sub> binding to native LG was achieved at a ratio of 2:1, but that the binding to rLG remained at a ratio of 1:1. The expressed rLG hence incompletely mimics the native LG structure with a loss of one vitamin D binding site or partial loss for both sites. Because palmitate and retinol bind to only the central calyx, not to the exosite,<sup>18</sup> we used each of these two ligands as a 'marker' to monitor whether they still interact with rLG. The results revealed that neither palmitate nor retinol interact with rLG, as judged by the absence of Trp fluorescence changes (Table 1) indicating that the correct conformation of the central calyx was not present in rLG.

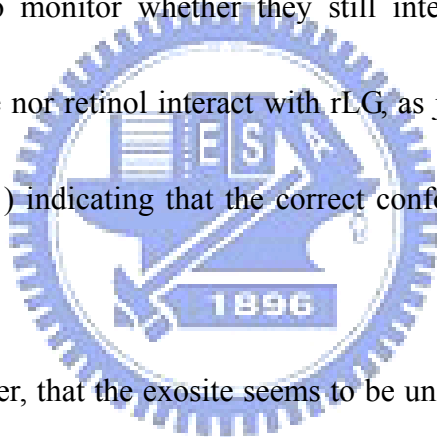


Figure 4A shows, however, that the exosite seems to be unaltered in rLG, as the binding ratio for vitamin D<sub>3</sub> remained at 1:1. Because heat treatment results in a loss of the central calyx but retention of the exosite,<sup>6,9,10</sup> we used heated LG (100 °C for 16 min) as a probe to compare its vitamin D<sub>3</sub> binding to rLG. The binding of heated LG attained a ratio of 1:1, similar to previous findings.<sup>9,10</sup> Interestingly, the ratios of vitamin D<sub>3</sub> binding to either heated LG or rLG were almost indistinguishable, and heat had no effect on rLG (Figure 4A, left panel). The affinities of heated LG, heated rLG and rLG for vitamin D<sub>3</sub> were also similar (Figure 4A; right panel). The number of vitamin D<sub>3</sub> binding sites predicted with a

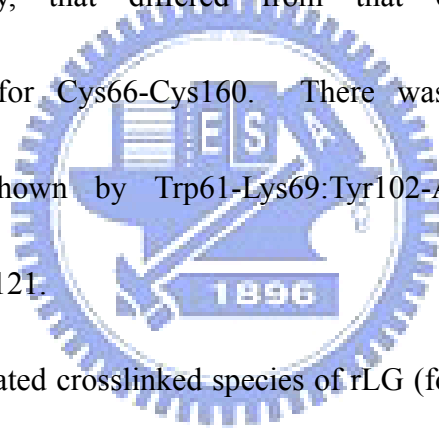
Cogan plot and the apparent dissociation constant calculated from the slope (Figure 4A, right panel) are listed in Table 1. The binding affinity of native LG (containing two binding sites) was about 5 nM ( $K_d^{app} = 4.7 \pm 0.37$  nM), which appears to be seven times that of rLG (containing exosite only) ( $K_d^{app} = 33.1 \pm 3.62$  nM).

Because the  $\beta$ -structure of LG is required to maintain the calyx,<sup>6,9</sup> we expected its structure to be altered in rLG. From analysis of the CD spectra, we verified the change of the typical  $\beta$ -structure in rLG according to a leftward shift of a symmetric dip at 215 nm characteristic of native LG (Figure 5A). Heat produced essentially no additional structural change in rLG. There was a minor difference in the CD spectra between heated LG and rLG, which might be due to the presence of His-tag in the rLG or to different disulfide linkages, described below. Notably, addition of vitamin D<sub>3</sub> to all LG species did not alter the overall CD spectra (data not shown). To confirm the loss of  $\beta$ -structure in expressed rLG, we used a  $\beta$ -structure-dependent specific LG monoclonal antibody (4H11E8)<sup>8</sup> to show that it recognized only native LG, not rLG, on a native gel Western blot (Figure 5B).

### **Further characterization of rLG using MALDI-TOF and carboxymethylation**

Recombinant LG apparently cannot fold to its native state in the *E. coli* expression system, which is a general issue when utilizing a given recombinant protein for the investigation of a structure-function relationship. In our case, the loss of the binding nature of the central calyx in rLG is probably due to the overall change in the  $\beta$ -structure (Figure 5).

Although the exact mechanism involved in such a change remains elusive, we attempted to further investigate whether the disulfide linkages (n=2 from a total of five Cys residues with one free –SH group at position 121 in native LG) are related. The use of limited trypsin-digested fragments of native, heated and recombinant LG in MALDI-TOF analysis revealed (Figure 6 A-D) that rLG contained two complicated intramolecularly crosslinked fragments, including Trp61-Lys69:Tyr102-Arg124 and Tyr102-Arg124:Leu149-Ile162 for Cys66-Cys106, Cys66-Cys119, or Cys66-Cys121 and Cys106-Cys160, Cys119-Cys160, or Cys121-Cys160, respectively, that differed from that of native LG, containing Trp61-Lys69:Leu149-Ile162 for Cys66-Cys160. There was an additional crosslinked fragment in heated LG shown by Trp61-Lys69:Tyr102-Arg124 for Cys66-Cys106, Cys66-Cys119, or Cys66-Cys121.



To elucidate the complicated crosslinked species of rLG (for example, dimerization was seen in both heated and recombinant LG), we irreversibly reduced all linkages by carboxymethylation using iodoacetic acid. Under these conditions, we found that native LG, heated LG and rLG were able to form monomers with almost the same homogeneity (Figure 6E). Interestingly, both carboxymethylated rLG and carboxymethylated heated LG had similar binding ratios (1:1) and affinities for vitamin D<sub>3</sub> to those without carboxymethylation, whereas carboxymethylated LG also exhibited a 1:1 ratio. Further heating of modified proteins did not affect the binding ratios (Table 1). These results indicate that disulfide

linkages are essential to maintain the necessary conformation of the central calyx, but are probably not particularly critical for exosite binding. The expressed rLG therefore provided us with a tool in the subsequent mutant tests involving monitoring of a single exosite interaction.

### **Vitamin D<sub>3</sub> binding to rLG mutants of $\gamma$ -turn loop residues 143-145**

According to the crystal structure of the LG-vitamin D<sub>3</sub> complex,<sup>9</sup> there is a direct interaction between vitamin D<sub>3</sub> and the side chains of Leu143 and Met145 in the  $\gamma$ -turn loop, because the distance between vitamin D<sub>3</sub> and each side chain is <3.8 Å (Figures 1D and 2B). We replaced each of these two residues with a positively charged Lys, a negatively charged Glu, or a hydrophobic Phe, by site-directed mutagenesis. The effect on the binding to vitamin D<sub>3</sub>, determined by fluorescence quenching, is shown in Figure 4B (Left and right panels) and Table 2. A markedly decreased binding affinity was seen when Leu143 was substituted with Lys or Glu (8.11-fold or 5.84-fold). Interestingly, there was only a slight decrease when it was replaced by a hydrophobic Phe residue (0.96-fold) (Figure 4B). A consistent pattern was likewise seen with the M145K, M145E and M145F mutants upon binding vitamin D<sub>3</sub> (Figure 4C).

Because Pro is typically found in a  $\gamma$ -turn, we tested the importance of Pro144 using P144A mutant. Figure 4D and Table 2 show significantly decreased binding of vitamin D<sub>3</sub> (4.6-fold) by the P144A mutant. Table 2 shows that the effects of these residues in the loop



region for vitamin D<sub>3</sub> interaction rank overall as Leu143 > Met145 > Pro144.

### **Interference of vitamin D<sub>3</sub> to $\gamma$ -turn specific mAb (1D8F8) binding with LG**

To select a mAb that might recognize the  $\gamma$ -turn region, we screened a LG mAb battery (n=900),<sup>5</sup> using a set of mutants as a probe. We found one LG mAb, 1D8F8, that was capable of reacting with the M145K, M145E and M145F mutants, but not with L143K, L143E and P144A mutants, according to a Western blot analysis (Figure 7A). MAb 1D8F8 is therefore specific for Leu143 and Pro144 located within the  $\gamma$ -turn loop. As Leu143 and Pro144 are located inside the exosite (Figure 1B,D), the presence of vitamin D<sub>3</sub> in the exosite is expected to interfere with the recognition of mAb 1D8F8, as depicted in our space-filling model (Figure 7B). As Figure 7C shows, the binding of vitamin D<sub>3</sub> to the “exosite” of native LG, heated LG or rLG attenuated the recognition of mAb 1D8F8, according to a dot-blot assay, but, with the use of retinol and palmitate as a control, neither ligands affected the binding of 1D8F8. This result provides additional evidence for the involvement of the  $\gamma$ -turn loop in the binding of vitamin D.

### **Biological activity of LG in vitamin D<sub>3</sub> uptake in mice**

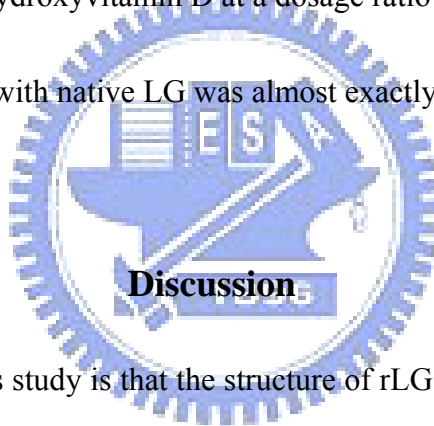
To investigate whether LG binding vitamin D can facilitate its uptake in an animal, we used the mouse as a model. We initially fed the animals (n=30) with milk and milk fractions (LG, whey protein or casein) all fortified with vitamin D<sub>3</sub> (final concentration 100  $\mu$ M) for 3 weeks, and then determined the plasma intake of 25-hydroxyvitamin D (a metabolite of

vitamin D). Figure 8A shows that the final mean concentrations of 25-hydroxyvitamin D in mice (n=5 in each group) fed with raw milk, whey protein (without casein) or LG each supplemented with vitamin D<sub>3</sub> were significantly greater than those without LG (containing no LG) (P<0.001). Casein, which lacks LG appears ineffective in the vitamin D uptake. The levels of 25-hydroxyvitamin D in all tested groups were elevated relative to the naive control without vitamin D<sub>3</sub> (P<0.001).

### **Role of the exosite in uptake of vitamin D<sub>3</sub> in mice**

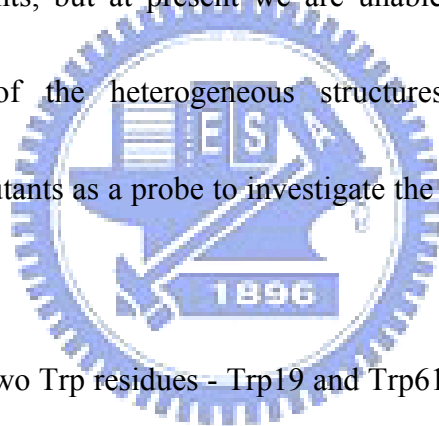
To test the hypothesis that the exosite of LG plays a role in the transport of vitamin D, we compared the uptake of vitamin D<sub>3</sub> between native LG (containing a calyx and an exosite) and heated LG (containing only an exosite) as a strategy to evaluate their variation in uptake, if any.<sup>6,9</sup> Mice (n=65) were separated into three major groups: those fed vitamin D<sub>3</sub> as a control (group 1), those fed LG supplemented with vitamin D<sub>3</sub> (group 2), and those fed heated LG supplemented with vitamin D<sub>3</sub> (group 3); mice fed with no vitamin D<sub>3</sub> were included as a baseline. Each subgroup of mice were then divided by increasing dosages of vitamin D<sub>3</sub> according to vitamin D<sub>3</sub>/LG ratios (0.4, 1, 2, and 3), while LG or heated LG was maintained at a constant concentration (250 μM). Under these conditions, we expected to see the effect of the dosage of vitamin D<sub>3</sub> on its transport by the exosite. Figure 8B shows a typical dose response in all three major groups supplemented with vitamin D<sub>3</sub>. Among these, the elevation of plasma 25-hydroxyvitamin D was prominent in group 2 (native LG supplemented

with vitamin D<sub>3</sub>). There seemed to be no saturation of 25-hydroxyvitamin D with vitamin D<sub>3</sub> at greater dosages in groups 2 and 3. When the values of the control group (group 1 fed vitamin D<sub>3</sub>) were subtracted from those of group 2 or 3, the levels of 25-hydroxyvitamin D appeared, remarkably, to be saturable (Figure 8C). The dose-response curves fit exactly the binding ratios of vitamin D<sub>3</sub> versus LG; native LG containing two sites to bind vitamin D<sub>3</sub> hence produces maximal concentrations of plasma 25-hydroxyvitamin D at a dosage ratio of 2:1 (vitamin D<sub>3</sub>/LG), whereas heated LG, consisting only the exosite, produces maximal concentrations of plasma 25-hydroxyvitamin D at a dosage ratio of 1:1. The final increase in plasma 25-hydroxyvitamin D with native LG was almost exactly twice that of heated LG.



The major concern of this study is that the structure of rLG produced in *E. coli* no longer mimics that of native LG. We demonstrated, using MALDI-TOF analysis, that this phenomenon is due primarily to the mis-crosslinking of five Cys residues present in rLG (Figure 6). rLG is composed of various dimeric and aggregated forms (Figure 6E). Interestingly, however, following the irreversible reduction of all disulfide linkages by carboxymethylation, these forms become a homogeneous species similar to that of carboxymethylated LG. The same is seen with heated LG. We then showed that all carboxymethylated proteins lost a calyx, as they failed to interact with retinol and palmitate,

but they still retained the ability to bind vitamin D<sub>3</sub>, with a binding affinity almost identical to that of reduced LG or nonreduced rLG (Table 1). These data indicate that disulfide linkages of LG probably do not greatly affect the secondary binding to vitamin D. The reason for using heated LG in this study was as a control to evaluate exosite binding for rLG, because almost identical binding was found with rLG and heated rLG (Figure 4A and Table 1). Whether the exosite of rLG maintains the same conformation as that of native LG is currently unknown. An ultimate solution is to obtain the crystal structure of the rLG-vitamin D complex, including the mutants, but at present we are unable to obtain a rLG-vitamin D crystal, probably because of the heterogeneous structures of rLG. We therefore subsequently used the rLG mutants as a probe to investigate the importance of the  $\gamma$ -turn loop in vitamin D binding.



Another concern is that two Trp residues - Trp19 and Trp61 - in LG were involved when binding is monitored using fluorescence quenching. Several previous studies suggested that the intrinsic fluorescence of LG is due almost exclusively to Trp19.<sup>24,25</sup> Trp19 is located at the bottom of the calyx, whereas Trp61 is more accessible to a solvent, and is thus able to make only a minor contribution to fluorescence emission.<sup>26</sup> On the basis of our previous studies,<sup>6,9,10</sup> at pH 2-6 or after thermal treatment to switch off the gate of the calyx, we showed that vitamin D<sub>3</sub> interacted with only the exosite (with 35~40% of maximal binding ability), but not retinol and palmitate. The change of fluorescence caused by the binding of

the exosite is 35~40% of that of the native LG containing two sites. The binding signal for the exosite is hence also attributed to Trp19, because Trp19 is located slightly away from the exosite. In addition, the fluorescence binding assay was conducted with a control (ethanol) and a blank (N-acetyl-L-tryptophanamide), to exclude the effects of a solvent and a ligand, respectively. Despite the small change in the fluorescence, Trp quenching in response to proximate ligand binding has served as a probe to investigate the dynamics of ligand and LG interactions.<sup>22</sup>

Regardless of the undesired structural changes in *E. coli*-expressed LG, we provide several observations that might support the idea that the  $\gamma$ -turn loop plays a role in the interaction between the exosite and vitamin D.<sup>9</sup> First, substituting each Leu143 and Met145 with charged amino acids resulted in a substantially decreased binding affinity of vitamin D<sub>3</sub> (4.7-fold to 8.1-fold in Table 2), which is consistent with a previous crystallographic report<sup>9</sup> showing the side chains of these two residues to be directly involved in vitamin D binding. It should be noted that these Leu and Met residues are projected into the interior of the protein, such that any mutation to charged residues would be highly disruptive of the structure of this loop; a change in vitamin D binding would therefore be expected. In contrast, such substitution might not greatly change the overall structure of the loop region, as demonstrated by the site-specific mAb 1D8F8 being able to recognize mutants M145K, M145E, and M145F (Figure 7A). The substitution of centered Pro144 by Ala also significantly

attenuated the binding affinity (4.6-fold in Table 2). Because Pro144 has no direct contact with vitamin D<sub>3</sub>,<sup>9</sup> we suggest that it might be essential to maintain the conformation of the loop structure. All mutants other than L143F and M145F impaired vitamin D binding. There is a strong inverse correlation ( $r = -0.94$ ) between the apparent dissociation constants and binding ratios for all mutants (Table 2). The binding ratios calculated from the Cogan plot are near 0.5 (Table 2), but the titration curve (Figure 4, left panel) revealed that maximal binding was achieved at a ratio of 1:1. In general, the Cogan plot might indicate only that an impaired binding ratio might be caused by a markedly decreased binding affinity due to a unique structural change in those mutants. For example, the L143F and M145F mutants still showed a ratio of 0.7. Hence, Phe residues maintain the necessary hydrophobicity, although the overall conformation in this region might undergo some change.

Second, the exosites of rLG, heated LG, carboxymethylated LG, carboxymethylated rLG and carboxymethylated heated LG recognize only vitamin D<sub>3</sub>, and neither palmitate nor retinol. This interaction appears to be ligand-specific and consistent with a previous study, in that there is no second binding site for palmitate and retinol.<sup>18</sup> Third, binding of vitamin D<sub>3</sub> to LG attenuated the recognition of a  $\gamma$ -turn loop specific mAb (1D8F8) (Figure 7).

With respect to the animal study, we found almost equal uptake of plasma 25-hydroxyvitamin D for mice dosed with equal concentration of LG in vitamin D<sub>3</sub>-fortified LG, whey protein (mainly LG and  $\alpha$ -lactoalbumin), and raw milk (Figure 8A). LG is

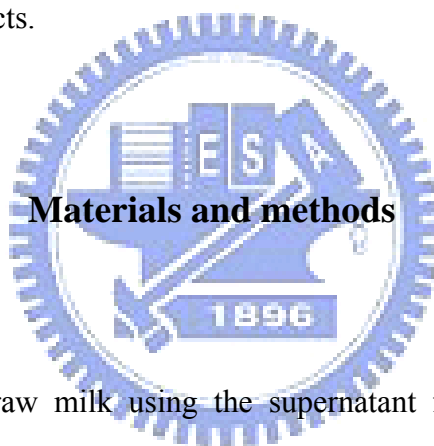
therefore probably the only vehicle that transports vitamin D in milk. Interestingly, the use of LG supplemented with vitamin D<sub>3</sub> at various dose revealed that native LG, comprising two vitamin D-binding sites, produced a maximal uptake of plasma vitamin D at a dosage ratio of 2:1 (vitamin D<sub>3</sub>/LG), whereas heated LG, possessing only an exosite, produced maximal uptake of plasma vitamin D at a dosage ratio of 1:1 (Figure 8). The final increase in plasma 25-hydroxyvitamin D caused by native LG was almost exactly twice that caused by heated LG. As a single mutation on the  $\gamma$ -turn loop (L143K) resulted in a maximal eight-fold decrease in binding affinity for vitamin D<sub>3</sub>, it would be of interest to investigate the effect of such a mutation on the uptake of vitamin D in animals. This experiment is, however, impracticable at present, because of the limited quantity of rLG isolated in our expression system.

Increased concentrations of vitamin D in plasma have been demonstrated to be associated with a decreased incidence of breast, ovarian, prostate and colorectal cancers.<sup>27,28</sup>

Because LG is a fraction that is directly responsible for enhancing the uptake of vitamin D in mice (Figure 8), there might be two advantages of the presence of an exosite in LG. The first is that the central calyx of LG is thought to be partially occupied by fatty acid in milk;<sup>29</sup> the available exosite might provide another route to transport vitamin D. Second, at present, the processing of many dairy products involves excessive heat for the purpose of sterilization. The presence of a thermally stable exosite might play a 'bypass' role in maintaining the binding and transport of vitamin D<sub>3</sub>. Such a unique property of LG is worth considering for

supplementing vitamin D in dairy products enriched with LG. It is worthy mentioning here that mice and humans lack an LG gene;<sup>30</sup> the present finding indicates that vitamin D supplementation in milk (the biochemical event) is therefore essential for general public health. This is well worth following up in species that do express LG.

In summary, this study indicates a potential role of the  $\gamma$ -turn (Leu-Pro-Met) in maintaining the structure of a secondary vitamin D binding site. The additional mouse experiment provides new insights into the transport role of LG and its supplementation with vitamin D used in dairy products.



### **Purification of native LG**

LG was purified from raw milk using the supernatant from a saturated ammonium sulfate fraction (40%), followed by chromatography on a G-150 column, as described previously.<sup>5</sup>

### **Analysis of the crystal structure of the LG-vitamin D<sub>3</sub> complex**

The crystal structure of LG in this context is deposited in the Protein Data Bank, code 2GJ5,<sup>9</sup> and the diagram created with RasMol<sup>31</sup> and O v7.0.<sup>32</sup>

### **Construction of plasmid pQE30-LG**



Total RNA was isolated from bovine mammary gland tissue; the cDNA was synthesized from RNA using M-MLV reverse transcriptase (Invitrogen, Carlsbad, CA, USA). The cDNA fragments encoding for LG<sup>33</sup> were amplified on proofreading DNA polymerase (Invitrogen) and cloned into the *Bam*HI-*Hind*III sites of an *E. coli* expression vector, pQE30 (Qiagen, Madison, WI, USA). The plasmids were screened in JM109 and expressed in M15 (pREP4) (Qiagen), with the final sequence of pQE30-LG being confirmed by DNA sequencing.<sup>34,35</sup>

#### **Site-directed mutagenesis**

Site-directed mutants (n=7) of LG (L143K, L143E, L143F, M145K, M145E, M145F, and P144A) were generated using oligonucleotides containing the desired mutation with the QuikChange PCR method (Stratagene, La Jolla, CA, USA); the pQE30-LG expression vector served as a template,<sup>36</sup> and the nucleotide sequencing confirmed. In addition, DNA nucleotide-sequencing analysis confirmed each inserted cDNA mutant of rLG to be correct.

#### **Expression and purification of rLG and its mutants**

*E. coli* [M15 (pREP4)] with pQE30-LG or its mutants were cultured in the LB medium (containing 100 µg/ml ampicillin and 1 mM isopropyl thio-β-D-galactoside) at 37 °C for 6 h on a rotary shaker. Cells were harvested at 8,000g for 20 min, resuspended in 40 ml of 20 mM Tris-HCl (pH 8.0), sonicated, and then centrifuged at 20,000g for 20 min at 4 °C. The pellet containing inclusion bodies was resuspended in 30 ml of 2 M urea containing 20 mM

Tris-HCl, 0.5 M NaCl, and 2% Triton X-100 (pH 8.0), sonicated as above, and then centrifuged at 20,000g for 20 min at 4 °C. The inclusion bodies were then lysed, dissolved in a binding buffer containing 20 mM Tris-HCl, 0.5 M NaCl, 5 mM imidazole, 6 M guanidine-HCl, and 1 mM 2-mercaptoethanol (pH 8.0), and passed through a syringe filter (0.45 µm). A HiTrap chelating column (GE Healthcare, Uppsala, Sweden) was washed with 0.1 M NiSO<sub>4</sub> and equilibrated with the binding buffer before the cell lysate was loaded as previously described.<sup>35</sup> The column-bound fraction was then treated with a binding buffer containing 6 M urea, and finished with the binding buffer without urea. The recombinant protein was finally eluted with a buffer containing 20 mM Tris-HCl, 0.5 M NaCl, and 250 mM imidazole without 2-mercaptoethanol (pH 8.0). Protein fractions were pooled, desalted on a P-2 column (Bio-Rad laboratories, Hercules, CA, USA), and lyophilized. The protein concentration was determined by the Lowry method,<sup>37</sup> using BSA as a standard.

### **Gel electrophoresis and immunoblot analysis**

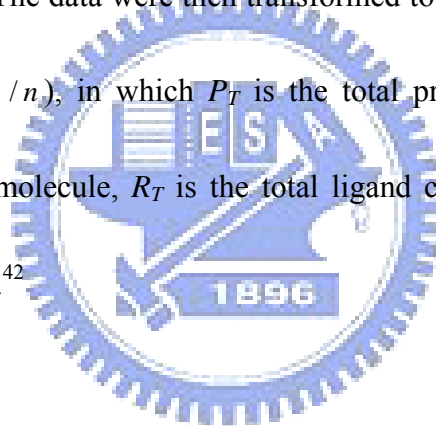
SDS-PAGE or native PAGE with 15% polyacrylamide gel was used to characterize rLG and its mutants, using a modified procedure similar to that described previously.<sup>7,38</sup> The sample for SDS-PAGE or native PAGE were mixed with a loading buffer (12 mM Tris-HCl, 0.4% SDS, 5% glycerol, and 0.02% bromphenol blue, pH 6.8) without thermal treatment to ensure the retention of the native structure of LG. For reducing PAGE, mercaptoethanol at a final concentration of 143 mM in the samples was used. Western blot analysis was

performed as described previously:<sup>6</sup> the electrotransferred samples were incubated with mAbs (4D11, 4H11E8, or 1D8F8),<sup>5</sup> and developed using 3,3'-di-aminobenzidine containing 0.01% H<sub>2</sub>O<sub>2</sub>.<sup>6</sup> Dot-blot to assess the interaction between vitamin D<sub>3</sub> and the exosite was performed using the samples of LG or LG-vitamin D<sub>3</sub> complex (ratio 1:10) spotted onto the membrane; the final binding was probed with a  $\gamma$ -loop specific mAb (1D8F8).

### **Vitamin D<sub>3</sub> binding to LG, rLG and rLG mutants**

The ligand-binding assay of LG was performed with fluorescence emission as previously established.<sup>6,9,10,21,22,24,25</sup> The binding of vitamin D<sub>3</sub> to LG was measured by fluorescence quenching of Trp19 of LG at 332 nm, using excitation at 287 nm. Fluorescence spectra (Cary Eclipse fluorescence spectrophotometer; Varian Inc., Palo Alto, CA, USA) were recorded at 24 °C. For the titration experiment, 5  $\mu$ M native LG, heated LG (preheated at 100 °C for 16 min), rLG or its mutants (in 10 mM phosphate buffer, pH 8.0) was instantly incubated with increased concentrations of vitamin D<sub>3</sub> (0.625-20  $\mu$ M in absolute ethanol). The final concentration of ethanol in the reaction mixture was such that it was < 3% at the endpoint of the titration. With this concentration, neither aggregation of LG nor a significant change in fluorescence emission was produced.<sup>39,40</sup> As in previous studies,<sup>6,9,10,21,22,25</sup> the titration of LG protein with various concentrations of ethanol (up to 3%) was evaluated and employed as an initial intrinsic fluorescence of LG before the addition of ligands. A solution of N-acetyl-L-tryptophanamide (Sigma-Aldrich, St Louis, MO, USA), with an absorbance at

287 nm that was equal to that of the tested protein, was also used as a blank during the ligand titration, according to the method previously established.<sup>21,22,25</sup> The decreased intensity of fluorescence of N-acetyl-L-tryptophanamide solution during the titration was thus not due to the interaction between ligand and tryptophanamide, but resulted from the inner filter effect as a consequence of ligand absorbance at 287 nm.<sup>41</sup> The change in fluorescence intensity at 332 nm depended on the amount of protein-ligand complex, allowing the calculation of  $a$  (the fraction of unoccupied ligand-binding sites), using the equation  $a = (F - F_{\text{sat}}) / (F_0 - F_{\text{sat}})$  as previously described.<sup>21,22,25</sup> The data were then transformed to a plot of the Cogan equation,  $(P_T a = (1/n)[R_T a / (1 - a)] - K_d^{\text{app}} / n)$ , in which  $P_T$  is the total protein concentration,  $n$  is the number of binding sites per molecule,  $R_T$  is the total ligand concentration, and  $K_d^{\text{app}}$  is the apparent dissociation constant.<sup>42</sup>



## CD

For CD measurement, 0.5 mg/ml of native or heated LG (100 °C for 16 min), rLG or its mutants (in 20 mM phosphate buffer, pH 7.0) was added to a cuvette of 1.0 mm path length.<sup>9,38</sup> The CD spectra were recorded 20 times on a Jasco-J715 spectropolarimeter (Jasco, Tokyo, Japan) at 24 °C over the range from 200 to 250 nm at a scan speed of 20 nm/min.

## MALDI-TOF MS analysis of trypsin-digested LG

For trypsin treatment, 100 µg of LG, heated LG or rLG in 50 µl of NaCl/Pi containing 0.02 M phosphate and 0.12 M NaCl (pH 7.4) was incubated with 1 µl of trypsin (0.5 mg/ml) at 37 °C for 16 h. The reaction was terminated by adding 1 mM phenylmethanesulfonyl fluoride. The trypsinized samples were then concentrated using C18 Zip-Tips and eluted with 50% acetonitrile/0.1% trifluoroacetic acid following the manufacturer's (Millipore, Billerica, MA, USA) standard protocol. MALDI-TOF MS was performed using a Microflex MALDI-TOF LRF20 mass spectrometer (Bruker Daltonics, Billerica, MA, USA). The Zip-Tips-purified peptide digests were spotted with an  $\alpha$ -cyano-4-hydroxycinnamic acid matrix and run in reflectron positive-ion mode at an accelerating voltage of 25 kV.

#### **Carboxymethylation of LG**

For carboxymethylation,<sup>6,8,38</sup> 5 mg of LG, heated LG or rLG was first dissolved in 2 ml of 0.1 M Tris-HCl buffer (pH 8.6) containing 6 M ultrapure urea and 0.02 M dithiothreitol. Following flushing with nitrogen for 2 h, 20 mg of iodoacetic acid was added to the reaction mixture, while the pH was maintained at 8.6 by the addition of 0.1 M NaOH, and incubation was performed for another 3 h. Finally, carboxymethylated LG, carboxymethylated heated LG and carboxymethylated rLG were desalted on a Bio-Gel P2 column, eluted with 0.05 M ammonium bicarbonate, and lyophilized.

#### **Animal experiments**

Female BALB/c mice (4 weeks old, n=95, obtained from the National Animal Center, National Science Council of Taiwan) were kept in an animal room (12 h light cycle, 21 °C) and fed with a standard diet; housing and management were according to guidelines established and approved by the National Science Council of Taiwan. In an initial test using milk fortified with vitamin D<sub>3</sub> and fortified milk components, mice (n=30) with body mass  $17.56 \pm 1.28$  g [mean  $\pm$  standard deviation (SD)] were randomly divided into six groups (n=5). Vitamin D<sub>3</sub> (100  $\mu$ M) was emulsified with raw milk, whey protein (milk without casein), casein (reconstituted to the milk volume), LG (250  $\mu$ M, approximately equivalent to the concentration in milk) or distilled water in a feeding bottle (*ad libitum*), and mice were fed with this for 3 weeks. Each mouse drank ~3-3.5 ml/day on average. The mean body mass of each group increased by 8% in general, and there was no significant difference among the groups at the end of the test. For the experiment dosing with vitamin D<sub>3</sub>, mice (n=65, with body mass  $17.73 \pm 1.17$  g, mean  $\pm$  SD) were divided into three major groups: group 1 (vitamin D<sub>3</sub>), group 2 (vitamin D<sub>3</sub> plus native LG), and group 3 (vitamin D<sub>3</sub> plus heated LG). The experiment was designed to investigate the relationship between the vitamin D-binding sites of LG and the uptake of vitamin D. LG serving as a vehicle was kept at a constant concentration (250  $\mu$ M) during the feeding period. Group 1 (n=20) without LG was dosed with only vitamin D<sub>3</sub>, as a control. All groups were given varied dosages: 100, 250, 500 or 750  $\mu$ M vitamin D<sub>3</sub> according to vitamin D<sub>3</sub>/LG ratios of 0.4, 1, 2 or 3, respectively. Group

2 (n=20) and group 3 (n=20) were provided with native LG (containing two binding sites) and heated LG (containing one binding site), respectively. As well as these three groups, one naive group given no vitamin D<sub>3</sub> and LG was included (n=5). Preparation of the vitamin D<sub>3</sub> supplement and the protocol (3 weeks) were as described above. Analysis of 25-hydroxyvitamin D in mouse plasma was conducted with a kit (25-Hydroxy Vitamin D Direct EIA, IDS Diagnostics, Fountain Hills, AZ, USA), according to the manufacturer's instructions.

### Acknowledgements

This work was supported by National Science Council (NSC) grants 92-2313-B-009-002, 93-2313-B009-002, 94-2313-B-009-001, 95-2313-B-009-001, and 97-2313-B-009-001-MY2 (Simon JT Mao), and NSC 94-2321-B-213-001, 95-2321-B-213-001-M (NSC), 963RSB02, and 973RSB02 (National Synchrotron Radiation Research Center) (Chun-Jung Chen).

### References

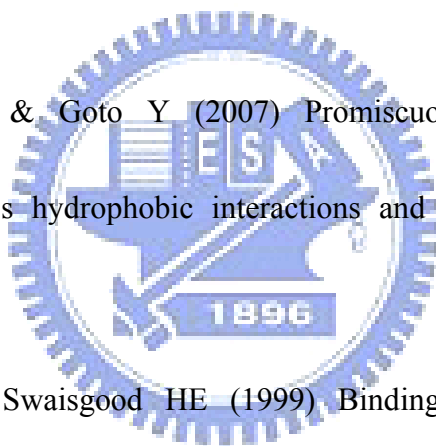
1. Hambling SG, MacAlpine AS & Sawyer L (1992) Beta-lactoglobulin. In *Advanced Dairy Chemistry I* (Fox PF eds) pp. 141-190. Elsevier, Amsterdam.
2. Sawyer L & Kontopidis G (2000) The core lipocalin, bovine beta-lactoglobulin. *Biochim Biophys Acta* **1482**, 136-148.

3. Marshall K (2004) Therapeutic applications of whey protein. *Altern Med Rev* **9**, 136-156.
4. Sava N, Van der Plancken I, Claeys W & Hendrickx M (2005) The kinetics of heat-induced structural changes of beta-lactoglobulin. *J Dairy Sci* **88**, 1646-1653.
5. Chen WL, Huang MT, Liu HC, Li CW & Mao SJT (2004) Distinction between dry and raw milk using monoclonal antibodies prepared against dry milk proteins. *J Dairy Sci* **87**, 2720-2729.
6. Song CY, Chen WL, Yang MC, Huang JP & Mao SJT (2005) Epitope mapping of a monoclonal antibody specific to bovine dry milk: involvement of residues 66-76 of strand D in thermal denatured beta-lactoglobulin. *J Biol Chem* **280**, 3574-3582.
7. Chen WL, Hwang MT, Liao CY, Ho JC, Hong KC & Mao SJT (2005)  $\beta$ -Lactoglobulin is a Thermal Marker in Processed Milk as Studied by Electrophoresis and Circular Dichroic Spectra. *J Dairy Sci* **88**, 1618-1630.
8. Chen WL, Liu WT, Yang MC, Hwang MT, Tsao JH & Mao SJT (2006) A novel conformation-dependent monoclonal antibody specific to the native structure of beta-lactoglobulin and its application. *J Dairy Sci* **89**, 912-921.
9. Yang MC, Guan HH, Liu MY, Lin YH, Yang JM, Chen WL, Chen CJ & Mao SJT (2008) Crystal structure of a secondary vitamin D<sub>3</sub> binding site of milk beta-lactoglobulin. *Proteins* **71**, 1197-1210.



10. Yang MC, Guan HH, Yang JM, Ko CN, Liu MY, Lin YH, Huang YC, Chen CJ & Mao SJT (2008) Rational design for crystallization of  $\beta$ -lactoglobulin and vitamin D<sub>3</sub> complex: revealing a secondary binding site. *Cryst Growth Des* **8**, 4268-4276.
11. Qin BY, Bewley MC, Creamer LK, Baker EN & Jameson GB (1999) Functional implications of structural differences between variants A and B of bovine beta-lactoglobulin. *Protein Sci* **8**, 75-83.
12. Greene LH, Hamada D, Eyles SJ & Brew K (2003) Conserved signature proposed for folding in the lipocalin superfamily. *FEBS Lett* **553**, 39-44.
13. Lüthy R, Bowie JU & Eisenberg D (1992) Assessment of protein models with three-dimensional profiles. *Nature* **356**, 83-85.
14. Kontopidis G, Holt C & Sawyer L (2004) Invited review: beta-lactoglobulin: binding properties, structure, and function. *J Dairy Sci* **87**, 785-796.
15. Adams JJ, Anderson BF, Norris GE, Creamer LK & Jameson GB (2006) Structure of bovine beta-lactoglobulin (variant A) at very low ionic strength. *J Struct Biol* **154**, 246-254.
16. Bello M, Pérez-Hernández G, Fernández-Velasco DA, Arreguín-Espinosa R & García-Hernández E (2008) Energetics of protein homodimerization: effects of water sequestering on the formation of beta-lactoglobulin dimer. *Proteins* **70**, 1475-1487.

17. Wu SY, Perez MD, Puyol P & Sawyer L (1999) beta-lactoglobulin binds palmitate within its central cavity. *J Biol Chem* **274**, 170-174.
18. Kontopidis G, Holt C & Sawyer L (2002) The ligand-binding site of bovine beta-lactoglobulin: evidence for a function? *J Mol Biol* **318**, 1043-1055.
19. Considine T, Singh H, Patel HA & Creamer LK (2005) Influence of binding of sodium dodecyl sulfate, all-trans-retinol, and 8-anilino-1-naphthalenesulfonate on the high-pressure-induced unfolding and aggregation of beta-lactoglobulin B. *J Agric Food Chem* **53**, 8010-8018.
20. Konuma T, Sakurai K & Goto Y (2007) Promiscuous binding of ligands by beta-lactoglobulin involves hydrophobic interactions and plasticity. *J Mol Biol* **368**, 209-218.
21. Wang Q, Allen JC & Swaisgood HE (1999) Binding of lipophilic nutrients to beta-lactoglobulin prepared by bioselective adsorption. *J Dairy Sci* **82**, 257-264.
22. Wang Q, Allen JC & Swaisgood HE (1997) Binding of vitamin D and cholesterol to beta-lactoglobulin. *J Dairy Sci* **80**, 1054-1059.
23. Kuwata K, Shastry R, Cheng H, Hoshino M, Batt CA, Goto Y & Roder H (2001) Structural and kinetic characterization of early folding events in  $\beta$ -lactoglobulin. *Nat Struct Biol* **8**, 151-155.



24. Cho Y, Batt CA & Sawyer L (1994) Probing the retinol-binding site of bovine beta-lactoglobulin. *J Biol Chem* **269**, 11102-11107.
25. Wang Q, Allen JC & Swaisgood HE (1997) Binding of retinoids to beta-lactoglobulin isolated by bioselective adsorption. *J Dairy Sci* **80**, 1047-1053.
26. Brownlow S, Morais Cabral JH, Cooper R, Flower DR, Yewdall SJ, Polikarpov I, North AC & Sawyer L (1997) Bovine beta-lactoglobulin at 1.8 Å resolution--still an enigmatic lipocalin. *Structure* **5**, 481-495.
27. Vieth R (2001) Vitamin D nutrition and its potential health benefits for bone, cancer and other conditions. *J Nutr Environ Med* **11**, 275-291.
28. Lappe JM, Travers-Gustafson D, Davies KM, Recker RR & Heaney RP (2007) Vitamin D and calcium supplementation reduces cancer risk: results of a randomized trial. *Am J Clin Nutr* **85**, 1586-1591.
29. Pérez MD, Díaz de Villegas C, Sánchez L, Aranda P, Ena JM & Calvo M (1989) Interaction of fatty acids with beta-lactoglobulin and albumin from ruminant milk. *J Biochem* **106**, 1094-1097.
30. Simons JP, McClenaghan M & Clark AJ (1987) Alteration of the quality of milk by expression of sheep beta-lactoglobulin in transgenic mice. *Nature* **328**, 530-532.
31. Sayle RA & Milner-White EJ (1995) RASMOL: biomolecular graphics for all. *Trends Biochem Sci* **20**, 374-376.

32. Jones TA, Zou JY, Cowan SW & Kjeldgaard M (1991) Improved methods for building protein models in electron density maps and the location of errors in these models. *Acta Crystallogr A* **47**, 110-119.
33. Jamieson AC, Vandeyar MA, Kang YC, Kinsella JE & Batt CA (1987) Cloning and nucleotide sequence of the bovine beta-lactoglobulin gene. *Gene* **61**, 85-90.
34. Lai IH, Tsai TI, Lin HH, Lai WY & Mao SJT (2007) Cloning and expression of human haptoglobin subunits in Escherichia coli: delineation of a major antioxidant domain. *Protein Expr Purif* **52**, 356-362.
35. Lai IH, Lin KY, Larsson M, Yang MC, Shiau CH, Liao MH & Mao SJT (2008) A unique tetrameric structure of deer plasma haptoglobin--an evolutionary advantage in the Hp 2-2 phenotype with homogeneous structure. *FEBS J* **275**, 981-993.
36. Ju M, Stevens L, Leadbitter E & Wray D (2003) The Roles of N- and C-terminal determinants in the activation of the Kv2.1 potassium channel. *J Biol Chem* **278**, 12769-12778.
37. Lowry OH, Rosebrough NJ, Farr AL & Randall RJ (1951) Protein measurement with the Folin phenol reagent. *J Biol Chem* **193**, 265-275.
38. Tseng CF, Lin CC, Huang HY, Liu HC & Mao SJT (2004) Antioxidant role of human haptoglobin. *Proteomics* **4**, 2221-2228.

39. Dufour E & Haertlé T (1990) Alcohol-induced changes of beta-lactoglobulin retinol-binding stoichiometry. *Protein Eng* **4**,185-190.
40. Dufour E, Genot C & Haertlé T (1994) beta-Lactoglobulin binding properties during its folding changes studied by fluorescence spectroscopy. *Biochim Biophys Acta* **1205**, 105-112.
41. Dufour E & Haertlé T (1991) Binding of retinoids and beta-carotene to beta-lactoglobulin. Influence of protein modifications. *Biochim Biophys Acta* **1079**, 316-320.
42. Cogan U, Kopelman M, Mokady S & Shinitzky M (1976) Binding affinities of retinol and related compounds to retinol binding proteins. *Eur J Biochem* **65**, 71-78.

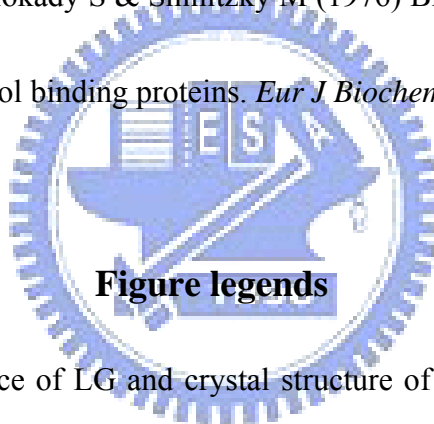


**Figure 1.** Amino acid sequence of LG and crystal structure of the LG-vitamin D<sub>3</sub> complex.

(A) LG comprises 162 amino acids with nine  $\beta$ -sheet strands (A-I). The  $\alpha$ -helix with three turns is located between residues 130 and 141 (yellow). (B) Space-filling drawing of the LG-vitamin D<sub>3</sub> complex at resolution 2.4 Å. Vitamin D<sub>3</sub> (carbon yellow and oxygen red) and LG are drawn on the basis of our previously refined model,<sup>9,10</sup> with one vitamin D<sub>3</sub> molecule penetrating inside the calyx (left) and the other lying on the surface pocket at the C-terminus (residues 136-149) (right). (C) Front view of vitamin D<sub>3</sub> binding to the exosite and chemical structure of vitamin D<sub>3</sub>. (D) The 3D ribbon model of the LG-vitamin D<sub>3</sub>

complex shows that the exosite combines an  $\alpha$ -helix (red) and  $\beta$ -strand I (pink) with a  $\gamma$ -turn loop (green). (A) and (B) are reproduced from our previous study,<sup>9</sup> with permission of the publisher.

**Figure 2.** Amphipathic  $\alpha$ -helix of LG and its interaction with vitamin D<sub>3</sub>. (A) Unique amphipathic  $\alpha$ -helix of LG. (B) Final refined model with the  $2|F_{obs} - F_{calc}|$  electron density showing that the bulk of the density is sufficient to cover the vitamin D<sub>3</sub> in the exosite. The figures are reproduced from our previous study,<sup>9</sup> with permission of the publisher.

**Figure 3.** Expression and purification of recombinant LG and its mutants from *E. coli*. (A) SDS-PAGE (in the presence of mercaptoethanol) of native LG isolated from milk, cell lysate (paired left), and isolated rLG (paired right). (B) Western blot of cell lysate and isolated rLG mutants using a LG specific mAb (4D11). M represents a molecular marker.

**Figure 4.** Fluorescence titration curves of native and heated LG, non-heated and heated rLG or rLG mutants with vitamin D<sub>3</sub>. Left panel: titration curve of native LG, heated LG, rLG and heated rLG (A) and mutants (B-D) with vitamin D<sub>3</sub>. Right panel: Cogan plot per titration curve.  $P_T$  = total protein concentration,  $R_T$  = total ligand concentration, and  $a$  = fraction of unoccupied ligand sites on the protein. The dashed line in each right-hand panel represents the titration plot of rLG only, used for reference. Each point represents the mean of triplicate determinations. The average SD was less than 5-8% of the mean.

**Figure 5.** CD and Western blot analysis of rLG. (A) Native LG exhibits primarily a typical

$\beta$ -sheet conformation with a symmetrical dip at 215 nm. (B) MAb (4H11E8) specific for the native  $\beta$ -structure.<sup>8</sup> Western blot was performed using a 15% native PAGE.

**Figure 6.** MALDI-TOF MS analysis of trypsin-digested LG and carboxymethylation of LG.

(A) Predicted trypsin cleavage sites (red bar, indicating cleavage probability) of LG isoform A obtained using a peptide cutter program (<http://au.expasy.org/tools/peptidecutter/>). The expected masses of peptide fragments (blue) and the disulfide linkages (orange bar) of native LG are depicted. LG isoform A with Asp64 and Val118 and isoform B with Gly64 and Ala118 in fragments 61-69 and 102-124 are shown in red. (B) MALDI-TOF spectrum of trypsin-digested native LG. Two mass spectra showing ions with  $m/z$  2721.286 for isoform B and  $m/z$  2779.288 for isoform A are representative for the fragment Trp61-Lys69:Leu149-Ile162 containing the disulfide linkage Cys66-Cys160. (C) Spectrum of trypsin-digested heated LG. Ions with  $m/z$  3317.565 and  $m/z$  3796.354 represent the dimeric Leu149-Ile162 and Trp61-Lys69:Tyr102-Arg124. (D) Spectrum of trypsin-digested rLG. Ions with  $m/z$  3805.000 and  $m/z$  4342.204 represent Trp61-Lys69:Tyr102-Arg124 and Tyr102-Arg124:Leu149-Ile162. (E) SDS-PAGE in the absence of mercaptoethanol of native LG, heated LG and rLG with or without carboxymethylation (CM). HLG, CM and HCM denote heated LG, carboxymethylated and heated carboxymethylated proteins, respectively. The molecular marker (M) is shown.

**Figure 7.** Identification and epitope mapping of a  $\gamma$ -turn-specific mAb and the

structure-function relationship between the  $\gamma$ -turn loop and vitamin D<sub>3</sub>. (A) Identification of a mAb (1D8F8) specific for a  $\gamma$ -turn loop of LG, utilizing rLG mutants on a Western blot. 1D8F8 recognizes native LG, rLG and some rLG mutants, but not mutants L143K, L143E, and P144A, indicating that  $\gamma$ -turn residues 143-144 are located within the epitope. (B) A space-filling model depicting residues 143 and 144 (green). They are within the vitamin D-binding exosite shared with 1D8F8. (C) Effect of vitamin D<sub>3</sub> binding on the immunoreactivity of LG, determined using dot-blot followed by scanning densitometric analysis (n=3). R, P and D<sub>3</sub> represent retinol, palmitate and vitamin D<sub>3</sub>, respectively.

**Figure 8.** Effect of LG on vitamin D<sub>3</sub> uptake in mice. (A) Concentration of 25-hydroxyvitamin D in plasma of mice fed (n=5 for each group) with milk or its components supplemented with vitamin D<sub>3</sub> (100  $\mu$ M). (B) Effect of native LG (containing the calyx and exosite) and heated LG (containing only the exosite) on uptake of vitamin D: each subgroup of mice (n=5) was dosed with vitamin D<sub>3</sub> in groups 2 and 3 (0, 100, 250, 500 and 750  $\mu$ M), according to ratios 0, 0.4, 1, 2 and 3, respectively, of vitamin D<sub>3</sub>/LG; vitamin D<sub>3</sub> alone (group 1) served as a control group. The concentration of LG was kept constant (250  $\mu$ M). (C) Final “adjusted” uptake of vitamin D after subtracting the value for the vitamin D<sub>3</sub> control group (group 1) from those for the vitamin D<sub>3</sub>-fortified native LG (group 2) or the vitamin D<sub>3</sub>-fortified heated LG group (group 3).



**Table 1.** Apparent dissociation constants and ratios for binding of ligands to native LG and rLG

Ligand	Protein	Binding ratio calculated from Cogan plot (ligand / LG)	$K_d^{app}$ ( $10^{-9}$ M)
		$\bar{X} \pm SD$	$\bar{X} \pm SD$
Vitamin D <sub>3</sub>	Native LG	1.76 ± 0.12	4.7 ± 0.37
	Heated LG	0.84 ± 0.05	45.7 ± 3.12
	rLG	0.73 ± 0.03	33.1 ± 3.62
	Heated rLG	0.72 ± 0.02	38.6 ± 3.56
	Carboxymethylated LG <sup>a</sup>	0.84 ± 0.02	35.2 ± 2.92
	Carboxymethylated heated LG <sup>a</sup>	0.84 ± 0.05	39.2 ± 3.08
	Carboxymethylated rLG <sup>a</sup>	0.79 ± 0.03	32.8 ± 3.61
	Carboxymethylated LG with heat treatment <sup>a</sup>	0.83 ± 0.02	35.2 ± 3.03
	Carboxymethylated heated LG with heat treatment <sup>a</sup>	0.83 ± 0.03	40.0 ± 2.38
	Carboxymethylated rLG with heat treatment <sup>a</sup>	0.78 ± 0.03	33.1 ± 3.41
Retinol	Native LG	0.91 ± 0.09	17.3 ± 1.62
	Heated LG	<sup>b</sup>	-
	rLG	-	-
	Heated rLG	-	-
	Carboxymethylated LG	-	-
	Carboxymethylated heated LG	-	-
	Carboxymethylated rLG	-	-
	Carboxymethylated LG with heat treatment	-	-
	Carboxymethylated heated LG with heat treatment	-	-
	Carboxymethylated rLG with heat treatment	-	-
Palmitate	Native LG	0.80 ± 0.072	44.0 ± 4.56
	Heated LG	-	-
	rLG	-	-
	Heated rLG	-	-
	Carboxymethylated LG	-	-
	Carboxymethylated heated LG	-	-
	Carboxymethylated rLG	-	-
	Carboxymethylated LG with heat treatment	-	-
	Carboxymethylated heated LG with heat treatment	-	-
	Carboxymethylated rLG with heat treatment	-	-

<sup>a</sup> The titration experiment was conducted as for other proteins, but is not shown in figure 4.

<sup>b</sup> No fluorescence change or no binding in titration experiment.

**Table 2.** Apparent dissociation constants and ratios for binding of vitamin D<sub>3</sub> to rLG and its  $\gamma$ -turn loop region mutants

	<b>Binding ratio calculated from Cogan plot (vitamin D<sub>3</sub> / LG)</b>	$K_d^{app}$ (10 <sup>-9</sup> M)	<b>Fold decrease in binding affinity</b>
	$\bar{X} \pm SD$	$\bar{X} \pm SD$	
Wild type	0.73 ± 0.03	33.1 ± 3.62 <sup>a</sup>	
L143K	0.50 ± 0.02	301.1 ± 13.16	8.11
L143E	0.50 ± 0.02	226.3 ± 9.83	5.84
L143F	0.70 ± 0.02	64.8 ± 3.91	0.96
P144A	0.50 ± 0.02	185.3 ± 8.18	4.6
M145K	0.53 ± 0.02	208.6 ± 9.19	5.31
M145E	0.56 ± 0.02	189.8 ± 8.47	4.74
M145F	0.71 ± 0.02	59.7 ± 3.87	0.81

<sup>a</sup> P < 0.001 as compared to mutants. Data represent means of triplicate determinations.

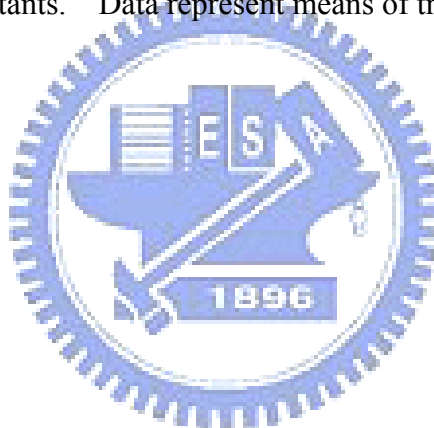


**Figure 1**

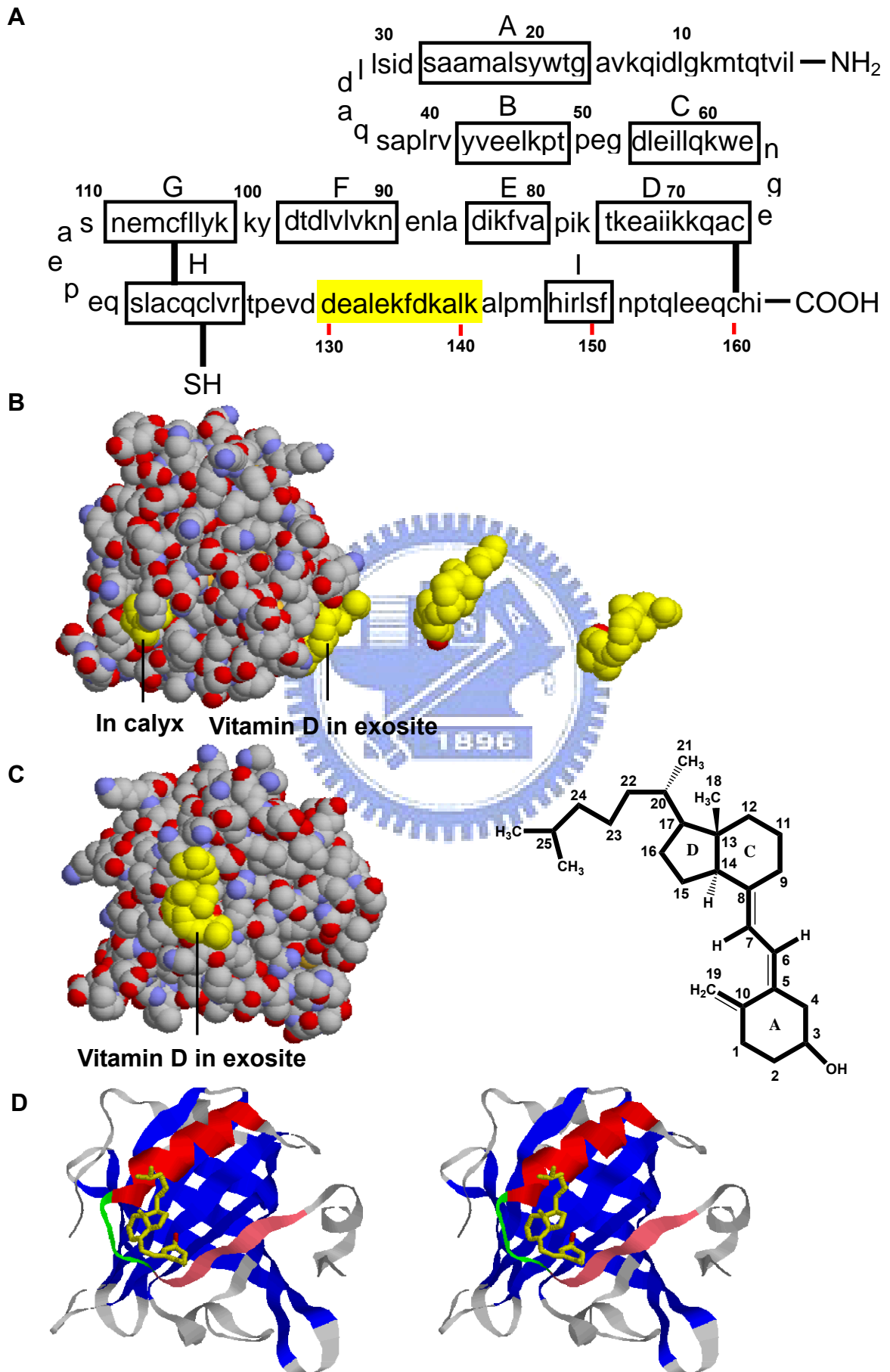
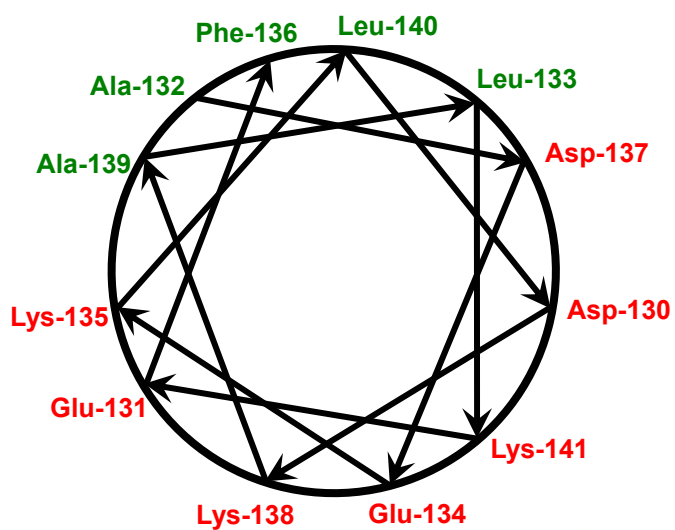


Figure 2

A. Amphipathic  $\alpha$ -helix in residues 130-141



B. Electron density map around the exosite containing the  $\gamma$ -turn loop

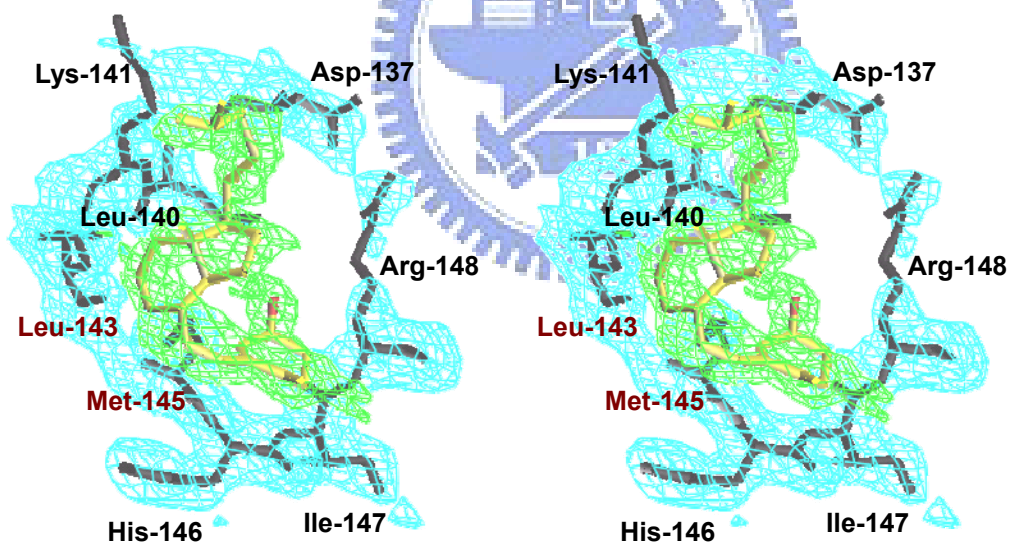


Figure 3

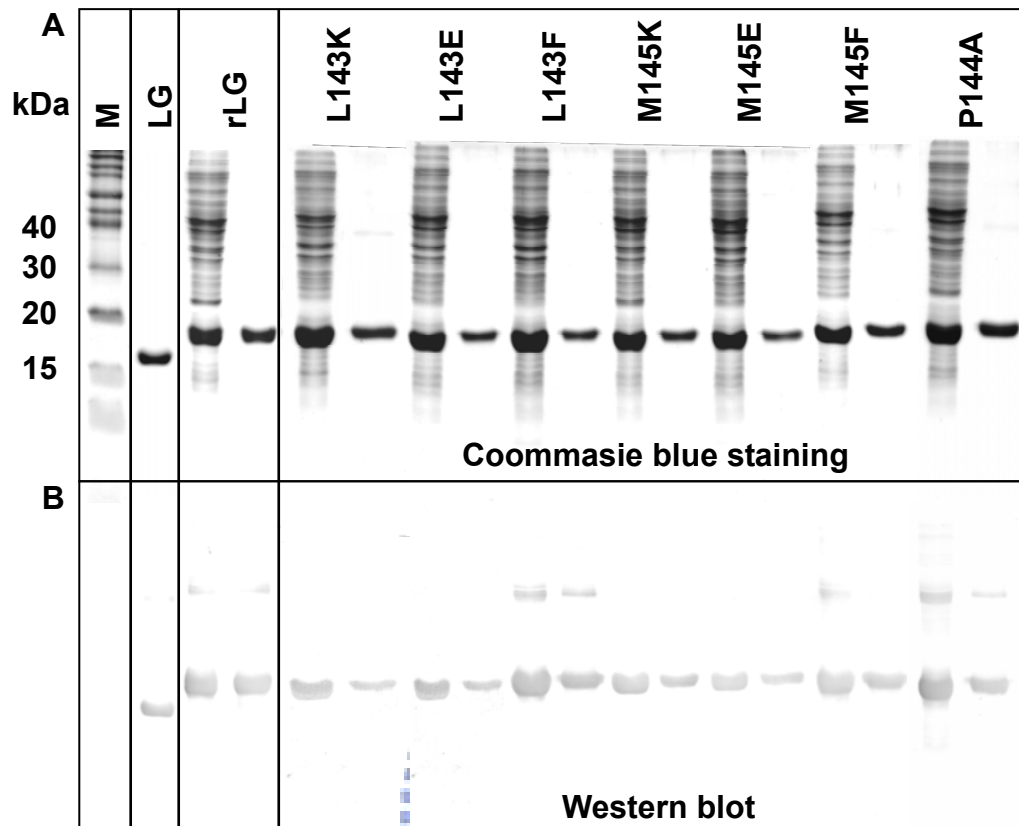


Figure 4

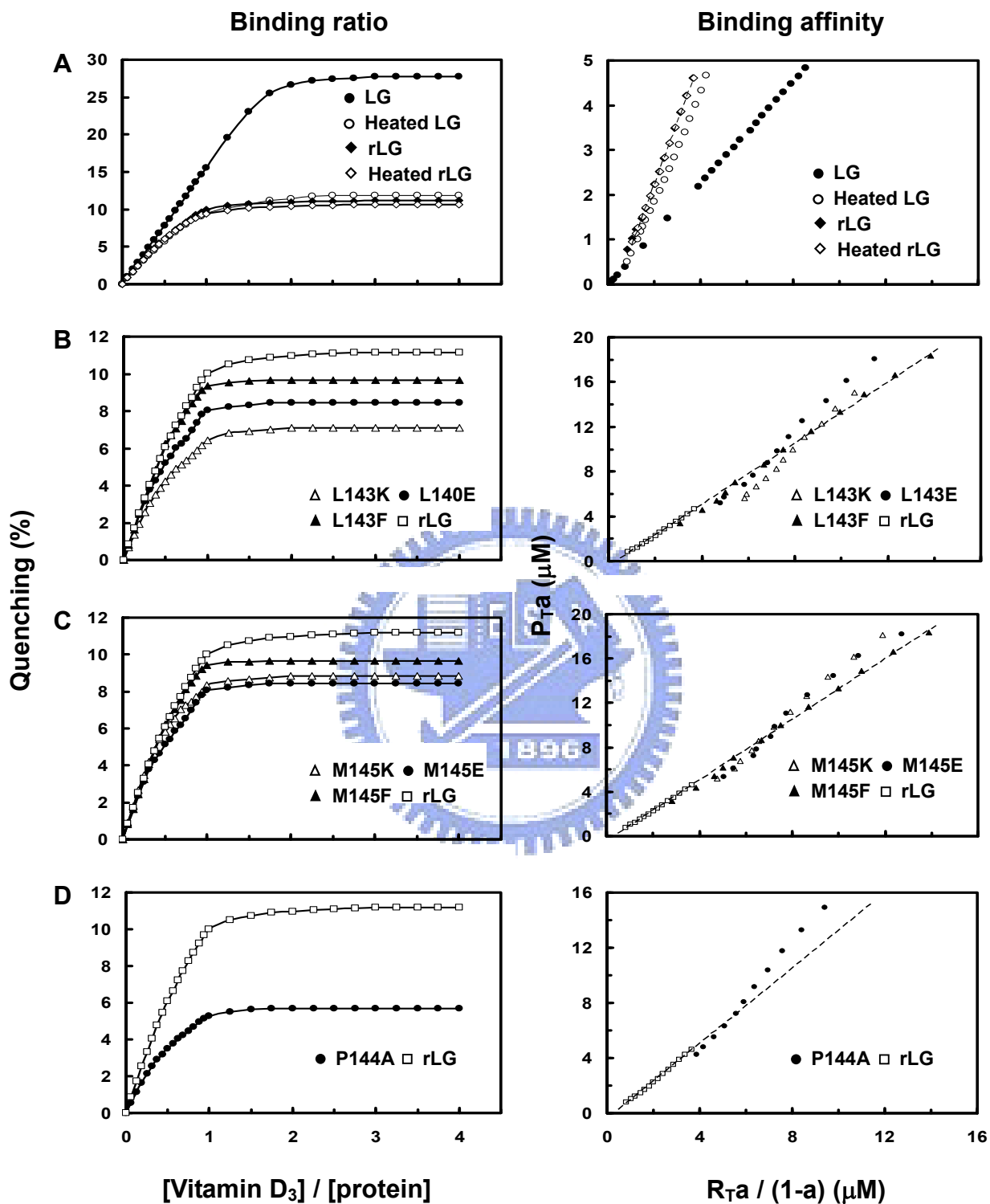
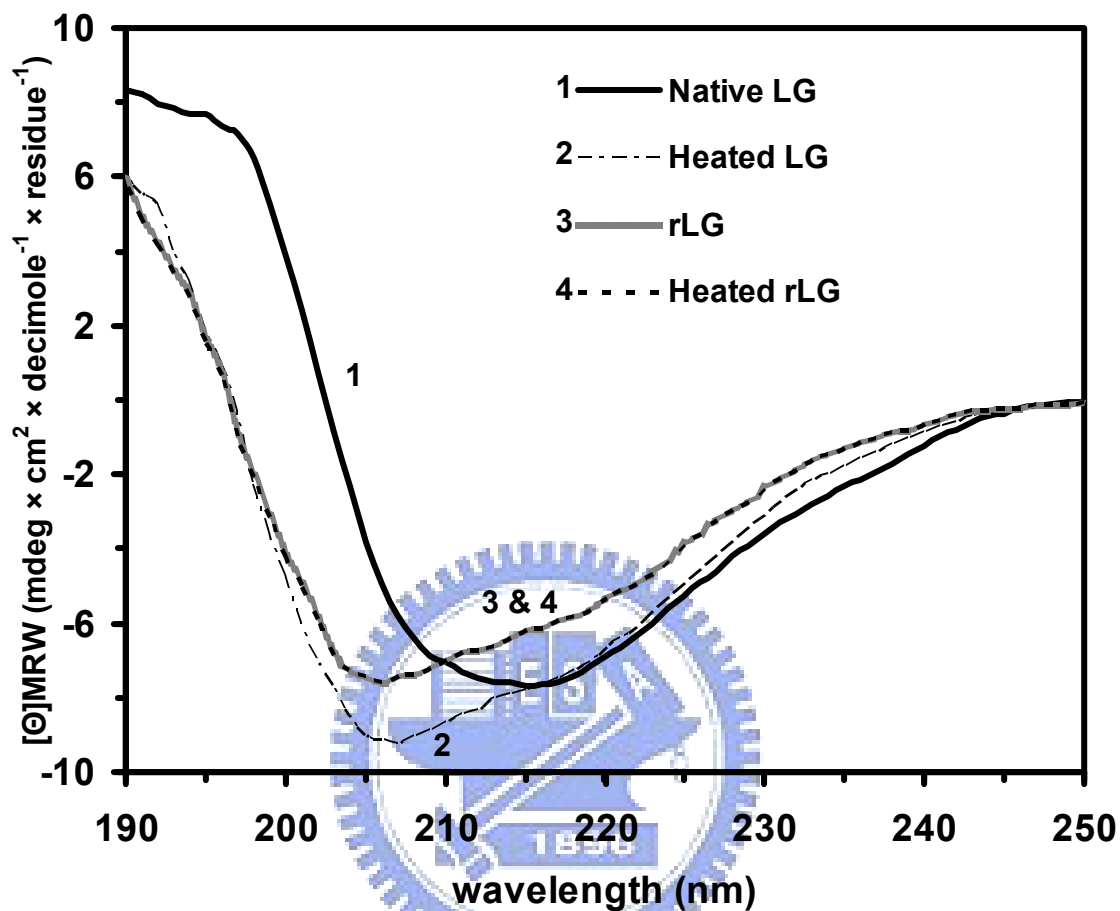


Figure 5

A. Circular Dichroic Spectra



B. Western blot using  $\beta$ -structure-dependent mAb (4H11E8) on native-PAGE



Figure 6

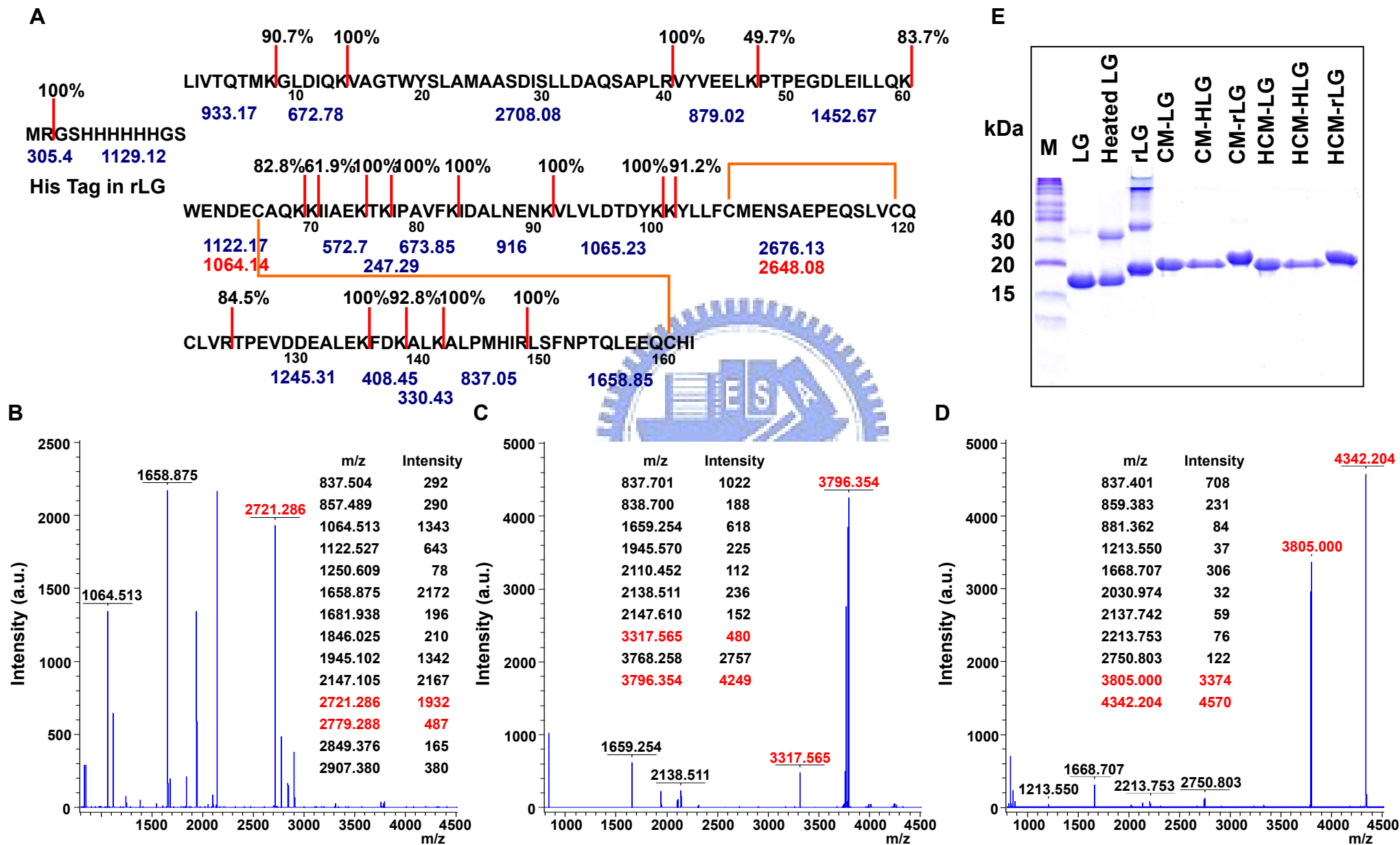
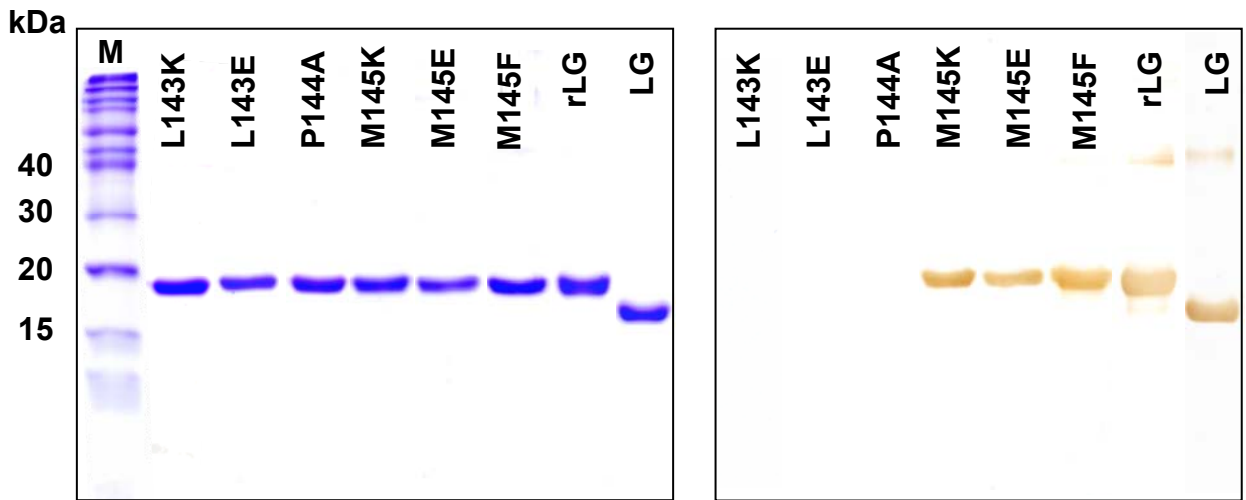


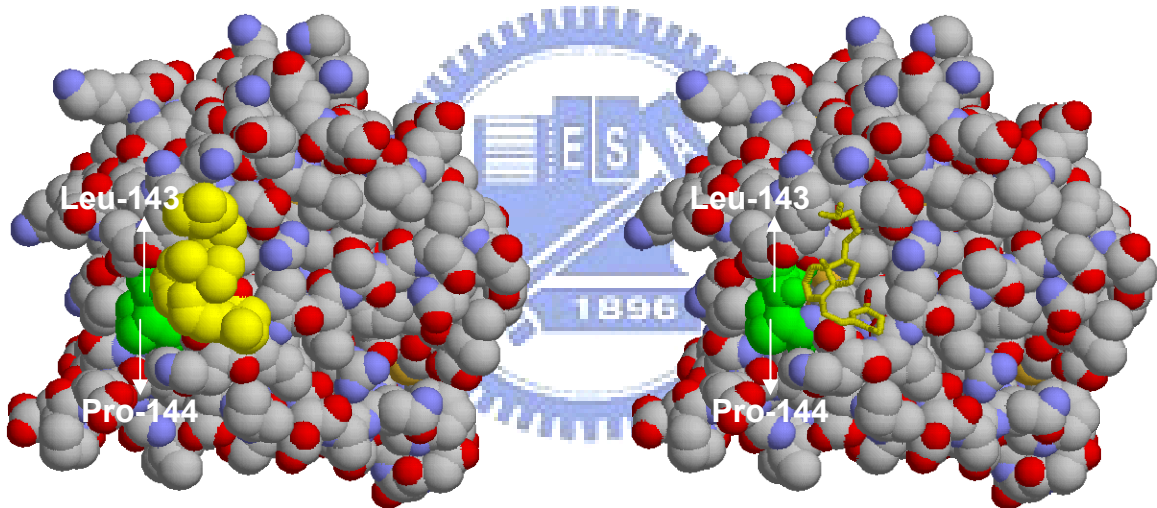


Figure 7

A. Mapping of exosite-specific mAb (1D8F8)



B. Antigenic epitope of  $\gamma$ -turn specific mAb (1D8F8)



C. Effect of vitamin D<sub>3</sub> binding on  $\gamma$ -turn specific mAb (1D8F8)

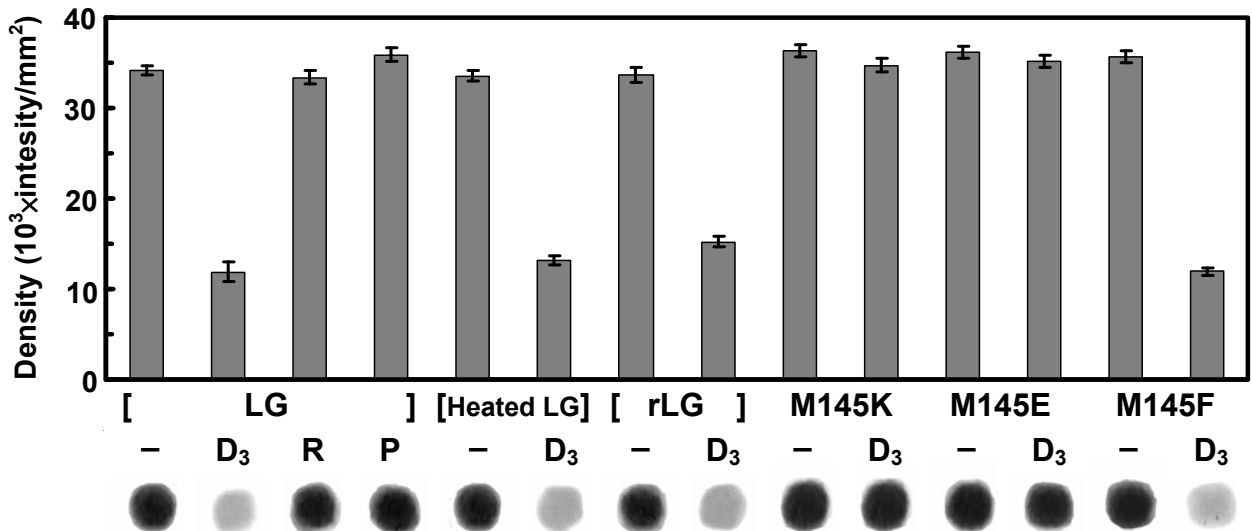
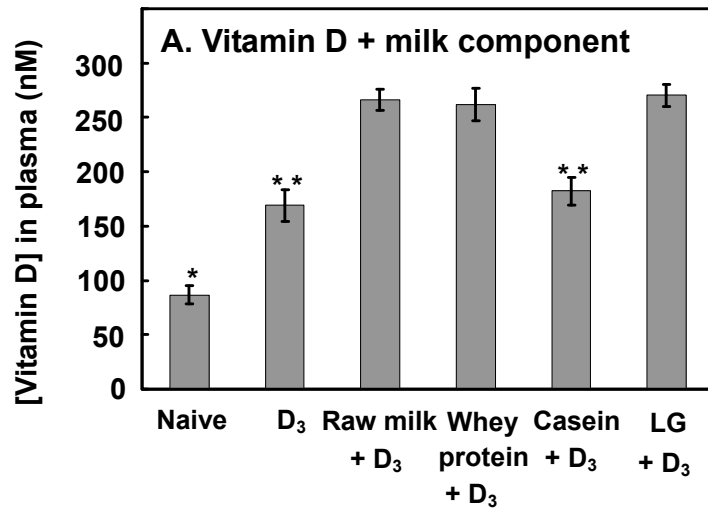
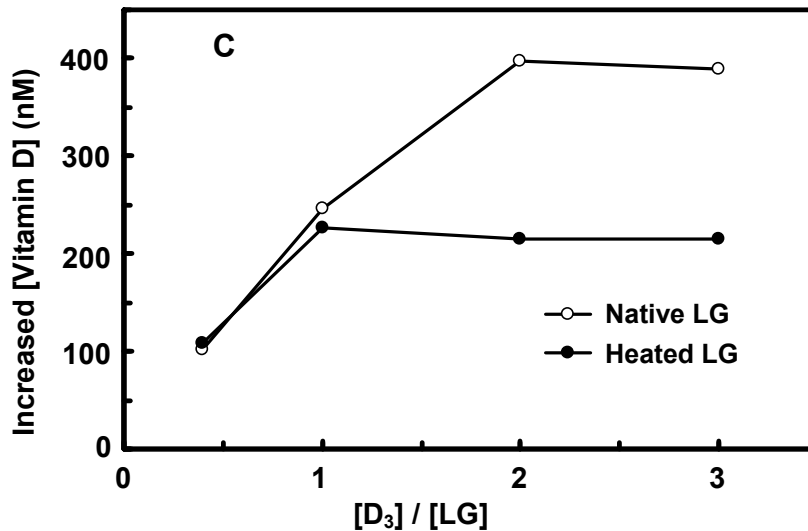
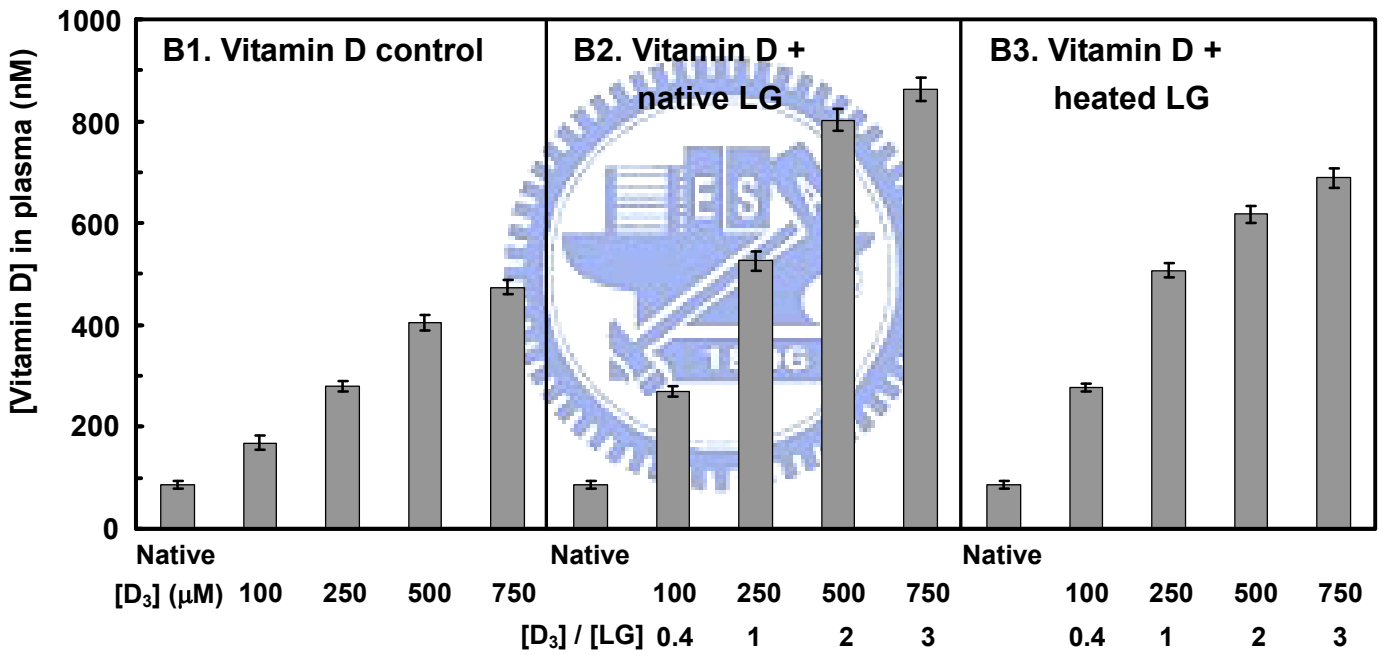


Figure 8



\* P < 0.001 as compared to all the other group.

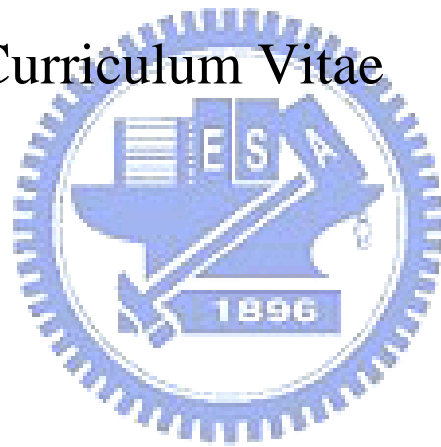
\*\* P < 0.001 as compared to all the other group.



# Appendix



# Curriculum Vitae



## Curriculum Vitae

**Ming Chi Yang (楊明誌), Ph.D.**

Date of Birth: October 10, 1981

Institute of Biochemical Engineering,  
National Chiao Tung University  
75 Po-Ai Street,  
Hsinchu 30050, Taiwan.  
Tel: +886-3-571-2121 ext. 56939  
Mobile Tel: +886-9-32936291  
Fax: +886-3-572-9288  
E-mail: b881641@life.nthu.edu.tw

國立交通大學  
生化工務研究所  
新竹市博愛街 75 號  
生科實驗館 101 室  
聯絡電話：03-5712121 ext.56939  
手機：0932936291  
傳真：03-5729288

### **Education**

**2005/9-present Ph.D.** Institute of Biochemical Engineering, National Chiao Tung University, Hsinchu, Taiwan (國立交通大學生化工程研究所)

**2004/9-2005/6 M.S.** Institute of Biochemical Engineering, National Chiao Tung University, Hsinchu, Taiwan (國立交通大學生化工程研究所)

**1999/9-2004/6 B.S.** Department of Life Science, National Tsing Hua University, Hsinchu, Taiwan (國立清華大學生命科學系)

### **Dissertation**

Physiological and physico-biochemical function of bovine milk  $\beta$ -lactoglobulin as probed by site-directed mutagenesis, bioinformatics and its crystal structure complexed with vitamin D  
Advisor: Chair Professor Simon J.T. Mao, Ph.D. (毛仁淡 講座教授)

This work constitutes identification of the secondary vitamin D binding site (exosite) of  $\beta$ -lactoglobulin, essential residues for exosite binding and vitamin D transport role of  $\beta$ -lactoglobulin. Most detail of the dissertation has been published as journal articles (see publication list).

### **Research Area**

#### **Doctoral and Graduate Research**

Institute of Biochemical Engineering, National Chiao Tung University, Hsinchu, Taiwan, 2004/9-2009 (research advisor: Dr. Simon J.T. Mao). (指導教授：毛仁淡 講座教授)

- Identification of the secondary vitamin D binding site (exosite) of  $\beta$ -lactoglobulin by fluorescence spectra, bioinformatic programs and X-ray diffraction.

- Determination of essential residues for exosite binding by site-directed mutagenesis and monoclonal antibody.
- Definition of vitamin D transport role of  $\beta$ -lactoglobulin with animal study.
- Ligand binding ability of  $\beta$ -lactoglobulin in native and thermal denatured state.
- Simulation of binding between haptoglobin and hemoglobin.

#### **Undergraduate Research:**

Division of Animal Medicine, Animal Technology Institute Taiwan, Maioli, Chunan, Taiwan, 2001/9-2003/6 (research advisor: Dr. Chao-Wei Liao). (指導教授：廖朝暉 研究員)

- Immune response of pig after immunization with alive vaccine of porcine reproductive and respiratory syndrome (PRRS) virus and a chimeric protein composed PRRSV ORF6 with Pseudomonas exotoxin A.
- Development of oral T-cell vaccine for porcine reproductive and respiratory syndrome (PRRS) virus.

#### **Teaching Experience**

##### **Teaching Assistant** “Biochemical Experiments”

Department of Biological Science and Technology, National Chiao Tung University, September 2006-January 2007

##### **Teaching Assistant** “Organic chemistry”

Department of Biological Science and Technology, National Chiao Tung University, February 2006-June 2006

##### **Teaching Assistant** “Drug delivery”

Department of Biological Science and Technology, National Chiao Tung University, September 2005-January 2006



#### **Technical Experience**

**Molecular genetics:** Genomic DNA and total RNA isolation; PCR and RT-PCR; Electrophoresis of nucleic acids; Gene cloning and expression; Site-directed mutagenesis.

**Biochemistry:** Polyacrylamide gel electrophoresis; Protein determination; Spectrophotometric enzyme assays; Microencapsulation; Affinity (monoclonal antibody) column chromatography; HPLC (gel filtration, ion exchange and reverse phase); Ligand binding assay by fluorescence spectrophotometer and isothermal calorimetry; Peptide synthesis; Protein array; Chemical modification of protein; Limited proteolysis; MALDI-TOF mass spectra; Confocal laser scanning microscopy; Protein crystallography.

**Immunology:** Operation and management of laboratory animal; Antisera generation and monoclonal antibody isolation; ELISA; Western blot; Immunoprecipitation;

Immunohistochemistry; Fluorescent and enzyme labeling of antibody and protein; FACS analysis.

### **Professional Certificate**

- Certificate in radiation safety training for operator (Radiation Protection Association R.O.C.) 「財團法人中華民國輻射防護協會操作人員輻射安全訓練班結訓證書 (94 輻協訓字第 0076 號)」
- Certificate in ethical training in animal experimentation (Council of Agriculture, Executive Yuan, Taiwan) 「行政院農業委員會實驗動物人道管理訓練合格證書 (實動訓字(九四)第一九〇號)」

### **Publications**

1. Song CY, Chen WL, **Yang MC**, Huang JP, Mao SJT. Epitope mapping of a monoclonal antibody specific to bovine dry milk. Involvement of residues 66-76 of strand D in thermal denatured  $\beta$ -lactoglobulin. *Journal of Biological Chemistry* 2005; 280: 3574-3582. (SCI IF: 5.6; Area of Biochemistry & Molecular Biology: 40/263)
2. Chen WL, Liu WT, **Yang MC**, Huang MT, Mao SJT. A novel conformation-dependent monoclonal antibody specific to native structure of  $\beta$ -lactoglobulin and its application. *Journal of Dairy Science* 2006; 89:912-921. (SCI IF: 2.4; Area of Agriculture, Dairy & Animal Science: 3/47)
3. **Yang MC**, Guan HH, Liu MY, Yang JM, Chen WL, Chen CJ, Mao SJT. Crystal structure of a secondary vitamin D<sub>3</sub> binding site of milk  $\beta$ -lactoglobulin. 2006 Protein Data Bank (PDB) access code: 2GJ5 (MMDB ID: 58939).
4. **Yang MC**, Guan HH, Liu MY, Lin YH, Yang JM, Chen WL, Chen CJ, Mao SJT. Crystal structure of a secondary vitamin D<sub>3</sub> binding site of milk  $\beta$ -lactoglobulin. *Proteins-Structure Function and Bioinformatics* 2008; 71:1197-1210. (SCI IF: 4.7 based on the year submitted; Area of Biophysics: 18/69)
5. Lai IH, Lin KY, Larsson M, **Yang MC**, Shiao CH, Liao MH, Mao SJT. A unique tetrameric structure of deer plasma haptoglobin: An evolutionary advantage in HP 2-2 phenotype with homogeneous structure. *FEBS Journal* 2008; 275: 981-993. (SCI IF: 3.4; Area of Biochemistry & Molecular Biology: 91/263)
6. **Yang MC**, Guan HH, Yang JM, Ko CN, Liu MY, Lin YH, Huang YC, Chen CJ, Mao SJT. Rational design for crystallization of  $\beta$ -lactoglobulin and vitamin D<sub>3</sub> complex: revealing a secondary binding site. *Crystal Growth & Design* 2008; 8: 4268-4276 (SCI IF: 4.0; Area of Crystallography: 1/25). **Selected as the cover of Journal Issue 2008, Dec.**
7. **Yang MC**, Chen NC, Chen CJ, Wu CY, Mao SJT. Evidence for  $\beta$ -lactoglobulin involvement in vitamin D transport *in vivo*- role of the  $\gamma$ -turn (Leu-Pro-Met) of  $\beta$ -lactoglobulin in vitamin D binding. *FEBS Journal* 2009; 276: 2251-2265 (SCI IF: 3.4;

Area of Biochemistry & Molecular Biology: 91/263)

8. **Yang MC**. Physiological and physico-biochemical function of bovine milk  $\beta$ -lactoglobulin as probed by site-directed mutagenesis, bioinformatics and its crystal structure complexed with vitamin D. 2009, Ph.D. thesis in the Institute of Biochemical Engineering, National Chiao Tung University, Hsinchu. Taiwan.

### **Presentations**

1. **Yang MC**, Chen WL, Mao SJT. Ligand binding ability of  $\beta$ -lactoglobulin in native and thermal denatured state. The Twentieth Joint Annual Conference of Biomedical Sciences, Taipei, Taiwan. Oral presentation. Programs & abstracts. P230 (March 26-27, 2005)
2. Chen WL, **Yang MC**, Song CY, Mao SJT. Thermal denaturation of  $\beta$ -lactoglobulin as probed by specific monoclonal antibodies. The Twentieth Joint Annual Conference of Biomedical Sciences, Taipei, Taiwan. Programs & abstracts. P396 (March 26-27, 2005)
3. **Yang MC**, Chen WL, Mao SJT. Secondary vitamin D binding domain of  $\beta$ -lactoglobulin: A thermal independent site. The 10th Conference on Biochemical Engineering, Taipei, Taiwan. Oral presentation. Programs & abstracts. P103 (June 24-25, 2005)
4. Mao SJT, Chen WL, **Yang MC**, Liu WT. Distinguish between native and thermally denatured  $\beta$ -lactoglobulin using a monoclonal antibody as a probe. 2005 Joint Annual Meeting of ADSA-ASAS-CSA, Cincinnati, OH, USA. Oral presentation. Programs & abstracts. P77 (July 24-28, 2005)
5. Song CY, **Yang MC**, Mao SJT. Residues 69-74 of  $\beta$ -lactoglobulin are responsible for a monoclonal antibody binding to thermal denatured lactoglobulin. 2005 Joint Annual Meeting of ADSA-ASAS-CSA, Cincinnati, OH, USA. Oral presentation. Programs & abstracts. P76 (July 24-28, 2005)
6. Chen WL, Liu WT, **Yang MC**, Huang MT, Mao SJT.  $\beta$ -lactoglobulin plays a provocative role in lymphocyte proliferation. The Fourteenth Symposium on Recent Advances in Cellular and Molecular Biology, Pingtung, Taiwan. Programs & abstracts. P159 (January 18-20, 2006)
7. Chen WL, Liu WT, **Yang MC**, Huang MT, Mao SJT.  $\beta$ -lactoglobulin plays a provocative role in lymphocyte proliferation. The Twenty-first Joint Annual Conference of Biomedical Sciences, Taipei, Taiwan. Programs & abstracts. P120 (March 18-19, 2006)
8. **Yang MC**, Chen C J, Liu MY, Mao SJT. Crystal structure of  $\beta$ -lactoglobulin and vitamin D complex. Identification of a second binding site for vitamin D. The Twenty-first Joint Annual Conference of Biomedical Sciences, Taipei, Taiwan. Programs & abstracts. P167 (March 18-19, 2006)
9. **Yang MC**, Chen C J, Liu MY, Mao SJT. Crystal structure of  $\beta$ -lactoglobulin and vitamin D complex. Identification of a second binding site for vitamin D. Experimental Biology 2006, San Francisco, CA, USA. FASEB. J. 20 :LB59 (April 1-5, 2006)



10. Chen WL, Liu WT, **Yang MC**, Huang MT, Mao SJT.  $\beta$ -lactoglobulin plays a provocative role in lymphocyte proliferation. Experimental Biology 2006, San Francisco, CA, USA. FASEB. J. 20 :A961 (April 1-5, 2006)
11. Guan HH, **Yang MC**, Liu MY, Yang JM, Chen WL, Mao SJT, Chen CJ. Crystal structure of  $\beta$ -lactoglobulin and vitamin D complex. NSRRC 12th Users' Meeting and Workshops, Hsinchu, Taiwan. Oral presentation. Programs & abstracts. O3-1 (October 3-4, 2006)
12. **Yang MC**, Guan HH, Liu MY, Lin YH, Yang JM, Chen WL, Chen CJ, Mao SJT. Crystal structure of a secondary vitamin D<sub>3</sub> binding site of milk  $\beta$ -lactoglobulin. 2006 Best Poster Competition of College of Biological Science & Technology, NCTU, Hsinchu, Taiwan. Programs & abstracts. P94 (November 17, 2006)
13. **Yang MC**, Guan HH, Liu MY, Lin YH, Yang JM, Chen WL, Chen CJ, Mao SJT. Crystal structure of a secondary vitamin D<sub>3</sub> binding site of milk  $\beta$ -lactoglobulin. 2007 NCTU Conference of Biological Technology, Hsinchu, Taiwan. Programs & abstracts. P9 (October 30, 2007)
14. Guan HH, **Yang MC**, Liu MY, Yang JM, Chen WL, Mao SJT, Chen CJ. Crystal structure of  $\beta$ -lactoglobulin and vitamin D complex. Identification of a second binding site for vitamin D: A thermal independent site. The 8th Conference of the Asian Crystallographic Association, Taipei, Taiwan Programs & abstracts. P06-074 (November 4-7, 2007)
15. **Yang MC**, Chen NC, Mao SJT. Physiological function of secondary vitamin D binding site on milk  $\beta$ -lactoglobulin. The Sixteenth Symposium on Recent Advances in Cellular and Molecular Biology, Pingtung, Taiwan. Programs & abstracts. P166 (January 23-25, 2008)
16. Lai IH, Lin KY, Larsson M, **Yang MC**, Shiao CH, Liao MH, Mao SJT. A unique tetrameric structure of deer plasma haptoglobin: an evolutionary advantage in hp 2-2 phenotype with homogeneous structure. The Sixteenth Symposium on Recent Advances in Cellular and Molecular Biology Pingtung, Taiwan. Programs & abstracts. P167 (January 23-25, 2008)
17. **Yang MC**, Chen NC, Lee J, Lai IH, Mao SJT. Interaction of deer Hp 2-2 with hemoglobin is superior to human Hp 2-2: an evolutionary advantage. The Sixteenth Symposium on Recent Advances in Cellular and Molecular Biology Pingtung, Taiwan. Programs & abstracts. P170 (January 23-25, 2008)
18. **Yang MC**, Chen NC, Mao SJT. Physiological Function of Secondary Vitamin D Binding Site on Milk  $\beta$ -Lactoglobulin. The Twenty-third Joint Annual Conference of Biomedical Sciences, Taipei, Taiwan. Oral presentation. Programs & abstracts. P82 (March 29-30, 2008)
19. Lai IH, Lin KY, Larsson M, **Yang MC**, Shiao CH, Liao MH, Mao SJT. A unique tetrameric structure of deer plasma haptoglobin: an evolutionary advantage in Hp 2-2 phenotype with homogeneous structure. The Twenty-third Joint Annual Conference of

- Biomedical Sciences, Taipei, Taiwan. Oral presentation. Programs & abstracts. P102 (March 29-30, 2008)
20. **Yang MC**, Chen NC, Lee J, Mao SJT. Interaction of deer Hp 2-2 with hemoglobin is superior to human Hp 2-2: an evolutionally advantage. The Twenty-third Joint Annual Conference of Biomedical Sciences, Taipei, Taiwan. Oral presentation. Programs & abstracts. P83 (March 29-30, 2008)
  21. **Yang MC**, Guan HH, Liu MY, Lin YH, Yang JM, Chen WL, Mao SJT, Chen CJ. Rational Design for Crystallization of  $\beta$ -Lactoglobulin and Vitamin D<sub>3</sub> complex Reveal a Secondary Binding Site. The 12th International Conference on the Crystallization of Biological Macromolecules, Cancun, Mexico. Oral presentation. (May 6-9, 2008)
  22. **Yang MC**, Chen NC Structural and functional importance of the secondary vitamin D binding of  $\beta$ -Lactoglobulin. 2008 Best Poster Competition of College of Biological Science & Technology, NCTU. Programs & abstracts. G1-21 (May 28, 2008)
  23. **Yang MC**, Chen NC Binding of deer Hp 2-2 with hemoglobin is superior to human Hp 2-2: an evolutionally advantage. 2008 Best Poster Competition of College of Biological Science & Technology, NCTU. Programs & abstracts. G1-20 (May 28, 2008)
  24. Lai IH, Lin KY, **Yang MC** A unique tetrameric structure of deer plasma haptoglobin: an evolutionary advantage in Hp 2-2 phenotype with homogeneous structure. 2008 Best Poster Competition of College of Biological Science & Technology, NCTU. Programs & abstracts. G1-23 (May 28, 2008)
  25. Lai IH, **Yang MC**, Shiau CH, Liao MH, Mao SJT. A unique tetrameric structure of deer plasma haptoglobin: an evolutionary advantage in Hp 2-2 phenotype with homogeneous structure. The Spring Symposium of the Taiwan Association of Veterinary Medicine and Animal Husbandry, Pingtung, Taiwan. Programs & abstracts. P78. (May 31, 2008)
  26. Chen CJ, Guan HH, **Yang MC**, Mao SJT. Rational crystallization of  $\beta$ -lactoglobulin and vitamin D<sub>3</sub> complex reveal a secondary binding site. The XXI Congress and Assembly of the International Union of Crystallography (IUCr2008), Osaka, Japan. Acta Cryst. A64: C242-C243. (August 23-31, 2008)
  27. **Yang MC**, Guan HH, Yang JM, Ko CN, Liu MY, Lin YH, Huang YC, Chen CJ, Mao SJT. Rational design for crystallization of  $\beta$ -lactoglobulin and vitamin D<sub>3</sub> complex: revealing a secondary binding site. 2008 NCTU Research Conference of Biological Technology, Hsinchu, Taiwan. Invited speech. (December 30, 2008)
  28. **Yang MC**, Guan HH, Yang JM, Ko CN, Liu MY, Lin YH, Huang YC, Chen CJ, Mao SJT. Rational design for crystallization of  $\beta$ -lactoglobulin and vitamin D<sub>3</sub> complex: revealing a secondary binding site. The Seventeenth Symposium on Recent Advances in Cellular and Molecular Biology Pingtung, Taiwan. Programs & abstracts. P214 (February 11-13, 2009)

29. Chen WL, Chen CL, Chao LS, Peng JY, Lai IH, **Yang MC**, Wang LS. The novel biomarkers for non-small cell lung carcinoma (NSCLC) by comparative proteomics: cytochrome c oxidase subunit Va is a potentially new biomarker for tumor invasion in NSCLC. The Twenty-fourth Joint Annual Conference of Biomedical Sciences, Taipei, Taiwan. Oral presentation. Programs & abstracts. P64 (March 21-22, 2009)
30. **Yang MC**, Guan HH, Yang JM, Ko CN, Liu MY, Lin YH, Huang YC, Chen CJ, Mao SJT. Rational design for crystallization of  $\beta$ -lactoglobulin and vitamin D<sub>3</sub> complex: revealing a secondary binding site. The Twenty-fourth Joint Annual Conference of Biomedical Sciences, Taipei, Taiwan. Oral presentation. Programs & abstracts. P66 (March 21-22, 2009)
31. Lai IH, Wang SH, Lee JW, Chen WL, **Yang MC**, Lin BR, Mao SJT. Neutrophils as one of the major haptoglobin sources in mastitic milk. The Twenty-fourth Joint Annual Conference of Biomedical Sciences, Taipei, Taiwan. Programs & abstracts. P374 (March 21-22, 2009)

#### **Honor**

1. **Award for outstanding oral presentation** in the **2005 10th Conference on Biochemical Engineering, Taipei, Taiwan**. "Secondary vitamin D binding domain of  $\beta$ -lactoglobulin: A thermal independent site."
2. **Excellent Research Award** in the **2007 NCTU Conference of Biological Technology, Hsinchu, Taiwan**. "Crystal structure of a secondary vitamin D<sub>3</sub> binding site of milk  $\beta$ -lactoglobulin."
3. **Outstanding Poster Award** in the **2008 Best Poster Competition of College of Biological Science & Technology, NCTU**. "Structural and functional importance of the secondary vitamin D binding of  $\beta$ -Lactoglobulin."
4. **Outstanding Research Award and Invited Speech** in the **2008 NCTU Research Conference of Biological Technology, Hsinchu, Taiwan**. "Rational design for crystallization of  $\beta$ -lactoglobulin and vitamin D<sub>3</sub> complex: revealing a secondary binding site."

# Publications



# Epitope Mapping of a Monoclonal Antibody Specific to Bovine Dry Milk

INVOLVEMENT OF RESIDUES 66–76 OF STRAND D IN THERMAL DENATURED  $\beta$ -LACTOGLOBULIN\*

Received for publication, June 23, 2004, and in revised form, November 1, 2004  
Published, JBC Papers in Press, November 9, 2004, DOI 10.1074/jbc.M407031200

Chun Ying Song<sup>‡</sup>, Wen Liang Chen<sup>‡</sup>, Ming Chi Yang<sup>‡</sup>, Jen Pin Huang<sup>§</sup>, and Simon J. T. Mao<sup>‡¶</sup>

From the <sup>‡</sup>Research Institute of Biochemical Engineering, Department of Biological Science and Technology, National Chiao Tung University, 75 Po-Ai Street, Hsinchu and <sup>§</sup>Genesis Biotech Inc., 131, Lane 235, Bao-Chiao Road, Hsintien, Taipei, Taiwan, Republic of China

**$\beta$ -Lactoglobulin ( $\beta$ -LG) is a bovine milk protein sensitive to thermal denaturation. Previously, we demonstrated that such structural change can be detected by a monoclonal antibody (mAb) specific to denatured  $\beta$ -LG. In the present study, we show a dramatic increase in  $\beta$ -LG immunoreactivity when heating raw milk between 70 and 80 °C. To map out the specific epitope of  $\beta$ -LG recognized by this mAb, we used a combined strategy including tryptic and CNBr fragments, chemical modifications (acetylation and carboxymethylation), peptide array containing *in situ* synthesized peptides, and a synthetic soluble peptide for immunoassays. The antigenic determinant we defined was exactly located within the D strand (residues 66–76) of  $\beta$ -LG. Circular dichroic spectral analysis shows that carboxymethylation on  $\beta$ -LG not only resulted in a substantial loss of  $\beta$ -configuration but also exerted a 10 times increase in immunoreactivity as compared with heated  $\beta$ -LG. The result suggests that a further disordered structure occurred in  $\beta$ -LG and thus rendered the mAb recognition. Mutations on each charged residue (three Lys and one Glu) revealed that Lys-69 and Glu-74 were extremely essential in maintaining the antigenic structure. We also show an inverse relationship between the immunoreactivity in heated  $\beta$ -LG and its binding to retinol or palmitic acid. Most interestingly, pH 9–10, which neutralizes the Lys groups of  $\beta$ -LG, not only reduced its immunoreactivity but also its binding to palmitic acid implicating a role of Lys-69. Taken together, we concluded that strand D of  $\beta$ -LG participated in the thermal denaturation between 70 and 80 °C and the binding to retinol and palmitic acid. The antigenic and biochemical roles of mAb specific to D strand are discussed in detail.**

unstable and molten globule nature,  $\beta$ -LG has been studied extensively for its physical and biochemical properties (2, 3). The protein comprises 162 amino acid residues, with one free cysteine and two disulfide linkages (Fig. 1). According to the three-dimensional crystallographic studies,  $\beta$ -LG is predominantly a  $\beta$ -sheet configuration containing nine antiparallel  $\beta$ -strands from A to I (4–6) (Fig. 1). Topographically, strands A–D form one surface of the barrel (calyx), and strands E–H form the other. The only  $\alpha$ -helical structure with three turns is at the COOH terminus, which follows strand H lying on the outer surface of the calyx (7). A remarkable property of the calyx is its ability to bind *in vitro* hydrophobic molecules such as retinol, fatty acids, vitamin D, and cholesterol (8–11). Spectroscopic studies have demonstrated that irreversible modification of the  $\beta$ -LG structure occurs upon thermal treatment above 65–70 °C. Thermodynamic analysis of the calorimetric signal reveals that there are two domains unfolding independently while heating (12). The exact regions involved in the thermal denaturation are still unclear. Whether the subtle unfolding changes can be detected by an immunochemical approach remains a question.

Regardless of intensive research, the biological function of this protein has not yet been satisfactorily resolved. Recently, we immunized the mice with commercially prepared dry milk and produced a panel of monoclonal antibodies (mAb). From the 900 hybridomas screened, a clone specific to dry milk, but not to raw milk, has been selected. Characterization of this dry milk-specific mAb reveals that this antibody recognizes thermally denatured  $\beta$ -LG (13). It suggests that a new antigenic epitope in  $\beta$ -LG is being exposed by a heating process used in the preparation of dry milk. In the present study, we defined the immunoreactive site that was recognized by this specific mAb, and we attempted to relate it to the thermal denaturation properties of  $\beta$ -LG. The strategy for epitope mapping combined several approaches, including tryptic and CNBr fragments, chemical modifications (acetylation and carboxymethylation), peptide array containing *in situ* synthesized peptides (with overlapped regions), and a synthetic peptide in solution for immunoassays. We demonstrate that the epitope was located exactly within the D strand of  $\beta$ -LG (residues 66–76). The immunoreactivity as recognized by this mAb was correlated to the thermal denaturation and conversion of  $\beta$ -sheet to a disordered structure of  $\beta$ -LG. Most interestingly, the D strand is associated with the A–C strands forming one domain at the opening of the calyx (Fig. 1). For this reason, we also studied

Bovine  $\beta$ -lactoglobulin ( $\beta$ -LG)<sup>1</sup> is one of the major proteins in milk consisting of about 10–15% (1). Because of the thermally

\* This work was supported by Grants NSC 90-2313-B-009-001, NSC 91-2313-B-009-001, NSC 92-2313-B-009-002, and NSC 93-2313-B-009-002 from the National Science Council of Taiwan, Republic of China. The costs of publication of this article were defrayed in part by the payment of page charges. This article must therefore be hereby marked "advertisement" in accordance with 18 U.S.C. Section 1734 solely to indicate this fact.

¶ To whom correspondence should be addressed: Dept. of Biological Science and Technology, College of Biological Science and Technology, National Chiao Tung University, 75 Po-Ai St., Hsinchu, Taiwan, Republic of China. Tel.: 886-3-571-2121 (ext. 56948); Fax: 886-3-572-9288; E-mail: mao1010@ms7.hinet.net.

<sup>1</sup> The abbreviations used are:  $\beta$ -LG,  $\beta$ -lactoglobulin; CM-LG, carboxymethylated- $\beta$ -LG; mAb, monoclonal antibody; ELISA, enzyme-linked immunosorbent assay; PBS, phosphate-buffered saline; PDB,

Protein Data Bank; HRP, horseradish peroxidase; ELISA, enzyme-linked immunosorbent assay; LDL, low density lipoprotein; CM, carboxymethylated.



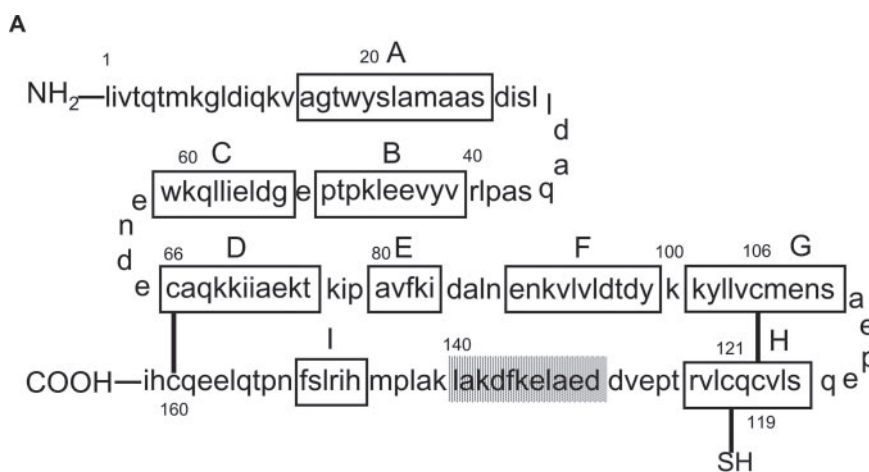
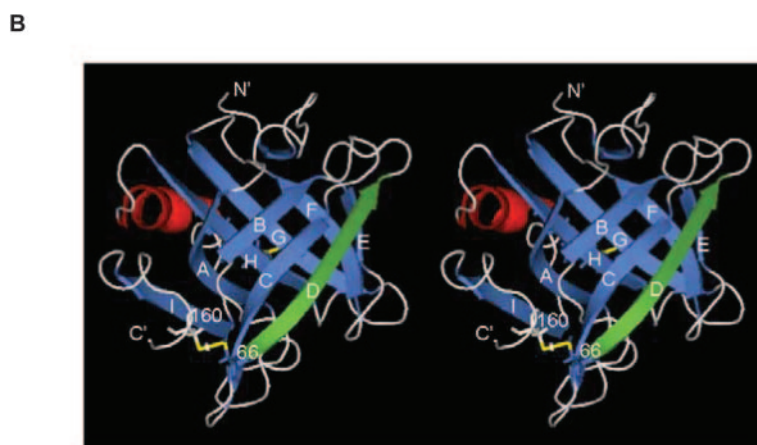


**FIG. 1. Amino acid sequence and three-dimensional structure of  $\beta$ -LG.** A,  $\beta$ -LG consisted of 162 amino acids with nine  $\beta$ -sheet strands (A–I) and one  $\alpha$ -helix (shadow). There are two disulfide bonds located between strand D and the carboxyl terminus (Cys-66 and Cys-160) and between strands G and H (Cys-106 and Cys-119), whereas a free buried thio group is at Cys-121. B, crystal structure of  $\beta$ -LG determined by Ref. 6 and created by PyMOL (25) (PDB code 1CJ5), shows that strands A–D form one surface of the barrel, and strands E–I form the other. The antigenic site recognized by the mAb is located within strand D (green) following thermal denaturation. The two disulfide linkages are also shown (yellow). Hydrophobic molecules such as retinol and palmitic acid are bound in the pocket of calyx.



the effect of heating and pH on  $\beta$ -LG binding to retinol and palmitic acid. Further epitope mapping shows that conversion of Glu-74 into either Ala or negatively charged Asp totally abolished its immunoreactivity. A similar result was seen in Lys-69 but not the other Lys residues. Finally, we propose that strand D plays a provocative role in the molten globule state of  $\beta$ -LG as probed by our mAb.

#### EXPERIMENTAL PROCEDURES

**Materials**— $\beta$ -LG was purified from fresh raw milk using 30% saturated ammonium sulfate top fraction followed by a G-150 column chromatography as described previously (13, 14).

**Preparation of Monoclonal Antibody Specific to Dry Milk**—Monoclonal antibodies were produced according to the standard procedures described previously by us (15, 16), in which dry milk (Nestle Australia Ltd., Sidney, Australia) was used for immunization (13). In brief, the myeloma cell line (FO) was fused with spleen cells from immunized BALB/c mice at a ratio of 1:5. The culture medium (between days 14 and 21 after fusion) was assayed for the production of specific antibodies by a solid-phase ELISA using both raw and dry milk as the respective antigen. Each monoclonal antibody was established by limiting dilutions at least two times (15, 16).

**Trypsin and CNBr Fragmentation**—For trypsin treatment, 50  $\mu$ g of  $\beta$ -LG in 100  $\mu$ l of phosphate-buffered saline (PBS) containing 0.02 M phosphate and 0.12 M NaCl, pH 7.4, were preheated at 100  $^{\circ}$ C for 10 min. After this, 1  $\mu$ l of trypsin (0.1 mg/ml) was added and incubated at room temperature for 4 h (13). Trypsinized LG was analyzed on an SDS-PAGE (18% polyacrylamide) followed by a Western blot. For CNBr fragmentation (17, 18), 5 mg of  $\beta$ -LG were first dissolved in 70% (v/v) trifluoroacetic acid with the addition of 10 mg of CNBr in the dark for 24 h at room temperature. After evaporating three times in a Speed Vac (CVE 200D, ELELA, Japan) with the addition of 5 $\times$  volume of deionized water, the dry material was dissolved in the 10 mM phosphate

buffer, pH 7.0. The immunoreactivity of CNBr fragments was then analyzed on an 18% SDS-PAGE, followed by a Western blot.

**Acetylation and Carboxymethylation of  $\beta$ -LG**—Chemical modification of  $\beta$ -LG by acetylation was conducted by a modification of the procedure described previously by us (19). To 5 mg of  $\beta$ -LG in 2 ml of 50 mM sodium bicarbonate, pH 8.0, containing 6 M urea, 5  $\mu$ l of acetic anhydride were slowly added into the reaction mixture step by step, while maintaining the pH at 8.0 by using 0.1 M NaOH. After 3 h of incubation at room temperature, the acetylated protein was desalted on Bio-Gel P-2 column eluted by 0.05 M ammonium bicarbonate and lyophilized. For carboxymethylation (19, 20), 5 mg of  $\beta$ -LG were first dissolved in 5 ml of 0.1 M Tris-HCl buffer, pH 8.6, containing 6 M ultra pure urea and 0.02 M dithiothreitol. Following flushing with nitrogen, 20 mg of iodoacetic acid were added into the reaction mixture, while maintaining the pH at 8.6 by the addition of 0.1 M NaOH, and were incubated for another 3 h. Finally, carboxymethylated (CM)  $\beta$ -LG was desalted on a Bio-Gel P2 column eluted by 0.05 M ammonium bicarbonate and lyophilized. By amino acid analysis, the CM- $\beta$ -LG contained 4.98 residues of CM cysteine per mol of  $\beta$ -LG.

**CD Spectrum**—The secondary structure of native, heated, or chemically modified  $\beta$ -LG was determined using a computerized Jasco J-715 CD spectropolarimeter. Each protein sample was dissolved in 10 mM phosphate buffer, pH 7.0, with a final concentration of 0.2 mg/ml. About 300  $\mu$ l of the protein solution were used for analysis within a cuvette of 1-mm path length. The obtained spectra were accumulated for 25 times at a scanning rate of 50 nm/min. All the data were shown as the mean residue molar ellipticity  $[\theta]_{MRW}$  (20, 21).

**Peptide Array**—Twelve synthetic peptides in one nitrocellulose array, each containing 15 amino acid residues, were designed corresponding to residues 25–107 of  $\beta$ -LG or to residues 67–75 within strand D (Fig. 1). The synthetic peptides were prepared under a contract with Genesis Biotech Inc. (Taipei, Republic of China). Briefly, the peptides were directly synthesized *in situ* on a nitrocellulose paper according to the method described previously (22). The nitrocellulose membrane in

0.01 M Tris-buffered saline containing 0.05% (v/v) Tween 20 (TBST) was blocked with 5% (w/v) gelatin in TBST for 2 h at room temperature followed by washing three times. After incubation with mAb for 2 h and three washes, goat anti-mouse IgG conjugated with horseradish peroxidase (HRP) in 0.5% gelatin/TBST was added and incubated. Finally, following the washes, the chemiluminescent substrate (ECL™ Western blotting System, Amersham Biosciences) was added, washed, and immediately developed by exposing onto a film.

**Competitive ELISA**—In brief, heated  $\beta$ -LG (1  $\mu$ g in 50  $\mu$ l of PBS) was first immobilized onto microtiter wells followed by three washes to remove unbound  $\beta$ -LG (13, 23). The wells were then blocked by 3% gelatin in PBS. After three washes, 50  $\mu$ l of the competitive protein ( $\beta$ -LG, heated  $\beta$ -LG, acetylated or carboxymethylated  $\beta$ -LG, or synthetic peptide residues 67–76) in PBS containing 0.3% gelatin were mixed with 50  $\mu$ l of mAb and incubated at room temperature for 1 h. Following washes and secondary antibody (goat anti-mouse IgG conjugated with HRP) incubation, the microtiter plate was developed with 2,2-azino-bis(3-ethylbenzothiazoline-6-sulfonic acid) and read at 415 nm.

**Effect of pH on  $\beta$ -LG Binding to mAb**— $\beta$ -LG (1  $\mu$ g/well) was immobilized onto a microtiter plate followed by blocking and washing at neutral pH. The immobilized  $\beta$ -LG was then incubated with mAb at various pH values for 2 h at room temperature. After removing the unbound mAb, the plate was developed according to the standard ELISA procedures at neutral pH (13, 23). Because pH itself can affect the antigen-antibody binding, a control experiment using mouse IgG as immobilized antigen was also conducted at various pH values for a parallel comparison.

**Retinol and Palmitic Acid Binding to  $\beta$ -LG**— $\beta$ -LG was reported to be a 1 to 1 binding ratio with retinol or palmitic acid as measured by fluorescence emission techniques (24). In general, binding of retinol to  $\beta$ -LG was measured by extrinsic fluorescence emission of the retinol molecule at 470 nm using excitation at 287 nm. Binding of palmitic acid to  $\beta$ -LG was measured by the fluorescence enhancement of Trp residues of  $\beta$ -LG at 332 nm by using excitation at 287 nm. For the effect of the pH experiment, 5 or 20  $\mu$ M of native  $\beta$ -LG was instantly incubated with 5  $\mu$ M of retinol or 20  $\mu$ M of palmitic acid, respectively, at various pH values at 24 °C. For the effect of the heat experiment,  $\beta$ -LG was preheated at 80 or 100 °C for 5 min and then incubated with retinol or palmitic acid at pH 8.0. Fluorescence spectra were recorded at 24 °C with a fluorescence Spectrophotometer F-4500 (Hitachi High-Tech Corp., Tokyo, Japan).

**Three-dimensional Analysis of  $\beta$ -LG Structure**—The three-dimensional structure of  $\beta$ -LG used in this context was provided by Protein Data Bank ([www.rcsb.org/pdb/](http://www.rcsb.org/pdb/)), code 1CJ5 (6), with the diagram created by PyMOL (25).

**Three-dimensional Analysis of  $\beta$ -LG and Palmitic Acid Complex Structure**—The three-dimensional structure of bovine  $\beta$ -LG complexed with palmitic acid used in this context was provided by Protein Data Bank code 1GXA (11), with the diagram created by RasMol (26).

## RESULTS

**Characterization of the Monoclonal Antibody Specific to Dry Milk**—Previous studies (13) show that the monoclonal antibody (mAb) used in this report is specific to processed dry milk but not to raw milk. It only recognizes  $\beta$ -LG, one of the major milk proteins. The mAb is apparently able to discriminate the denatured  $\beta$ -LG from a given milk product (13). Because heating procedures are used to process the dry milk, the finding indicates that  $\beta$ -LG undergoes a conformational rearrangement, which facilitates the binding of this mAb. In the present study, we show a dramatic and sharp increase in  $\beta$ -LG immunoreactivity when raw milk was heated between 70 and 80 °C over time (Fig. 2). It was of interest that the increase in immunoreactivity was concomitant with the reported transition temperature for converting native to denatured  $\beta$ -LG (27). The finding suggests that the immunoreactive site recognized by this mAb lies in the thermal denatured region of  $\beta$ -LG.

**Mapping of Antigenic Determinant of Denatured  $\beta$ -LG Utilizing Tryptic Digestion and Acetyl Modification**—To initially map out the specific immunoreactive region, heated  $\beta$ -LG was limitedly digested by trypsin. On Western blot, we demonstrated that the immunoreactivity was totally abolished after the trypsin treatment (13), suggesting that Lys, Arg, or both

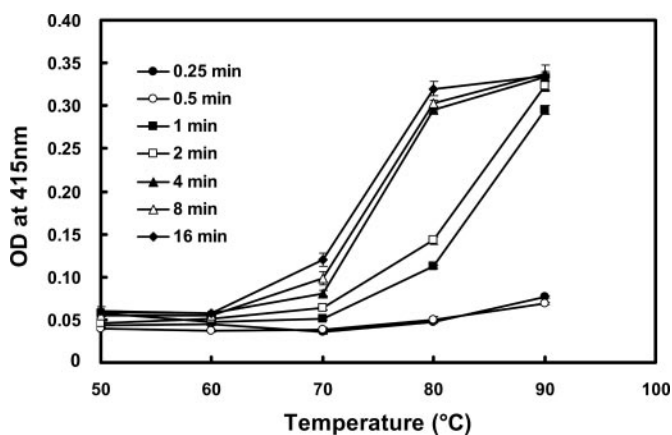
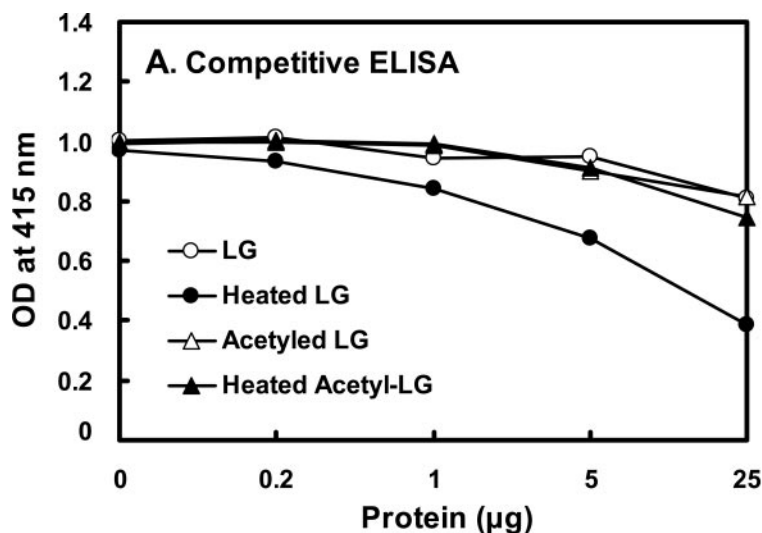


FIG. 2. Immunoreactivity of  $\beta$ -LG in raw milk heated at different temperatures over time. Immunoreactivity was monitored using an ELISA on raw milk heated at various temperatures. The increase in immunoreactivity of  $\beta$ -LG assessed by dry milk-specific mAb is correlated to the molten globule state of  $\beta$ -LG with a transition between 70 and 80 °C.

residue(s) were probably involved in maintaining the antigenic structure for  $\beta$ -LG. Chemical modification using acetylation (pH 8.0) on positively charged residues (mostly Lys) attenuated the immunoreactivity of  $\beta$ -LG on a competitive ELISA (Fig. 3A). These two experiments support the notion that positively charged amino acids of  $\beta$ -LG attributed for the mAb recognition.

**Immunoreactivity of CNBr Fragments of  $\beta$ -LG**—To delineate further the major antigenic domain, CNBr cleavage on  $\beta$ -LG was conducted. Western blot analysis shows that there was a major immunoreactive fragment corresponding to a molecular mass of about 9 kDa (Fig. 3B). As estimated from its Met cleavage site, this fragment was presumed a peptide containing residues 25–107 (Fig. 1). Subsequently, the amino-terminal sequence of this fragment was determined. The first six amino acid residues (AASDIS) confirmed that the immunoreactive site was located between residues 25 and 107 of  $\beta$ -LG (Fig. 1).

**Final Antigenic Mapping Using a Solid-phase Peptide Array**—As described above, Lys-enriched areas were assumed to participate in maintaining the antigenic structure. Pro residues are also considered to be involved as they are located at or near the antigenic determinant by forming a loop at the surface of a given protein. By using an EMBOSS program for searching a possible antigenic determinant within residues 25–107 of  $\beta$ -LG (Fig. 4), we predicted that two domains, namely residues 42–56 and 67–81, were most likely to be immunoreactive. Accordingly, a solid-phase peptide array containing the above predicted regions and 10 other overlapped synthetic peptides (each with 15 residues) was prepared. These peptides were directly synthesized on a nitrocellulose membrane (Fig. 4). After binding of mAb and HRP-conjugated secondary antibody, the array was developed by a chemiluminescent agent. We show that only peptides 4 (residues 70–84), 8 (residues 61–75), and 12 (residue 67–81) were immunoreactive (Fig. 4). Peptide 4 gave partial immunoreactivity, suggesting that residues 67–70 were essentially involved in the reactive site (Fig. 4). Because the size of an epitope is relatively small, usually containing 6–9 amino acid residues (16, 23, 28–30), it was possible to narrow down the reactive site from the immunoreactivity in overlapped peptides. We proposed that the reactive site was closely associated with AQKKIIAEK (or nine residues 67–75) (Fig. 4). Notably, this region is highly positive in charges. By observing the high resolution crystal structure of  $\beta$ -LG (6), it is fascinating to see that this proposed region is exactly located within the D strand of surfaced  $\beta$ -sheet (residues 66–76) (Fig.



**FIG. 3. Effect of acetylation and CNBr cleavage on immunoreactivity of  $\beta$ -LG.** A, competitive ELISA using heated  $\beta$ -LG as an immobilized antigen, while competing with native, heated, acetylated, and heat-acetylated  $\beta$ -LG. Immunoreactivity of  $\beta$ -LG was significantly increased upon heating at 100 °C for 5 min but not of acetylated and heated acetyl-LG. B, immunoreactivity of CNBr fragments of  $\beta$ -LG. About 10  $\mu$ g of native and CNBr cleaved  $\beta$ -LG were used for SDS-PAGE containing  $\beta$ -mercaptoethanol as a reducing agent (left) followed by a Western blot (right). A major immunoreactive peptide with a molecular mass of about 9 kDa was found to be in residues 25–107 as determined by an amino-terminal sequence analysis. In theory, fragments with a molecular weight greater than 9 kDa represent those incompletely cleaved peptides (Fig. 1). Lane M, molecular markers. Lane 1, native  $\beta$ -LG. Lane 2, CNBr fragments of  $\beta$ -LG.

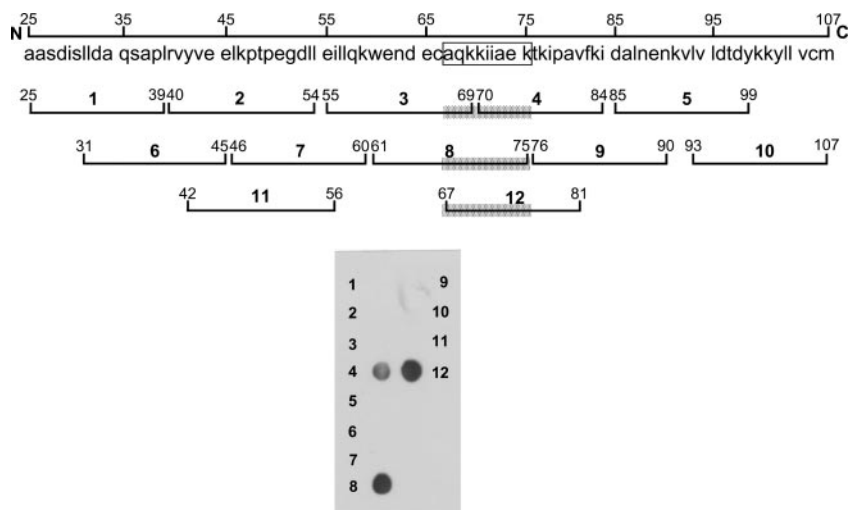
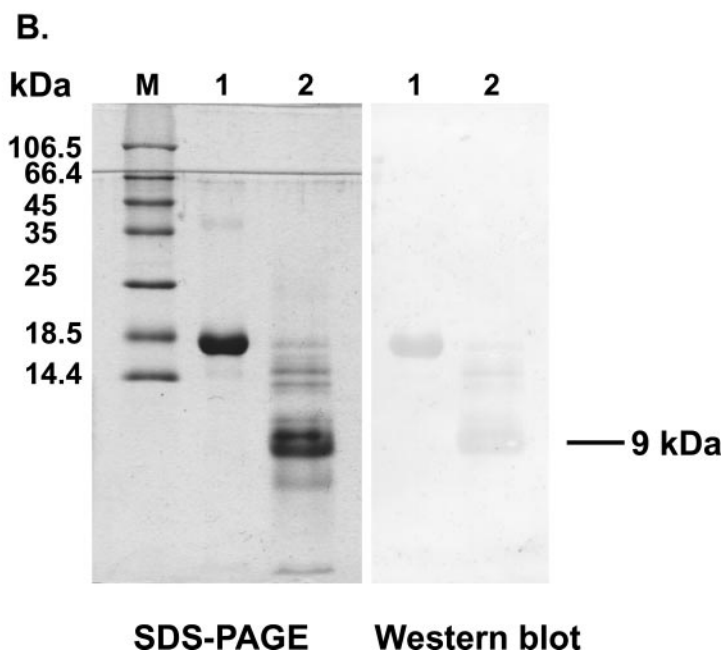


**FIG. 4. Delineation of an epitope recognized by mAb.** Twelve peptides corresponding to a 9-kDa CNBr fragment of  $\beta$ -LG (residues 25–107) were directly synthesized *in situ* on nitrocellulose membrane. Peptides 11 and 12 were prepared due to the presence of Pro residues thought to be potentially antigenic and Lys thought to be involved per our trypsin and acetylation experiments. The entire peptide array was commercially prepared under a contract for customer designing. Binding of antibody was conducted by using HRP-labeled secondary antibody with chemiluminescent agent as a developer. The shaded region represents the proposed epitope.

1). We therefore defined this immunoreactive site as an epitope. Another noticed point is that there is a disulfide linkage between strand D (Cys-66) and the carboxyl terminus (Cys-160). This disulfide linkage plays an important role in

stabilizing the  $\beta$ -structure by forming antiparallel sheets of  $\beta$ -LG. The proposed epitope (residues 67–75) in its native state is rather ordered with a  $\beta$ -sheet span about 28 Å in length. As such, the orientation in native  $\beta$ -LG may prohibit the binding



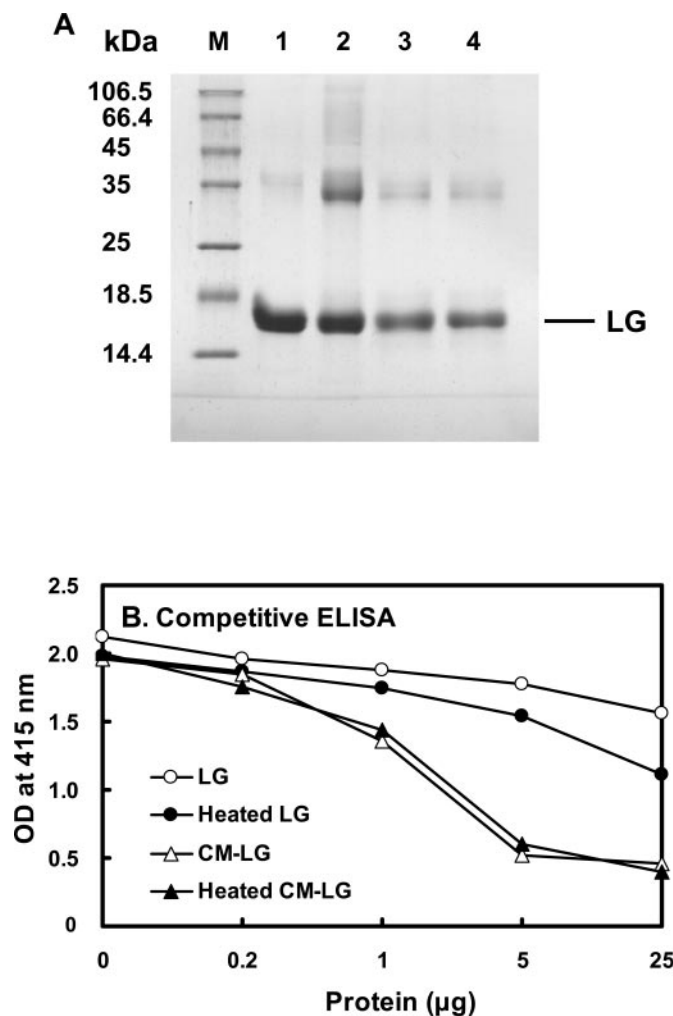


FIG. 5. SDS-PAGE profile and immunoreactivity of carboxymethylated  $\beta$ -LG (CM-LG). A, about 10  $\mu$ g of  $\beta$ -LG and CM-LG were loaded on 15% SDS-PAGE. Lane M, molecular markers. Lanes 1,  $\beta$ -LG. Lane 2, heated  $\beta$ -LG. Lane 3, CM-LG. Lane 4, heated CM-LG. Significant increase in  $\beta$ -LG dimer and high molecular forms are seen, while heating at 100  $^{\circ}$ C for 5 min, but not in CM-LG. B, competitive ELISA of native, heated  $\beta$ -LG, CM and heated CM-LG. The plate was immobilized with heated  $\beta$ -LG.

of our specific mAb. We hypothesized when the D strand underwent disordered structure, it would then allow the “denatured” mAb binding.

**Carboxymethylated  $\beta$ -LG and CD Spectrum**—To test the above hypothesis by which the conformational change of the D strand would enhance the binding of our mAb, we chemically modified all the Cys residues to irreversibly block the disulfide linkages within the native  $\beta$ -LG (Fig. 5A). By using a competitive ELISA with heated  $\beta$ -LG as a positive control, it revealed that carboxymethylation on  $\beta$ -LG resulted in a striking increase in its immunoreactivity. The increase was about 10 $\times$  greater than that of heated  $\beta$ -LG (Fig. 5B). Meanwhile, analysis of CD spectra on carboxymethylated  $\beta$ -LG further confirmed a significant conformational change by converting a  $\beta$ -sheet (typically at 215 nm) to a more disordered structure than that of heated  $\beta$ -LG (Fig. 6).

**Immunoreactivity of a Soluble Synthetic Peptide**—Finally, a soluble peptide corresponding to the linear sequence of strand D (residues 67–76 or AQKKIIAEKT) was synthesized. Fig. 7 shows that this linear sequence was able to inhibit completely mAb binding to heated  $\beta$ -LG on a competitive ELISA. Furthermore, this synthetic peptide exhibited a typical disordered structure rather than a  $\beta$ -configuration (Fig. 6).

**Role of Charged Residues in Epitope Specificity**—To determine which lysines were responsible for the mAb recognition, mutation on each Lys (Lys-69, Lys-70, and Lys-75) with Ala was conducted. As shown in Fig. 8, only Lys-69 was very specific for the mAb binding. Replacement with positively charged Arg did not salvage the immunoreactivity. Glu-74 played a similar role; replacement with Ala or negatively charged Asp failed to show any immunoreactivity. Ile-71 and Ile-72 also played an essential hydrophobic role, although the exact residue has not been identified. Meanwhile, negative control peptides (Fig. 8, peptides 11–12) retaining all the Lys residues did not show any binding.

**Effect of pH on  $\beta$ -LG Binding to mAb**—Because the structural stability of  $\beta$ -LG is pH-dependent (31), we tested whether changes of pH could also induce an increase in  $\beta$ -LG immunoreactivity. Fig. 9A shows that the CD structure of  $\beta$ -LG was stable at pH 2 with some changes between 3 and 7, whereas a transition to disorder was seen from 8 to 10. However, such a disordered structure did not facilitate the mAb binding (Fig. 9B). Because Lys-69 was essential (Fig. 8) and the overall positive charge of this residue started to become neutralized under pH 8–10, the immunoreactivity was decreased (Fig. 9B). A control experiment showing a typical pH-dependent antigen-antibody reaction was performed (Fig. 9C), and there was a slight decrease in immunoreactivity at pH 9–10.

**Effect of pH and Heating on  $\beta$ -LG Binding to Retinol and Palmitic Acid**—To explore the correlation between the structural change of  $\beta$ -LG (at various pH) and its retinol binding, we monitored the extrinsic fluorescent change of retinol upon the binding to  $\beta$ -LG. The optimal binding for retinol appeared to be at pH between 8 and 10 (Fig. 10A). Heating  $\beta$ -LG at temperatures greater than 80  $^{\circ}$ C almost completely abolished its binding for retinol (Fig. 10B). The data support the notion that the striking increase in immunoreactivity of the D strand at this temperature (Fig. 2) was negatively correlated to the retinol binding, which requires the integrity of a  $\beta$ -sheet structure of  $\beta$ -LG.

Most interestingly, the binding to palmitic acid was decreased to some extent at pH 9–10 (Fig. 10C), which correlated with the binding to mAb (Fig. 9B). Because Lys-69 played a very essential role in the antigenic site (Fig. 8), such correlation suggests that the protonated state of this residue might be involved in stabilizing both the mAb binding and  $\beta$ -LG-palmitic acid complex formation (see more details under “Discussion”). Similarly, heating on  $\beta$ -LG substantially reduced the binding for palmitic acid.

## DISCUSSION

Molten globules are thought to be general intermediates in protein folding and unfolding (32, 33).  $\beta$ -LG, a major moiety of bovine whey proteins, is one of the most investigated models for understanding the mechanism involved in protein stability upon heating. Although the three-dimensional crystal structure of  $\beta$ -LG has been elucidated, the area involved in thermal denaturation remains unclear. On the other hand the region responsible for Tanford transition (4), occurring at pH from 6.5 to 8.0 is known to be within the residues 85–90 (EF loop). This region opens or blocks the entrance of the calyx (34).

The present study (13) demonstrates that denatured strand D of  $\beta$ -LG was responsible for the binding of our thermally sensitive mAb. Several unique features of the binding are identified. First, heating on native  $\beta$ -LG resulted in a loss of  $\beta$ -sheet to more disordered structure (Fig. 6) in which the immunoreactivity was concomitantly increased (Fig. 5). Second, blocking the disulfide linkage between the D strand (Cys-66) and COOH terminus (Cys-160) of  $\beta$ -LG by carboxymethylation not only produced a disordered structure (Fig. 6) but also markedly

FIG. 6. Circular dichroic spectra of native  $\beta$ -LG, heated  $\beta$ -LG, carboxymethylated LG (CM-LG), and synthetic peptide 67–76. Samples at a final concentration of 0.2 mg/ml in 10 mM phosphate buffer, pH 7.4, were used for the study. A typical  $\beta$ -structure of native  $\beta$ -LG is shown at 215 nm.  $\beta$ -LG was heated at 100 °C for 5 min.

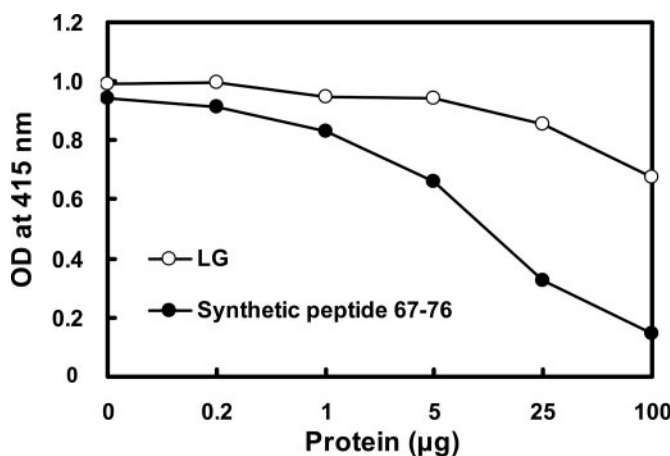
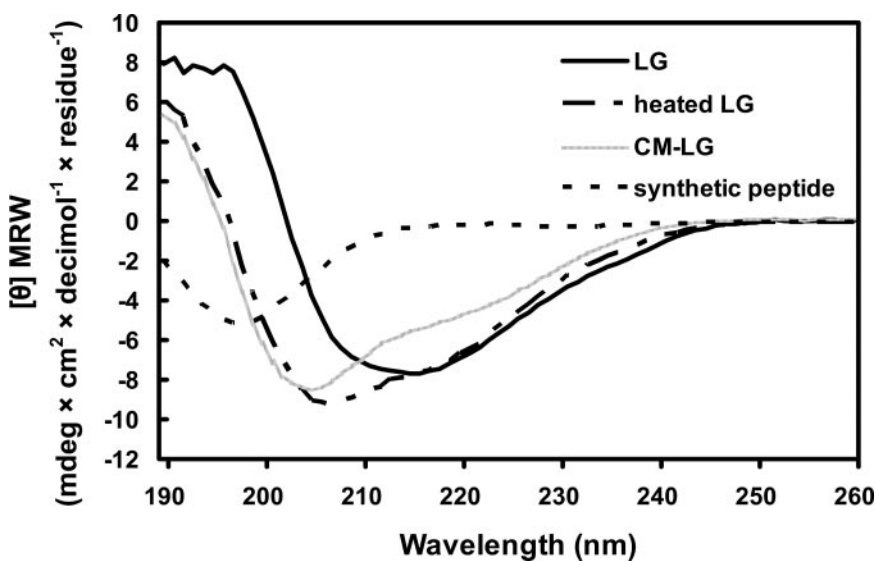


FIG. 7. Immunoreactivity of the synthetic peptide determined by an ELISA. A synthetic peptide corresponding to residues 67–76 (AQKKIIAEKT) in strand D was prepared as a soluble form. The plate was immobilized with heated  $\beta$ -LG.

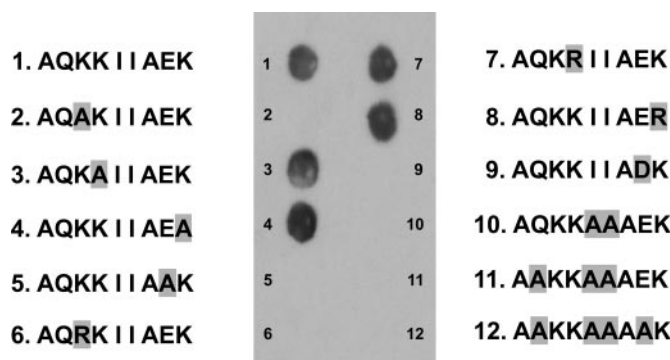


FIG. 8. Role of charged residues in antigenic specificity determined by a peptide array. Peptide 1 represents the native sequence 67–75 of  $\beta$ -LG. Substitution of Lys-69 and Glu-74 by Ala or a same charged amino acid, respectively, resulted in a total loss of immunoreactivity (peptides 2–9). Hydrophobic residues Ile-71 and Ile-71 were essential in maintaining the antigenic structure, whereas peptides 11 and 12 retaining all the Lys residues were used as randomized negative controls.

enhanced the mAb binding. Further heating on carboxymethylated  $\beta$ -LG did not give more binding. Such enhancement was even greater than heated  $\beta$ -LG (10 $\times$ ) on competitive ELISA (Fig. 5B). Presumably, this was because of the augmented degree of freedom of the D strand without the disulfide linkage rendering more antibody binding. It is of interest to point out

that the secondary structure of strand D alone, without including strand C, is predicted as 50% random coiled (residues 66–70) and 50% helical (residues 71–76) by using the parameters from three-dimensional PSSM; the folding recognition server at the Imperial Cancer Research Fund (ICRF) ([www.sbg.bio.ic.ac.uk/~3dpssm/](http://www.sbg.bio.ic.ac.uk/~3dpssm/)). However, in the presence of strand C as an anti-parallel orientation, the predicted structure of strand D becomes  $\beta$ -configuration. Obviously, the formation of an anti-parallel  $\beta$ -structure in native  $\beta$ -LG molecule is stabilized through the help of a disulfide linkage (Cys-66 and Cys-160) between strand D and the helical domain at COOH terminus (Fig. 1). Thus, conformational change on strand D played a vital role for the mAb recognition. It is worth mentioning that although severe heating might break the disulfide linkage at Cys-66, it would be immediately “stabilized” via re-oxidation by forming high molecular or self-associated polymers as shown in our previous report (13). Thus, the immunoreactivity of heated  $\beta$ -LG was less than that of carboxymethylated  $\beta$ -LG. Third, the soluble synthetic peptide (residues 67–76) corresponding to strand D (without Cys-66) was able to completely inhibit the binding of mAb to  $\beta$ -LG. Fourth, the D strand is topographically located at the surface of  $\beta$ -LG (Fig. 1), which is agreeable to the general concept of a given antigenic epitope (35). Fifth, the buried side chain of Lys-69 was exposed upon heating and then recognized by the mAb (described below).

With respect to the exact size of the epitope that was recognized by our mAb, we excluded the possibility of Cys-66 as part of the epitope from the D strand. First, peptide 67–81 without Cys-66 gave an almost equal immunoreactivity to that of peptide 61–75 with Cys-66 in a peptide array assay (Fig. 4) suggesting that Cys-66 might not be located in antigenic determinant. Second, carboxymethylation on whole  $\beta$ -LG molecules with Cys-66 included in the modification markedly increased its immunoreactivity. If Cys-66 were involved in the antigenic site, introduction of such a bulky group (carboxymethyl) on this residue would have resulted in a significant loss of immunoreactivity (30). It should be noted here that Cys-66 was only responsible for the conformational restraint by cross-linking Cys-66 and Cys-160; as such it limited the binding for denatured mAb. Third, the length of a linear epitope can be as short as 6–7 residues as demonstrated by our previous work (16, 23, 28) and the work of others (29, 30). The present study shows the involvement of Glu-74 in the epitope (Fig. 8), which is eight residues apart from Cys-66. Finally, our synthetic soluble peptide without Cys-66 could completely inhibit the mAb binding

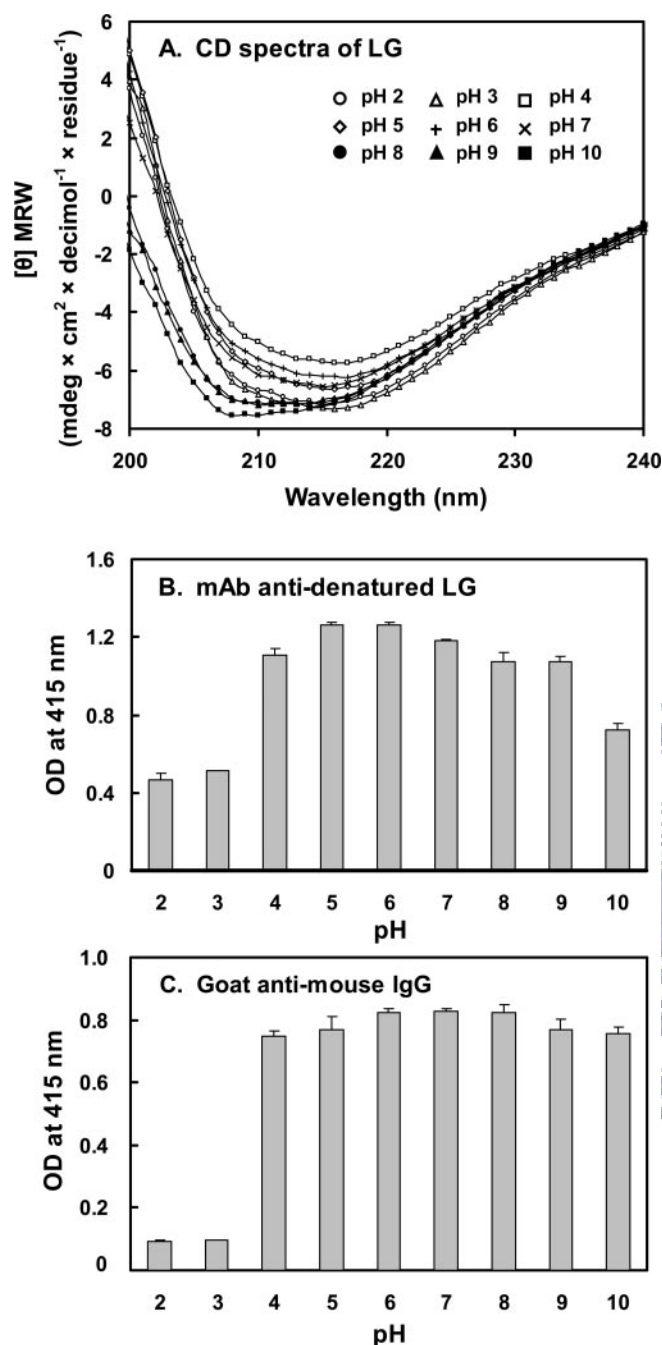


FIG. 9. Effect of pH on  $\beta$ -LG binding to mAb. A, CD spectra of  $\beta$ -LG at pH from 2 to 10. B, binding of mAb to  $\beta$ -LG at various pH values determined by ELISA. The primary mAb binding was conducted at the pH values indicated; all other reactions, including coating, blocking, washing, and secondary antibody binding, were performed at pH 7.4 according to standard procedures. The binding was significantly decreased at pH 8–10. C, control experiment evaluating the effect of pH on antigen-antibody interaction. This experiment was designed to study the pH effect on the binding of antigen and antibody in general. Antigen (mouse IgG) was coated on the plate and allowed the binding of HRP-labeled anti-IgG (goat) at various pH values. The plate was then developed after removing unbound antibody using PBS at pH 7.4. The binding was slightly decreased at pH 9–10.

(Fig. 7). Regardless, our antigenic mapping suggests that strand D located on the surface is involved in the molten globule and the unfolding structure of  $\beta$ -LG while heated. Coincidentally, the transition temperature of native  $\beta$ -LG was between 70 and 80 °C, which is in agreement with the increase in immunoreactivity for this mAb. On the other hand, the polyclonal antibody raised against the native  $\beta$ -LG did not

exhibit such a unique property (13).

The antigenic mapping from this study also provides some interesting insight as to the specificity of antigen-antibody interaction. Lys-69 and Glu-74 in the epitope were found to be extremely essential in maintaining the antigenic structure (Fig. 8), and substituting each with uncharged Ala diminished the mAb binding. Replacing each with the same charged amino acid Arg and Asp, respectively, could not restore the immunoreactivity. However, such point mutation in a given protein between the same charged residues Lys/Arg or Glu/Asp is very common within or among the species, while still maintaining its biological function. Notably, fragment 70–84 (Fig. 4) without Lys-69 gave a partial immunoreactivity, which differed from the mutation experiment (Fig. 8). Although the mechanism involved remains elusive, one possible explanation was the different solution property between the peptide with and without Lys-69. We speculate that the binding was more specific with the increase of chain length of the epitope, such as “lock and key.” Another interesting feature is that the span between Lys-69 and Glu-74 is six amino acids, which are sufficient to form an epitope as described previously by us using a mAb against fibrin (16). It is consistent with our observations for the interaction of protein antigens with antibodies, in which six determining residues, for the most part, were involved in binding with antigen (16, 29). We also demonstrate the importance of Ile-72 and Ile-73 within residues 69–74; substituting these two hydrophobic residues by Ala diminished its immunoreactivity. However, a further delineation using point mutation to each residue is needed to draw a final conclusion.

Using mAb as a probe to study the structural and functional relationship of a given protein has been popular and has been reviewed (36). It provides a powerful tool in defining the functional location within the molecule. Previously, we have shown mAb prepared against human hepatic lipase can distinguish between active and inactive forms of lipase (15). Some unique low density lipoprotein (LDL) mAbs have been used for discriminating between patients with and without coronary artery disease (37, 38). Those LDL mAbs have also been utilized for probing the thermal changes of human LDL (39), whereas the immunoreactivity was conversely correlated to the temperature with the optimal binding at 4 °C (38, 39). Because the three-dimensional structures of lipase and LDL were lacking, the exact mechanism involved remains elusive. The epitope of the  $\beta$ -LG we mapped in this study, however, is known and provides a better understanding for its interaction with mAb. We propose that because of a highly ordered  $\beta$ -configuration of the D strand in its native state, the binding to our specific mAb is prohibited. But the D strand underwent a conformational change upon heating, which would then allow the denatured mAb binding.

With respect to physiologic significance, the epitope region we defined is located at one of the critical domains forming a conical central calyx that is responsible for the binding of retinol and fatty acids (10, 11). An *in vivo* experiment shows that  $\beta$ -LG enhances the intestinal uptake of retinol in preruminant calves (40). It has been suggested that conformational changes in the calyx and the exposure of the surface hydrophobic site of  $\beta$ -LG in the molten globule state reduces the retinol affinity (24). The binding specificity may be determined by the dynamic motion of loops between the  $\beta$ -strands (34, 41). It is not known which  $\beta$ -strand(s) is involved for the exposure of the surface hydrophobic site. In this study we show a substantially decreased binding of retinol to  $\beta$ -LG that was preheated at a transition temperature of 80 °C (Fig. 10), with a significant increase in immunoreactivity (Fig. 2). Notably, two hydrophobic residues Ile-71 (buried in native state) and Ile-72 (exposed in native state) are located within the epitope and participate



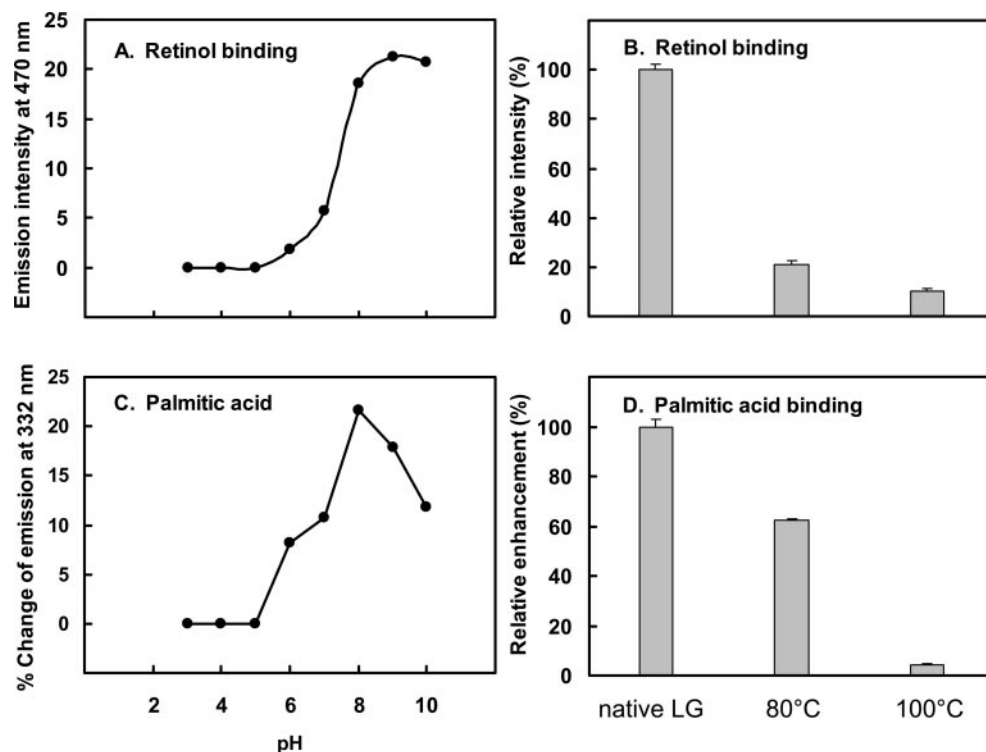


FIG. 10. Effect of pH and heating on  $\beta$ -LG binding to retinol and palmitic acid. A, fluorescence emission for binding of  $\beta$ -LG to retinol was measured at 470 nm with excitation at 287 nm. Binding was determined by the enhancement of extrinsic fluorescence of retinol at 24 °C. B, effect of  $\beta$ -LG heating (5 min) on retinol binding. C, fluorescence emission for binding of  $\beta$ -LG to palmitic acid was measured at 332 nm with excitation at 287 nm. Binding was determined by the enhancement of intrinsic fluorescence of  $\beta$ -LG at 24 °C. D, effect of  $\beta$ -LG heating (5 min) on palmitic acid binding.

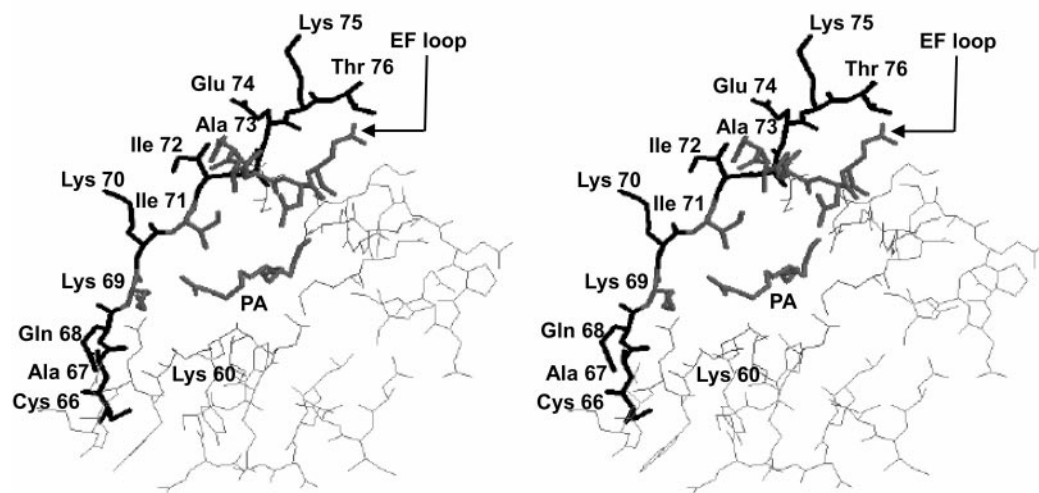


FIG. 11. Three-dimensional view of  $\beta$ -LG complexed with palmitic acid. The diagram is constructed according to the RasMol wire frame model (26), showing the D strand (residues 66–76) and other residues (28–43, 60–65, 84–93, and 107–117) (light wire frame) close to the calyx of  $\beta$ -LG. Notably, palmitic acid (PA) is almost perpendicularly oriented against the D strand, whereas Lys-69 is capable of interacting with the acidic group of palmitic acid. A hydrophobic interaction between the side chain of Ile-71 and palmitic acid is speculated. The EF loop (85–89), which controls the opening or closing of the calyx, is also seen. During the thermal denaturation, the conformational change of strand D results in the exposure of buried side chains of Lys-69 and Ile-71 and thereby attenuates and enhances the binding to palmitic acid and mAb, respectively.

in the binding to mAb (Fig. 8). One or both of these two residues must be exposed to the surface during thermal transition for rendering mAb binding. Thus, it is conceivable that Ile-71 might have become exposed on the surface during heating. Using co-crystallized  $\beta$ -LG with palmitic acid, the refined structure (at 2.5-Å resolution) reveals that the carboxyl group of palmitic acid binds to both Lys-60 and Lys-69 (9, 10). Fig. 11

shows a stereo view in which Lys-69 lies exactly within the antigenic epitope and orients at the entrance of the binding pocket, whereas the side chain of Ile-71 may interact with the fatty acyl chain. For the retinol binding, there is no obvious contact between the hydroxyl group of retinol and Lys-69 (11), although Lys-69 is closely oriented to the hydroxyl group (42). Again, we show a decreased binding of palmitic acid to  $\beta$ -LG

that was preheated at 80 °C (Fig. 10), and a significant increase in immunoreactivity (Fig. 2).

We demonstrate that the binding of retinol to  $\beta$ -LG was pH-dependent with initial binding at pH 7, while reaching a maximal pH between 8 and 10 (Fig. 10A). The data are consistent with the Tanford transition occurring at pH values from 6.5 to 9.5 (43). The calyx opens at pH 7.1–8.2 (4) and closes at pH 2.6 (7). Most interestingly, the binding of palmitic acid was attenuated at pH values from 8 to 10 (Fig. 10C). One of the possible explanations is that the protonated state of buried side chain of Lys-69 was neutralized at a pH value above 8 and resulted in weakening the ionic interaction with the carboxyl group of palmitic acid. Of course we could not rule out the other part of  $\beta$ -LG that might also undergo conformational changes at high pH, affecting the interaction with palmitic acid (Fig. 10C). We also speculate that the change of protonated state of Lys-69 contributed to the decreased immunoreactivity at pH 8–10 (Fig. 9B).

As mentioned above, the immunoreactivity assessed by this mAb was positively correlated to its molten globule state (between 70 and 80 °C in Fig. 3). This epitope in strand D was not only thermal sensitive but was also negatively correlated to retinol and palmitic acid binding. Lys-69 in native state participates in the binding for palmitic acid (10), but in the heat-denatured state it contributes to the binding for mAb. Therefore, this mAb may be used as a probe to study the thermal changes and the physiologic activity of  $\beta$ -LG, such as its binding to fatty acids and retinol.

Much is known about the physicochemical properties of  $\beta$ -LG (3). However, the biological function of this protein in addition to the transport of retinol and fatty acids has not yet been satisfactorily resolved. Recent studies have shown that  $\beta$ -LG produces hypocholesterolemic (44, 45) and antioxidant effects (46, 47) and may also serve as a growth factor for mammalian cells (48). The protein is acid-resistant in the gastrointestinal tract with a superior absorption capability via a receptor-mediated process (49–51). Because  $\beta$ -LG is a major protein consisting of about 10–15% of total milk proteins (1) and is labile to heat treatment by forming large polymers with other milk proteins (13, 52), it is conceivable that overheating should be avoided in order to maintain the physiologic role of  $\beta$ -LG. Therefore, our mAb may be useful for monitoring the immunochemical and biochemical nature of  $\beta$ -LG in heat-processed milk. From a technological standpoint, the monoclonal antibody prepared against the strand D region may be relevant to the design and operation of appropriate processes for thermal sanitation of milk and of other dairy products.

Taken together, we conclude that our mAb was able to discriminate the dry milk from the raw milk. The immunoreactivity of thermal denatured  $\beta$ -LG was correlated to its molten globule state and structural changes from primarily  $\beta$ -sheet to disordered conformation. Epitope mapping reveals that Lys-69, Ile-71, Ile-72, and Glu-74 in denatured D strand were directly involved in binding to mAb. The data suggest that the D strand plays a critical role in  $\beta$ -LG thermal denaturation, in which the buried side chains of Lys-69 and Ile-71 were exposed to the surface of  $\beta$ -LG calyx. At thermal transition temperature 80 °C, the increased immunoreactivity was associated with the decreased retinol and palmitic acid binding. We propose the mAb produced in this study may be used as a probe to study the thermal changes and the physiologic activity of  $\beta$ -LG, such as its binding to fatty acids and retinol. Whether the other  $\beta$ -strands may also participate in this role upon the heating between 70 and 80 °C, remains to be addressed.

**Acknowledgment**—We thank C. W. Li for preparing some artistic drawings.

## REFERENCES

- Hambling, S. G., MacAlpine, A. S., and Sawyer, L. (1992) in *Advanced Dairy Chemistry* (Fox, P. F., ed) pp. 141–190, Elsevier, Amsterdam
- Qi, X. L., Brownlow, S., Holt, C., and Sellers, P. (1995) *Biochim. Biophys. Acta* **1248**, 43–49
- Sawyer, L., and Kontopidis, G. (2000) *Biochim. Biophys. Acta* **1482**, 136–148
- Qin, B. Y., Bewley, M. C., Creamer, L. K., Baker, E. N., Baker, E. N., and Jameson, G. B. (1998) *Biochemistry* **37**, 14014–14023
- Qin, B. Y., Bewley, M. C., Creamer, L. K., Baker, E. N., and Jameson, G. B. (1999) *Protein Sci.* **8**, 75–83
- Kuwata, K., Hoshino, M., Forge, V., Era, S., Batt, C. A., and Goto, Y. (1999) *Protein Sci.* **8**, 2541–2545
- Uhrinova, S., Smith, M. H., Jameson, G. B., Uhrin, D., Sawyer, L., and Barlow, P. N. (2000) *Biochemistry* **39**, 3565–3574
- Narayan, M., and Berliner, L. J. (1997) *Biochemistry* **36**, 1906–1911
- Qin, B. Y., Creamer, L. K., Baker, E. N., and Jameson, G. B. (1998) *FEBS Lett.* **438**, 272–278
- Wu, S. Y., Perez, M. D., Puyol, P., and Sawyer, L. (1999) *J. Biol. Chem.* **274**, 170–174
- Kontopidis, G., Holt, C., and Sawyer, L. (2002) *J. Mol. Biol.* **318**, 1043–1055
- Fessas, D., Iametti, S., Schiraldi, A., and Bonomi, F. (2001) *Eur. J. Biochem.* **268**, 5439–5448
- Chen, W. L., Huang, M. T., Liu, H. C., Li, C. W., and Mao, S. J. T. (2004) *J. Dairy Sci.* **87**, 2720–2729
- McCreath, G. E., Owen, R. O., Nash, D. C., and Chase, H. A. (1997) *J. Chromatogr. A* **773**, 73–83
- Mao, S. J. T., Rehtin, A. E., and Jackson, R. L. (1988) *J. Lipid Res.* **29**, 1023–1029
- Mao, S. J. T., Rehtin, A. E., Krstenansky, J. L., and Jackson, R. L. (1990) *Thromb. Haemostasis* **63**, 445–448
- Mao, S. J. T., Gotto, A. M., Jr., and Jackson, R. L. (1975) *Biochemistry* **14**, 4127–4131
- Mao, S. J. T., Sparrow, J. T., Gilliam, E. B., Gotto, A. M., Jr., and Jackson, R. L. (1977) *Biochemistry* **16**, 4150–4156
- Mao, S. J. T., Sparrow, J. T., Gotto, A. M., and Jackson, R. L. (1980) *Biochim. Biophys. Acta* **617**, 245–253
- Tseng, C. F., Lin, C. C., Huang, H. Y., Liu, H. C., and Mao, S. J. T. (2004) *Proteomics* **4**, 2221–2228
- Chen, L., Mao, S. J. T., McLean, L. R., Powers, R. W., and Larsen, W. J. (1994) *J. Biol. Chem.* **269**, 28282–28287
- Frank, R. (1992) *Tetrahedron* **48**, 9217–9232
- Mao, S. J. T., Yates, M. T., Owen, T. J., and Krstenansky, J. L. (1989) *J. Immunol. Methods* **120**, 45–50
- Yang, J., Powers, J. R., Clark, S., Dunker, A. K., and Swanson, B. G. (2002) *J. Agric. Food Chem.* **50**, 5207–5214
- Delano, W. L. (2002) *The PyMOL Molecular Graphics System*, DeLano Scientific, San Carlos, CA
- Sayle, R. A., and Milner-White, E. J. (1995) *Trends Biochem. Sci.* **20**, 374–376
- de Wit, J. N., and Swinkels, G. A. (1980) *Biochim. Biophys. Acta* **624**, 40–50
- Bhatnagar, P. K., Mao, S. J. T., Gotto, A. M., Jr., and Sparrow, J. T. (1983) *Peptides (Elmsford)* **4**, 343–349
- Davies, D. R., and Cohen, G. H. (1996) *Proc. Natl. Acad. Sci. U. S. A.* **93**, 7–12
- Atassi, M. Z. (1984) *Eur. J. Biochem.* **145**, 1–20
- Casal, H. L., Köhler, U., and Mantsch, H. H. (1988) *Biochim. Biophys. Acta* **957**, 11–20
- Pittsytyn, O. B., Pain, R. H., Semisotnov, G. V., Zerovnik, E., and Razgulyaev, O. I. (1990) *FEBS Lett.* **262**, 20–24
- Chang, J. Y., and Li, L. (2001) *J. Biol. Chem.* **276**, 9705–9712
- Ragona, L., Fogolari, F., Catalano, M., Ugolini, R., Zetta, L., and Molinari, H. (2003) *J. Biol. Chem.* **278**, 38840–38846
- Atassi, M. Z. (1980) *Mol. Cell. Biochem.* **32**, 21–43
- Miller, E. J., and Cohen, A. B. (1991) *Am. J. Physiol.* **260**, 1–12
- Patton, J. G., Badimon, J. J., and Mao, S. J. T. (1983) *Clin. Chem.* **29**, 1898–1903
- Mao, S. J. T., Patton, J. G., Badimon, J. J., Kottke, B. A., Alley, M. C., and Cardin, A. D. (1983) *Clin. Chem.* **29**, 1890–1897
- Mao, S. J. T., Kazmar, R. E., Silverfield, J. C., Alley, M. C., Kluge, K., and Fathman, C. G. (1982) *Biochim. Biophys. Acta* **713**, 365–374
- Kushibiki, S., Hodate, K., Kurisaki, J., Shingu, H., Ueda, Y., Watanabe, A., and Shinoda, M. (2001) *J. Dairy Res.* **68**, 579–586
- Abduragimov, A. R., Gasyimov, O. K., Yusifov, T. N., and Glasgow, B. (2000) *Curr. Eye Res.* **21**, 824–832
- Cho, Y., Batt, C. A., and Sawyer, L. (1994) *J. Biol. Chem.* **269**, 11102–11107
- Tanford, C., Bunville, L. G., and Nozaki, Y. (1959) *J. Am. Chem. Soc.* **81**, 4032–4036
- Nagaoka, S., Futamura, Y., Miwa, K., Awano, T., Yamauchi, K., Kanamaru, Y., Tadashi, K., and Kuwata, T. (2001) *Biochem. Biophys. Res. Commun.* **281**, 11–17
- Yamauchi, R., Ohinata, K., and Yoshikawa, M. (2003) *Peptides (Elmsford)* **24**, 1955–1961
- Zommara, M., Toubo, H., Sakono, M., and Imaizumi, K. (1998) *Biosci. Biotechnol. Biochem.* **62**, 710–717
- Chevalier, F., Chobert, J. M., Genot, C., and Haertle, T. (2001) *J. Agric. Food Chem.* **49**, 5031–5038
- Francis, G. L., Regester, G. O., Webb, H. A., and Ballard, F. J. (1995) *J. Dairy Sci.* **78**, 1209–1218
- Guo, M. R., Fox, P. F., Flynn, A., and Kindstedt, P. S. (1995) *J. Dairy Sci.* **78**, 2336–2344
- Papiz, M. Z., Sawyer, L., Eliopoulos, E. E., North, A. C., Findlay, J. B., Sivaprasadarao, R., Jones, T. A., Newcomer, M. E., and Kraulis, P. J. (1986) *Nature* **324**, 383–385
- Caillard, I., and Tome, D. (1994) *Am. J. Physiol.* **266**, 1053–1059
- Havea, P., Singh, H., and Creamer, L. K. (2001) *J. Dairy Res.* **68**, 483–497

## A Novel Conformation-Dependent Monoclonal Antibody Specific to the Native Structure of $\beta$ -Lactoglobulin and Its Application

W. L. Chen,\* W. T. Liu,\* M. C. Yang,\* M. T. Hwang,\* J. H. Tsao,† and S. J. T. Mao\*<sup>1</sup>

\*Research Institute of Biochemical Engineering, Department of Biological Science and Technology,

National Chiao Tung University, Hsinchu, Taiwan, Republic of China

†Yong Rong Dairy, Chyayi, Taiwan, Republic of China

### ABSTRACT

Molten globules are thought to be general intermediates in protein folding and unfolding.  $\beta$ -lactoglobulin ( $\beta$ -LG) is one of the major bovine whey proteins, constituting ~10 to 15% of total milk proteins. We have recently identified  $\beta$ -LG as a superior marker for evaluating thermally processed milk. Strand D of  $\beta$ -LG participates in irreversible thermal unfolding as probed by a monoclonal antibody (mAb) specific to thermally denatured  $\beta$ -LG. In the present study, we used native  $\beta$ -LG as an immunogen to test the hypothesis that a specific mAb against the native  $\beta$ -LG could be established. As result, a mAb (4H11E8) directed against the native structure of  $\beta$ -LG was made. The antibody did not recognize the heat-denatured form of  $\beta$ -LG, such as its dimer and aggregates. Immunoassay using this “native” mAb showed that the stability of  $\beta$ -LG was at temperatures  $\leq 70^\circ\text{C}$ .  $\beta$ -Lactoglobulin began to deteriorate between 70 and  $80^\circ\text{C}$  over time. The denaturation was correlated with the transition temperature of  $\beta$ -LG. Further chemical modification of Cys (carboxymethylation) or positively charged residues (acetylation) of  $\beta$ -LG totally abolished its immunoreactivity, confirming the conformation-dependent nature of this mAb. Using competitive ELISA, the 4H11E8 mAb could determine the native  $\beta$ -LG content in commercially processed milks. Concentrations of native  $\beta$ -LG varied significantly among the local brands tested. From a technological standpoint, the mAb prepared in this study is relevant to the design and operation of appropriate processes for thermal sanitation of milk and of other dairy products. **Key words:**  $\beta$ -lactoglobulin structure, immunoassay, native monoclonal antibody, thermal denaturation

### INTRODUCTION

Molten globules are thought to be general intermediates in protein folding and unfolding (Chang et al.,

2000; Yang et al., 2001; Croguennec et al., 2004; Chen et al., 2005; Song et al., 2005).  $\alpha$ -Lactalbumin and  $\beta$ -LG are 2 of the major protein moieties of bovine whey proteins;  $\beta$ -LG constitutes 50% of the whey or about 10 to 15% of total milk proteins (Braunschweig et al., 2000; de Jongh et al., 2001; Wang and Lucey, 2003; Chen et al., 2005). Both of them are the most investigated models for understanding the mechanisms involved in protein stability, folding, and unfolding upon heating.

$\beta$ -Lactoglobulin consists of 162 AA residues with 1 free Cys and 2 disulfide linkages (Pérez and Calvo, 1995; Sava et al., 2005). According to 3-D crystallographic studies,  $\beta$ -LG is predominantly a  $\beta$ -sheet configuration containing 9 antiparallel  $\beta$ -strands from A to I (Qin et al., 1999; Forge et al., 2000). Topographically, strands A through D form one surface of the barrel (calyx), and strands E through H form the other. The only  $\alpha$ -helical structure with 3 turns is at the COOH-terminus, which follows strand H lying on the outer surface of the calyx (Uhrinova et al., 2000). A remarkable property of the calyx is its ability to bind in vitro hydrophobic molecules such as retinoids, fatty acids, vitamin D, and cholesterol (Qin et al., 1998; Wu et al., 1999; Kontopidis et al., 2002). We have recently identified that strand D of  $\beta$ -LG participates in the irreversibly thermal unfolding (Song et al., 2005) of which a new antigenic epitope in  $\beta$ -LG is being exposed between AA residues 66 and 76 when heating to  $>70^\circ\text{C}$  (Chen et al., 2005; Song et al., 2005). The unique structural and conformational changes made  $\beta$ -LG a superior marker for evaluating thermal processed milk (Chen et al., 2005).

In the present study, a conformation-dependent mAb (4H11E8) directed against native  $\beta$ -LG was prepared. The decreased immunoreactivity of  $\beta$ -LG as recognized by this “native” mAb was correlated to the thermal denaturation and conversion of  $\beta$ -sheet to the disordered structure of  $\beta$ -LG. Chemical modification of Cys and positively charged residues totally abolished the immunoreactivity of  $\beta$ -LG, confirming the nature of conformational dependency of this mAb. Using competitive ELISA, the mAb was able to determine the native  $\beta$ -LG content in commercially processed milk. We showed

Received August 17, 2005.

Accepted November 2, 2005.

<sup>1</sup>Corresponding author: mao1010@ms7.hinet.net



that the native  $\beta$ -LG concentrations varied significantly among the brands. The utility of this native mAb in monitoring the quality of dairy products and the biological consequences is discussed in detail.

## MATERIALS AND METHODS

### *Preparation of Milk Samples and $\beta$ -LG*

Fresh, bulked, whole raw milk obtained from a local dairy farm (Chyayi, Taiwan) was used for PAGE, Western blot, and ELISA analyses. For the heating experiments, each milk sample was heated at each temperature for the indicated time and immediately cooled down in an ice bath before the study.  $\beta$ -Lactoglobulin was purified from freshly skimmed milk using 40% saturated ammonium-sulfate top fraction followed by a  $\beta$ -LG antibody affinity column chromatography (Chen et al., 2004, 2005).

### *Animal Care and Use*

Balb/c mice were purchased from the National Animal Center of the National Science Council of Taiwan. The mice were maintained and fed in light-cycled animal rooms; facilities and management were according to guidelines established and approved by the National Science Council.

### *Immunization of Mice*

Female Balb/c mice, aged 5 to 7 wk, were used for immunization according to the method described previously (Yang and Mao, 1999; Chen et al., 2004, 2005). In brief, native  $\beta$ -LG [200  $\mu$ g in 200  $\mu$ L of PBS containing 0.02 M phosphate and 0.12 M NaCl (pH 7.4)] was homogenized with an equal volume of complete Freund's adjuvant by a 3-way stopcock for the first injection. The other 2 injections were then followed using incomplete Freund's adjuvant at d 7 and 14. Seven days following a final booster, plasma was obtained from blood collected in 0.1% EDTA (wt/vol) and was then used as a source for conventional  $\beta$ -LG polyclonal antibody. The titers of this antiserum were typically >1:10,000 as judged by an ELISA (Chen et al., 2004). The spleen obtained was used for preparing hybridoma fusion.

### *Production of mAb*

Monoclonal antibodies were produced according to the standard procedures previously described (Mao et al., 1982, 1988, 1990; Chen et al., 2004). In brief, a myeloma cell line (FO) was fused with spleen cells from immunized mice at a ratio of 1:5. Fusion was carried

out within 2 min at 37°C using 1 mL of 50% (wt/vol) polyethylene glycol containing 10% (vol/vol) DMSO (Hybri-Max, Sigma Chemical Co., St. Louis, MO). The cell mixture was then washed and resuspended in a hypoxanthine-aminopterin-thymidine medium (Hybri-Max) containing approximately  $1 \times 10^4$  FO cells/100  $\mu$ L. The suspended cells were distributed at 100  $\mu$ L per well in 96-well microtiter plates and incubated at 37°C in a 5% CO<sub>2</sub> incubator followed by the addition of 100  $\mu$ L of fresh hypoxanthine-aminopterin-thymidine medium after 7 d. Subsequently, culture medium was assayed for the production of specific mAb, between 14 and 21 d following fusion, using a solid-phase ELISA as described subsequently.

### *Screening of mAb Specific for Native $\beta$ -LG Using ELISA*

About 0.5  $\mu$ g of raw or dry milk protein in 50  $\mu$ L of PBS was coated onto a microtiter plate (Nunc, Roskilde, Denmark). Unbound  $\beta$ -LG was washed and subsequently blocked by the addition of 350  $\mu$ L of 1% gelatin (wt/vol) for 30 min (Mao et al., 1983, 1988; Patton et al., 1983; Chen et al., 2004, 2005; Song et al., 2005). Following washes with PBS, 50  $\mu$ L of hybridoma culture medium (2 to 3 wk following the fusion) was added and incubated at room temperature for 60 to 90 min. Each well was then washed 3 $\times$  with gelatin-PBS containing 0.1% gelatin and 0.05% Tween-20. Bound  $\beta$ -LG antibodies were detected using a goat antimouse IgG conjugated with horseradish peroxidase in gelatin-PBS for 30 min. Finally, each well was washed and developed with 0.04% (wt/vol) 2,2-Azino-bis(3-ethylbenz-thiazoline-6-sulfonic acid) (ABTS) in PBS containing 0.01% H<sub>2</sub>O<sub>2</sub> (vol/vol). For primary screening, mAb that differentially reacted with native  $\beta$ -LG were selected, and those that reacted equally with native and thermally denatured  $\beta$ -LG were ignored. The selected hybridomas were expanded and subcloned by limiting dilutions for at least 2 $\times$  to establish the monoclonals (Mao et al., 1988, 1990). The specificity of the mAb that recognized the native structure of  $\beta$ -LG was further confirmed by Western blot using native and heated  $\beta$ -LG (95°C for 5 min).

### *Gel Electrophoresis*

Sodium dodecyl sulfate-PAGE or native PAGE containing 15% (wt/vol) polyacrylamide (unless specified) was used for the characterization of the milk proteins via a modified procedure (Yang and Mao, 1999; Chen et al., 2005) similar to that described previously (Oldfield et al., 1998; Chen et al., 2005). All samples (5 to 20  $\mu$ g) for SDS-PAGE were equilibrated in 10 mM Tris-

HCl and 0.1% SDS (pH 7.6) before loading to the gel. A preheat treatment used in the conventional SDS-PAGE was omitted in this study to ensure the native structure of unheated  $\beta$ -LG or milk proteins. The same procedures were conducted for native PAGE.

### Western Blot Analysis

Following the SDS-PAGE or native PAGE, the gel was soaked instantly and briefly in a transfer buffer containing 25 mM Tris-HCl, 192 mM glycine, 20% methanol, and 0.0375% SDS (pH 8.3) for 30 s (Chen et al., 2004, 2005). The gel was then immediately electrotransferred to a nitrocellulose membrane (Hybond-ECL extra, Amersham, Buckingham, UK) at 90 mA for 45 min in a semidry transfer cell (BioRad, Hercules, CA). The membrane was immersed in 1% gelatin for 1 h with gentle shaking. Following 3 washes with PBS for 5 min, the membrane was incubated with tested mAb (with appropriate dilution in PBS containing 0.1% gelatin and 0.05% Tween-20) for 1 h followed by 3 washes and incubation with horseradish peroxidase-conjugated goat antimouse IgG for 1 h. Finally, the membrane was developed with 0.1 mg/mL of 3-3'-diaminobenzidine (3,3',4,4'-tetra-amino-biphenyl) containing 0.01% H<sub>2</sub>O<sub>2</sub> in PBS.

### Trypsin and Cyanogen Bromide Fragmentation

For trypsin treatment, 50  $\mu$ g of  $\beta$ -LG in 100  $\mu$ L of PBS was incubated with 1  $\mu$ L of trypsin (0.1 mg/mL) at room temperature for 4 h (Chen et al., 2004; Song et al., 2005). Trypsinized  $\beta$ -LG was analyzed on SDS-PAGE (18% polyacrylamide) followed by a Western blot. Cyanogen bromide (CNBr) fragmentation was conducted according to the method previously described with some modifications (Mao et al., 1977; Song et al., 2005). In general, 5 mg of  $\beta$ -LG was first dissolved in 70% (vol/vol) trifluoroacetic acid as previously described (Caprioli et al., 1991; Andrews et al., 1992) with the addition of 10 mg of CNBr in the dark for 24 h at room temperature. After 3 $\times$  evaporation in a lyophilizer with the addition of 5 $\times$  volume of deionized water, the dry material was dissolved in the 10 mM phosphate buffer (pH 7.0). The immunoreactivity of CNBr fragments was then analyzed on an 18% SDS-PAGE followed by a Western blot.

### Acetylation and Carboxymethylation of $\beta$ -LG

Chemical modification of  $\beta$ -LG by acetylation was conducted by a modification of the procedure previously described (Mao et al., 1980; Song et al., 2005). To 5 mg of  $\beta$ -LG in 2 mL of 50 mM sodium bicarbonate (pH

8.0) containing 6 M urea, 5  $\mu$ L of acetic anhydride was slowly added into the reaction mixture step by step while maintaining the pH at 8.0 using 0.1 M NaOH. After 3 h of incubation at room temperature, the acetylated protein was desalted on a Biogel P-2 column eluted by 0.05 M ammonium bicarbonate and lyophilized.

For carboxymethylation (Mao et al., 1980; Tseng et al., 2004; Song et al., 2005), 5 mg of  $\beta$ -LG was first dissolved in 5 mL of 0.1 M Tris-HCl buffer (pH 8.6) containing 6 M ultra-pure urea and 0.02 M 2-mercaptoethanol. Following flushing with nitrogen, 20 mg of iodoacetic acid was added into the reaction mixture while maintaining the pH at 8.6 via the addition of 0.1 M NaOH and incubation for another 3 h. Finally, carboxymethylated (CM)  $\beta$ -LG was desalted on a Bio-Gel P2 column eluted by 0.05 M ammonium bicarbonate and lyophilized. According to AA analysis, the CM  $\beta$ -LG contained 4.9 residues of CM Cys/mol of  $\beta$ -LG.

### Standard Displacement Curve of Milk Samples and Determination of $\beta$ -LG Concentration

In brief,  $\beta$ -LG (0.5  $\mu$ g in 50  $\mu$ L of PBS) was first immobilized onto each microtiter well followed by washes and blocking as described for ELISA. After washes, 50  $\mu$ L of the milk samples (raw or commercially processed milks) at various dilutions in 0.1% gelatin-PBS was mixed with 50  $\mu$ L of the 4H11E8 mAb and incubated at room temperature for 1 h. Following washes, a secondary antibody (goat antimouse IgG conjugated with horseradish peroxidase) was added, incubated, washed, and then developed with ABTS. To determine the native  $\beta$ -LG content of each milk sample, the  $\beta$ -LG concentration was based on the equivalent immunoreactivity extrapolated from that using purified  $\beta$ -LG as a standard. The mean value of each unknown sample was obtained from triplicated determinations with an intraassay variation of <8%.

### Milk Samples for Native PAGE

Different brands of commercially processed milk were purchased from the local market, and one was from the US market (Kroger, Cincinnati, OH). Freshly bulked, whole raw milk was obtained from a local dairy farm. Samples were immediately centrifuged at 13,000 rpm (15,500  $\times$ g) for 1 h at 4°C. The top layer in the supernatant was carefully removed, and the remaining fraction (whey protein) containing minimal casein was used for the analysis of PAGE and Western blot.

## RESULTS

Using dry milk as an immunogen, we have recently produced a mAb that can distinguish dry milk from raw



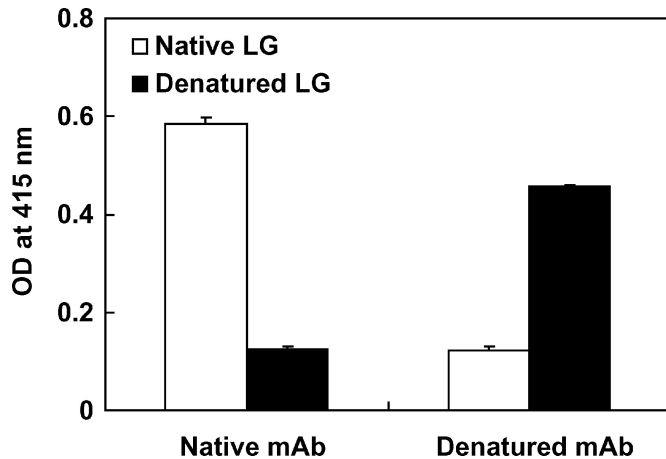


**Figure 1.** Typical example of a monoclonal antibody (mAb) that differentially reacted with native and heated  $\beta$ -LG. Immunoreactivity was monitored using an ELISA, and an equal amount of native and heated  $\beta$ -LG protein (1  $\mu$ g) was coated onto the microtiter plate.  $\beta$ -Lactoglobulin was heated at 95°C for 5 min prior to the coating. Each bar represents the mean  $\pm$  SEM of triplicate determinations. OD = optical density.

milk (Chen et al., 2004). Antigenic mapping shows that the epitope is located between residues 66 and 76 in strand D of thermally denatured  $\beta$ -LG (Song et al., 2005). When heated to >80°C, the epitope region of  $\beta$ -LG is exposed and bound by the mAb (3E7G7). Therefore, the antibody is defined as “denatured” mAb. In the present study, we tested the hypothesis that a native  $\beta$ -LG mAb could be prepared when native  $\beta$ -LG was used for immunization. Approximately 500 hybridoma clones were screened, among which 1 mAb was established (4H11E8) that specifically reacted with the native  $\beta$ -LG, but not heat-denatured  $\beta$ -LG. A typical example is shown in Figure 1: mAb 4H11E8 bound primarily to native  $\beta$ -LG in contrast to denatured mAb that bound to heated  $\beta$ -LG.

### Western Blot Analysis

Using SDS-PAGE and Western blot analysis, mAb 4H11E8 only recognized the native monomeric  $\beta$ -LG of raw and dry milk, but not denatured  $\beta$ -LG dimer or polymers of dry milk (Figure 2). The denatured  $\beta$ -LG was almost nondetectable by Coomassie blue staining. Such minimal denatured forms, however, were observed using a denatured mAb prepared previously [Figure 2 (right panel); Chen et al., 2004, 2005]. To demonstrate the specificity and sensitivity of the 4H11E8 mAb, we heated raw milk at 95°C over time. Following a native PAGE and Western blot analysis,  $\beta$ -LG was found to be severely denatured after heating of milk at 95°C for >2 min (Figure 3A). Formation of

large polymers from either self-associated  $\beta$ -LG or  $\beta$ -LG conjugates (with other milk proteins) was observed for denatured mAb (Figure 3B). Because more  $\beta$ -LG aggregates formed after heating for >4 min, less denatured  $\beta$ -LG could run into the gel; such that some of the sample became undetectable by the denatured mAb on the blot (Figure 3B). It was obvious that mAb 4H11E8 only recognized the native  $\beta$ -LG. We herein define it as “native” mAb.

### Effect of Heat on the Immunoreactivity of Raw Milk

Quantitative ELISA was then used to analyze immunoreactivity of native mAb against raw milk heated at different temperatures over time (Figure 4). The  $\beta$ -LG thermal denaturation curve shows that, in general,  $\beta$ -LG was stable at the temperatures  $\leq$ 70°C. It began to deteriorate between 70 and 80°C. Most interestingly, the thermal denaturation curve determined by the immunoassay in this study is almost identical to that determined by the structural change of  $\beta$ -LG using a physical-chemical approach: a circular dichroic spectrum (Chen et al., 2005). A severe decrease in immunoreactivity was observed when heating was >80°C. This finding demonstrated that the structural loss of native  $\beta$ -LG could be probed by the native 4H11E8 mAb.

### Effect of Conformational Change on the Immunoreactivity of $\beta$ -LG

We anticipated that the overall structure of  $\beta$ -LG might determine the specific nature of this native mAb. To test this hypothesis, we chemically modified  $\beta$ -LG by carboxymethylation to break up the disulfide linkage in altering its overall structure. As shown in Figure 5A, the native mAb reacted with native  $\beta$ -LG, but not that CM using a Western blot analysis. Notably, an extra band was present in the modified  $\beta$ -LG (Coomassie blue staining), which might have been generated during the modification by an unknown mechanism. Additional acetylation on the lysyl residues, limited trypsin treatment, and CNBr fragmentation also diminished the immunoreactivity (Figure 5, B through D). It should be noted here that both of these 2 chemical modifications were carried out in the presence of 6 M urea. The modified  $\beta$ -LG was dialyzed against PBS prior to the Western blot to remove the urea. After dialysis, the immunoreactivity of  $\beta$ -LG treated with 6 M urea was retained because of the renaturation of the conformation. Also, sample treated with trifluoroacetic acid alone (without the presence of cleavage reagent CNBr) did not show the loss of immunoreactivity after removing the trifluoroacetic acid by lyophilization. However,  $\beta$ -LG treated with 8 M urea without dialysis resulted in a complete

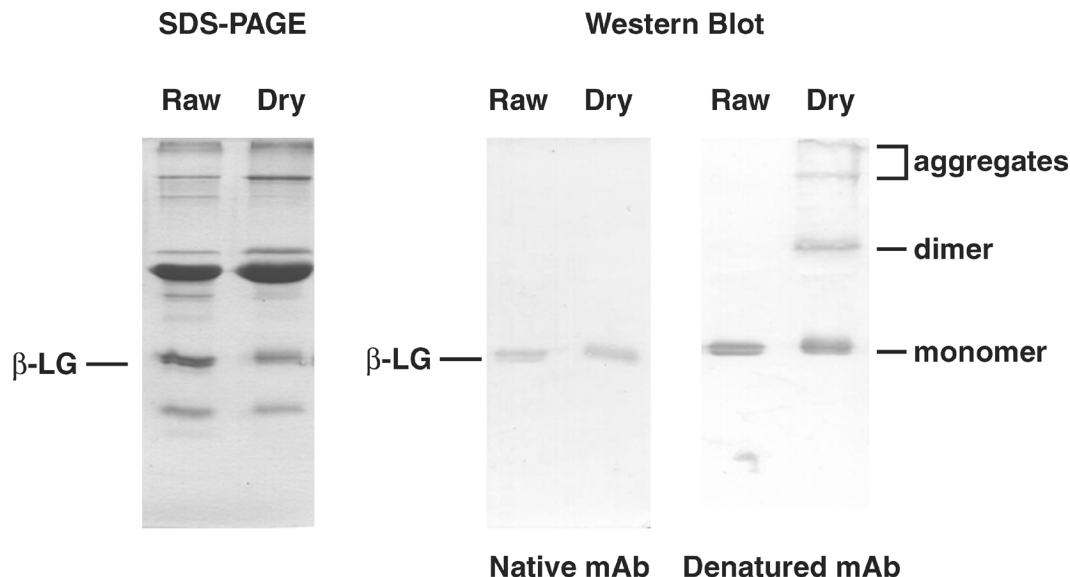


**Figure 2.** Characterization of native monoclonal antibody (mAb) 4H11E8 using Western blot. Left: raw and dry milk on a 15% SDS-PAGE followed by Coomassie blue staining. Right: raw and dry milk on SDS-PAGE followed by Western blot using native and denatured mAb. The data show that native mAb only recognizes the native form of  $\beta$ -LG, but not  $\beta$ -LG dimer, polymers, or aggregates. The denatured forms of  $\beta$ -LG cannot be seen by Coomassie staining.

loss of the immunoreactivity on a nitrocellulose using a dot-blot assay (data not shown). Taken together, these results suggest that the native mAb was not sequentially dependent.

#### **Determination of Native $\beta$ -LG in Processed Milk from the Local Market**

Using competitive ELISA by native mAb, we monitored the immunoreactivity of native  $\beta$ -LG in processed milk. A typical example for the standard displacement curves resulting from the samples purchased from the local market is shown in Figure 6. Optical density is inversely correlated with the expression of native  $\beta$ -LG in tested milks. The raw milk shows a superior  $\beta$ -LG immunoreactivity to most of the brands tested (Figure 6) and was almost superimposed with one brand that was claimed to be pasteurized at  $<65^{\circ}\text{C}$  for 30 min (low temperature; long pasturization). Using a standard curve of native  $\beta$ -LG (data not shown), the extrapolated  $\beta$ -LG content for each brand is listed in Table 1. The  $\beta$ -LG left over in each processed brand varied significantly. Interestingly, the native  $\beta$ -LG values in a US brand (No. 3) and domestic brand (No. 2; low temperature and long pasteurization) were essentially identical to those in raw milk. Finally, we characterized the native  $\beta$ -LG content in processed milk using a native PAGE.  $\beta$ -Lactoglobulin was found severely denatured in some of the brands (Figure 7) and was almost consis-

tent with the quantitative ELISA using native mAb (Table 1).

#### **DISCUSSION**

It is well established that the heating process during the preparation of dry milk causes structural changes in some milk proteins (Needs et al., 2000; Chen et al., 2004). Although such changes are subtle, we have demonstrated that the denatured mAb can distinguish minor differences between the dry and raw milks (Chen et al., 2004). Subsequently,  $\beta$ -LG was found to be the component responsible for the specificity of that denatured mAb (Chen et al., 2004). Following antigenic mapping using synthetic peptides, we have recently delineated the epitope to be located between residues 66 and 76 of the denatured D strain of  $\beta$ -LG (Song et al., 2005). Thus, this suggests that  $\beta$ -LG is a sensitive thermal marker that can be probed by a mAb specific to denatured  $\beta$ -LG. Conversely, it predicts that a mAb specific to native  $\beta$ -LG can be made following appropriate immunization and screening. For this reason, in the present study, we used native  $\beta$ -LG as an immunogen to test the hypothesis that a specific mAb against the native structure of  $\beta$ -LG could be established.

Because those monoclonals that cross-reacted with denatured  $\beta$ -LG had already been eliminated in the initial screening, the remaining clones that were specific to native  $\beta$ -LG should be most likely directed

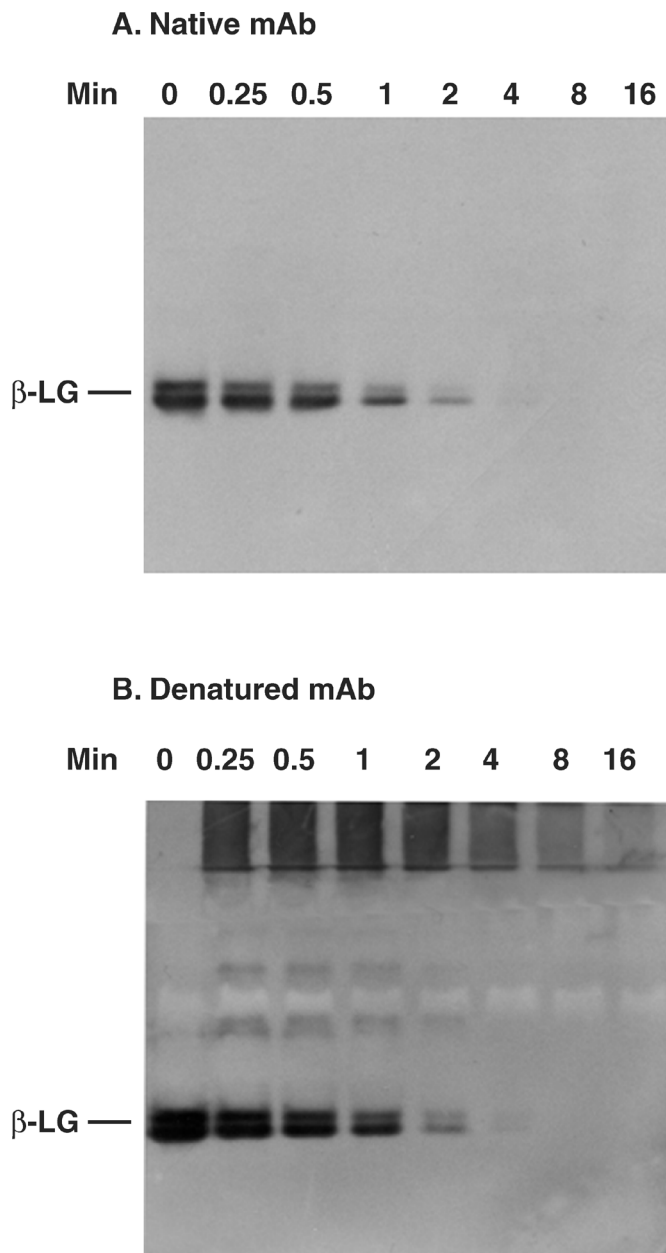


**Figure 3.** Thermal denaturation of  $\beta$ -LG characterized by native monoclonal antibody (mAb) 4H11E8 and denatured mAb on native PAGE. The experiment was carried out by heating raw milk at 95°C over time (0 to 16 min) followed by a Western blot using mAb (A) and denatured mAb (B). Two isoforms of  $\beta$ -LG were seen on native PAGE. The native mAb does not recognize the thermally denatured  $\beta$ -LG.

against a conformational dependent epitope. Several lines of evidence support this possibility. First, from the known 3-D structure, Cys residues are responsible for stabilizing the overall structure of  $\beta$ -LG by cross-linking the positions strand D Cys-66 and carboxyl terminus Cys-160 (Creamer et al., 2004; Song et al., 2005).

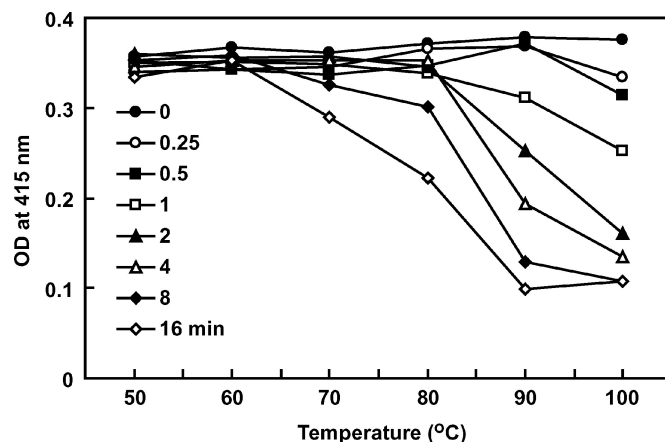


**Figure 4.** Immunoreactivity of  $\beta$ -LG in raw milk heated at different temperatures over time. Each milk sample was independently heated at each respective temperature with the time as indicated and immediately cooled in an ice bath before immobilizing onto the ELISA plate. Immunoreactivity was monitored by an ELISA using native mAb 4H11E8. Each point represents a mean of duplicated determinations. The decrease in immunoreactivity assessed by native mAb is essentially correlated to the molten globule state of  $\beta$ -LG with a transition between 70 and 80°C. OD = optical density.

Our chemical modification (carboxymethylation) on Cys residues not only resulted in the conformational change of  $\beta$ -LG as shown in our previous study (Song et al., 2005.), but also completely abolished the immunoreactivity in the present study (Figure 4). Second, acetylation, which neutralizes the positively charged lysyl residues (at pH 10), resulted in a total loss of the immunoreactivity of  $\beta$ -LG (Figure 5B). These charged residues are also crucial in maintaining the overall 3-D structure of a given protein or  $\beta$ -LG (Song et al., 2005). Third, in contrast to the denatured  $\beta$ -LG mAb (Chen et al., 2004; Song et al., 2005), this native mAb did not recognize the CNBr fragment (Figure 4). It is conceivable that this mAb may not be sequence dependent. It was tempting to speculate that the entire  $\beta$ -LG molecule was required in maintaining the antigenic structure, but we could not rule out that such fragmentation might directly cleave the epitope, resulting in a loss of immunoreactivity. We then denatured the  $\beta$ -LG using 8 M urea and demonstrated that it was not immunoreactive using a dot-blot assay (data not shown). Thus, it further supports the notion that conformation of  $\beta$ -LG plays a role in this native mAb. With respect to CNBr cleavage, we used 70% trifluoroacetic acid instead of formic acid. Although formic acid is commonly used because of its good solubility and denaturation for a given protein, it may damage Trp and Tyr residues (Morrison et al., 1990). It may also result in formylation and so increase peptide mass (Beavis and Chait, 1990). Conversely, trifluoroacetic acid is preferable to formic acid, giving a

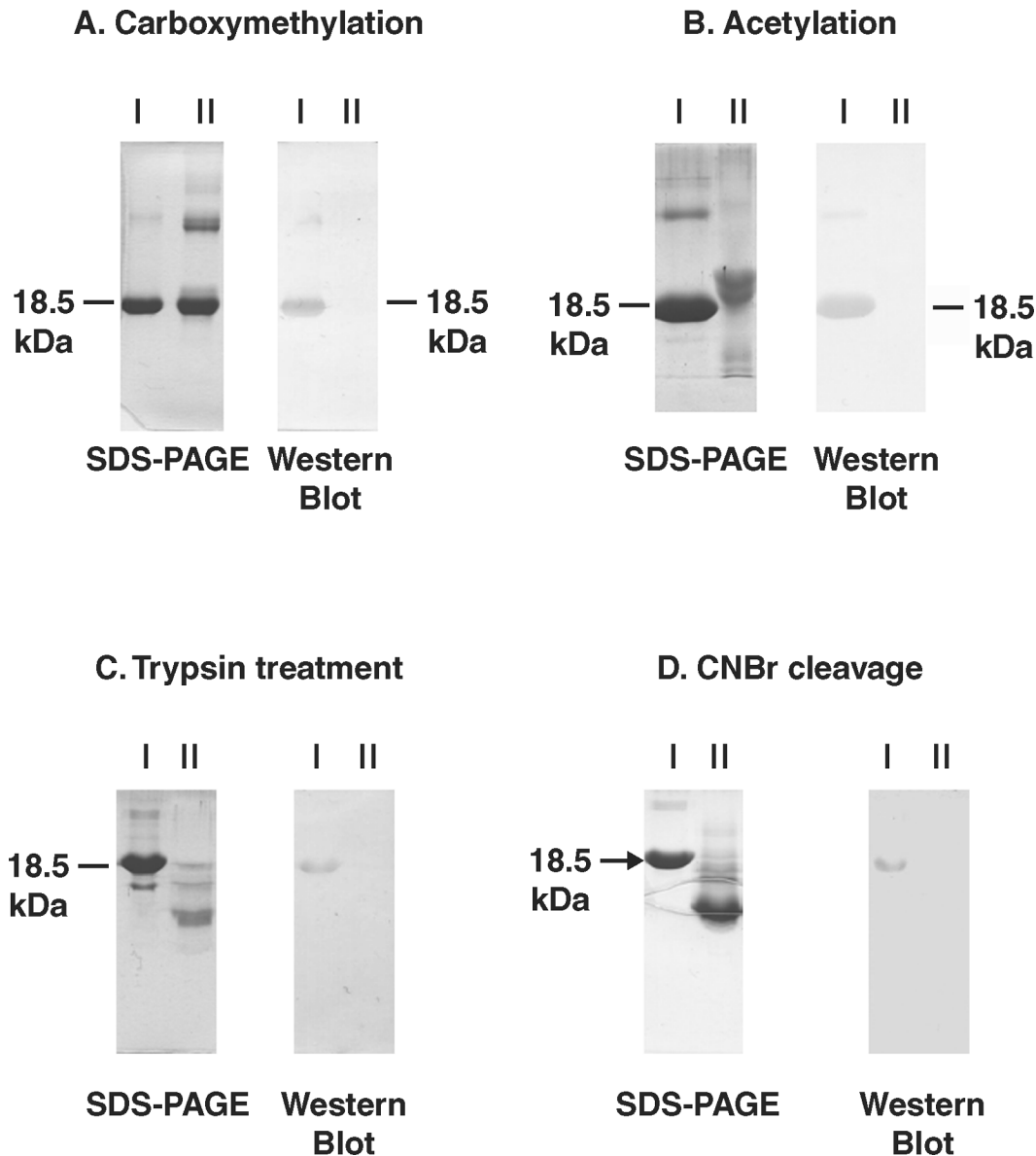


**Figure 5.** Role of disulfide linkage in maintaining the antigenic structure of  $\beta$ -LG and the effect of chemical modifications on its immunoreactivity. A)  $\beta$ -LG was irreversibly reduced by carboxymethylation; lane I: native  $\beta$ -LG and lane II: carboxymethylated  $\beta$ -LG. B)  $\beta$ -LG was modified before (lane I) and after (lane II) acetylation at pH 10. C)  $\beta$ -LG was treated before (lane I) and after (lane II) trypsin cleavage. D)  $\beta$ -LG was treated before (lane I) and after (lane II) cyanogen bromide (CNBr) cleavage. The left side of each panel represents the analysis of 20% SDS-PAGE using Coomassie blue staining, except for Panel A, where staining was at 15% SDS-PAGE. The right side of each panel represent the Western blot analysis using native monoclonal antibody 4H11E8. The data suggest that the immunoreactivity is dependent on the overall structure of  $\beta$ -LG (A and B), and the epitope is likely not located in the  $\beta$ -LG fragments (C and D).

satisfactory result (Caprioli et al., 1991; Andrews et al., 1992), but the reaction time is somewhat slower than that of formic acid.

Taken together, our study reveals that this native mAb is conformationally dependent on the overall structure of  $\beta$ -LG. It is difficult for us to map out the specific antigenic determinant at the present time, but it is very possible that Cys-121 or its neighboring resi-

dues might play an essential role in the recognition of the native mAb. Because the free Cys-121 residue is known to be involved in the simplest form of covalently linked  $\beta$ -LG dimer upon heating (Panick et al., 1999; Farrell et al., 2004; Kontopidis et al., 2004), such dimerization causes the loss of our mAb binding (Figure 2). The covalent linkage may eventually block the 4H11E8 binding via steric hindrance (Figure 2). Furthermore,



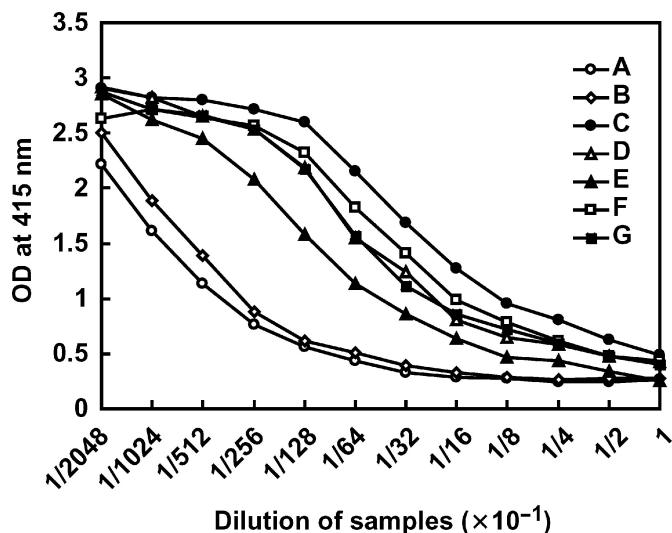


**Figure 6.** Typical example of immunoreactivity of native  $\beta$ -LG in raw and processed milk as determined by a competitive ELISA. Native  $\beta$ -LG was used as an immobilized antigen while competing the binding of raw and processed milks for native monoclonal antibody 4H11E8. A) raw milk, B) processed milk from a local market pasteurized at 60°C for 30 min, and C through G) processed milks purchased from the local market with undisclosed heating procedures. Apparently, the immunoreactivity of  $\beta$ -LG in most of the processed milk was attenuated as compared with the raw milk. OD = optical density.

the Cys-121 is also responsible for cross linking with  $\beta$ -LG aggregates or with other milk proteins upon heating (Chen et al., 2004; Creamer et al., 2004; Croguennec et al., 2004; Chen et al., 2005). We have attempted to map out the antigenic structure for this native mAb using

**Table 1.** Determination of native  $\beta$ -LG from commercially processed milk

Processed milk from market <sup>1</sup>	Amount of native $\beta$ -LG (mg/mL) <sup>2</sup>
1	5.50 ± 0.06
2	5.35 ± 0.15
3	5.40 ± 0.12
4	2.98 ± 0.27
5	0.60 ± 0.08
6	0.36 ± 0.02
7	0.55 ± 0.08
8	1.84 ± 0.36
9	0.39 ± 0.03
10	0.34 ± 0.08
11	0.68 ± 0.18
12	1.05 ± 0.16
13	0.49 ± 0.04
14	0.48 ± 0.05

<sup>1</sup>Samples 1, 2, and 3 represent a raw milk and a processed milk of a local market pasteurized at 60°C for 30 min and a processed milk of a U.S. market pasteurized with a standard procedure, respectively. Samples 4 through 13 represent various processed milks of a local market with an undisclosed heating procedure.

<sup>2</sup>Determination of  $\beta$ -LG was by competitive ELISA. Each value represents the mean ± SEM of triplicate determinations.

the peptide array technique previously established in our laboratory (Song et al., 2005), but we failed to show any immunoreactivity against the synthetic peptides. Therefore, we can only speculate that Cys-121 (or its neighboring residues) is essential for mAb recognition, but the antigen-antibody interaction may still need the integrity of the native structure of  $\beta$ -LG. Final conclusive interpretation of the involvement of Cys-121 with respect to the native mAb recognition probably lies in the use of recombinant  $\beta$ -LG with a single mutation on Cys-121. This experiment is now in progress in our laboratory using site-directed mutagenesis. In addition, the acetylation experiment conducted in this study (Figure 5) tended to suggest the possible involvement of lysyl residues in the antigenic determinant similar to that found previously (Song et al., 2005), in which the positively charged residues are frequently expressed on a surface epitope.

As to the biological function of  $\beta$ -LG, studies have shown that it produces hypocholesterolemic (Nagaoka et al., 2001) and antioxidant effects (Peña-Ramos and Xiong, 2001; Wong and Kitts, 2003; Hernandez-Ledesma et al., 2005) and may also serve as a growth factor for mammalian cells (Feuermann et al., 2004). It can transport and complex with retinol and fatty acids via its hydrophobic binding pocket calyx of  $\beta$ -LG (Song et al., 2005). Interestingly,  $\beta$ -LG is not only acid resistant in gastrointestinal tracts, but it also possesses a superior absorption capability via a receptor-mediated process (Dew and Ong, 1997). Our recent study demonstrates the loss of this binding capability when  $\beta$ -LG is denatured by heating to >80°C. We have further suggested that it is the exposure of hydrophobic region (residues 66 to 76) of the D strand to a polar environment that destabilizes the calyx structure and complex formation with retinol and palmitic acid (Song et al., 2005). Because  $\beta$ -LG is also labile to heat treatment by forming large polymers with other milk proteins (Chen et al., 2004, 2005), it is tempting to speculate that heat may reduce the extent of absorption of  $\beta$ -LG through the gut. Conceivably, additional overheating should be avoided to maintain the physiologic role of  $\beta$ -LG. Our mAb may provide a novel mean for monitoring the native structure of  $\beta$ -LG in heat-processed milks. It is of interest to note that the reported transition temperature of native  $\beta$ -LG (between 70 and 80°C) is almost completely agreeable with the decrease in immunoreactivity for the native mAb (Figure 4). From a technological standpoint, this mAb may be relevant to the design and operation of appropriate processes for thermal sanitation of milk and other dairy products. For example, using a standard Ohio State University method of manufacturing whey protein curd, milk is short-time pasteurized (about 72°C for 30 s) and held overnight at

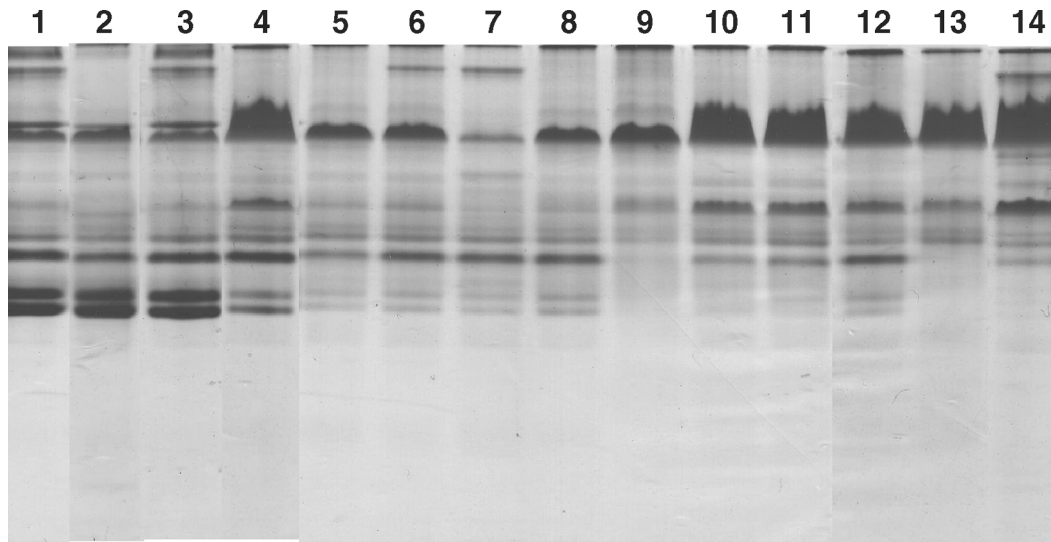


**Figure 7.** Characterization of  $\beta$ -LG content in processed milk using native PAGE. Whey protein of skimmed milk ( $n = 14$ ;  $10 \mu\text{g}$  each) was loaded on a 15% native PAGE and stained by Coomassie blue. For the preparation of whey protein, milk samples were immediately centrifuged at 13,000 rpm ( $15,500 \times g$ ) for 1 h at  $4^\circ\text{C}$ . The top layer in the supernatant was carefully removed, and the remaining fraction (whey protein) containing minimal casein was used for the analysis. Lane 1: raw milk; lane 2: processed milk from a local market pasteurized at  $60^\circ\text{C}$  for 30 min; lane 3: processed milk from a US market pasteurized with a standard procedure; lanes 4 to 14: processed milk of various brands from a local market with undisclosed heating procedures.  $\beta$ -Lactoglobulin concentration in each milk was determined by native mAb using an ELISA. The designated sample number of each tested milk was the same as that shown in Table 1 ( $n = 14$ ).

$40^\circ\text{C}$ . The next morning, the mixture is cooled to  $30^\circ\text{C}$ , inoculated with a lactic acid culture, and incubated for 30 min. Rennet extract is added, and the mixture is stirred, resulting in coagulation of curd (Marshall, 2004). According to our curve for thermal denaturation constructed by the mAb (Figure 4),  $\beta$ -LG is likely intact using these standard procedures. The present study shows the use of native mAb in determining the native  $\beta$ -LG concentration in processed milk (Table 1), but not of the polyclonal antibodies, as they recognized both native and denatured  $\beta$ -LG (Chen et al., 2005). Table 1 illustrates that the  $\beta$ -LG content varied significantly among the brands we tested. Although the status for the manufactured process is not disclosed and is not yet readily known, our study indicates the remarkable difference among the procedures for thermal sterilization and pasteurization as previously indicated (Douglas et al., 1981). Therefore, it is recommended that the heating process should be eventually standardized to avoid unnecessary overheating by our domestic manufacturers. In conclusion, the present study provides evidence that a novel conformation-dependent  $\beta$ -LG mAb can be prepared via an appropriate immunization strategy and screening. Such native mAb can be used as a unique reagent to routinely monitor the quality of dairy products when  $\beta$ -LG is considered to be an essential ingredient.

## ACKNOWLEDGMENT

This work was supported by grants 90-2313-B-009-001, 91-2313-B-009-001, 92-2313-B-009-002, 93-2313-B-009-002, and 94-2313-B-009-001 from the National Science Council, Taiwan, Republic of China.

## REFERENCES

- Andrews, P. C., M. M. Allen, M. L. Vestal, and R. W. Nelson. 1992. Large scale protein mapping using infrequent cleavage reagents, LD TOF MS, and ES MS. Pages 515–523 in *Techniques in Protein Chemistry II*. R. M. Angeletti, ed. Academic Press, San Diego, CA.
- Beavis, R. C., and B. T. Chait. 1990. Rapid, sensitive analysis of protein mixtures by mass spectrometry. *Proc. Natl. Acad. Sci. USA* 87:6873–6877.
- Braunschweig, M., C. Hagger, G. Stranzinger, and Z. Puhan. 2000. Associations between casein haplotypes and milk production traits of Swiss brown cattle. *J. Dairy Sci.* 83:1387–1395.
- Caprioli, R. M., B. Whaley, K. K. Mock, and J. S. Cottrell. 1991. Sequence-ordered peptide mapping by time-course analysis of protease digests using laser description mass spectrometry. Pages 497–510 in *Techniques in Protein Chemistry II*. R. M. Angeletti, ed. Academic Press, San Diego, CA.
- Chang, J. Y., A. Bulychev, and L. Li. 2000. A stabilized molten globule protein. *FEBS Lett.* 487:298–300.
- Chen, W. L., M. T. Hwang, C. Y. Liao, J. C. Ho, K. C. Hong, and S. J. T. Mao. 2005. Beta-lactoglobulin is a thermal marker in processed milk as studied by electrophoresis and circular dichroic spectra. *J. Dairy Sci.* 88:1618–1630.
- Chen, W. L., M. T. Hwang, H. C. Liu, C. W. Li, and S. J. T. Mao. 2004. Distinction between dry and raw milk using monoclonal antibodies prepared against dry milk proteins. *J. Dairy Sci.* 87:2720–2729.

- Creamer, L. K., A. Bienvenue, H. Nilsson, M. Paulsson, M. van Wanroij, E. K. Lowe, S. G. Anema, M. J. Boland, and R. Jimenez-Flores. 2004. Heat-induced redistribution of disulfide bonds in milk proteins. 1. Bovine beta-lactoglobulin. *J. Agric. Food Chem.* 52:7660–7668.
- Croguennec, T., D. Molle, R. Mehra, and S. Bouhallab. 2004. Spectroscopic characterization of heat-induced nonnative beta-lactoglobulin monomers. *Protein Sci.* 13:1340–1346.
- de Jongh, H. H. J., T. Gröneveld, and J. de Groot. 2001. Mild isolation procedure discloses new protein structural properties of  $\beta$ -lactoglobulin. *J. Dairy Sci.* 84:562–571.
- Dew, S. E., and D. E. Ong. 1997. Absorption of retinol from the retinol:retinol-binding protein complex by small intestinal gut sheets from the rat. *Arch. Biochem. Biophys.* 338:233–236.
- Douglas, F. W., Jr., R. Greenberg, H. M. Farrell, Jr., and L. F. Edmondson. 1981. Effects of ultra-high-temperature pasteurization on milk proteins. *J. Agric. Food Chem.* 29:11–15.
- Farrell, H. M., R. Jimenez-Flores, G. T. Bleck, E. M. Brown, J. E. Butler, L. K. Creamer, C. L. Hicks, C. M. Hollar, K. F. Ng-Kwai-Hang, and H. E. Swaisgood. 2004. Nomenclature of the proteins of cows' milk—Sixth revision. *J. Dairy Sci.* 87:1641–1674.
- Feuermann, Y., S. J. Mabeesh, and A. Shamay. 2004. Leptin affects prolactin action on milk protein and fat synthesis in the bovine mammary gland. *J. Dairy Sci.* 87:2941–2946.
- Forge, V., M. Hoshino, K. Kuwata, M. Arai, K. Kuwajima, C. A. Batt, and Y. Goto. 2000. Is folding of beta-lactoglobulin non-hierarchical? Intermediate with native-like beta-sheet and non-native alpha-helix. *J. Mol. Biol.* 296:1039–1051.
- Hernandez-Ledesma, B., A. Davalos, B. Bartolome, and L. Amigo. 2005. Preparation of antioxidant enzymatic hydrolysates from alpha-lactalbumin and beta-lactoglobulin. Identification of active peptides by HPLC-MS/MS. *J. Agric. Food Chem.* 53:588–593.
- Kontopidis, G., C. Holt, and L. Sawyer. 2002. The ligand-binding site of bovine beta-lactoglobulin: Evidence for a function? *J. Mol. Biol.* 318:1043–1055.
- Kontopidis, G., C. Holt, and L. Sawyer. 2004. Invited review: Beta-lactoglobulin: Binding properties, structure, and function. *J. Dairy Sci.* 87:785–796.
- Mao, S. J. T., R. E. Kazmar, J. C. Silverfield, M. C. Alley, K. Kluge, and C. G. Fathman. 1982. Immunochemical properties of human low density lipoproteins as explored by monoclonal antibodies. Binding characteristics distinct from those of conventional serum antibodies. *Biochim. Biophys. Acta* 713:365–374.
- Mao, S. J. T., J. G. Patton, J. J. Badimon, B. A. Kottke, M. C. Alley, and A. D. Cardin. 1983. Monoclonal antibodies to human plasma low-density lipoproteins. I. Enhanced binding of 125I-labeled low-density lipoproteins by combined use of two monoclonal antibodies. *Clin. Chem.* 29:1890–1897.
- Mao, S. J. T., A. E. Rechten, and R. L. Jackson. 1988. Monoclonal antibodies that distinguish between active and inactive forms of human postheparin plasma hepatic triglyceride lipase. *J. Lipid Res.* 29:1023–1029.
- Mao, S. J. T., A. E. Rechten, J. L. Krstenansky, and R. L. Jackson. 1990. Characterization of a monoclonal antibody specific to the amino terminus of the alpha-chain of human fibrin. *Thromb. Haemost.* 63:445–448.
- Mao, S. J. T., J. T. Sparrow, E. B. Gilliam, A. M. Gotto, and R. L. Jackson. 1977. Mechanism of lipid-protein interaction in the plasma lipoproteins: Lipid-binding properties of synthetic fragments of apolipoprotein A-II. *Biochemistry* 16:4150–4156.
- Mao, S. J. T., J. T. Sparrow, A. M. Gotto, and R. L. Jackson. 1980. The phospholipid-binding and immunochemical properties of amidinated, guanidinated and acetylated apolipoprotein A-II. *Biochim. Biophys. Acta* 617:245–253.
- Marshall, K. 2004. Therapeutic applications of whey protein. *Altern. Med. Rev.* 9:136–156.
- Morrison, J. R., N. H. Fidge, and B. Grego. 1990. Studies on the formation, separation, and characterization of cyanogen bromide fragments of human AI apolipoprotein. *Anal. Biochem.* 186:145–152.
- Nagaoka, S., F. Yu, M. Keiji, A. Takako, Y. Kouhei, K. Yoshihiro, T. Kojima, and K. Tamotsu. 2001. Identification of novel hypocholesterolemic peptides derived from bovine milk  $\beta$ -lactoglobulin. *Biochem. Biophys. Res. Commun.* 281:11–17.
- Needs, E. C., M. Capellas, A. P. Bland, P. Manoj, D. MacDougall, and G. Paul. 2000. Comparison of heat and pressure treatments of skim milk, fortified with whey protein concentrate, for set yogurt preparation: Effects on milk proteins and gel structure. *J. Dairy Res.* 67:329–348.
- Oldfield, D. J., H. Singh, M. W. Taylor, and K. N. Pearce. 1998. Kinetics of denaturation and aggregation of whey protein in skim milk heated in an ultra-high temperature (UHT) plant. *Int. Dairy J.* 8:311–318.
- Panick, G., R. Malessa, and R. Winter. 1999. Differences between the pressure- and temperature-induced denaturation and aggregation of beta-lactoglobulin A, B, and AB monitored by FT-IR spectroscopy and small-angle X-ray scattering. *Biochemistry* 38:6512–6519.
- Patton, J. G., J. J. Badimon, and S. J. T. Mao. 1983. Monoclonal antibodies to human plasma low-density lipoproteins. II. Evaluation for use in radioimmunoassay for apolipoprotein B in patients with coronary artery disease. *Clin. Chem.* 29:1898–1903.
- Peña-Ramos, E. A., and Y. L. Xiong. 2001. Antioxidative activity of whey protein hydrolysates in a liposomal system. *J. Dairy Sci.* 84:2577–2583.
- Pérez, M. D., and M. Calvo. 1995. Interaction of  $\beta$ -lactoglobulin with retinol and fatty acids and its role as a possible biological function for this protein: A review. *J. Dairy Sci.* 78:978–988.
- Qin, B. Y., M. C. Bewley, L. K. Creamer, H. M. Baker, E. N. Baker, and G. B. Jameson. 1998. Structural basis of the Tanford transition of bovine beta-lactoglobulin. *Biochemistry* 37:14014–14023.
- Qin, B. Y., M. C. Bewley, L. K. Creamer, E. N. Baker, and G. B. Jameson. 1999. Functional implications of structural differences between variants A and B of bovine beta-lactoglobulin. *Protein Sci.* 8:75–83.
- Sava, N., I. Van der Plancken, W. Claeys, and M. Hendrickx. 2005. The kinetics of heat-induced structural changes of  $\beta$ -lactoglobulin. *J. Dairy Sci.* 88:1646–1653.
- Song, C. Y., W. L. Chen, M. C. Yang, J. P. Huang, and S. J. T. Mao. 2005. Epitope mapping of a monoclonal antibody specific to bovine dry milk: Involvement of residues 66–76 of strand D in thermal denatured beta-lactoglobulin. *J. Biol. Chem.* 280:3574–3582.
- Tsang, C. F., C. C. Lin, H. Y. Huang, H. C. Liu, and S. J. T. Mao. 2004. Antioxidant role of human haptoglobin. *Proteomics* 4:2221–2228.
- Uhrinova, S., M. H. Smith, G. B. Jameson, D. Uhrin, L. Sawyer, and P. N. Barlow. 2000. Structural changes accompanying pH-induced dissociation of the beta-lactoglobulin dimer. *Biochemistry* 39:3565–3574.
- Wang, T., and J. A. Lucey. 2003. Use of multi-angle laser light scattering and size-exclusion chromatography to characterize the molecular weight and types of aggregates present in commercial whey protein products. *J. Dairy Sci.* 86:3090–3101.
- Wong, P. Y. Y., and D. D. Kitts. 2003. Chemistry of buttermilk solid antioxidant activity. *J. Dairy Sci.* 86:1541–1547.
- Wu, S. Y., M. D. Perez, P. Puyol, and L. Sawyer. 1999. Beta-lactoglobulin binds palmitate within its central cavity. *J. Biol. Chem.* 274:170–174.
- Yang, J., A. K. Dunker, J. R. Powers, S. Clark, and B. G. Swanson. 2001. Beta-lactoglobulin molten globule induced by high pressure. *J. Agric. Food Chem.* 49:3236–3243.
- Yang, S. J., and S. J. T. Mao. 1999. A simple HPLC purification procedure for porcine plasma haptoglobin. *J. Chromatogr. B* 731:395–402.



# Crystal structure of a secondary vitamin D<sub>3</sub> binding site of milk $\beta$ -lactoglobulin

Ming-Chi Yang,<sup>1</sup> Hong-Hsiang Guan,<sup>2,3</sup> Ming-Yih Liu,<sup>2</sup> Yih-Hung Lin,<sup>2</sup> Jinn-Moon Yang,<sup>1</sup> Wen-Liang Chen,<sup>1</sup> Chun-Jung Chen,<sup>2,3\*</sup> and Simon J. T. Mao<sup>1,4\*</sup>

<sup>1</sup> Department of Biological Science and Technology, College of Biological Science and Technology, National Chiao Tung University, Taiwan, Republic of China

<sup>2</sup> Life Science Group, Research Division, National Synchrotron Radiation Research Center, Taiwan, Republic of China

<sup>3</sup> Department of Physics, Institute of Bioinformatics and Structural Biology, National Tsing Hua University, Taiwan, Republic of China

<sup>4</sup> Department of Biotechnology and Bioinformatics, Asian University, Taiwan, Republic of China

## ABSTRACT

$\beta$ -lactoglobulin ( $\beta$ -LG), one of the most investigated proteins, is a major bovine milk protein with a predominantly  $\beta$  structure. The structural function of the only  $\alpha$ -helix with three turns at the C-terminus is unknown. Vitamin D<sub>3</sub> binds to the central calyx formed by the  $\beta$ -strands. Whether there are two vitamin D binding-sites in each  $\beta$ -LG molecule has been a subject of controversy. Here, we report a second vitamin D<sub>3</sub> binding site identified by synchrotron X-ray diffraction (at 2.4 Å resolution). In the central calyx binding mode, the aliphatic tail of vitamin D<sub>3</sub> clearly inserts into the binding cavity, where the 3-OH group of vitamin D<sub>3</sub> binds externally. The electron density map suggests that the 3-OH group interacts with the carbonyl of Lys-60 forming a hydrogen bond (2.97 Å). The second binding site, however, is near the surface at the C-terminus (residues 136–149) containing part of an  $\alpha$ -helix and a  $\beta$ -strand I with 17.91 Å in length, while the span of vitamin D<sub>3</sub> is about 12.51 Å. A remarkable feature of the second exosite is that it combines an amphipathic  $\alpha$ -helix providing nonpolar residues (Phe-136, Ala-139, and Leu-140) and a  $\beta$ -strand providing a nonpolar (Ile-147) and a buried polar residue (Arg-148). They are linked by a hydrophobic loop (Ala-142, Leu-143, Pro-144, and Met-145). Thus, the binding pocket furnishes strong hydrophobic force to stabilize vitamin D<sub>3</sub> binding. This finding provides a new insight into the interaction between vitamin D<sub>3</sub> and  $\beta$ -LG, in which the exosite may provide another route for the transport of vitamin D<sub>3</sub> in vitamin D<sub>3</sub> fortified dairy products. Atomic coordinates for the crystal structure of  $\beta$ -LG-vitamin D<sub>3</sub> complex described in this work have been deposited in the PDB (access code 2GJ5).

Proteins 2008; 71:1197–1210.  
© 2007 Wiley-Liss, Inc.

**Key words:** fluorescence ligand binding assay; crystallography; localized alternative vitamin D binding site; thermal denaturation; amphipathic helix.

## INTRODUCTION

Bovine  $\beta$ -lactoglobulin ( $\beta$ -LG) is a major whey protein in milk to an extent of about 50%.<sup>1</sup> Because of its thermally unstable and molten-globule nature,  $\beta$ -LG has been studied extensively for its physical and biochemical properties in the past 40 years.<sup>2–6</sup> Although the biological functions of the protein still remain elusive, some essential functions of  $\beta$ -LG, such as cholesterol lowering, modulation of immune system, transport of retinol, fatty acid, and vitamin D,<sup>7–9</sup> and prevention of oxidative-stress,<sup>10,11</sup> have been reported.

Several crystal forms of bovine  $\beta$ -LG have been described.<sup>12–21</sup> Of these, lattices X and Z (Space group *P*1 and *P*3<sub>2</sub>21) have been investigated at a low resolution.<sup>14</sup> A high resolution study of another crystal form, lattice Y, has yielded a chain trace and a preliminary model.<sup>14</sup> The overall folding turns out to be remarkably similar to that of the human plasma retinol binding protein<sup>15,16,22,23</sup> and human tear lipocalin,<sup>24</sup> known as members of the lipocalin superfamily. As shown in Figure 1(A),  $\beta$ -LG comprises of 162 amino acid residues with two disulfide linkages and one free cysteine. It has predominantly a  $\beta$ -sheet configuration containing nine antiparallel  $\beta$ -strands from A to I.<sup>18,19,25</sup> Topographically,  $\beta$ -strands A–D form one surface of the barrel (calyx), whereas strands E–H form the other.

The only  $\alpha$ -helical structure with three turns is at the COOH-terminus (residues 130–141), which is followed by a  $\beta$ -strand I lying on the outer surface of the calyx.<sup>26</sup> The

Grant sponsor: National Science Council (NSC); Grant numbers: 92-2313-B-009-002, 93-2313-B009-002, 94-2313-B-009-001, 95-2313-B-009-001, 94-2321-B-213-001; Grant sponsor: National Synchrotron Radiation Research Center (NSRRC); Grant numbers: 944RSB02, 954RSB02.

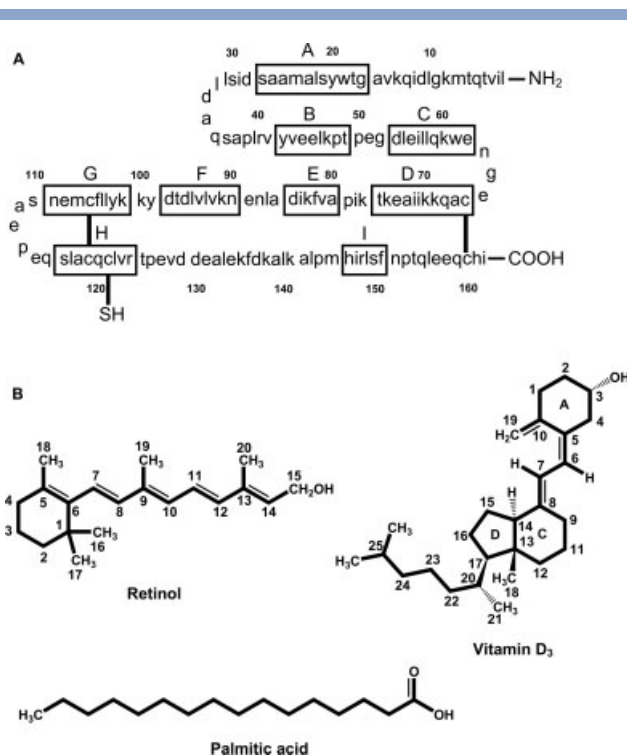
\*Correspondence to: Simon J. T. Mao, Department and College of Biological Science and Technology, National Chiao Tung University, 75 Po-Ai Street, Hsinchu, 30068 Taiwan, ROC. E-mail: mao1010@ms7.hinet.net and Chun-Jung Chen, Life Science Group, Research Division, National Synchrotron Radiation Research Center, 101 Hsin-Ann Road, Hsinchu, 30076 Taiwan, ROC. E-mail: cjchen@nsrrc.org.tw

Received 13 April 2007; Revised 16 August 2007; Accepted 22 August 2007

Published online 14 November 2007 in Wiley InterScience (www.interscience.wiley.com).

DOI: 10.1002/prot.21811



**Figure 1**

Amino acid sequence of  $\beta$ -LG and chemical structure of its binding ligands. (A)  $\beta$ -LG is consisted of 162 amino acids with nine  $\beta$ -sheet strands (A-I) and one  $\alpha$ -helix at the COOH-terminus. There are two disulfide linkages located between strand D and COOH-terminus (Cys-66 and Cys-160) and between strands G and H (Cys-106 and Cys-119), with a free buried thio-group at Cys-121.  $\alpha$ -helix with three turns is located between residues 130 and 141 (in light gray). (B) Chemical structure of retinol, palmitic acid, and vitamin D<sub>3</sub>.

structural and functional relationship of this helical region is not yet clearly defined. Studies on the crystal structure of  $\beta$ -LG-retinol complex at 2.5 Å resolution by Monaco *et al.* have pointed out that there is a surface pocket consisting of almost completely hydrophobic residues near the helical region.<sup>16</sup>

The remarkable ability of the calyx to bind hydrophobic molecules, such as retinol, fatty acids, and vitamin D [Fig. 1(B)],<sup>27–29</sup> has recently been reviewed by Kontopidis *et al.*<sup>9</sup> It seems clear that the binding of fatty acid, retinol, and vitamin D is within the central calyx of the protein; however, the existence of a second ligand binding site beyond the calyx is a matter of controversy.<sup>9</sup> Interestingly, an early study has suggested that a hydrophobic pocket, formed by the  $\alpha$ -helix and the surface of the barrel, also exists.<sup>16</sup> This surface pocket, limited by Phe-136 and followed by residues 139–143 (Ala-Leu-Lys-Ala-Leu), has been suspected to potentially bind retinol;<sup>16</sup> however, later studies by X-ray diffraction did not reveal that retinol could occupy this site.<sup>9,29</sup> Using *cis*-parinaric acid as a ligand, Dufour *et al.*<sup>30</sup> have suggested that this ligand is bound in this hydrophobic pocket. It

remains unclear what type of ligands may interact with this surface site. The binding of vitamin D to  $\beta$ -LG is also controversial.<sup>9,31</sup> It has been postulated that there is another binding site, in addition to the calyx, for vitamin D based on the work of Swaisgood and de Wolf<sup>31–35</sup> by using biochemical binding assays. Subsequently, they also suggested that one vitamin D is bound in that hydrophobic site. Nevertheless, the location of the secondary binding site remote from the calyx has been implicated,<sup>15,16</sup> but has not yet been identified by the crystal structure of bovine  $\beta$ -LG with vitamin D<sub>2</sub>.<sup>9</sup>

Spectroscopic studies and thermodynamic analysis of the calorimetric signal have demonstrated that irreversible unfolding of the  $\beta$ -LG structure occurs upon thermal treatment above its transition temperature, 65–70°C.<sup>36</sup> Recently, we have shown that the conformational changes of  $\beta$ -LG are rapid and extensive at temperatures above the transition,<sup>5</sup> and  $\beta$ -strand D of the calyx is directly involved in the unfolding during the thermal denaturation.<sup>4</sup> As a result, the binding of palmitate or retinol to the central calyx is diminished. In the present study, we also demonstrated that the maximal binding ratios of vitamin D<sub>3</sub> to  $\beta$ -LG were 2:1, similar to that established by Wang *et al.*<sup>31</sup> Our next strategy was to denature the conformation of the calyx by heating at 100°C for 16 min; under this condition the calyx pocket was thermally “removed.” We then tested whether the thermally denatured  $\beta$ -LG was able to bind vitamin D<sub>3</sub>, palmitate, and retinol. Interestingly, only vitamin D<sub>3</sub> bound the heated  $\beta$ -LG and the binding ratio of vitamin D<sub>3</sub> to the heated  $\beta$ -LG was found to be 1:1. Thus, it suggests that there is a secondary site for vitamin D<sub>3</sub> binding, which is thermally independent. To confirm the hypothesis that a second vitamin D<sub>3</sub> binding site exists, we determined the crystal structure of  $\beta$ -LG-vitamin D<sub>3</sub> complex and attempted to identify, localize, and characterize such a site.

## MATERIALS AND METHODS

### Materials

$\beta$ -LG was purified from raw milk using saturated ammonium sulfate (40%) followed by a G-150 column chromatography of the upper fraction as described previously.<sup>3</sup> All-*trans* retinol, palmitic acid, vitamin D<sub>3</sub> (cholecalciferol), and *N*-acetyl-L-tryptophanamide were purchased from Sigma-Aldrich (St. Louis, MO).

### Ligand binding to $\beta$ -LG

$\beta$ -LG stock solution was prepared in 0.01M phosphate buffered solution, pH 8.0 (PB). Retinol, palmitate, and vitamin D<sub>3</sub> were prepared using absolute ethanol and purged with nitrogen and stored at –80°C in the dark. All the binding assays described below were conducted at

24°C. The ligand binding assay of  $\beta$ -LG was measured by fluorescence emission techniques similar to that previously described.<sup>4,31,32</sup> In general, the binding of retinol to  $\beta$ -LG was measured by extrinsic fluorescence emission of a retinol molecule at 470 nm using excitation at 287 nm, whereas binding of palmitate or vitamin D<sub>3</sub> to  $\beta$ -LG was measured by the fluorescence enhancement or quenching of Trp-19 of  $\beta$ -LG at 332 nm using excitation at 287 nm. Fluorescence spectra were recorded with a fluorescence spectrophotometer (Hitachi F-4500; Tokyo, Japan). For the titration experiment, 5  $\mu$ M of native  $\beta$ -LG was instantly incubated with various proportions of retinol or vitamin D<sub>3</sub> (0.625–25  $\mu$ M) at pH 8.0. For palmitate (2.5–100  $\mu$ M), 20  $\mu$ M of native  $\beta$ -LG was used. A solution of *N*-acetyl-L-tryptophanamide with an absorbance at 287 nm—equal to that of the protein—served as a blank. The change in fluorescence of this solution with titration caused by an inner filter effect was corrected as described by Cogan *et al.*<sup>37</sup> The change in fluorescence intensity at 332 nm or 470 nm was assumed to depend on the amount of protein-ligand complex, which allowed the calculation of *a*, the fraction of unoccupied ligand-binding sites on the protein:  $a = (F - F_{\text{sat}})/(F_0 - F_{\text{sat}})$ . Here *F* is the fluorescence intensity at a certain titration ratio, *F*<sub>sat</sub> is the corrected fluorescence intensity of  $\beta$ -LG solution with its sites saturated, and *F*<sub>0</sub> is the initial corrected fluorescence intensity. These data were then used to construct a plot of *P<sub>T</sub>a* versus *R<sub>T</sub>a/(1 - a)* according to the equation:  $P_T a = (1/n)[R_T a/(1 - a)] - K_d^{\text{app}}/n$ , where *P<sub>T</sub>* is the total protein concentration, *n* is the number of binding sites per molecule, *R<sub>T</sub>* is the total ligand concentration, and *K<sub>d</sub><sup>app</sup>* is the apparent dissociation constant.

To study the effect of pH on the binding capacity, native  $\beta$ -LG between 5 and 20  $\mu$ M was instantly incubated with retinol, vitamin D<sub>3</sub>, or palmitate between 5 and 20  $\mu$ M. To determine the effect of heat on the binding ability,  $\beta$ -LG was preheated at between 50 and 100°C for 15 s to 16 min and stopped using a 20°C water bath. The preheated  $\beta$ -LG was then incubated with retinol, palmitate, or vitamin D<sub>3</sub> at pH 8.0. The final concentration of ethanol in the reaction mixture was kept less than 3% (vol/vol) for all the experiments mentioned above. The ligand binding ability of  $\beta$ -LG was calculated as described previously.<sup>4,31</sup> For the titration curve experiment, the data were expressed as the percentage of emission of  $\beta$ -LG that had the maximal binding ratio. For the heat denaturation experiment, the data were expressed as the percentage relative to native  $\beta$ -LG. All the data were collected in triplicate determinations.

### Circular dichroism spectrum

For the circular dichroism (CD) spectral measurements, each sample (0.5 mg/mL) was heated in 20 mM Tris, pH 8.0.<sup>4,38</sup> The CD spectra were recorded on a

spectropolarimeter (Jasco-J715; Tokyo, Japan) at 24°C over wavelength ranges from 200 to 250 nm, and recorded at a scan speed of 20 nm/min. All spectra were measured twenty times in a cuvette with a path length of 1.0 mm. Each  $\beta$ -LG sample (100  $\mu$ L) was preheated at 50, 60, 70, 80, 90, and 100°C for 16 min and instantly stopped in a 20°C water bath before an immediate measurement.

### Crystallization

Purified  $\beta$ -LG was concentrated to 20 mg/mL in 20 mM Tris, pH 8.0. Vitamin D<sub>3</sub> stock solution made up as 50 mM in ethanol was added to  $\beta$ -LG solution to give a molar ratio of 3:1 and incubated for 3 h at 37°C. Precipitation immediately occurred when  $\beta$ -LG and vitamin D<sub>3</sub> were mixed, and the solution drops became clear on the slides after 3–4 days. Crystallization of the  $\beta$ -LG-vitamin D<sub>3</sub> complex was achieved using the hanging-drop vapor-diffusion method at 18°C with 2  $\mu$ L hanging drops containing equal amounts of  $\beta$ -LG-vitamin D<sub>3</sub> complex and a reservoir solution (0.1M HEPES containing 1.4M trisodium citrate dehydrate, pH 7.5). Crystals 0.1–0.2 mm long grew after 7 days.

### Crystallographic data collection and processing

The crystals were mounted on a Cryoloop (0.1–0.2 mm), dipped briefly in 20% glycerol as a cryoprotectant solution, and frozen in liquid nitrogen. X-ray diffraction data at 2.4 Å resolution were collected at 110 K using the synchrotron radiation on the beamlines BL12B2 at SPring-8 (Harima, Japan) and BL13B at NSRRRC (Hsinchu, Taiwan). The data were processed using the *HKL2000* program.<sup>39</sup> The crystals belong to the space group *P*<sub>3</sub><sub>2</sub><sub>1</sub> with unit cell dimensions of *a* = *b* = 53.78 Å and *c* = 111.573 Å. There is one molecule per asymmetric unit according to an estimated solvent content in a reasonable region. Details of the data statistics are given in a table in the text.

### Crystal structure determination and refinement

The structure of the  $\beta$ -LG-vitamin D<sub>3</sub> was determined by molecular replacement<sup>40</sup> as implemented in *CNS v1.1*<sup>41</sup> using the crystal structure of bovine  $\beta$ -LG (PDB code 2BLG)<sup>18</sup> as a search model. The  $\beta$ -LG molecule was located in the asymmetric unit after rotation and translation function searches. All refinement procedures were performed using *CNS v1.1*. The composite omitted electron density maps with coefficients  $|2F_o - F_c|$  were calculated and visualized using *O v7.0*,<sup>42</sup> and the model was rebuilt and adjusted iteratively as required. Throughout the refinement, a random selection (8%) of the data was placed aside as a “free data set,” and the model was

refined against the rest of the data with  $F \geq 0$  as a working set.<sup>43–45</sup> The monomer protein model was initially refined by rigid-body refinement using the data from 15.0 to 3.0 Å resolution, for which the group temperature  $B$  values were first restrained at 20 Å<sup>2</sup>. This refinement was followed by simulated annealing using a slow cooling protocol with a starting temperature of 2500 K, provided in CNS, applied to all data between 15.0 and 2.4 Å. The bulk solvent correction was then applied, and group  $B$  factors were adjusted. After several cycles of positional and grouped  $B$  factor refinement interspersed with interactive modeling, the  $R$ -factor for the  $\beta$ -LG-vitamin D<sub>3</sub> complex decreased to about 28% with the  $R_{\text{free}}$  around 36%. Two elongated extra electron densities with one  $\beta$ -LG molecule were clearly visible and recognized as the vitamin D<sub>3</sub> in  $\sigma_A$ -weighted  $|F_o - F_c|$  difference maps. Two vitamin D<sub>3</sub> molecules were then adjusted and well fitted into the density map. The refinement then proceeded with another cycle of simulated annealing with a slow cooling, starting at a temperature of 1000 K. The vitamin D<sub>3</sub> molecules were adjusted iteratively according to the omitted electron density maps. Finally, water molecules were added using the program CNS v1.1.

### Model validation

The final model of  $\beta$ -LG and vitamin D<sub>3</sub> complex contains 1272 nonhydrogen protein atoms for the monomer  $\beta$ -LG, 28 atoms for one vitamin D<sub>3</sub> molecule, and 38 water molecules. The refinement statistics are given in the text. The correctness of stereochemistry of the model was verified using PROCHECK.<sup>46</sup> The calculations of r.m.s. deviations from ideality<sup>47</sup> for bonds, angles, and dihedral and improper angles performed in CNS showed satisfactory stereochemistry. In a Ramachandran plot,<sup>48</sup> all main chain dihedral angles were in the most favored and additionally allowed regions except for Tyr-99.

### Coordinates

Atomic coordinates for the crystal structure of  $\beta$ -LG-vitamin D<sub>3</sub> complex described in this work have been deposited in the PDB (access code 2GJ5).

## RESULTS

### Binding of $\beta$ -LG to retinol, palmitate, and vitamin D<sub>3</sub>

Using the titration method previously established by Wang *et al.*,<sup>31,32</sup> we show that the maximal binding of vitamin D<sub>3</sub> with  $\beta$ -LG was achieved at a 2:1 ratio; whereas the binding for retinol or palmitate remained to be 1:1 (Fig. 2). This result is similar to that reported previously by Wang *et al.*<sup>31,32</sup> and tends to support a notion that  $\beta$ -LG binds two vitamin D<sub>3</sub> molecules. The

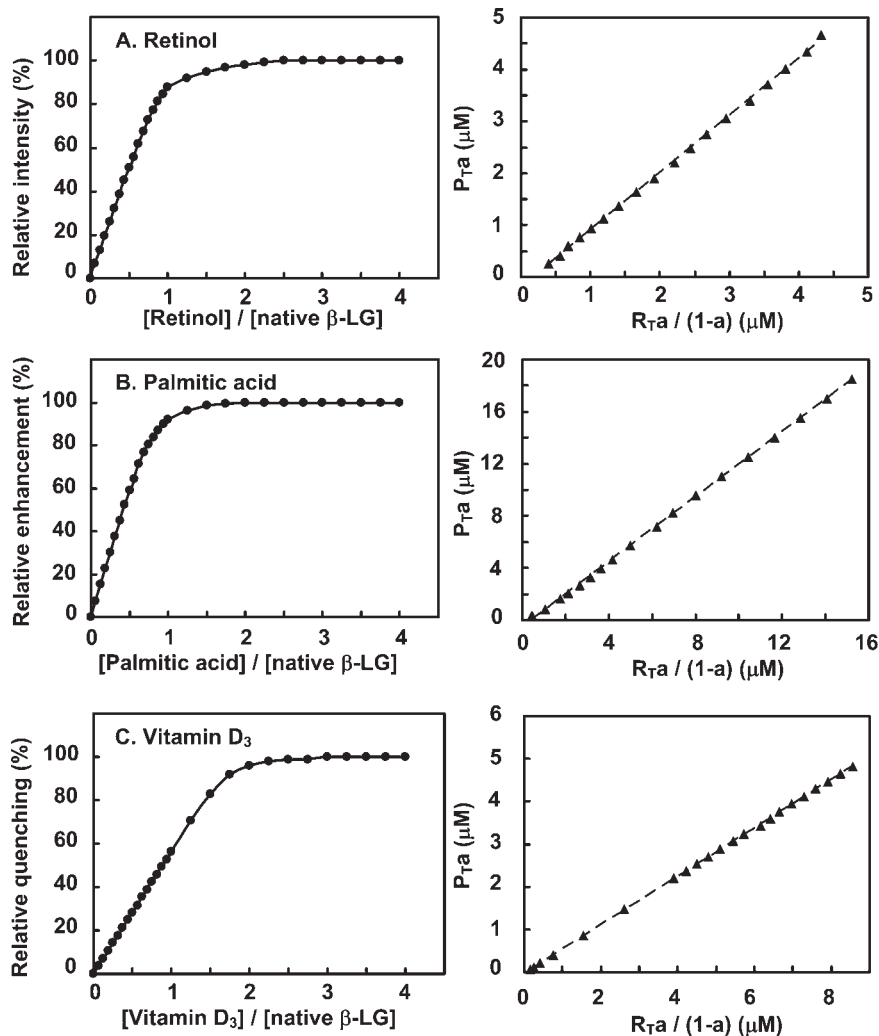
two possibilities for this result are either that  $\beta$ -LG has the same binding site for two vitamin D<sub>3</sub> molecules or it possesses two independent vitamin D<sub>3</sub> binding sites.

### Effect of pH on $\beta$ -LG binding to retinol, palmitate, and vitamin D<sub>3</sub>

It has been postulated that pH plays a crucial role in controlling the opening of the calyx to allow the entrance of  $\beta$ -LG ligands. At low pH or below the Tanford transition (about pH 6), the EF loop (the calyx cap) is closed, disallowing the binding of the ligands. To explore whether there is another vitamin D<sub>3</sub> binding site that may not be affected by the Tanford transition, we monitored the binding of vitamin D<sub>3</sub> at various pH while using retinol or palmitate as a reference. A notable transition of vitamin D<sub>3</sub> binding to  $\beta$ -LG was found to occur between pH 6.0 and 8.0 (Fig. 3), similar to that of retinol and palmitate. The binding to vitamin D<sub>3</sub> or palmitate was decreased to some extent at pH 9–10 (Fig. 3). This could be due to the protonated state of Lys-69 inside the calyx being neutralized at a high pH as suggested previously.<sup>4,29</sup> It is of interest to note that unlike retinol and palmitate;  $\beta$ -LG at a pH between 2 and 6 still retains about 35% of the maximal binding for vitamin D<sub>3</sub> [Fig. 3(C)]. The data imply that there is a possible secondary binding site for vitamin D<sub>3</sub> that is independent of the calyx.

### Effect of heating on $\beta$ -LG binding to retinol, palmitate, and vitamin D<sub>3</sub>

The pH titration experiment described above was unable to yield an accurate explanation of the existence of another binding site for vitamin D<sub>3</sub>. Our previous work showed that thermally denatured  $\beta$ -LG (heated to 100°C for 5 min) was unable to bind to retinol and palmitate because of the unfolding of the calyx.<sup>4</sup> In the next experiment, our strategy was to thermally “remove” the calyx and then test whether heated  $\beta$ -LG retained an activity allowing vitamin D<sub>3</sub> binding. Figure 4 shows a notable and sharp decrease in retinol, palmitate, and vitamin D<sub>3</sub> binding to  $\beta$ -LG heated between 70°C and 80°C over time. The change of binding is consistent to the molten-globule nature of  $\beta$ -LG, which correlates to its transition temperature.<sup>4</sup> At temperatures above 80°C, the protein lost its binding ability to retinol and palmitate in a time-dependent fashion, but it still retained 40% of the binding to vitamin D<sub>3</sub> even after being heated at 100°C for 16 min [Fig. 4(C)]. The heated  $\beta$ -LG (100°C for 16 min) was further titrated with the binding of vitamin D<sub>3</sub> in excess. Figure 4(D) reveals that there was about 42% of maximal binding of vitamin D<sub>3</sub> relative to that using native  $\beta$ -LG. There was no fluorescence change while titrating with retinol or palmitate (data not shown). Remarkably, a maximal stoichiometry of 1:1 was observed between the denatured  $\beta$ -LG and vitamin D<sub>3</sub>.

**Figure 2**

Binding ratio of  $\beta$ -LG with ligands. (A) Titration experiment for binding of  $\beta$ -LG to retinol measured at 470 nm with excitation at 287 nm (pH 8.0). Binding was determined by the enhancement of extrinsic fluorescence of retinol. (B, C) Titration experiment for binding of  $\beta$ -LG to palmitate and vitamin D<sub>3</sub> measured at 332 nm with excitation at 287 nm (pH 8.0). Binding was determined by the fluorescence enhancement (palmitate) and quenching (vitamin D<sub>3</sub>) of intrinsic fluorescence of  $\beta$ -LG. The maximal binding ratio of vitamin D<sub>3</sub> to  $\beta$ -LG is 2:1. Right panels:  $P_T$  = Total protein concentration,  $R_T$  = Total ligand concentration, and  $a$  = Fraction of unoccupied ligand sites on the protein. Each point represents the mean of triplicate determinations with an average of standard deviation (SD) less than 5–8% of the mean.

Thus, it suggests that a thermally stable site exists in  $\beta$ -LG to bind vitamin D<sub>3</sub>.

### Comparison of binding affinity of $\beta$ -LG to retinol, palmitate, and vitamin D<sub>3</sub>

We further determined the binding affinities of  $\beta$ -LG for retinol, palmitate, and vitamin D<sub>3</sub> using the method previously described by Wang *et al.*<sup>31,32</sup> The fluorescence data obtained for retinol, palmitate, and vitamin D<sub>3</sub> binding to native  $\beta$ -LG are shown in Figure 2 (right panels), while the vitamin D<sub>3</sub> binding to heated  $\beta$ -LG (100 °C for 16 min) is shown in Figure 4(D) (inserted panel).

Yielding values for the number of binding sites per molecule and apparent dissociation constant from the slope are listed in Table I. The binding affinity of vitamin D<sub>3</sub> to native  $\beta$ -LG using this method was about 5 nM ( $K_d^{app} = 4.74 \pm 0.37$  nM) and appears to be 5–10 times greater than that of retinol and palmitate. On the other hand, the binding affinity of vitamin D<sub>3</sub> to heated  $\beta$ -LG was attenuated at about 45 nM ( $K_d^{app} = 45.67 \pm 3.12$  nM), but is within the same order as that between native  $\beta$ -LG and retinol or palmitate. Because heating  $\beta$ -LG also induces the aggregation of  $\beta$ -LG,<sup>5</sup> the overall attenuated binding affinity of the “secondary site” indicates a structural change in the second binding site in heated  $\beta$ -LG.



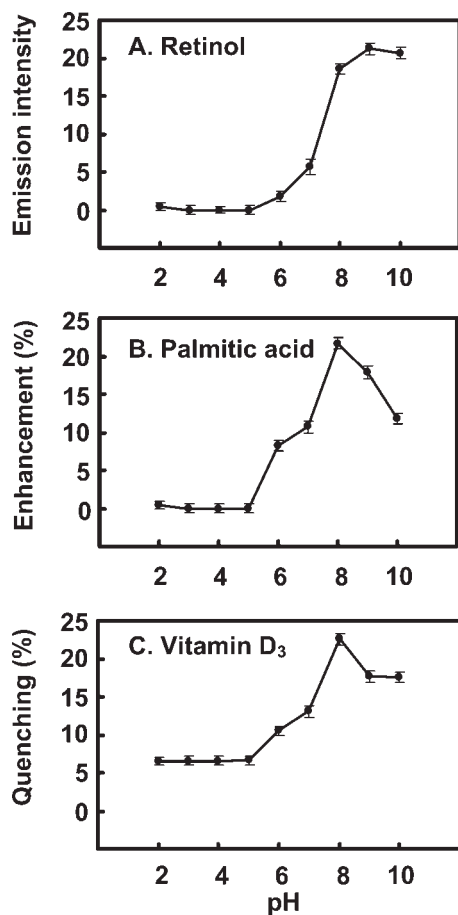


**Figure 3**

Effect of pH (Tanford transition) on  $\beta$ -LG binding with ligands. (A) Emission fluorescence of retinol. (B) Enhanced fluorescence of  $\beta$ -LG upon the binding of palmitate. (C) Quenched intrinsic fluorescence of  $\beta$ -LG upon the binding of vitamin D<sub>3</sub>. All the measurements are identical to that described in Figure 2. Each point represents the mean of triplicate determinations  $\pm$  SD.

Nevertheless, the data temptingly suggest that the putative second binding site is somewhat heat resistant.

### Overall crystal structure of $\beta$ -LG-vitamin D<sub>3</sub> complex

We have clarified that there are two vitamin D binding sites on  $\beta$ -LG according to ligand binding assay performed in solution. Protein crystallography was used to locate the secondary vitamin D binding site of  $\beta$ -LG. There are several crystal forms of bovine  $\beta$ -LG that have been well reported, including the triclinic (lattice X), orthorhombic (lattice Y), and trigonal (lattice Z) forms belonging to space groups  $P1$ ,  $C222_1$ , and  $P3_221$ , respectively.<sup>12–21</sup> The crystal of the  $\beta$ -LG-vitamin D<sub>3</sub> complex we obtained was found to be a trigonal (lattice Z) space group  $P3_221$  based on the data of 2.4 Å resolution. The final model comprised of 161 residues and its refinement

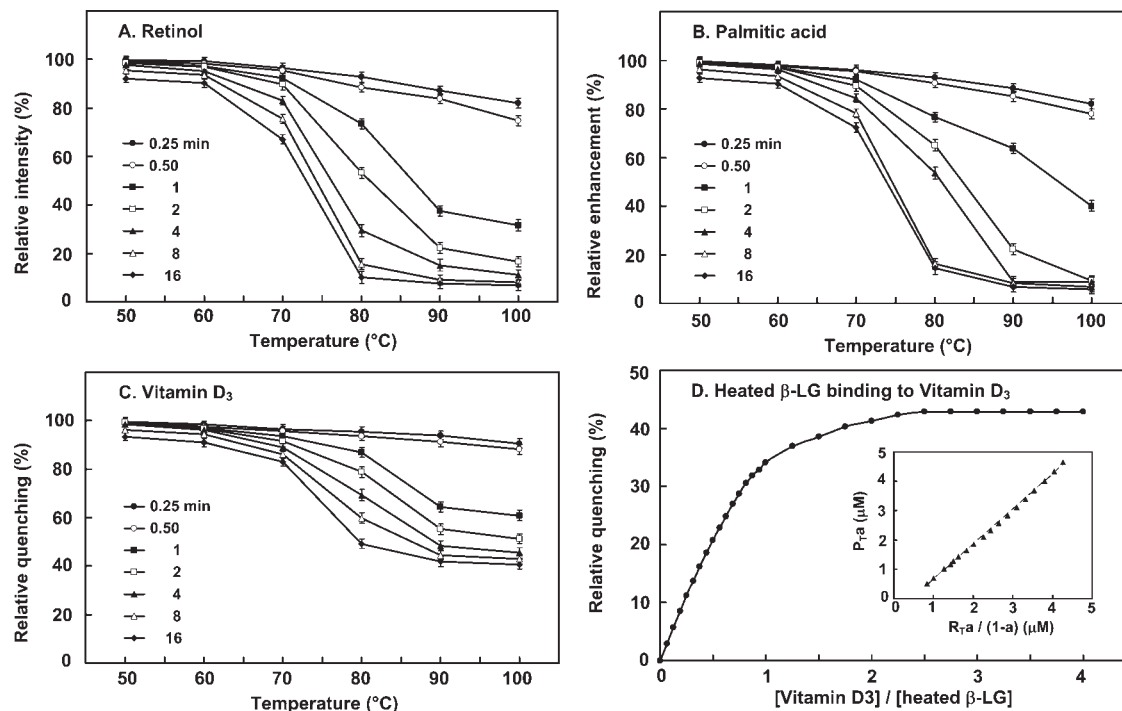
statistics of the complex are given in Table II. The discrepancy indices for  $R$  and  $R_{\text{free}}$  are 23.86% and 26.12%, respectively. The  $\beta$ -LG-vitamin D<sub>3</sub> complex possesses a well geometry similar to that reported by CNS<sup>27</sup> with a root-mean-square (r.m.s.) bond length and bond angle deviation from ideality 0.007 Å and 1.264°, respectively (Table II). A Ramachandran plot reveals that only one residue is in the disallowed regions (Tyr-99), which arises in most of the lipocalin family as a result of the  $\gamma$ -turn associated with the sequence “TDY” (residues 97–99). The average temperature factor for all protein atoms is 55.02 Å<sup>2</sup>, which is considered to be inadequate for established crystallographic standards. This may be explained by  $\beta$ -LG having nearly 25% of the residues located around flexible surface loops and NH<sub>2</sub>- and COOH-terminal regions. Previously published statistics of  $\beta$ -LG complexes<sup>9,27,29</sup> show a  $B$ -factor range of 41.3–57.27 (Table III), which accommodates for the elevated values acquired in this study that seem to deviate from the norm.

The overall topology of  $\beta$ -LG is similar to that previously described<sup>15–19</sup> with a well-defined antiparallel  $\beta$ -sheet structure and flexible loops connecting the secondary structure elements. The loops AB, CD, EF, and GH are more flexible than the others, consistent with the observations from other reported crystal structures.<sup>15–19</sup> The EF loop that acts as a flap is in the open position of the central calyx, which is expected when vitamin D<sub>3</sub> is present.

Space-filling drawings of the  $\beta$ -LG-vitamin D<sub>3</sub> complex show that there are two domains for vitamin D<sub>3</sub> binding (Fig. 5). One vitamin D<sub>3</sub> molecule inserts almost perpendicularly into the calyx cavity as expected and is consistent to the previous reports.<sup>9,29</sup> The other binds to the surface near the COOH-terminus of  $\beta$ -LG (residues 136–149), including part of the  $\alpha$ -helix and  $\beta$ -strand I (Fig. 1) as shown in Figure 6. The  $B$ -factor for the vitamin D<sub>3</sub> molecules in the calyx and the second site are 39.19 and 46.90, respectively (Table II). Proximity of these values to the published data<sup>9,27,29</sup> reveals the rigidity of vitamin D<sub>3</sub> bound to  $\beta$ -LG (Table III). For the second site, vitamin D<sub>3</sub> is close to the surface of  $\beta$ -LG with 17.91 Å in length, while the span of vitamin D<sub>3</sub> is about 12.51 Å. Under this orientation, the A ring or the aliphatic tail following the C/D rings of vitamin D<sub>3</sub> interacts with the  $\beta$ -strand I or the  $\alpha$ -helix of  $\beta$ -LG, respectively (Fig. 6). We putatively defined this second vitamin D<sub>3</sub> binding site as an exosite.

Figure 6 depicts that the bulk of the electron density is sufficient to cover the entire extent of vitamin D<sub>3</sub> in the calyx (in stereo view) as well as that in the exosite. The aliphatic tail of vitamin D<sub>3</sub> (C17–27) is oriented inside the calyx with the 3-OH group of vitamin D<sub>3</sub> near the outside of the pocket.

Superimposing the current  $\beta$ -LG-vitamin D<sub>3</sub> and previously described  $\beta$ -LG models (PDB codes 1BSQ) in the

**Figure 4**

Effect of heating on  $\beta$ -LG binding with ligands. (A–C)  $\beta$ -LG was heated between 50 and 100 °C for 15 s to 16 min before the addition of retinol, palmitate, and vitamin D<sub>3</sub>. (D) Titration curve of heated  $\beta$ -LG (100 °C for 16 min) with vitamin D<sub>3</sub>. Only vitamin D<sub>3</sub>, but not retinol and palmitate, was able to bind denatured  $\beta$ -LG with a molar ratio of  $\sim$ 1:1. The data suggest that there is another thermally independent vitamin D<sub>3</sub> binding site, which is remote from the calyx pocket. Each point in panels A–C represents the mean of triplicate determinations  $\pm$  SD. While, each point in panel D represents the mean of triplicate determinations with a SD less than 5–8% of the mean.

region of the calyx [Fig. 7(A)] reveals that the movement of the external EF “gate loop” of  $\beta$ -LG-vitamin D<sub>3</sub> is quite similar to that of the  $\beta$ -LG-retinol complex<sup>18,29</sup> (data not shown). Some side chains, such as Lys-60, Glu-62, Phe-105, and Met-107, require significant reposition to make room for vitamin D<sub>3</sub> insertion into the calyx. The atoms of vitamin D<sub>3</sub> near or at the “mouth” of the calyx possess higher values of *B*-factors suggesting their higher mobility. Figure 7(B) depicts the distance of vitamin D<sub>3</sub> to the  $\beta$ -LG calyx. The shortest interaction distance is hydrogen bonding between the 3-OH group of vitamin D<sub>3</sub> and Lys-60 (2.97 Å) of  $\beta$ -LG; whereas the only hydrogen bond involving retinol binding is that to Glu-62.<sup>29</sup> Hydrophobic interaction and the distances between the carbons of vitamin D<sub>3</sub> and Pro-38, Leu-39, Val-41, Ile-71, Ala-86, Phe-105, and Met-107 of  $\beta$ -LG are also displayed.

With respect to the second binding site for vitamin D<sub>3</sub>, it appears that vitamin D<sub>3</sub> is bound to a surface pocket between the COOH-terminal  $\alpha$ -helix and  $\beta$ -strand I (residues 136–149). The current  $\beta$ -LG-vitamin D<sub>3</sub> and previously described native  $\beta$ -LG models in this region (PDB codes 1BSQ) are superimposed and shown in Figure 8(A). Notably, there is not much conforma-

tional change near the exosite of  $\beta$ -LG upon the vitamin D<sub>3</sub> binding. Figure 8(B) shows the distance between vitamin D<sub>3</sub> and the amino acids involved (Asp-137, Leu-140, Lys-141, Leu-143, Met-145, His-146, Ile-147, and Arg-148). Although some charged residues of the exosite are involved, their interaction with vitamin D<sub>3</sub> is mainly hydrophobic with the charged groups of  $\beta$ -LG sticking out of the pocket. The data suggest that the contact is via a hydrophobic interaction. There is no evidence that the hydroxyl group of vitamin D<sub>3</sub> interacts with  $\eta$ 1 N of Arg-148 as the distance (4.9 Å) is greater than that of

**Table I**

Apparent Dissociation Constants and Binding Ratio for Binding Ligands to Native or Heated  $\beta$ -LG

Ligand	Binding ratio (ligand/ $\beta$ -LG)	$K_d^{app}$ (10 <sup>-9</sup> M)
	$\bar{X} \pm \text{SD}$	$\bar{X} \pm \text{SD}$
Retinol with native $\beta$ -LG	0.908 $\pm$ 0.089	17.28 $\pm$ 1.62
Palmitate with native $\beta$ -LG	0.801 $\pm$ 0.072	44.03 $\pm$ 4.56
Vitamin D <sub>3</sub> with native $\beta$ -LG	1.761 $\pm$ 0.121	4.74 $\pm$ 0.37
heated $\beta$ -LG	0.835 $\pm$ 0.054	45.67 $\pm$ 3.12

**Table II**Data Collection and Refinement Statistics of  $\beta$ -LG-Vitamin D<sub>3</sub> Complex

<b>Data collection</b>	
Space group	<i>P</i> 3 <sub>2</sub> 21
Cell dimensions	
<i>a</i> , <i>b</i> , <i>c</i> (Å)	53.780, 53.780, 111.573
$\alpha$ , $\beta$ , $\gamma$ (°)	90, 90, 120
Resolution (Å)	30–2.4 (2.49–2.4)
<i>R</i> <sub>sym</sub>	0.034 (0.226)
$\langle I/\sigma_I \rangle$	43.3 (10.3)
Completeness (%)	98.5% (99.5%)
Redundancy	7.0
<b>Refinement</b>	
Resolution (Å)	15–2.4
No. of unique reflections	7422
<i>R</i> <sub>work</sub> / <i>R</i> <sub>free</sub>	23.86%/26.12%
No. of atoms	
Protein	1272
Ligand	56
Water	38
<i>B</i> -factors	
Protein	55.02
Ligand in calyx/exosite	39.19/46.90
Water	52.47
R.m.s. deviations	
Bond lengths (Å)	0.007
Bond angles (°)	1.264

hydrogen bonding (bond length less than 3.13 Å) [Fig. 8(B)].

Furthermore,  $\beta$ -LG is primarily oriented as a  $\beta$  structure (50%); the only  $\alpha$ -helix region of  $\beta$ -LG consisting of three turns is located at the COOH-terminus between residues 130 and 141. Remarkably interesting, the  $\alpha$ -helix is arranged as amphipathic consisting of all the charged residues (Asp-130, Glu-131, Glu-134, Asp-137, Lys-138, and Lys-141) clustered at one face with hydrophobic or noncharged residues (Ala-132, Leu-133, Phe-136, Ala-139, and Leu-140) at another face without an exception [Fig. 9(A)]. A remarkable feature is that the exosite is comprised of an amphipathic  $\alpha$ -helix providing hydrophobic residues (Phe-136, Ala-139, and Leu-140) at one side and a  $\beta$ -strand providing a hydrophobic Ile-147 and a backbone His-146 at the other side [Fig. 9(B)]. These two sides are linked by a loop containing hydrophobic residues Ala-142, Leu-143, and Pro-144. Thus, the binding pocket provides a strong hydrophobic force to stabilize vitamin D<sub>3</sub> binding. The stereo view of such an interaction is also drawn in Figure 9(B), depicting the binding on the surface of  $\beta$ -LG. The carbons of vitamin

D<sub>3</sub> (*n* = 27 in total) close to the surface are C5, C8, C10, C13, C14, C15, C16, C17, C18, C19, C22, C24, C25, and C26 (*n* = 14). They are oriented toward the surface consistent with the analysis of Figure 5.

### CD spectrum analysis of heated $\beta$ -LG

In general, the CD spectrum at 222 nm is used for the calculation of the  $\alpha$ -helical content of a given protein. Because the  $\alpha$ -helix region of  $\beta$ -LG is located in the second binding site and heating  $\beta$ -LG retains ~40% of the maximal vitamin D<sub>3</sub> binding to the whole  $\beta$ -LG molecule, we monitored whether there were spectral changes of  $\beta$ -LG at 222 nm of  $\beta$ -LG upon heating at 50, 60, 70, 80, 90, and 100°C. Figure 10 reveals that there were no significant changes in spectra at 222 nm. As expected, the  $\beta$ -configuration was disordered at temperatures above 70°C, consistent with our previous observation.<sup>4</sup> Thus, it temptingly offers support that the proposed exosite is somewhat thermally stable.

## DISCUSSION

During the past 40 years,  $\beta$ -LG has been extensively studied for its biochemical properties, and an abundance of literature exists about its physicochemical nature.<sup>9</sup> Although the exact physiological functions of  $\beta$ -LG are not fully explored, one of its roles is to transport hydrophobic molecules, such as retinol, fatty acids, and vitamin D.<sup>49,50</sup> The active form of vitamin D is 1 $\alpha$ , 25(OH)<sub>2</sub> vitamin D<sub>3</sub>, which maintains calcium homeostasis and plays important roles on the immune system and prevents the growth and differentiation of cancer cells. Recent studies indicate that increased plasma vitamin D<sub>3</sub> concentrations are associated with decreased incidence of breast, ovarian, prostate and colorectal cancers,<sup>51</sup> and osteoporotic fractures.<sup>52</sup> The concentration of vitamin D<sub>3</sub> in plasma is about 80 nM. A double-blind placebo controlled study conducted in Europe indicated this level to be significantly reduced over the winter season (about 37%) due to the lack of exposure to sunlight.<sup>53</sup> However, drinking vitamin D<sub>3</sub> fortified milk (312 nM) significantly compensated the seasonal loss of vitamin D by greater than 50%. For this reason, it has been recommended that milk enriched with vitamin D<sub>3</sub> be provided in high-latitude European countries. Thus, we chose vitamin D<sub>3</sub>, instead of vitamin D<sub>2</sub>, to form a

**Table III**Mean B-Factor for  $\beta$ -LG Complexes with Ligands Extracted from Previously Published Papers

Ligand	Retinol	Retinoic acid	Palmitate	Cholesterol	Vitamin D <sub>2</sub>	Mercury	12-Bromododecanoic acid
Mean B-factor for protein atoms (Å <sup>2</sup> )	56.1	48.8	54.2	44.5	57.27	50.0	41.3
Mean B-factor for ligand atoms (Å <sup>2</sup> )	65.0	66.8	58.4	69.9	72.6	53.5	52.1
Mean B-factor for water molecules (Å <sup>2</sup> )	67.4	59.0	68.1	53.0	56.9	55.9	72.6

## Space-filling model

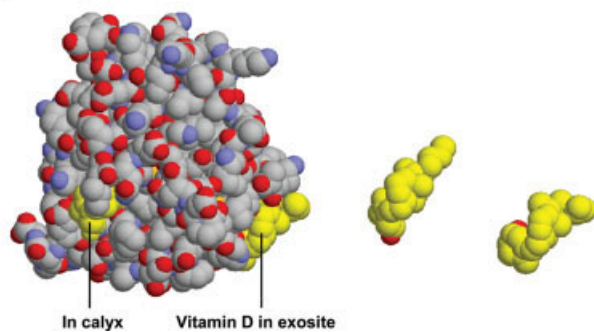


## Figure 5

Structure of  $\beta$ -LG complexed with vitamin D<sub>3</sub> at 2.4 Å resolution. Space-filling drawing of  $\beta$ -LG-vitamin D<sub>3</sub> complex. Vitamin D<sub>3</sub> (colored in yellow) and  $\beta$ -LG are drawn based on our final refined model with carbon, oxygen, and nitrogen atoms depicted in gray, red, and blue, respectively. Sulfur molecules (in orange) are buried inside at this face. It demonstrates that there are two distinct vitamin D<sub>3</sub> binding sites on each  $\beta$ -LG molecule. One is penetrated inside the calyx (left) and the other is lying on the surface between the  $\alpha$ -helix and  $\beta$ -strand I at the COOH-terminus (residues 136–149) (right).

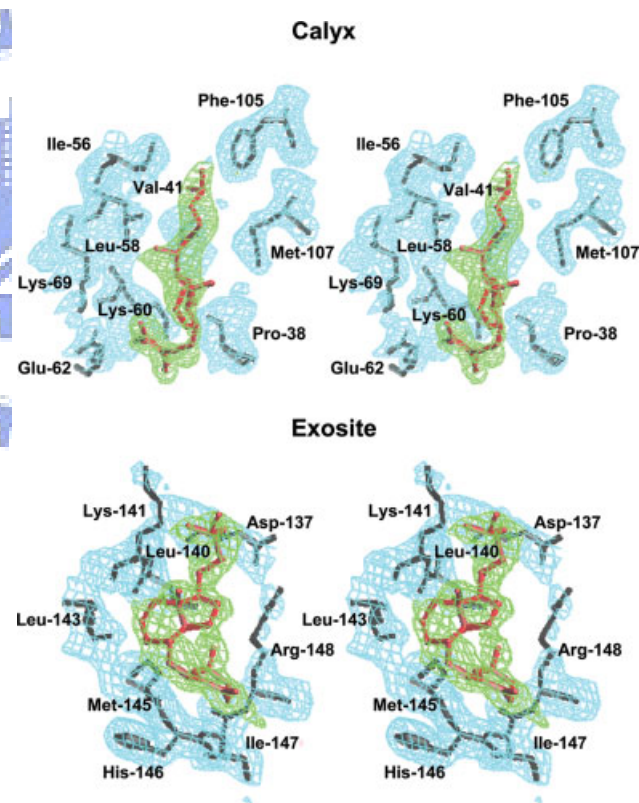
$\beta$ -LG-vitamin D<sub>3</sub> complex in this study. Structurally, the only difference of vitamin D<sub>3</sub> from D<sub>2</sub> is the latter being a double bond between the carbon positions 22 and 23 (Fig. 1). Despite the minor difference, their binding characteristics to  $\beta$ -LG are similar.<sup>31</sup> One additional goal in the present study is to test the possibility of binding vitamin D<sub>3</sub> to thermally denatured milk, which is often produced in the processing of milk.

With respect to the ligand binding of  $\beta$ -LG, many research groups<sup>28,31,32</sup> have shown that the stoichiometry for binding retinol or palmitate to  $\beta$ -LG is 1:1, and most experimental evidence points to the calyx of  $\beta$ -LG as the binding site for retinol and palmitate.<sup>29</sup> However, there remains a debate about the stoichiometry for vitamin D<sub>3</sub> binding being 1 or 2. Wang *et al.*<sup>31,34</sup> proposed that  $\beta$ -LG has another binding site for vitamin D in addition to the central calyx, but doubt has been raised based on crystallographic analysis.<sup>9,29</sup> In fact, the presence of a secondary site for ligand binding has been described and proposed for some time,<sup>16</sup> but the identity of a  $\beta$ -LG-ligand complex by an X-ray crystal structure has not been elucidated.<sup>9</sup>

In the present work, using the method of extrinsic fluorescence emission and fluorescence enhancement and quenching established previously,<sup>4,31,32</sup> we show the maximal binding ratios of retinol or palmitate with  $\beta$ -LG to be 1:1, whereas it was 2:1 for that of vitamin D<sub>3</sub> (Fig. 2). The latter result is consistent to that reported by Wang *et al.*<sup>31,32</sup> It is worth mentioning that using the intrinsic fluorescence of Trp can give results that indicate significantly tighter ligand binding than other methods, especially equilibrium dialysis. This effect is particularly noticeable when the Trp fluorescence decreases with

ligand addition.<sup>9,35</sup> A recent review<sup>9</sup> suggests that a surface low-affinity binding site together with a central high-affinity binding site (calyx) would appear to satisfy most of the reported experimental observations. In brief, the diverse reports of more than a single binding site may be dependent on the method used.

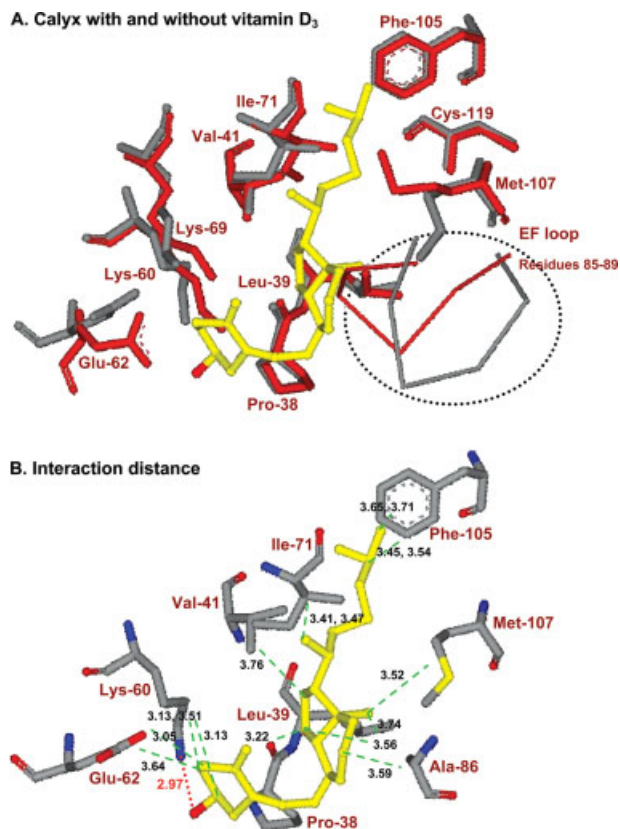
In an attempt to resolve the controversy about an additional binding site for vitamin D<sub>3</sub>, we used several additional approaches involving structural change to study the interaction between vitamin D<sub>3</sub> and  $\beta$ -LG. First, it has been established that the EF loop acts as a gate over the calyx.<sup>9,18,29,54</sup> At a low pH, the loop is in a “closed” position, and the ligand binding into the calyx is inhibited. On the contrary, at a high pH above the Tanford transition, the loop is “open” allowing ligands to penetrate into the calyx.<sup>4,54,55</sup> We explored the binding ability between  $\beta$ -LG and vitamin D<sub>3</sub> at various pH. Similar to that of retinol and palmitate, the present study shows that there is a notable transition of vitamin D<sub>3</sub>



## Figure 6

Electron density map around the calyx and the exosite of vitamin D<sub>3</sub>- $\beta$ -LG complex at 2.4 Å resolution. Final refined model together with the  $2F_{obs} - F_{calc}$  electron density show that the bulk of the electron density is sufficient to cover a vitamin D<sub>3</sub> molecule, both in the calyx (top) and the exosite (bottom). In the central calyx binding mode, the aliphatic tail of vitamin D<sub>3</sub> clearly inserts into the binding cavity, where the 3-OH group of vitamin D<sub>3</sub> binds externally. In exosite binding mode, vitamin D<sub>3</sub> interacts mostly with the hydrophobic moiety of the pocket.



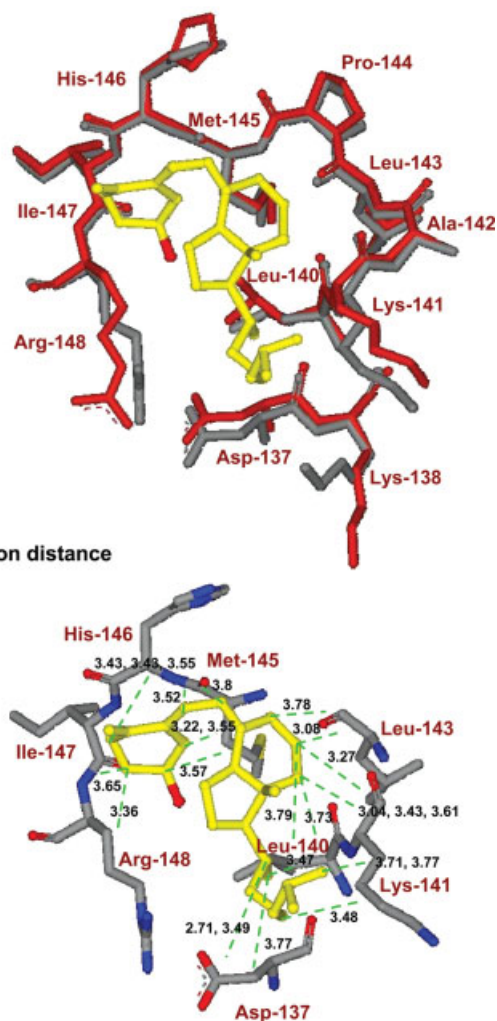
**Figure 7**

Superimposed structure of the calyx before and after binding of vitamin D<sub>3</sub> and a diagram showing their contacts less than 3.8 Å. (A) Superimposing the current model for vitamin D<sub>3</sub>-β-LG (colored in gray) with previously described native β-LG (in red) (PDB code 1BSQ) in the calyx shows that there is a significant repositioning of Glu-62 and Met-107 to make room for the ligand into the calyx. Notably, vitamin D<sub>3</sub> binding has resulted in a local conformational change by opening the EF loop as shown in a dotted circle (residues 85–89). Such conformational change in the loop is similar to the binding of retinol (data not shown). (B) The calyx of β-LG offers mainly hydrophobic interactions to vitamin D<sub>3</sub> binding (less than 3.8 Å). The shortest distance, 2.97 Å, is the hydrogen bond between the 3-OH group of vitamin D<sub>3</sub> and Lys-60 (dotted red). [Color figure can be viewed in the online issue, which is available at [www.interscience.wiley.com](http://www.interscience.wiley.com).]

binding to the calyx of β-LG occurring between pH 6.0 and 8.0 (Fig. 3). Most interestingly, at pH between 2 and 6 we show vitamin D<sub>3</sub> interacting with β-LG (with about 35% of maximal binding ability), but not retinol and palmitate [Fig. 3(C)]. Because the EF loop is “closed” below the Tanford transition, such binding suggests the presence of another binding site for vitamin D<sub>3</sub>. Physiologically, such low pH binding could be essential, since β-LG is well known to be stable at low pH<sup>1,2</sup> and resistant to acid hydrolysis and protease digestion in the gastrointestinal tract.<sup>56,57</sup> Notably, the binding of vitamin D<sub>3</sub> or palmitate to β-LG was decreased to some extent at pH 9–10 (Fig. 3). One of the possible explanations is that the positively charged groups of lysine residues inside calyx are neutralized at pH above 8 resulting in a

weakening of the interaction with the carboxyl group of palmitate.<sup>4</sup>

Second, we have shown that the β-strand D of the calyx is directly involved in the thermal denaturation.<sup>4</sup> The conformational changes of β-LG were rapid, extensive, and irreversible upon heating over 70–80°C.<sup>5</sup> As a result, it completely diminishes the binding of palmitate and retinol. To test the hypothesis that there is a putative second binding site for vitamin D<sub>3</sub> located independently

**A. Exosite with and without vitamin D<sub>3</sub>****Figure 8**

Superimposed structure of the exosite before and after binding of vitamin D<sub>3</sub> and a diagram showing their contacts of less than 3.8 Å. (A) Superimposing the current model for vitamin D<sub>3</sub>-β-LG (colored in gray) with previously described native β-LG (in red) (PDB code 1BSQ) in the exosite reveals that the overall conformation is not substantially changed upon the binding of vitamin D<sub>3</sub>. (B) The exosite is near the surface of C-terminal α-helix and β-strand I, where the 3-OH group of vitamin D<sub>3</sub> does not apparently form hydrogen bonding with β-LG. [Color figure can be viewed in the online issue, which is available at [www.interscience.wiley.com](http://www.interscience.wiley.com).]

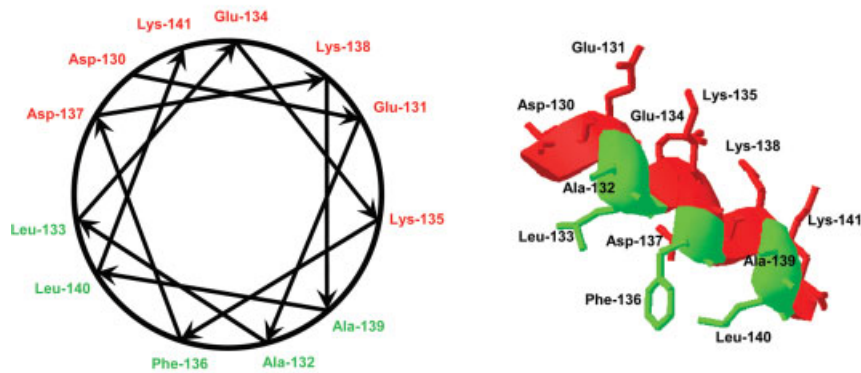
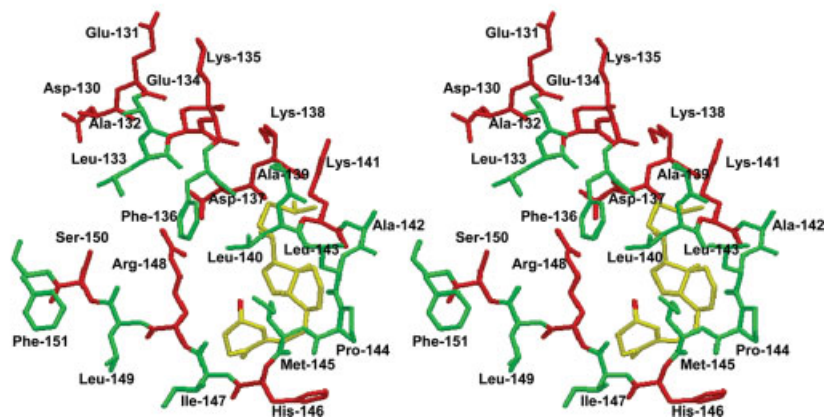
A. Amphipathic  $\alpha$ -helixB. Stereo view of vitamin D<sub>3</sub>-exosite complex

Figure 9

Amphipathic helix of  $\beta$ -LG and its interaction with vitamin D<sub>3</sub>. (A) The only  $\alpha$ -helix region of  $\beta$ -LG is located between residues 130 and 141 (Fig. 1). Most interestingly, the  $\alpha$ -helix is oriented as amphipathic with all the charged residues clustered on one side without an exception. (B) The crystal structure reveals that the hydrophobic side of the  $\alpha$ -helix forms a stable hydrophobic pocket with  $\beta$ -strand I. They are linked by a hydrophobic loop (residues 142–145) and thus facilitate the binding to vitamin D<sub>3</sub>. The stereo view shows that part of vitamin D<sub>3</sub> is near the surface, particularly for the aliphatic tail, which is consistent with that depicted in Figure 5.

from the calyx, we thermally denatured the calyx (between 50 and 100°C) and then conducted the binding for retinol, palmitate, or vitamin D<sub>3</sub> over time (Fig. 4). It is of interest that only vitamin D<sub>3</sub> was able to bind to heated  $\beta$ -LG (at 100°C for 16 min) with a stoichiometry of almost 1:1, instead of 2:1 [Fig. 4(D)]. Our data suggests that the second binding site for vitamin D<sub>3</sub> is heat stable to some extent.

Third, analysis of the binding shows that the binding affinity between native  $\beta$ -LG and vitamin D<sub>3</sub> is relatively high within a nM range, about 10 times greater than palmitate and retinol (Table I). The result is almost the same as that of vitamin D<sub>2</sub> reported by Wang *et al.*,<sup>31</sup> but somewhat higher than the affinity reported for vitamin D<sub>3</sub>.<sup>31</sup> The reason contributing to such discrepancy remains elusive. One possibility may be due to the 5  $\mu$ M concentration (pH 8.0) of  $\beta$ -LG that we employed, while

Wang *et al.* used a 20  $\mu$ M concentration (pH 7.0) for a typical emission spectrum.<sup>34</sup> The other possibility may be due to the pH; the fluorescence of Trp may be affected by ionization of neighboring prototropic groups or by conformation changes due to the dimerization of the protein.<sup>2,34</sup> Nevertheless, the calculated affinity for vitamin D<sub>3</sub> ( $K_d^{\text{app}} = 45.67 \pm 3.12$  nM) to putative second or thermally stable binding site is about 10 times lower than that to native  $\beta$ -LG (calyx plus second site) (Table I). Thus, it seems to be consistent with the hypothesis proposed by Kontopidis *et al.*<sup>9</sup> that the central site (calyx) is a main binding site possessing a high affinity for most of the hydrophobic ligands, whereas the affinity for the secondary site is low. Ultimately, the secondary binding may depend on the nature of the ligands, such as their size, structure, and hydrophobicity. It would be of interest to further investigate other ligand bindings to

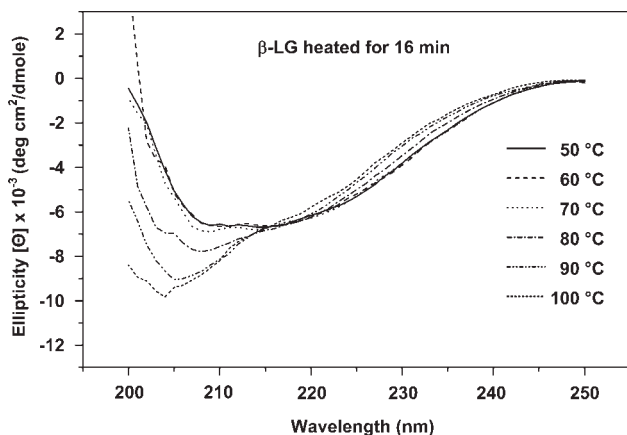


**Figure 10**

Circular dichroic spectra of native and heated  $\beta$ -LG.  $\beta$ -LG preheated between 50 and 100°C for 16 min was recorded by circular dichroism at a final concentration of 0.2 mg/mL. The  $\beta$ -structure of  $\beta$ -LG underwent disordering upon continuous heating as significant changes of ellipticity at 205–208 nm occurred above 80°C. The negative ellipticity at 222 nm, commonly a criteria for  $\alpha$ -helical structure, was identical between native and heated  $\beta$ -LG.

heated  $\beta$ -LG, although the calculation of binding affinity of heated  $\beta$ -LG is somewhat complicated owing to the formation of large  $\beta$ -LG polymers as mentioned (see Results).

Finally, to confirm our hypothesis that there exists a second vitamin D<sub>3</sub> binding site remote from the calyx, we used a synchrotron radiation X-ray to determine the crystal structure of the  $\beta$ -LG-vitamin D<sub>3</sub> complex. Our crystal of the complex is defined in trigonal (lattice Z) space group  $P3_221$ . This final model reveals that one vitamin D<sub>3</sub> molecule binds to the calyx (central internal binding-site) of  $\beta$ -LG and the other binds to the surface of  $\beta$ -LG between the  $\alpha$ -helix and  $\beta$ -strand I (external binding site; Fig. 5).

In the electron density map at 2.4 Å resolution, vitamin D<sub>3</sub> is well fitted into the bulk of electron density around the calyx or the exosite (Fig. 6). In central calyx binding mode, the aliphatic tail of vitamin D<sub>3</sub> clearly inserts into the binding cavity where the 3-OH group of vitamin D<sub>3</sub> binds externally. In an early report using vitamin D<sub>2</sub>,<sup>9</sup> the end that inserted into the calyx was not conclusively identified because the electron density was not enough to cover the entire ligand. It is not clear whether vitamin D<sub>3</sub> is superior to vitamin D<sub>2</sub> in binding to  $\beta$ -LG. The other difference is that in our study the 3-OH group of vitamin D<sub>3</sub> forms a hydrogen bond with the carbonyl of Lys-60 [Fig. 7(B)] instead of Lys-69 as proposed using vitamin D<sub>2</sub>.<sup>9</sup> Again, the electron density was not strong enough for the outer extremity of vitamin D<sub>2</sub> making the exact conclusion difficult. Another explanation is that there might be a significant difference in the orientation between vitamin D<sub>2</sub> and D<sub>3</sub>, although the

difference in chemical structure is subtle. Regardless, the vitamin D<sub>3</sub>- $\beta$ -LG binding mode is quite similar to that of retinol- $\beta$ -LG interaction over the calyx.<sup>29</sup> Pro-38, Leu-39, Val-41, Ile-71, Ala-86, Phe-105, and Met-107 are all involved in providing hydrophobic interactions with the displayed distance of less than 3.8 Å to the carbon backbone of vitamin D<sub>3</sub> [Fig. 7(B)].

In exosite binding mode, the vitamin D<sub>3</sub> molecule attaches at a pocket between the C-terminal  $\alpha$ -helix and  $\beta$ -strand I (Fig. 5). We specifically demonstrated that the exosite of  $\beta$ -LG provides a hydrophobic force to stabilize vitamin D<sub>3</sub> [Fig. 8(B)] and concluded that the exosite is located near the surface of the C-terminal  $\alpha$ -helix and  $\beta$ -strand I, where there is no strong evidence to show that the 3-OH group of vitamin D<sub>3</sub> is capable of interacting with  $\beta$ -LG [Fig. 8(B)]. A stereo view shown in Figure 9(B) reveals that part of the vitamin D<sub>3</sub> molecule is exposed toward the surface, consistent to that depicted in Figure 5. Although this second binding is located near the surface of  $\beta$ -LG, our data suggest that the binding affinity of vitamin D<sub>3</sub> to exosite is reasonably high and almost equivalent to that of retinol or palmitate to calyx (Table I). Apparently, vitamin D<sub>3</sub> interacts mostly with those hydrophobic amino acids within residues 136–149 with distances less than 3.8 Å [Fig. 8(B)]. The linking-loop residues 142–145 (Ala-Leu-Pro-Met) between the helix and strand I are all hydrophobic. With such an orientation, a hydrophobic pocket is constructed in facilitating the binding for vitamin D<sub>3</sub>. It is worth mentioning that this exosite is very similar to the surface hydrophobic site (mentioned and discussed above) that has been described by Monaco *et al.*<sup>16</sup> and proposed by Wang *et al.*<sup>31</sup>

It is of interest that the  $\alpha$ -helix involved in the exosite is typically amphipathic. This amphipathic region could be heat resistant as suggested from our binding experiment for vitamin D<sub>3</sub> and heated  $\beta$ -LG. A similar situation is seen in a typically amphipathic apolipoprotein A-I; its conformation and lipid binding properties are completely maintained upon heating over 100°C.<sup>58</sup> It might be worthwhile to study the crystal structure of the heated- $\beta$ -LG-vitamin D<sub>3</sub> complex to finally prove its heat resistance. Unfortunately, we are not able to crystallize such a complex at the present time. This could be due to the formation of multiple aggregated forms of  $\beta$ -LG upon heating.<sup>3–6</sup>

Vitamin D is found in only a few foods, such as fish oil, liver, milk, and eggs, in which milk is a major source for vitamin D in the diet. The level of vitamin D in bovine milk has been reported to be low. In many sophisticated food industries, processed milk, dry milk, margarine, and other dairy products are fortified with vitamin D<sub>3</sub> to a level of about 0.35  $\mu$ M. The concentration of  $\beta$ -LG in milk is about 270  $\mu$ M, providing a sufficient amount of  $\beta$ -LG to transport spiked vitamin D. It is of interest to point out that recent studies have demon-



strated that intact β-LG is acid resistant with a super permeability to cross the epithelium cells of the gastrointestinal tract.<sup>56,57</sup> Such a unique property of β-LG is worthy of consideration for transporting vitamin D in the milk.

There are two advantages for the presence of vitamin D<sub>3</sub> binding exosite in β-LG. First, central calyx of β-LG is thought to be primarily occupied by the fatty acid in milk.<sup>59</sup> The available exosite may provide another route for transporting the vitamin D. Second, many dairy products today are processed under excessive heat for the purpose of sterilization. The presence of a heat stable exosite may maintain the binding for vitamin D<sub>3</sub>.

Finally, since the putative exosite is located at the surface of β-LG, an approach using site-directed mutagenesis may eventually be served as to probe the structural and vitamin D binding relationship. The experiment is now in progress in our laboratory.

## ACKNOWLEDGMENTS

We are grateful to our colleagues, Dr. Yuch-Cheng Jean and Dr. Chun-Shiun Chao, and the supporting staffs for the technical assistance and discussion of the synchrotron radiation X-ray facility on data collection at BL13B1 of NSRRC, Taiwan, and Dr. Yu-San Huang and Dr. Kuan-Li Yu at BL12B2 of SPring-8, Japan. We also thank Dr. Su-Ying Wu of National Health Research Institutes (NHRI, Taiwan) for the useful discussion in preparing this manuscript.

## REFERENCES

1. Hambling SG, MacAlpine AS, Sawyer L. Beta-lactoglobulin. In: Fox PF, editor. *Advanced dairy chemistry II*. Amsterdam: Elsevier; 1992. pp 141–190.
2. Sawyer L, Kontopidis G. The core lipocalin, bovine beta-lactoglobulin. *Biochim Biophys Acta* 2000;1482:136–148.
3. Chen WL, Huang MT, Liu HC, Li CW, Mao SJT. Distinction between dry and raw milk using monoclonal antibodies prepared against dry milk proteins. *J Dairy Sci* 2004;87:2720–2729.
4. Song CY, Chen WL, Yang MC, Huang JP, Mao SJT. Epitope mapping of a monoclonal antibody specific to bovine dry milk: involvement of residues 66–76 of strand D in thermal denatured beta-lactoglobulin. *J Biol Chem* 2005;280:3574–3582.
5. Chen WL, Hwang MT, Liao CY, Ho JC, Hong KC, Mao SJT. β-lactoglobulin is a thermal marker in processed milk as studied by electrophoresis and circular dichroic spectra. *J Dairy Sci* 2005;88:1618–1630.
6. Chen WL, Liu WT, Yang MC, Hwang MT, Tsao JH, Mao SJT. A novel conformation-dependent monoclonal antibody specific to the native structure of beta-lactoglobulin and its application. *J Dairy Sci* 2006;89:912–921.
7. Nagaoka S, Futamura Y, Miwa K, Awano T, Yamauchi K, Kanamaru Y, Tadashi K, Kuwata T. Identification of novel hypocholesterolemic peptides derived from bovine milk beta-lactoglobulin. *Biochem Biophys Res Commun* 2001;281:11–17.
8. Zsila F, Bikadi Z, Simonyi M. Retinoic acid binding properties of the lipocalin member beta-lactoglobulin studied by circular dichroism, electronic absorption spectroscopy and molecular modeling methods. *Biochem Pharmacol* 2002;64:1651–1660.
9. Kontopidis G, Holt C, Sawyer L. Invited review: beta-lactoglobulin: binding properties, structure, and function. *J Dairy Sci* 2004;87:785–796.
10. Chevalier F, Chobert JM, Genot C, Haertle T. Scavenging of free radicals, antimicrobial, and cytotoxic activities of the Maillard reaction products of beta-lactoglobulin glycosylated with several sugars. *J Agric Food Chem* 2001;49:5031–5038.
11. Marshall K. Therapeutic applications of whey protein. *Altern Med Rev* 2004;9:136–156.
12. Steinrauf LK. Preliminary X-ray data for some new crystalline forms of β-lactoglobulin and hen-egg-white lysozyme. *Acta Crystallogr* 1959;12:77–79.
13. Aschaffenburg R, Green DW, Simmons RM. Crystal forms of Beta-lactoglobulin. *J Mol Biol* 1965;13:194–201.
14. Green DW, Aschaffenburg R, Camerman A, Coppola JC, Dunnill P, Simmons RM, Komorowski E S, Sawyer L, Turner EM, Woods KE. Structure of bovine beta-lactoglobulin at 6 Å resolution. *J Mol Biol* 1979;131:375–397.
15. Papiz MZ, Sawyer L, Eliopoulos EE, North AC, Findlay JB, Sivaprasadarao R, Jones TA, Newcomer ME, Kraulis PJ. The structure of beta-lactoglobulin and its similarity to plasma retinol-binding protein. *Nature* 1986;324:383–385.
16. Monaco HL, Zanotti G, Spadon P, Bolognesi M, Sawyer L, Eliopoulos EE. Crystal structure of the trigonal form of bovine beta-lactoglobulin and of its complex with retinol at 2.5 Å resolution. *J Mol Biol* 1987;197:695–706.
17. Brownlow S, Morais Cabral JH, Cooper R, Flower DR, Yewdall SJ, Polikarpov I, North AC, Sawyer L. Bovine beta-lactoglobulin at 1.8 Å resolution—still an enigmatic lipocalin. *Structure* 1997;5:481–495.
18. Qin BY, Bewley MC, Creamer LK, Baker HM, Baker EN, Jameson GB. Structural basis of the Tanford transition of bovine beta-lactoglobulin. *Biochemistry* 1998;37:14014–14023.
19. Qin BY, Bewley MC, Creamer LK, Baker EN, Jameson GB. Functional implications of structural differences between variants A and B of bovine beta-lactoglobulin. *Protein Sci* 1999;8:75–83.
20. Oliveira KM, Valente-Mesquita VL, Botelho MM, Sawyer L, Ferreira ST, Polikarpov I. Crystal structures of bovine beta-lactoglobulin in the orthorhombic space group C222(1). Structural differences between genetic variants A and B and features of the Tanford transition. *Eur J Biochem* 2001;268:477–483.
21. Adams JJ, Anderson BF, Norris GE, Creamer LK, Jameson GB. Structure of bovine beta-lactoglobulin (variant A) at very low ionic strength. *J Struct Biol* 2006;154:246–254.
22. Sawyer L, Papiz MZ, North ACT, Eliopoulos EE. Structure and function of bovine β-lactoglobulin. *Biochem Soc Trans* 1985;13:265–266.
23. Newcomer ME, Jones TA, Aqvist J, Sundelin J, Eriksson U, Rask L, Peterson PA. The three-dimensional structure of retinol-binding protein. *EMBO J* 1984;3:1451–1454.
24. Redl B. Human tear lipocalin. *Biochim Biophys Acta* 2000;1482:241–248.
25. Kuwata K, Hoshino M, Forge V, Era S, Batt CA, Goto Y. Solution structure and dynamics of bovine beta-lactoglobulin A. *Protein Sci*. 1999;8:2541–2545.
26. Uhrinova S, Smith MH, Jameson GB, Uhrin D, Sawyer L, Barlow PN. Structural changes accompanying pH-induced dissociation of the beta-lactoglobulin dimer. *Biochemistry* 2000;39:3565–3574.
27. Qin BY, Creamer LK, Baker EN, Jameson GB. 12-Bromododecanoic acid binds inside the calyx of bovine beta-lactoglobulin. *FEBS Lett* 1998;438:272–278.
28. Wu SY, Perez MD, Puyol P, Sawyer L. beta-lactoglobulin binds palmitate within its central cavity. *J Biol Chem* 1999;274:170–174.
29. Kontopidis G, Holt C, Sawyer L. The ligand-binding site of bovine beta-lactoglobulin: evidence for a function. *J Mol Biol* 2002;318:1043–1055.

30. Dufour E, Genot C, Haertle T. beta-Lactoglobulin binding properties during its folding changes studied by fluorescence spectroscopy. *Biochim. Biophys. Acta* 1994;1205:105–112.
31. Wang Q, Allen JC, Swaisgood HE. Binding of vitamin D and cholesterol to beta-lactoglobulin. *J Dairy Sci* 1997;80:1054–1059.
32. Wang Q, Allen JC, Swaisgood HE. Binding of retinoids to beta-lactoglobulin isolated by bioselective adsorption. *J Dairy Sci* 1997;80:1047–1053.
33. Wang Q, Allen JC, Swaisgood HE. Protein concentration dependence of palmitate binding to beta-lactoglobulin. *J Dairy Sci* 1998;81:76–81.
34. Wang Q, Allen JC, Swaisgood HE. Binding of lipophilic nutrients to beta-lactoglobulin prepared by bioselective adsorption. *J Dairy Sci* 1999;82:257–264.
35. Muresan S, van der Bent A, de Wolf FA. Interaction of beta-lactoglobulin with small hydrophobic ligands as monitored by fluorometry and equilibrium dialysis: nonlinear quenching effects related to protein–protein association. *J Agric Food Chem* 2001;49:2609–2618.
36. Fessas D, Iametti S, Schiraldi A, Bonomi F. Thermal unfolding of monomeric and dimeric beta-lactoglobulins. *Eur J Biochem* 2001;268:5439–5448.
37. Cogan U, Kopelman M, Mokady S, Shinitzky M. Binding affinities of retinol and related compounds to retinol binding proteins. *Eur J Biochem* 1976;65:71–78.
38. Tseng CF, Lin CC, Huang HY, Liu HC, Mao SJT. Antioxidant role of human haptoglobin. *Proteomics* 2004;4:2221–2228.
39. Otwinowski Z, Minor W. Processing of X-ray Diffraction Data Collected in Oscillation Mode. *Methods Enzymol* 1997;276:307–326.
40. Rossmann MG. The molecular replacement method. *Acta Crystallogr A* 1990;46:73–82.
41. Brunger AT, Adams PD, Clore GM, DeLano WL, Gros P, Grosse-Kunstleve RW, Jiang JS, Kuszewski J, Nilges M, Pannu NS, Read RJ, Rice LM, Simonson T, Warren GL. Crystallography and NMR system: a new software suite for macromolecular structure determination. *Acta Crystallogr D Biol Crystallogr* 1998;54:905–921.
42. Jones TA, Zou JY, Cowan SW, Kjeldgaard Improved methods for building protein models in electron density maps and the location of errors in these models. *Acta Crystallogr A* 1991;47:110–119.
43. Lee SC, Guan HH, Wang CH, Huang WN, Tjong SC, Chen CJ, Wu WG. Structural basis of citrate-dependent and heparan sulfate-mediated cell surface retention of cobra cardiotoxin A3. *J Biol Chem* 2005;280:9567–9577.
44. Covarrubias AS, Bergfors T, Jones TA, Hogbom M. Structural mechanics of the pH-dependent activity of beta-carbonic anhydrase from *Mycobacterium tuberculosis*. *J Biol Chem* 2006;281:4993–4999.
45. Brünger AT. Free R value: a novel statistical quantity for assessing the accuracy of crystal structures. *Nature* 1992;355:472–475.
46. Laskowski RA, MacArthur MW, Moss DS, Thornton JM. PROCHECK: a program to check the stereochemical quality of protein structures. *J Appl Crystallogr* 1993;26:283–291.
47. Engh RA, Huber R. Accurate bond and angle parameters for X-ray protein structure refinement. *Acta Crystallogr A* 1991;47:392–400.
48. Ramachandran GN, Sasisekharan V. Conformation of polypeptides and proteins. *Adv Protein Chem* 1968;23:283–438.
49. Said HM, Ong DE, Shingleton JL. Intestinal uptake of retinol: enhancement by bovine milk beta-lactoglobulin. *Am J Clin Nutr* 1989;49:690–694.
50. Kushibiki S, Hodate K, Kurisaki J, Shingu H, Ueda Y, Watanabe A, Shinoda M. Effect of beta-lactoglobulin on plasma retinol and triglyceride concentrations, and fatty acid composition in calves. *J Dairy Res* 2001;68:579–586.
51. Vieth R. Vitamin D nutrition and its potential health benefits for bone, cancer and other conditions. *J Nutr Environ Med* 2001;11:275–291.
52. Chapuy MC, Arlot ME, Duboeuf F, Brun J, Crouzet B, Arnaud S, Delmas PD, Meunier PJ. Vitamin D<sub>3</sub> and calcium to prevent hip fractures in the elderly women. *N Engl J Med* 1992;327:1637–1642.
53. McKenna MJ, Freaney R, Byrne P, McBrinn Y, Murray B, Kelly M, Donne B, O'Brien M. Safety and efficacy of increasing wintertime vitamin D and calcium intake by milk fortification. *QJM* 1995;88:895–898.
54. Ragona L, Fogolari F, Catalano M, Ugolini R, Zetta L, Molinari H. EF loop conformational change triggers ligand binding in beta-lactoglobulins. *J Biol Chem* 2003;278:38840–38846.
55. Yang J, Powers JR, Clark S, Dunker AK, Swanson BG. Hydrophobic probe binding of beta-lactoglobulin in the native and molten globule state induced by high pressure as affected by pH, KIO(3) and N-ethylmaleimide. *J Agric Food Chem* 2002;50:5207–5214.
56. Mäkinen-Kiljunen S, Palosuo T. A sensitive enzyme-linked immunosorbent assay for determination of bovine beta-lactoglobulin in infant feeding formulas and in human milk. *Allergy* 1992;47:347–352.
57. Lovegrove JA, Osman DL, Morgan JB, Hampton SM. Transfer of cow's milk beta-lactoglobulin to human serum after a milk load: a pilot study. *Gut* 1993;34:203–207.
58. Saito H, Dhanasekaran P, Nguyen D, Holvoet P, Lund-Katz S, Phillips MC. Domain structure and lipid interaction in human apolipoproteins A-I and E, a general model. *J Biol Chem* 2003;278:23227–23232.
59. Perez MD, Diaz de Villegas C, Sanchez L, Aranda P, Ena JM, Calvo M. Interaction of fatty acids with beta-lactoglobulin and albumin from ruminant milk. *J Biochem* 1989;106:1094–1097.

# A unique tetrameric structure of deer plasma haptoglobin – an evolutionary advantage in the Hp 2-2 phenotype with homogeneous structure

I. H. Lai<sup>1</sup>, Kung-Yu Lin<sup>1</sup>, Mikael Larsson<sup>2</sup>, Ming Chi Yang<sup>1</sup>, Chuen-Huei Shiau<sup>3</sup>, Ming-Huei Liao<sup>4</sup> and Simon J. T. Mao<sup>1,5</sup>

1 Institute of Biochemical Engineering, College of Biological Science and Technology, National Chiao Tung University, Hsinchu, Taiwan

2 Department of Chemical and Biological Engineering, Chalmers University of Technology, Gothenburg, Sweden

3 Pingtung County Livestock Disease Control Center, Pingtung, Taiwan

4 Department of Veterinary Medicine, National Pingtung University of Science and Technology, Pingtung, Taiwan

5 Department of Biotechnology and Bioinformatics, Asia University, Taichung, Taiwan

## Keywords

amino acid sequence; deer and human haptoglobin; monoclonal antibody; phenotype; purification

## Correspondence

S. J. T. Mao, Institute of Biochemical Engineering, College of Biological Science and Technology, National Chiao Tung University, 75 Po-Ai Street, Hsinchu 30050, Taiwan

Fax: +886 3 572 9288

Tel: +886 3 571 2121 ext. 56948

E-mail: mao1010@ms7.hinet.net

## Database

The sequence corresponding to deer Hp is available in the DDBJ/EMBL/GenBank database under the accession number EF601928

(Received 21 November 2007, revised 20 December 2007, accepted 28 December 2007)

doi:10.1111/j.1742-4658.2008.06267.x

Similar to blood types, human plasma haptoglobin (Hp) is classified into three phenotypes: Hp 1-1, 2-1 and 2-2. They are genetically inherited from two alleles **Hp 1** and **Hp 2** (represented in bold), but only the Hp 1-1 phenotype is found in almost all animal species. The Hp 2-2 protein consists of complicated large polymers cross-linked by  $\alpha$ 2- $\beta$  subunits or  $(\alpha$ 2- $\beta$ )<sub>n</sub> (where  $n \geq 3$ , up to 12 or more), and is associated with the risk of the development of diabetic, cardiovascular and inflammatory diseases. In the present study, we found that deer plasma Hp mimics human **Hp 2**, containing a tandem repeat over the  $\alpha$ -chain based on our cloned cDNA sequence. Interestingly, the isolated deer Hp is homogeneous and tetrameric, i.e.  $(\alpha$ - $\beta$ )<sub>4</sub>, although the locations of -SH groups (responsible for the formation of polymers) are exactly identical to that of human. Denaturation of deer Hp using 6 M urea under reducing conditions (143 mM  $\beta$ -mercaptoethanol), followed by renaturation, sustained the formation of  $(\alpha$ - $\beta$ )<sub>4</sub>, suggesting that the Hp tetramers are not randomly assembled. Interestingly, an  $\alpha$ -chain monoclonal antibody (W1), known to recognize both human and deer  $\alpha$ -chains, only binds to intact human Hp polymers, but not to deer Hp tetramers. This implies that the epitope of the deer  $\alpha$ -chain is no longer exposed on the surface when Hp tetramers are formed. We propose that steric hindrance plays a major role in determining the polymeric formation in human and deer polymers. Phylogenetic and immunochemical analyses revealed that the **Hp 2** allele of deer might have arisen at least 25 million years ago. A mechanism involved in forming Hp tetramers is proposed and discussed, and the possibility is raised that the evolved tetrameric structure of deer Hp might confer a physiological advantage.

Haptoglobin (Hp) is an acute-phase protein (responsive to infection and inflammation) that is present in the plasma of all mammals [1–4]. A recent study has found that Hp also exists in lower vertebrates (bony

fish) but not in frog and chicken [5]. The most frequently reported biological functions of the protein are to capture released hemoglobin during excessive hemolysis [6] and to scavenge free radicals during oxidative

## Abbreviations

Hp, haptoglobin;  $\beta$ -ME,  $\beta$ -mercaptoethanol.

stress [7]. The captured hemoglobin is internalized by a macrophage/monocyte receptor, CD163, via endocytosis. Interestingly, the CD163 receptor only recognizes Hp and hemoglobin in complex, which indicates exposure of a receptor-binding neo-epitope [6]. Thus, CD163 is identified as a hemoglobin scavenger receptor. Recently, we have shown that Hp is an extremely potent antioxidant that directly protects low-density lipoprotein (LDL) from  $\text{Cu}^{2+}$ -induced oxidation. The potency is markedly superior to that of probucol, one of the most potent antioxidants used in antioxidant therapy [8–10]. Transfection of Hp cDNA into Chinese hamster ovary (CHO) cells protects them against oxidative stress [9].

Human Hp is one of the largest proteins in the plasma, and is originally synthesized as a single  $\alpha\beta$  polypeptide. Following post-translational cleavage by a protease,  $\alpha$ - and  $\beta$ -chains are formed and then linked by disulfide bridges producing mature Hp [11]. The gene is characterized by two common alleles, *Hp 1* and *Hp 2b*, corresponding to  $\alpha 1$ - $\beta$  and  $\alpha 2$ - $\beta$  polypeptide chains, respectively, resulting in three main phenotypes: Hp 1-1, 2-1 and 2-2. All the phenotypes share the same  $\beta$ -chain containing 245 amino acid residues. As shown in Fig. 1A, the  $\alpha 1$ -chain containing 83 amino acid residues possesses two available –SH groups; that at the C-terminus always cross-links with a  $\beta$ -chain to form a basic  $\alpha\beta$  unit, and that at the N-terminus links with another  $(\alpha\beta)_1$ , resulting in an Hp dimer  $(\alpha 1\text{-}\beta)_2$ , i.e. a Hp 1-1 molecule. In contrast, the  $\alpha 2$ -chain, containing a tandem repeat of residues 12–70 of  $\alpha 1$  with 142 amino acid residues, is ‘trivalent’ providing an additional available –SH group (Cys15) that is able to interact with another  $\alpha\beta$  unit. As such,  $\alpha 2$ -chains can bind to either  $\alpha 1$ - $\beta$  or  $\alpha 2$ - $\beta$  units to form large polymers  $[(\alpha 1\text{-}\beta)_2\text{-}(\alpha 2\text{-}\beta)]_n$  in Hp2-1 and  $(\alpha 2\text{-}\beta)_n$  in Hp2-2] as shown in Fig. 1B.

Because of its weaker binding affinity to hemoglobin and retarded mobility (or penetration) between the cells, the polymeric structure of Hp 2-2 is dramatically more prevalent in some groups of patients with certain diseases, such as diabetes and inflammation-related diseases [7,12–14]. The human *Hp 2* allele has been proposed to have originated from *Hp 1* about two million years ago and then gradually displaced *Hp 1* as a consequence of nonhomologous crossing-over between the structural alleles (*Hp 1*) during meiosis [15–17], and is the first example of partial gene duplication of human plasma proteins [15,18,19]. Thus, only humans possess additional Hp 2-1 and 2-2 phenotypes.

In the present study, deer Hp protein was initially shown to be a homogeneous polymer using an electrophoretic hemoglobin typing gel. Following isolation

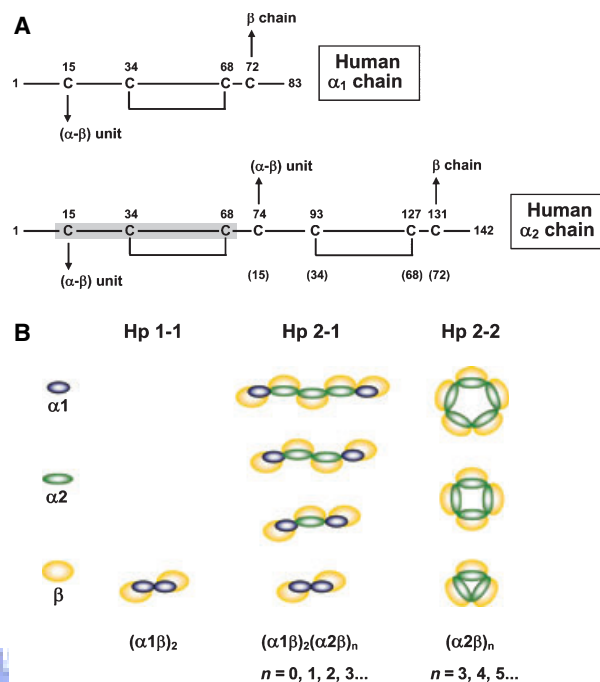


**Fig. 1.** Schematic drawing of the human Hp  $\alpha$ -chain and the molecular arrangement of Hp phenotypes. (A) The human Hp  $\alpha 1$ -chain includes two available –SH groups. That at the C-terminus always links to a  $\beta$ -chain to form a basic  $\alpha 1\text{-}\beta$  unit, and that at the N-terminus links either an  $\alpha 1\text{-}\beta$  unit or  $(\alpha 2\text{-}\beta)_n$  units. The sequence of  $\alpha 2$  is identical to that of  $\alpha 1$  except for a partial repeat insertion of residues 12–70. However, the extra Cys74 means that Hp 2-1 and 2-2 form complicated polymers. (B) Hp 1-1 forms the simplest homodimer  $(\alpha 1\text{-}\beta)_2$ , whereas Hp 2-1 is polymeric in linear form, forming a homodimer  $(\alpha 1\text{-}\beta)_2$ , trimer  $(\alpha\text{-}\beta)_3$  and other polymers. Here,  $\alpha$  represents  $\alpha 1$ - or  $\alpha 2$ -chains. Hp 2-2 forms cyclic structures: a trimer  $(\alpha 2\text{-}\beta)_3$  and other cyclic polymers.

and identification of the protein, the  $\alpha$ -chain was found to be similar to the human  $\alpha 2$ -chain based on its apparent molecular mass. We then cloned the cDNA of deer Hp, showing that the putative amino acid sequence mimics that of human Hp 2-2 (81.7% and 67.9% sequence homology in the  $\beta$ - and  $\alpha$ -chains, respectively), and that the  $\alpha$ -chain of deer Hp also possesses a unique tandem repeat. Interestingly, deer Hp  $\alpha$ -chain comprises seven –SH groups, that are oriented exactly the same as in human Hp 2-2, but the molecular arrangement of deer Hp is strictly tetrameric, i.e.  $(\alpha\text{-}\beta)_4$ . It is thus totally different from human Hp 2-2, which has  $(\alpha\text{-}\beta)_n$  polymers, where  $n \geq 3$ . Using an  $\alpha$ -chain mAb as a probe and denaturing/renaturing experiments, we further demonstrated that steric hindrance of the Hp  $\alpha$ -chain plays a major role in determining the polymeric formation of human  $(\alpha\text{-}\beta)_n$  and the deer  $(\alpha\text{-}\beta)_4$  tetramer. Amino acid sequence alignment demonstrated that the evolved amino acid



sequences of the ruminant  $\beta$ -chain are the most divergent among all mammals. By phylogenetic tree analysis, we identified the  $\alpha$ -chain of dolphin and whale (a branch before the deer) as belonging to the  $\alpha 1$  type. This suggests that the deer tandem repeat sequence arose between 25 and 45 million years ago, which is much earlier than the two million years proposed for humans. It is possible that the evolved tetrameric structure of deer Hp might confer a physiological advantage. We further proposed that a steric hindrance mechanism is involved in forming Hp tetramers.

## Results

### Identification of Hp phenotype

It has been claimed that the Hp of ruminants (cattle, sheep and goat) cannot enter polyacrylamide gels due to the large polymeric nature of the protein [20,21]. We tested whether this was also the case for the Hp of deer (another ruminant). Using a hemoglobin typing gel, we unexpectedly found deer plasma Hp to be a simple homogeneous molecule that is small enough to enter a 7% electrophoretic gel. An example of its phenotype and the electrophoretic properties of deer Hp, compared to human Hp 1-1, 2-1 and 2-2, is shown in Fig. 2. This shows that deer Hp mimics one of the polymeric forms of human Hp 2-1 or 2-2: either a linear or cyclic tetramer.

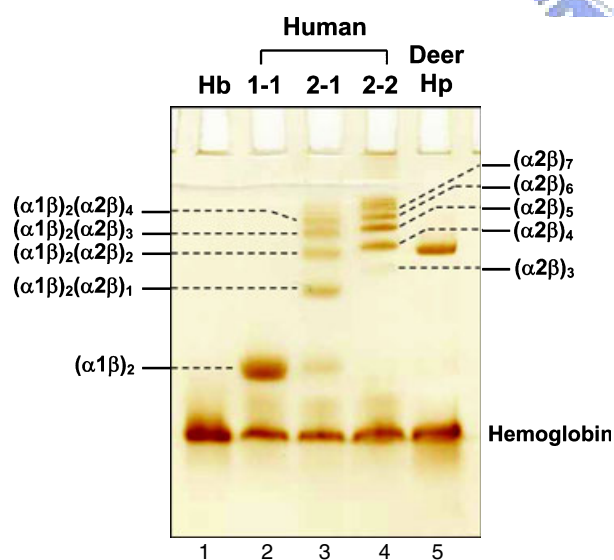


**Fig. 2.** Hemoglobin-binding patterns of deer and human plasma Hp on 7% native PAGE. Lane 1, hemoglobin only. Lanes 2, 3 and 4, human plasma of Hp 1-1, 2-1 and 2-2 phenotypes with hemoglobin, respectively. Lane 5, deer plasma with hemoglobin.

### Isolation of deer Hp

The molecular size of the Hp  $\alpha$ -chain has been conventionally used for identifying the phenotype of a given Hp protein. To further characterize the molecular form of deer plasma Hp, we attempted to isolate the protein using a Sepharose-based immunoaffinity column [22,23]. A mouse mAb prepared against the human  $\alpha$ -chain (W1) was utilized for coupling to the Sepharose because this mAb was able to react with both human and deer  $\alpha$ -chains on a western blot (described below). First, plasma samples enriched with Hp were pooled and applied to the affinity column. This procedure, however, failed to isolate deer Hp from the plasma due to the lack of binding of deer proteins to the column. Next, we used combined ammonium-sulfate fractionation and size-exclusion chromatography procedures [24] for the isolation. A size-exclusion chromatographic profile for the fractions containing Hp is shown in Fig. 3A (second peak). The homogeneity of isolated Hp was approximately 90%, as determined by SDS-PAGE (Fig. 3B). The presence of  $\alpha$ -chains was

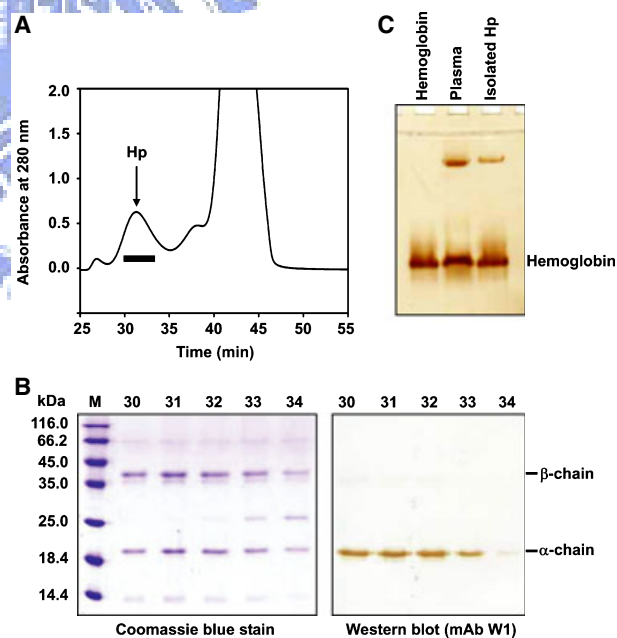


**Fig. 3.** Isolation of deer Hp using a size-exclusion Superose-12 column on an HPLC system. (A) A dialyzed supernatant of the 50% saturated ammonium sulfate fraction from plasma was applied to Superose-12 column ( $1 \times 30$  cm) at a flow rate of  $0.3 \text{ mL} \cdot \text{min}^{-1}$ , using NaCl/Pi as the mobile phase. The bar represents the pooled fractions corresponding to Hp. (B) SDS-PAGE and western blot analyses of eluted Hp fractions. (C) Hemoglobin-binding properties of isolated Hp and plasma containing native Hp on 7% native PAGE. Lane M, molecular markers in kDa (Invitrogen).



confirmed by western blot using W1 mAb (Fig. 3B; right panel).

### Hemoglobin binding of isolated Hp

In the next experiment, we tested the hemoglobin-binding ability of isolated deer Hp. Fig. 3C shows that the isolated Hp was able to form an Hp-hemoglobin complex under 7% native PAGE. Furthermore, it demonstrates that the deer protein consists of one major molecular form that is identical to its native form in the plasma based on electrophoretic mobility. It appears that the Hp isolated under our experimental conditions was not significantly altered with regard to its molecular and biochemical properties.

### Molecular mass estimation of deer and human Hp 2-2 using SDS-PAGE and western blot

Western blot analysis using the  $\alpha$  chain-specific mAb W1 indicated that the mAb recognizes both human and deer  $\alpha$  chains (Fig. 4A). It also reveals that the deer  $\alpha$ -chain belongs to the  $\alpha 2$  group, with a molecular mass of approximately 18 kDa on both SDS-PAGE and western blot. We therefore tentatively classified the deer Hp as phenotype 2-2. In isolated deer Hp, there was a trace amount of hemoglobin (approximately 14 kDa), with a molecular mass comparable to that of the human Hp  $\alpha 1$ -chain. The estimated molecular mass of the deer  $\beta$ -chain was about 36 kDa, slightly lower than that of human. The isolated deer Hp was further characterized using 4% SDS-PAGE under non-reducing conditions. Consistent with our hemoglobin binding assay, Fig. 4B (left panel) demonstrates that isolated deer Hp consists of only one specific tetrameric form, i.e.  $(\alpha\beta)_4$ , with a molecular mass about 216 kDa, which is close to that of the human Hp 2-2 tetramer (230 kDa) based on the gel profile.

### Unique immunoreactivity of deer Hp defined by mAb W1

We then attempted to ensure that the polymeric forms of human and deer protein were an Hp by western blot analysis using W1 mAb. Figs 3B and 4A clearly showed that this antibody was capable of binding both human and deer  $\alpha$ -chains in its reduced form. Interestingly, Fig. 4B (right panel) shows that this mAb recognized all the human Hp 2-2 polymers, but not intact deer Hp 2-2. However, after adding a reducing reagent ( $\beta$ -mercaptoethanol;  $\beta$ -ME) directly to intact deer Hp, the immunoreactivity was recovered on a dot-blot

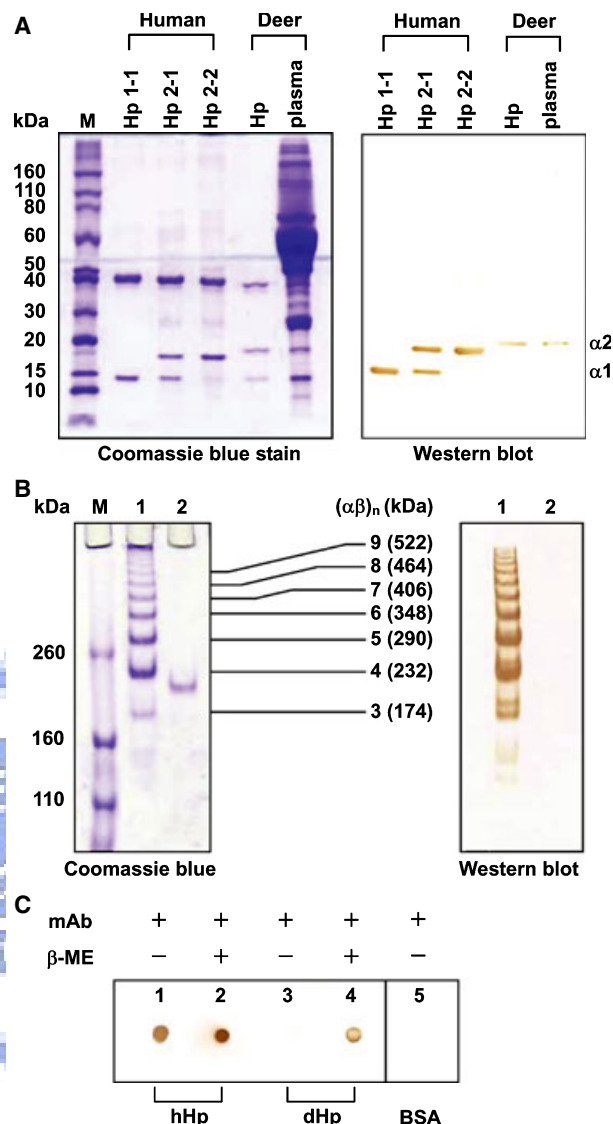


**Fig. 4.** SDS-PAGE, western blot and molecular mass analyses of isolated deer and human Hp. (A) The isolated proteins were run on 10–15% PAGE under reducing conditions. The western blot was performed using a human  $\alpha$ -chain-specific mAb (W1) that cross-reacts with the deer  $\alpha$ -chain. Lane M, molecular markers in kDa (Invitrogen). (B) Left panel: western blot analysis of the polymeric structure of isolated human and deer Hp under 4% non-reducing SDS-PAGE using  $\alpha$ -chain-specific mAb W1. Lane M, molecular markers in kDa (Invitrogen). Lane 1, isolated human Hp 2-2. Lane 2, isolated deer Hp. Right panel: On the western blot, mAb W1 only recognizes human polymeric Hp, but not intact deer tetrameric Hp. (C) Dot-blot analysis of isolated human Hp (hHp) and deer Hp (dHp) using  $\alpha$ -chain-specific mAb W1 in the presence or absence of the reducing reagent  $\beta$ -ME (143 mM). BSA was used as a negative control.

assay (Fig. 4C). It appears that the antigenic epitope of deer  $\alpha$ -chain is masked in the tetrameric form. This also explains why the W1 mAb-coupled affinity

column failed to bind deer plasma Hp in the purification procedure described above.

### Cloning of deer Hp cDNA

Evidently, the molecular form of deer 'Hp 2-2' totally differs from that of human Hp 2-2, with the latter found as typical polymers or the form  $(\alpha\beta)_n$ , where  $n = 3-12$  (Fig. 4B). It remains ambiguous as to whether deer Hp should be designated as a typical Hp 2-2. The most significant feature of the molecular structure of human Hp 2-2 is that it includes a tandem repeat in the  $\alpha$ 2-chain. To determine whether this is also true in deer Hp, we cloned the deer Hp cDNA. The complete linear nucleotide sequence corresponding to the  $\alpha$ - $\beta$  chain as determined by our laboratory has been submitted to GenBank (accession number EF601928). Based on the cDNA sequence, the deer  $\alpha$ - and  $\beta$ -chains comprise 136 and 245 amino acid residues, respectively, which is similar to that of human, with 142 ( $\alpha$ 2) and 245 ( $\beta$ ) residues (Fig. 5A,B). A tandem repeat of the deer  $\alpha$ -chain was observed (discussed below).

### Amino acid sequence alignment of deer and human Hp 2-2

The putative amino acid sequence alignment reveals that deer Hp is somewhat homologous to human Hp 2-2 (80% and 68% for  $\beta$ - and  $\alpha$ -chains, respectively). The divergence and identity of the  $\beta$ -chain with that of other mammals are shown in Fig. 5C. The sequence for deer is relatively similar to that of cattle [25], another ruminant. We also created a brief phylogenetic tree for possible molecular evolution of the Hp  $\beta$ -chain using the CLUSTAL method in DNASTAR MEGALIGN software. The result shows that the evolved amino acid sequences of ruminant Hp  $\beta$ -chains are the most divergent among all mammals (Fig. 5D).

### Analysis of -SH groups of the deer Hp $\alpha$ -chain and their implication for formation of the tetramer

As shown in Fig. 6 in the form of simplified ABC domains, the human  $\alpha$ 2-chain contains identical ABC

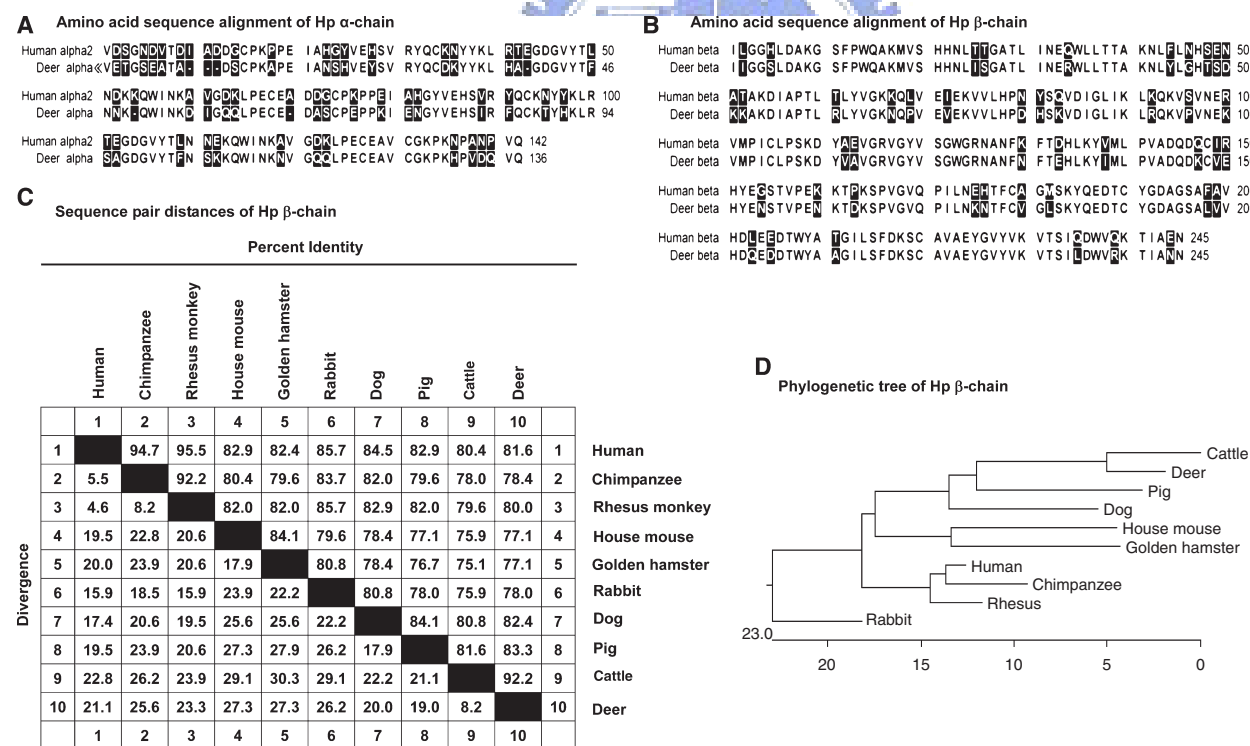


**Fig. 5.** Putative amino acid sequence analysis and divergence of mammal Hps. (A,B) Amino acid sequence alignment of the  $\alpha$ - and  $\beta$ -chains of human and deer. Variable regions are shaded in black. The cDNA nucleotide sequence corresponding to deer Hp in this study has been deposited in GenBank under the accession number of EF601928. (C) Divergence of the amino acid sequences of Hp  $\beta$ -chains among ten mammals. (D) Phylogenetic tree constructed according to the amino acid sequences of Hp  $\beta$ -chains for ten mammals. The tree was plotted using the MEGALIGN program in the DNASTAR package. Branch lengths (%) are proportional to the level of sequence divergence, while units at the bottom indicate the number of substitution events.

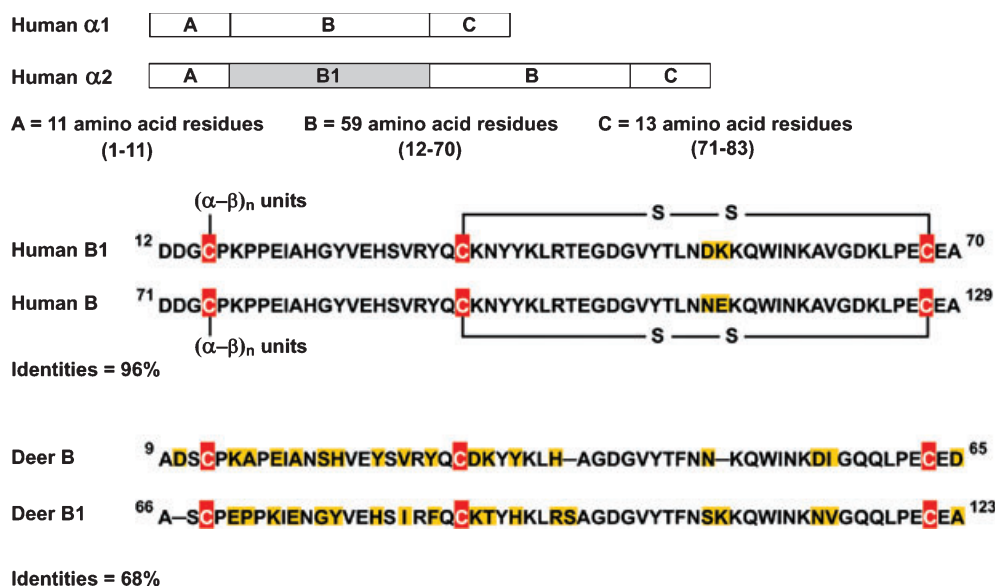


**Fig. 6.** Schematic drawing of tandem repeat region (B and B1) of deer and human  $\alpha$ -chain. The most significant feature of human  $\alpha 2$  is that it matches the ABC domains of  $\alpha 1$  but with an additional insertion of a redundant sequence (B1 region). The repeat unit contains 59 amino acid residues between Asp12 and Ala70. The sequence homology in the repeat region of human is 96% (two amino acids mutated). Deer also have a redundant sequence (B and B1), but the sequence homology between the two repeat units is approximately 68%. The full length of the  $\alpha$ -chain contains 142 and 136 residues in human and deer, respectively. The positions and number of Cys residues (total of seven) are completely identical between the two species (the one at the C-terminal region is not shown). Divergence of the amino acids within the species is marked in yellow.

domains to  $\alpha 1$  with insertion of a tandem repeat region (B1). The latter contains amino acid residues between Asp12 and Ala70 (a total of 59 residues). The sequence homology between the repeat regions of the human  $\alpha 2$ -chain is 96%, with only two amino acids mutated (replacement of Asn52 and Glu53 in the B region by Asp52 and Lys53 in the B1 region). This tandem repeat is responsible for the formation of Hp polymers due to the extra -SH group (Fig. 1A). Such repeats also exist within the deer  $\alpha$ -chain (B1 and B repeat), where the B1 region is residues 9–65. Thus, at the molecular level, the deer  $\alpha$ -chain belongs to the  $\alpha 2$  group, and is identical to the human  $\alpha 2$ -chain in possessing a tandem repeat. Interestingly, the sequence homology between the two repeat units (B1 and B) of deer is only 68% (Fig. 6).

As shown schematically in Fig. 1A, the human  $\alpha 2$ -chain consists of seven -SH groups (Cys15, 34, 68, 74, 93, 127 and 131) in 142 residues. Among these, there are two disulfide linkages within the  $\alpha$ -chain (Cys34 and 68 and Cys93 and 127), and the one at the C-terminal region (Cys131) cross-links with the  $\beta$ -chain (Cys105) to form a basic  $\alpha$ - $\beta$  unit. Under such an arrangement, Cys15 and Cys74 are available to link with other  $\alpha$ - $\beta$  units. As a result, human  $\alpha 2$  forms  $(\alpha$ - $\beta$ ) $_n$  polymers (where  $n \geq 3$ ) as shown in Fig. 4B. Interestingly, the number and location of -SH groups in the deer

$\alpha 2$ -chain are identical to those in human (Fig. 6), but the deer Hp only yields a tetrameric  $(\alpha$ - $\beta$ ) $_4$  form. As the identity between the tandem repeats of deer is only 68% (compared with 96% in human), we hypothesized that these amino acid differences determine the conformation between Cys15 and 74 and drive the construction of the  $(\alpha$ - $\beta$ ) $_4$  structure of deer Hp (see Discussion).

To test whether the deer Hp can also form multiple polymers *in vitro*, we denatured the protein using 6 M urea with addition of 143 mM  $\beta$ -ME. Under these conditions, the deer protein was completely dissociated, similar to the profile shown in Fig. 4A for SDS-PAGE analysis (data not shown). We then slowly renatured the deer Hp by stepwise dialysis in order to determine possible formation of other large polymers (greater than tetramer). Figure 7 shows that the renatured protein retained the tetramer form, and no other polymers larger than tetramers were observed on SDS-PAGE, although some trimers were produced. Under the same conditions, human Hp 2-2 was renatured to  $(\alpha$ - $\beta$ ) $_n$ . The data suggest that formation of deer Hp tetramer is specific, not randomly assembled. This assembly seems to be dependent on the unique orientation of the -SH groups within the Hp. In addition, each renatured protein retained its hemoglobin-binding ability (Fig. 7). A hypothetical model explaining the formation of Hp tetramers is described below.

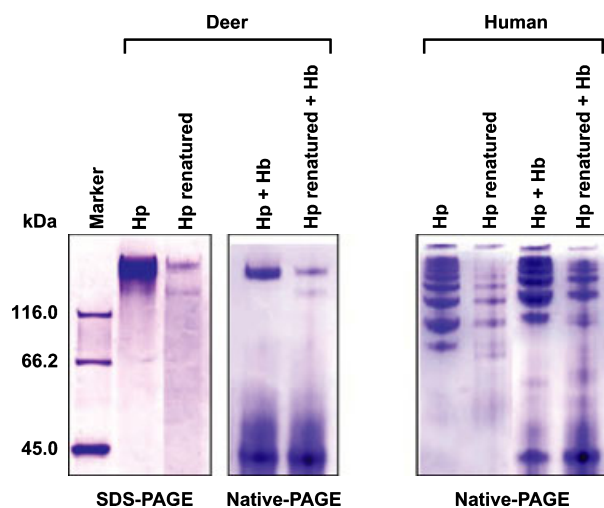


**Fig. 7.** SDS-PAGE and native PAGE analyses of renaturation of deer and human Hp polymers. Denaturation of deer Hp using 6 M urea under reducing conditions (143 mM  $\beta$ -ME) followed by renaturation resulted in the formation of  $(\alpha\text{-}\beta)_4$  and some  $(\alpha\text{-}\beta)_3$ .

## Discussion

### Isolation of deer native Hp

We have recently developed several lines of human Hp mAb and routinely utilized these antibodies for the isolation of human Hp 1-1, 2-1 and 2-2 phenotypes [22,26]. As only W1 (specific to the  $\alpha$ -chain) is able to cross-react with the deer  $\alpha$ -chain on a western blot, we attempted to utilize this mAb for the affinity isolation of deer Hp in this study. Interestingly, the W1 mAb only recognizes the human Hp but not deer Hp in its intact form (Fig. 4B,C). We therefore used a previously described HPLC-based size-exclusion chromatography procedure [24] for the isolation of deer Hp. However, this procedure is only suitable for isolating the Hps with a homogeneous structure, and is not suitable for human Hp 2-2 or 2-1 [22]. One minor disadvantage of the method was the contamination of the isolated Hp by a trace amount of hemoglobin (Fig. 4A). This is observed mainly because Hp-hemoglobin complexes are formed prior to the purification; as such, hemolysis should be kept to a minimum in order to reduce the hemoglobin level while collecting the blood.

### Presence of Hp in deer plasma

Not all deer possess a high level of plasma Hp. About 30% of the plasma samples that we screened (total  $n = 15$ ) exhibited low Hp levels in the hemoglobin-binding assay (Fig. 2). Based on chromogeneity, the

concentrations of deer plasma were approximately  $1 \text{ mg}\cdot\text{mL}^{-1}$  of those used for purification when compared with human Hp 1-1 standard. In reindeer ( $n = 6$ ), a mean plasma value of  $0.6 \text{ mg}\cdot\text{mL}^{-1}$  has been reported [27].

### Primary structure of the deer $\alpha$ -chain and its relationship to Hp polymers

There are several lines of evidence support the conclusion that the genotype of deer Hp is *Hp 2*, with an Hp 2-2 phenotype. First, analysis of mercaptoethanol-reduced plasma indicates a molecular mass of 18 kDa for the  $\alpha$ -chain, which is similar to that of human  $\alpha_2$  based on a western blot (Fig. 4A). Second, the molecular mass of the  $\alpha$ -chain from a purified sample was also similar to that of human  $\alpha_2$  (Fig. 4A). Third, by putative amino acid sequence alignment, the deer  $\alpha$ -chain contains a tandem repeat that is consistent with that found in human. Fourth, the total number of  $-\text{SH}$  groups and their location resulting from the tandem repeat are completely identical to that of human, although the sequence homology between the repeats was 68% in deer, compared to 96% in human (Fig. 6).

It remains unclear why the apparent molecular mass of the deer  $\alpha$ -chain on PAGE is somewhat higher than that of human. We therefore attempted to determine whether it was due to additional carbohydrate moieties on the deer  $\alpha$ -chain. However, using Pro-Q Emerald glycoprotein gel stains (Molecular Probes, Eugene, OR, USA), we did not identify any carbohydrates associated with the  $\alpha$ -chain of either species (data not shown).

### Hypothetical model for the formation of the deer Hp tetramer

The ability of the deer Hp to refold and reassemble into its tetrameric form *in vitro* indicates that the assembly of  $\alpha$ - and  $\beta$ -chains into predetermined polymers is dependent on their biochemical nature (Fig. 7). As shown in Fig. 8A, we proposed a model to explain the formation of tetramers. This suggests that the two  $-\text{SH}$  groups of the deer  $\alpha$ -chain are located on two flat surfaces at different angles to each other. Under these conditions, a homodimer cannot form due to the availability of another free  $-\text{SH}$  group of the  $\alpha\text{-}\beta$  unit for cross-linking with another  $\alpha\text{-}\beta$  unit. Figure 8B illustrates that there is no steric hindrance for tetramer formation, although there are two possible configurations for the tetramer. Some trimers may form, but there is some hindrance preventing the subunits from coming



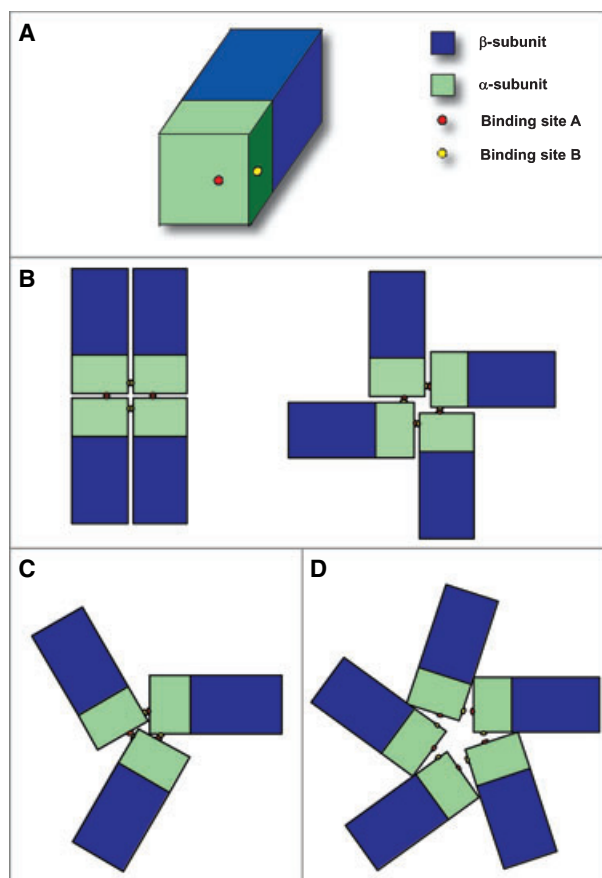


**Fig. 8.** A hypothetical model illustrating the steric hindrance involved in formation of a deer Hp tetramer. (A) A basic Hp subunit comprising one  $\alpha$ - and one  $\beta$ -subunit. The  $-SH$  groups that connect the Hp subunits into polymers are assumed to be located with steric hindrance between the SH binding sites A and B. (B) The two different possible forms of tetramers. (C) A trimeric form of deer Hp is possible to assemble according to this model, but steric hindrance is seen which prevents the  $-SH$  groups from linking to some extent. (D) Formation of a pentamer or higher-order polymer is not possible.

close together in the cyclic center (Fig. 8C). Therefore, the formation of trimers takes place to a much lower extent than that of tetramers. No higher-order polymers are formed, because the distance between the  $-SH$  groups is too great to allow cross-linking for  $(\alpha\text{-}\beta)_5$  pentamers or other larger polymers (Fig. 8D).

For a higher-order polymer ( $n > 5$ ), the angle ( $\theta$ ) between the sides containing the  $-SH$  groups of two polymers would be  $90\text{--}360/n$  degrees. If the distance between the  $-SH$  sites is approximately  $90^\circ$ , and the side of the Hp subunit contributes the base of the triangle, the distance is proportional to  $\sin \theta$ . As  $\theta$  approaches  $90^\circ$  as  $n$  approaches infinity, the distance between the  $-SH$  sites also comes close to a maximum

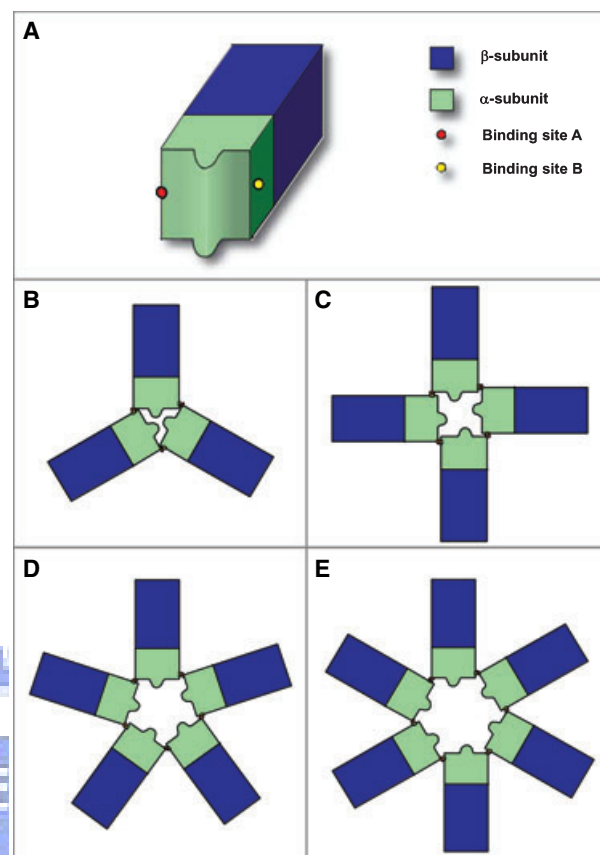


**Fig. 9.** Model of formation of human Hp 2-2 polymers. The positioning of the  $-SH$  groups involved in polymer formation differs from those in deer Hp. (A) A basic human Hp 2-2 subunit comprising one  $\alpha$ - and one  $\beta$ -subunit. The  $-SH$  groups that connect the subunits into polymers are located at the edge of the surface. The hindrance between the  $-SH$  binding sites A and B prevents formation of a dimer. (B) A trimer is able to form to some extent with some steric hindrance. (C–E) Polymers of a higher order than tetramers can form without any steric hindrance.

as  $n$  increases. In fact, few trimers are seen in our renaturing experiment (Fig. 7) and no polymers of an order of five or higher are observed.

For human Hp 2-2, on the other hand, the formation of higher-order polymers is possible (Fig. 9). The assumed positions of the  $-SH$  groups differ from those in deer Hp. They are located at the edges of the same plane, so formation of an identical 'stacking' dimer or  $(\alpha\text{-}\beta)_2$  is not possible due to steric hindrance between the two  $-SH$  groups (Fig. 9A). However, formation of some trimers by linking together via the two  $-SH$  groups at the edge is possible, but not to a great extent due to the limited space in the cyclic center (Fig. 9B). This explains why there are only trace amount of trimers in all the human Hp 2-2 samples (Fig. 2). The cyclic center provides sufficient room to facilitate

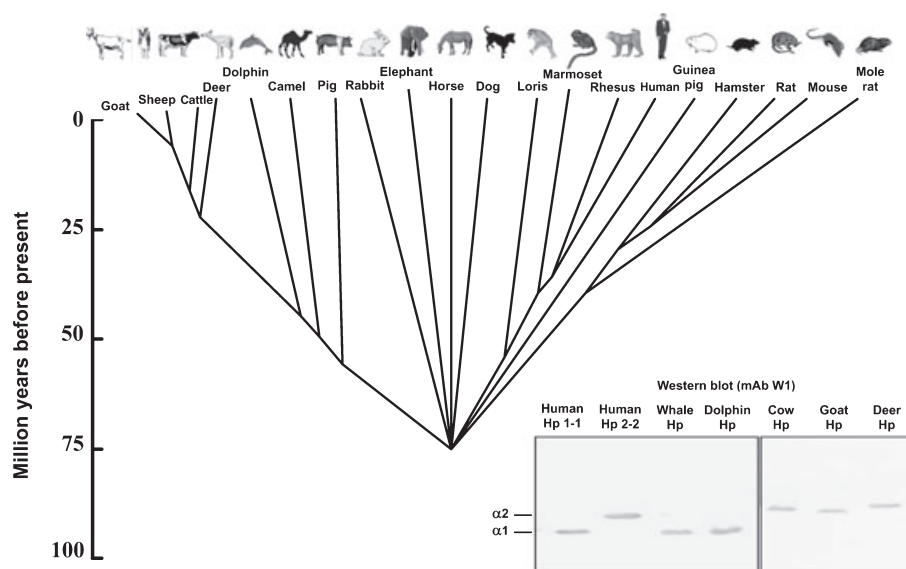


**Fig. 10.** Phylogenetic tree illustrating the molecular evolution of mammals, and phenotyping of human, whale, dolphin and ruminant  $\alpha$ -chains. The tree is constructed by assuming that all eutherian orders radiated at about the same point in evolutionary time, approximately 75 million years ago. Alternative branching orders give essentially identical results. Within a eutherian order, branch points are assigned using evolutionary times based on fossil records [30]. Western blot analysis of Hp of six mammals (with a branching point before and after deer) was conducted using a 10–15% SDS-PAGE gradient gel under reducing conditions with an  $\alpha$ -chain-specific mAb (W1) prepared against human Hp.

formation of polymers of an order greater than four  $\alpha$ - $\beta$  units. Such configuration also allows binding of the W1 mAb. In contrast, the cyclic center of deer Hp tetramers is totally blocked and is not accessible for mAb binding (Fig. 4B,C).

## Evolution

In vertebrates, a recent study has suggested that the Hp gene appeared early in vertebrate evolution, between the emergence of urochordates and bony fish [5]. All mammalian species studied to date have been shown to possess Hp. Analysis of the electrophoretic patterns of Hp-hemoglobin complexes has suggested that most of these Hps are similar to human Hp 1-1 [28]. Only the protein found in ruminants (cattle, sheep and goat) resembled polymeric forms of human Hp 2-2 [20], but whether they also possess a tandem repeat remains unexplored [25].

It is thought that humans originally had a single Hp 1-1 phenotype [29]. Maeda *et al.* [15] proposed that the tandem repeat sequence of human  $\alpha$ 2 evolved two million years ago from a nonhomologous unequal crossover between two *Hp 1* alleles (*Hp 1S* and *Hp 1F*) during meiosis. A unique feature of the *Hp 2* allele is that it is present only in humans and is not found in any primates, including New and Old

World monkeys, chimpanzees and gorillas [17]. We have recently found that cattle also possess *Hp 2* as the sole genotype [25]. It is likely that ruminants including deer, cattle, goat and sheep may all possess a sole *Hp 2*-type allele. In the present study, we have shown that the inserted tandem repeat region in deer Hp appears to have extensively evolved, as 32% of the repeated region has undergone mutation, compared to that of only 4% (two amino acid residues) in human Hp (Fig. 6). Thus, we propose that the occurrence of the tandem repeat in deer was much earlier than in humans.

Figure 10 depicts a phylogenetic tree constructed by assuming that all eutherian orders (mammals) radiated at about the same point in evolutionary time (approximately 75 million years ago) [30]. The phylogenetic analysis indicates that crossing-over of deer  $\alpha$ -chains occurred after divergence of the line leading to ruminants and pig, as pig possesses only the Hp 1-1 phenotype [24]. As dolphins and whales are the closest divergences before the ruminants, we further examined the size of the  $\alpha$ -chain in whales and dolphins as well as other ruminants (cattle and goat) to determine the possible time of the tandem repeat evolution in deer Hp. Interestingly, the inserted panel of Fig. 10 shows that the  $\alpha$ -chains of all the ruminants tested are the  $\alpha$ 2 type, except for dolphins ( $n = 5$ ) and whales ( $n = 5$ ).

These data suggests that the crossing-over resulting in the tandem repeat in ruminants occurred at least 25 million years ago or between 25 and 45 million years ago (Fig. 10), which is much earlier than the two million years proposed in humans [15]. The molecular evolution of the ruminants, which are the latest mammals in the phylogenetic tree (diverging after dolphins), is remarkably rapid, based on molecular evolution models for growth hormone and prolactin, when compared with other mammals [31,32]. This model appears to be consistent with the overall amino acid alterations (32%) within the tandem repeat of deer Hp  $\alpha$ -chain. A similar alteration in cattle has also been reported recently [25].

Whether this alteration is adaptive during evolution remains to be addressed. For example, in cattle, there is an extensive family of at least eight prolactin-like genes that are expressed in the placenta [33,34]. These genes appear to be arranged as a cluster on the same chromosome. Phylogenetic analysis suggests that all of these genes are the consequence of one or more duplications of the prolactin gene; detailed analysis suggests that a rapid adaptive change has played a role in molecular evolution [35].

### Evolutionary advantage of deer Hp protein being a tetramer

In addition to the superior binding affinity of Hp to hemoglobin, Hp is an anti-inflammatory molecule and a potent antioxidant [9]. In humans, the large complicated polymers of Hp 2-2 are a risk in the association of diabetic nephropathy [36,37]. One explanation is that the large polymer dramatically retards penetration of the molecule into the extracellular space [36]. We have shown in the present study that deer Hp 2-2 was not able to form complicated polymers, because the diversity in amino acid sequence between the tandem repeat of  $\alpha$ -chain has produced steric hindrance (Fig. 8) that may be advantageous to deer.

In conclusion, we have shown that deer possess an *Hp 2* allele with a tandem repeat that could have occurred at least 25 or between 25 and 45 million years ago based on the phylogenetic analysis. The phenotypic and biochemical structure of their Hp is markedly homogeneous, with a tetrameric arrangement due to the orientation of the two available -SH groups, preventing the formation of the complicated Hp polymers found for human Hp 2-2. In terms of molecular evolution, this steric hindrance may have conferred an advantage on deer Hp that compensates for the undesired tandem repeat in the  $\alpha$ -chain.

## Experimental procedures

### Animal plasma

Animal plasma of deer (*Cervus unicolor swinhoei*), goat (*Capra hircus*), cattle (*Bos taurus*), pig (*Sus scrofa domestica*), dolphin (*Steno bredanensis*) and whale (*Delphinapterus leucas*) were obtained from the Pingtung County Livestock Disease Control Center and the Veterinary Medicine Teaching Hospital, National Pingtung University of Science and Technology, Taiwan.

### Phenotyping

Hp phenotyping was performed by native PAGE using hemoglobin-supplemented serum or plasma [22]. Briefly, 6  $\mu$ L plasma were premixed with 3  $\mu$ L of 40 mg mL<sup>-1</sup> hemoglobin for 15 min at room temperature. The reaction mixture was then equilibrated with 3  $\mu$ L of a sample buffer containing 0.625 M Tris (pH 6.8), 25% glycerol and 0.05% bromophenol blue, followed by electrophoresis on a 7% native polyacrylamide gel (pH 8). Electrophoresis was performed at 20 mA for 2 h, after which time the Hp-hemoglobin complexes were visualized by shaking the gel in a freshly prepared peroxidase substrate (30 mL NaCl/P<sub>i</sub> containing 25 mg of 3,3'-diaminobenzidine in 0.5 mL dimethyl sulfoxide and 0.01% H<sub>2</sub>O<sub>2</sub>). The results were confirmed by western blot using an  $\alpha$ -chain-specific mAb prior to phenotyping.

### Preparation of mouse mAb and human Hp

Mouse mAb W1 specific to the human Hp  $\alpha$ -chain was produced in our laboratory according to standard procedures [38]. Native human Hp was isolated from plasma using an immunoaffinity column followed by size-exclusion chromatography on an HPLC system using previously described procedures [22].

### Purification of deer haptoglobin

Plasma samples enriched with Hp were prepared from deer blood containing 0.1% EDTA, followed by centrifugation at 1200 g for 15 min at 4 °C to remove the cells. Isolation was performed according to the method previously established for porcine Hp [24]. Saturated ammonium sulfate solution was added to the plasma to a final saturated concentration of 50%. After gentle stirring for 30 min at room temperature, the precipitate was discarded by centrifugation at 4000 g for 30 min at 4 °C. The supernatant was then dialyzed at 4 °C for 16 h against NaCl/P<sub>i</sub> containing 10 mM phosphate (pH 7.4) and 0.12 M NaCl with three changes. After dialysis, the sample was concentrated and filtered through a 0.45  $\mu$ m nylon fibre prior to size-exclusion chromatography. An HPLC system (Waters, Milford, MA, USA), consisting of two pumps, an automatic sample

injector and a photodiode array detector, with a Superose-12 column (1 × 30 cm) (GE Healthcare, Uppsala, Sweden) pre-equilibrated with NaCl/P<sub>i</sub>, was used for further purification. The column was run for 60–80 min at room temperature with a flow rate of 0.3 mL·min<sup>-1</sup> using NaCl/P<sub>i</sub> as the mobile phase. Fractions containing Hp were pooled and concentrated to a final volume of 1 mL using an Amicon centrifugal filter (Millipore, Billerica, MA, USA), and stored at -20 °C until use.

### Gel electrophoresis

SDS-PAGE was performed according to the method described by Laemmli [39] with some modifications, using 5% polyacrylamide as the stacking gel [40]. In general, samples containing 143 mM β-ME were preheated at 100 °C for 10 min in a buffer containing 12 mM Tris-HCl (pH 6.8), 0.4% SDS, 5% glycerol and 0.02% bromophenol blue before loading to the gel. The samples were run on a step gradient of polyacrylamide gel (10 and 15%) for about 1.5 h at 100 V and stained using Coomassie brilliant blue. For determination of the molecular mass of Hp, the tested samples were prepared under the non-reducing conditions using the SDS gel. Alternatively, the SDS gel was prepared in a 0.04 M phosphate buffer (pH 7.0) containing 4% polyacrylamide, and the samples were run for about 6 h at 30V. The molecular mass standard for SDS-PAGE, containing three pre-stained proteins (260, 160 and 110 kDa), was purchased from Invitrogen (Carlsbad, CA, USA).

### Immunoblot analysis

Western blot analysis was performed using a method similar to that described previously [40]. In brief, the electrotransferred and blocked nitrocellulose was incubated with anti-Hp mAb W1, followed by washes and incubation with horseradish peroxidase-conjugated goat anti-mouse IgG (Chemicon, Temecula, CA). The membrane was developed using 3,3'-diaminobenzidine containing 0.01% H<sub>2</sub>O<sub>2</sub>. Dot blots were performed by applying the samples (reduced or non-reduced) onto a nitrocellulose membrane using anti-Hp mAb W1 as the primary antibody.

### Cloning and sequencing analysis of deer Hp

The entire procedure was similar to that described previously [9,10]. Briefly, total RNA was extracted from deer whole blood using an RNeasy Mini Kit (Qiagen, Hilden, Germany) according to the manufacturer's instructions. The gene for deer Hp from total RNA was reverse-transcribed and PCR-amplified using proofreading DNA polymerase (Invitrogen), forward primer 5'-TTCCTGC AGTGGAACCCGGCAGTGAGGCCA-3' and reverse

primer 5'-CGGAAAACCATCGCTAACAACTAAGCTT GGG-3'. The PCR cycling profile was as follows: denaturation at 94 °C for 5 min, then 35 cycles of denaturation at 94 °C for 30 s, annealing at 55 °C for 30 s and extension at 72 °C for 90 s, then final extension at 72 °C for 10 min. The PCR product was analyzed by electrophoresis through a 1% agarose gel, and purified using a gel extraction kit (BD Biosciences, Palo Alto, CA). The purified PCR product was cloned into a pGEM-T Easy vector (Promega, Madison, WI, USA), and then the ligated plasmid was transformed into *Escherichia coli* JM109 (Qiagen). Finally, the sequence of deer Hp was confirmed by DNA sequencing.

### Sequence alignment and phylogenetic analysis

The cDNA and amino acid sequence alignment, sequence pair distances and phylogenetic tree construction were performed using DNASTAR software (Lasergene, Madison, WI, USA).

### Denaturation and renaturation of deer and human Hp 2-2

Purified deer Hp (0.1 mg·mL<sup>-1</sup>) or human Hp 2-2 (2 mg·mL<sup>-1</sup>) were mixed with NaCl/P<sub>i</sub> containing 6 M urea and 143 mM β-ME and incubated at room temperature for 30 min. The reaction mixture was first dialyzed in 200 mL NaCl/P<sub>i</sub> at 4 °C for 6 h, and this was repeated three times (total 24 h) to allow renaturation. The mixture was finally dialyzed against 2 L NaCl/P<sub>i</sub> overnight. The concentrated Hp samples with or without reduction were incubated with hemoglobin for use on a typing gel as that for plasma phenotyping, and then stained by Coomassie brilliant blue.

### Acknowledgements

This work was supported by NSC grant 95-2313-B-009-003-MY2 from the National Science Council, Taiwan. We especially thank Drs Suen-Chuain Lin (Veterinary Medicine Teaching Hospital, National Pingtung University of Science and Technology) and Yi-Ping Lu (Pingtung Livestock Disease Control Center) for kindly providing the animal plasma. We also acknowledge James Lee of National Chiao University for his scientific critiques and editorial comments.

### References

- 1 González-Ramón N, Hoebe K, Alava MA, Van Leengoed L, Piñeiro M, Carmona S, Iturralde M, Lampreave F & Piñeiro A (2000) Pig MAP/ITIH4 and haptoglobin are interleukin-6-dependent acute-phase



- plasma proteins in porcine primary cultured hepatocytes. *Eur J Biochem* **267**, 1878–1885.
- 2 Wang Y, Kinzie E, Berger FG, Lim SK & Baumann H (2001) Haptoglobin, an inflammation-inducible plasma protein. *Redox Rep* **6**, 379–385.
  - 3 Raijmakers MT, Roes EM, te Morsche RH, Steegers EA & Peters WH (2003) Haptoglobin and its association with the HELLP syndrome. *J Med Genet* **40**, 214–216.
  - 4 Gervois P, Kleemann R, Pilon A, Percevault F, Koenig W, Staels B & Kooistra T (2004) Global suppression of IL-6-induced acute phase response gene expression after chronic *in vivo* treatment with the peroxisome proliferator-activated receptor- $\alpha$  activator fenofibrate. *J Biol Chem* **279**, 16154–16160.
  - 5 Wicher KB & Fries E (2006) Haptoglobin, a hemoglobin-binding plasma protein, is present in bony fish and mammals but not in frog and chicken. *Proc Natl Acad Sci USA* **103**, 4168–4173.
  - 6 Kristiansen M, Gravarsen JH, Jacobsen C, Sonne O, Hoffman H, Law SKA & Moestrup SK (2001) Identification of the haemoglobin scavenger receptor. *Nature* **409**, 198–201.
  - 7 Langlois MR & Delanghe JR (1996) Biological and clinical significance of haptoglobin polymorphism in humans. *Clin Chem* **42**, 1589–1600.
  - 8 Mao SJT, Yates MT & Jackson RL (1994) Antioxidant activity and serum levels of probucol and probucol metabolites. *Methods Enzymol* **234**, 505–513.
  - 9 Tseng CF, Lin CC, Huang HY, Liu HC & Mao SJT (2004) Antioxidant role of human haptoglobin. *Proteomics* **4**, 2221–2228.
  - 10 Lai IH, Tsai TI, Lin HH, Lai WY & Mao SJT (2007) Cloning and expression of human haptoglobin subunits in *Escherichia coli*: delineation of a major antioxidant domain. *Protein Express Purif* **52**, 356–362.
  - 11 Kurosky A, Barnett DR, Lee TH, Touchstone B, Hay RE, Arnott MS, Bowman BH & Fitch WM (1980) Covalent structure of human haptoglobin: a serine protease homolog. *Proc Natl Acad Sci USA* **77**, 3388–3392.
  - 12 Miyoshi H, Ohshiba S, Matsumoto A, Takada K, Umegaki E & Hirata I (1991) Haptoglobin prevents renal dysfunction associated with intravariceal infusion of ethanalamine oleate. *Am J Gastroenterol* **86**, 1638–1641.
  - 13 Engstrom G, Lind P, Hedblad B, Wollmer P, Stavenow L, Janzon L & Lindgarde F (2002) Lung function and cardiovascular risk: relationship with inflammation-sensitive plasma proteins. *Circulation* **106**, 2555–2560.
  - 14 Hochberg I, Roguin A, Nikolsky E, Chandrasekhar PV, Cohen S & Levy AP (2002) Haptoglobin phenotype and coronary artery collaterals in diabetic patients. *Atherosclerosis* **161**, 441–446.
  - 15 Maeda N, Yang F, Barnett DR, Bowman BH & Smithies O (1984) Duplication within the haptoglobin Hp2 gene. *Nature* **309**, 131–135.
  - 16 Maeda N (1985) Nucleotide sequence of the haptoglobin and haptoglobin-related gene pair. The haptoglobin-related gene contains a retrovirus-like element. *J Biol Chem* **260**, 6698–6709.
  - 17 McEvoy SM & Maeda N (1988) Complex events in the evolution of the haptoglobin gene cluster in primates. *J Biol Chem* **263**, 15740–15747.
  - 18 Smithies O & Walker NF (1955) Genetic control of some serum proteins in normal humans. *Nature* **176**, 1265–1266.
  - 19 Black JA & Dixon GH (1968) Amino-acid sequence of alpha chains of human haptoglobins. *Nature* **218**, 736–741.
  - 20 Busby WH Jr & Travis JC (1978) Structure and evolution of artiodactyla haptoglobins. *Comp Biochem Physiol B* **60**, 389–396.
  - 21 Eckersall PD & Conner JG (1990) Plasma haptoglobin in cattle (*Bos taurus*) exists as polymers in association with albumin. *Comp Biochem Physiol B* **96**, 309–314.
  - 22 Tseng CF, Huang HY, Yang YT & Mao SJT (2004) Purification of human haptoglobin 1-1, 2-1, and 2-2 using monoclonal antibody affinity chromatography. *Protein Express Purif* **33**, 265–273.
  - 23 Yueh CH, Lai YA, Hsu HH, Chen WL & Mao SJT (2007) An improved method for haptoglobin 1-1, 2-1, 2-2 purification using monoclonal antibody affinity chromatography in the presence of sodium dodecyl sulfate. *J Chromatogr B Biomed Sci Appl* **845**, 210–217.
  - 24 Yang SJ & Mao SJT (1999) Simple high-performance liquid chromatographic purification procedure for porcine plasma haptoglobin. *J Chromatogr B Biomed Sci Appl* **731**, 395–402.
  - 25 Lai YA, Lai IH, Tseng CF, Lee J & Mao SJT (2007) Evidence of tandem repeat and extra thiol-groups in the polymeric formation of bovine haptoglobin: a unique structure of Hp 2-2 phenotype. *J Biochem Mol Biol* **40**, 1028–1038.
  - 26 Cheng TM, Pan JP, Lai ST, Kao LP, Lin HH & Mao SJT (2007) Immunochemical property of human haptoglobin phenotypes: determination of plasma haptoglobin using type-matched standards. *Clin Biochem* **40**, 1045–1056.
  - 27 Orro T, Sankari S, Pudas T, Oksanen A & Soveri T (2004) Acute phase response in reindeer after challenge with *Escherichia coli* endotoxin. *Comp Immunol Microbiol Infect Dis* **27**, 413–422.
  - 28 Bowman BH (1993) Haptoglobin. In *Hepatic Plasma Proteins: Mechanisms of Function and Regulation* (Bowman BH ed.), pp. 159–167. Academic Press, San Diego, CA.
  - 29 Smithies O, Connell GE & Dixon GH (1962) Chromosomal rearrangements and the evolution of haptoglobin genes. *Nature* **196**, 232–236.

- 30 Forsyth IA & Wallis M (2002) Growth hormone and prolactin-molecular and functional evolution. *J Mammary Gland Biol Neoplasia* **7**, 291–312.
- 31 Wallis M (1994) Variable evolutionary rates in the molecular evolution of mammalian growth hormones. *J Mol Evol* **38**, 619–627.
- 32 Wallis M (2000) Episodic evolution of protein hormones: molecular evolution of pituitary prolactin. *J Mol Evol* **50**, 465–473.
- 33 Schuler LA & Kessler MA (1992) Bovine placental prolactin-related hormones. *Trends Endocrinol Metab* **3**, 334–338.
- 34 Goffin V, Shiverick KT, Kelly PA & Martial JA (1996) Sequence–function relationships within the expanding family of prolactin, growth hormone, placental lactogen, and related proteins in mammals. *Endocr Rev* **17**, 385–410.
- 35 Wallis M (1993) Remarkably high rate of molecular evolution of ruminant placental lactogens. *J Mol Evol* **37**, 86–88.
- 36 Nakhoul FM, Zoabi R, Kanter Y, Zoabi M, Skorecki K, Hochberg I, Leibur R, Miller B & Levy AP (2001) Haptoglobin phenotype and diabetic nephropathy. *Diabetologia* **44**, 602–604.
- 37 Asleh R, Guetta J, Kalet-Litman S, Miller-Lotan R & Levy AP (2005) Haptoglobin genotype and diabetes-dependent differences in iron-mediated oxidative stress *in vitro* and *in vivo*. *Circ Res* **96**, 435–441.
- 38 Chen WL, Huang MT, Liu HC, Li CW & Mao SJT (2004) Distinction between dry and raw milk using monoclonal antibodies prepared against dry milk proteins. *J Dairy Sci* **87**, 2720–2729.
- 39 Laemmli UK (1970) Cleavage of structural proteins during assembly of the head of bacteriophage T4. *Nature* **227**, 680–685.
- 40 Song CY, Chen WL, Yang MC, Huang JP & Mao SJT (2005) Epitope mapping of a monoclonal antibody specific to bovine dry milk: involvement of residues 66–76 of strand D in thermal denatured  $\beta$ -lactoglobulin. *J Biol Chem* **280**, 3574–3582.





Journals A-Z

Books | Authors &amp; Reviewers | Librarians | ACS Members | About Us | e-Alerts | Help

CRYSTAL  
GROWTH  
& DESIGN

Quick Search

Advanced Search

Enter Title, Keywords, Authors, or DOI

Search


 Crystal Growth & Design
  All Journals/Website
Personalize your experience: [Log In](#) | [Register](#) | [Cart](#)

## About the Cover

## December 2008: Vol. 8, Iss. 12

Cartoon representation of the *in meso* crystallization process. Membrane protein (blue, b<sub>2</sub>AR-T4L, PDB ID: 2RH1) is embedded in the lipid bilayer of the lipidic cubic phase (LCP) (lower left corner). Addition of a precipitant induces crystal nucleation, in the vicinity of which the LCP transforms into a multilamellar phase serving as a portal connecting the bulk cubic phase to the growing crystal (upper right corner) (Adapted from Cherezov, V.; Caffrey, M. *Faraday Discuss.* 2007, 136, 195-212).

Membrane proteins are expected to diffuse following the single lipid bilayer of the LCP and approach the crystal through the lamellar phase portal. If proteins form irreversible micro-aggregates (such as shown in the middle-bottom part of the cubic phase), their diffusion through the narrow channels in the LCP will be highly restricted and no crystals will grow. The LCP-fluorescence recovery after a photobleaching (LCP-FRAP) assay is focused on measuring diffusion properties of membrane proteins embedded in the LCP at different screening conditions (*Cryst. Growth Des.* 2008, 8, 4307-4315). (Left inset) The electron density of vitamin D<sub>3</sub>

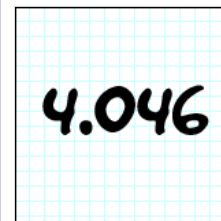
was optimized in the exosite for rational-designed crystallization by preparing a b-lactoglobulin (LG)-vitamin D<sub>3</sub> complex at various pH values (4-8) and initial ratios of vitamin D<sub>3</sub>/LG (1-3). The optimum electron density (in cyan) of vitamin D<sub>3</sub> (in red) in the exosite of the complex prepared at pH 8 with a vitamin D<sub>3</sub>/LG ratio of 3:1 was obtained (*Cryst. Growth Des.* 2008, 8, 4268-4276). [View the article.](#)

## Go to:

- » [Table of Contents for this issue](#)
- » [Cover Art Gallery for this journal](#)



## Advertisements



Info for Advertisers

## Browse By Issue

Select Volume

Select Issue

List of Issues

## Search By Citation

Vol # Page #

## Digital Object Identifier (DOI)

10.1021/

## Stay Current

Get your research ASAP.

e-Alerts | RSS Feeds

## Advertisements

Rational Design for Crystallization of  $\beta$ -Lactoglobulin and Vitamin D<sub>3</sub> Complex: Revealing a Secondary Binding Site<sup>†</sup>Ming Chi Yang,<sup>‡</sup> Hong-Hsiang Guan,<sup>§,#</sup> Jinn-Moon Yang,<sup>‡</sup> Cheng-Neng Ko,<sup>‡</sup> Ming-Yih Liu,<sup>§</sup> Yih-Hung Lin,<sup>§</sup> Yen-Chieh Huang,<sup>§</sup> Chun-Jung Chen,<sup>\*,§,||,∇</sup> and Simon J. T. Mao<sup>\*,‡,⊥</sup>

Department and College of Biological Science and Technology, National Chiao Tung University, 75 Po-Ai Street, Hsinchu 30068, Taiwan, ROC, Life Science Group, Scientific Research Division, National Synchrotron Radiation Research Center, 101 Hsin-Ann Road, Hsinchu 30076, Taiwan, ROC, Department of Physics, Institute of Bioinformatics and Structural Biology, National Tsing Hua University, 101, Section 2 Kuang Fu Road, Hsinchu 30013, Taiwan, ROC, Department of Biotechnology, Asian University, 500, Luifeng Road, Wufeng, Taichung 41354, Taiwan, ROC, and Institute of Biotechnology, National Cheng Kung University, 1 University Road, Tainan 70101, Taiwan, ROC

Received June 30, 2008; Revised Manuscript Received September 30, 2008

**ABSTRACT:**  $\beta$ -Lactoglobulin (LG) is a major milk whey protein containing primarily a calyx for vitamin D<sub>3</sub> binding, although the existence of another site beyond the calyx is controversial. Using fluorescence spectral analyses in the previous study, we showed the binding stoichiometry for vitamin D<sub>3</sub> to LG to be 2:1 and a stoichiometry of 1:1 when the calyx was “disrupted” by manipulating the pH and temperature, suggesting that a secondary vitamin D binding site existed. To help localize this secondary site using X-ray crystallography in the present study, we used bioinformatic programs (Insight II, Q-SiteFinder, and GEMDOCK) to identify the potential location of this site. We then optimized the occupancy and enhanced the electron density of vitamin D<sub>3</sub> in the complex by altering the pH and initial ratios of vitamin D<sub>3</sub>/LG in the cocrystal preparation. We conclude that GEMDOCK can aid in searching for an extra density map around potential vitamin D binding sites. Both pH (8) and initial ratio of vitamin D<sub>3</sub>/LG (3:1) are crucial to optimize the occupancy and enhance the electron density of vitamin D<sub>3</sub> in the complex for rational-designed crystallization. The strategy in practice may be useful for future identification of a ligand-binding site in a given protein.

## 1. Introduction

Bovine  $\beta$ -lactoglobulin (LG) is a major protein in milk comprising about 10–15%.<sup>1</sup> Because of its thermally unstable and molten-globule nature, LG has been studied extensively for its physical and biochemical properties.<sup>2–7</sup> Some essential functions of LG including hypocholesterolemic effect,<sup>8</sup> retinol transport,<sup>9,10</sup> and antioxidant activity<sup>11–14</sup> have been reported. According to the crystal structure, LG comprises predominantly a  $\beta$ -sheet configuration containing nine antiparallel  $\beta$ -strands from A to I (Figure 1a).<sup>15–17</sup> Topographically,  $\beta$ -strands A–D form one surface of the barrel (calyx), whereas  $\beta$ -strands E–H form the other. The only  $\alpha$ -helical structure with three turns is located at the COOH-terminus, which follows the  $\beta$ -strand H beyond the calyx.<sup>18</sup> A remarkable feature of the calyx is its ability to bind hydrophobic molecules such as retinol, fatty acids, and vitamin D<sub>3</sub> (Figure 1b).<sup>19–22</sup>

The location of vitamin D binding sites has been controversial, yet most evidence points toward the calyx. It has been postulated that another site exists,<sup>23–25</sup> but it could not be verified by the crystal structure using the vitamin D<sub>2</sub>–LG complex.<sup>10</sup> In a previous study, we first conducted a ligand binding assay using the fluorescence changes by retinol, palmitic

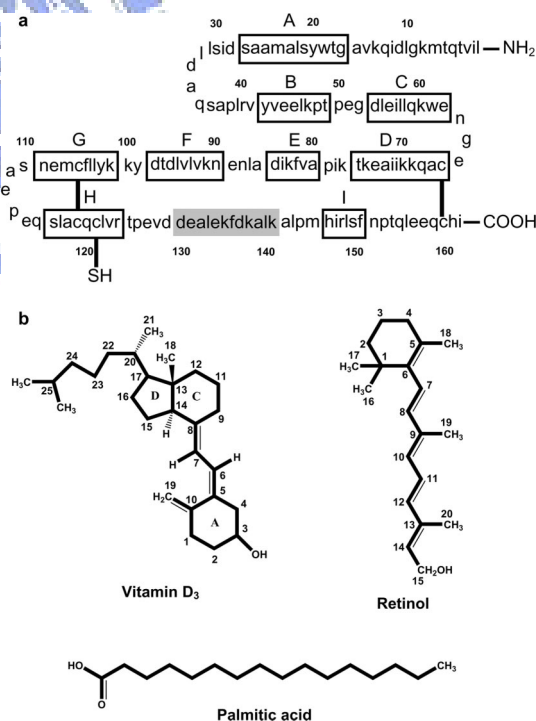


**Figure 1.** Primary structure of LG and chemical structure of its binding ligands. (a) LG comprises 162 amino acids with nine antiparallel  $\beta$ -sheet strands (A–I) and one  $\alpha$ -helix (in gray). There are two disulfide bonds located between  $\beta$ -strand D and carboxyl-terminus (Cys-66 and Cys-160) and between  $\beta$ -strands G and H (Cys-106 and Cys-119), while a free buried thiol group is at Cys-121. (b) Chemical structure of ligands which bind to LG, such as vitamin D<sub>3</sub>, retinol, and palmitic acid.

<sup>†</sup> Part of the special issue (Vol 8, issue 12) on the 12th International Conference on the Crystallization of Biological Macromolecules, Cancun, Mexico, May 6–9, 2008.

<sup>\*</sup> To whom correspondence should be addressed. (S.J.T.M.) E-mail: mao1010@ms7.hinet.net; (C.-J.C.) E-mail: cjchen@nsrrc.org.tw.

<sup>‡</sup> National Chiao Tung University.

<sup>§</sup> National Synchrotron Radiation Research Center.

<sup>#</sup> Institute of Bioinformatics and Structural Biology, National Tsing Hua University.

<sup>||</sup> Department of Physics, National Tsing Hua University.

<sup>∇</sup> National Cheng Kung University.

<sup>⊥</sup> Asian University.



**Table 1. Relative Ligand Binding Ability of LG at the Various pH and Preheated Temperatures Extracted from Our Published Paper<sup>26</sup>**

titration experiment				relative binding (%)				effect of heating (preheated for 16 min)			
[ligand]/ [native LG]	vitamin D <sub>3</sub>	retinol	palmitic acid	pH	vitamin D <sub>3</sub>	retinol	palmitic acid	temperature (°C)	vitamin D <sub>3</sub>	retinol	palmitic acid
0.125	7.1	13.2	15.1	2.0	<b>29.1</b>	2.2	2.0	50	93.4	92.1	92.6
0.25	14.1	26.0	30.0	3.0	<b>29.0</b>	0	0	60	91.1	90.2	90.4
0.375	21.2	38.8	44.9	4.0	<b>29.3</b>	0	0	70	83.0	67.0	72.3
0.5	28.1	50.6	59.0	5.0	<b>29.3</b>	0	0	80	49.2	10.2	14.4
0.625	35.3	62.0	71.5	6.0	46.7	8.5	38.0	90	41.9	7.5	6.8
0.75	42.3	72.7	80.4	7.0	58.1	27.0	49.4	100	<b>40.7</b>	6.7	5.8
0.875	49.3	81.3	86.9	8.0	100	87.7	100				
1.0	<b>56.2</b>	88.0	91.9	9.0	78.2	100	82.6				
1.25	70.6	91.8	96.0	10.0	77.7	97.6	54.3				
1.5	82.9	95.0	98.5								
1.75	92.0	96.7	99.2								
2.0	96.0	98.0	99.7								

**Table 2. Possible Sites Predicted by Insight II, Q-SiteFinder, and GEMDOCK**

programs	Insight II	Q-SiteFinder	GEMDOCK	
			vitamin D <sub>3</sub> docking for whole protein	vitamin D <sub>3</sub> docking for other parts of protein besides sites 1 and 2
ranking fitness (ratio)	1	1	-87.2 (50%)	
Site 1 (calyx)				
Site 2	2	2	-88.4 (20%)	
Site 3	3	8	-85.4 (6%)	-83.9 (40%)
Site 4		3	-82.4 (6%)	-81.2 (20%)
Site 5		5	-75.4 (3%)	-80.1 (3%)
Site 6		4	-83.4 (3%)	-87.0 (3%)

acid, and vitamin D<sub>3</sub> to address the existence of another site for vitamin D binding. This data demonstrated that the maximal binding stoichiometry of vitamin D<sub>3</sub> with LG was 2:1, whereas that of retinol or palmitic acid was 1:1 (Table 1),<sup>26</sup> suggesting that there was another binding site for the vitamin D<sub>3</sub> molecule. Second, we manipulated the binding capability by switching off the gate of calyx at low pH (2–6)<sup>15</sup> to further substantiate the “two site hypothesis”. As expected, the binding capability of retinol and palmitic acid diminished under this condition, but it retained the vitamin D binding with a vitamin D<sub>3</sub> to LG stoichiometry of 1:1 (Table 1).<sup>26</sup> We also used a strategy to denature the conformation of the calyx by heat treatment<sup>7</sup> and conducted the binding assay after the calyx was thermally “disrupted”. Under this condition, the binding stoichiometry of vitamin D<sub>3</sub> to heated LG (100 °C for 16 min) was found to be 1:1 (Table 1).<sup>26</sup> These previous binding experiments<sup>26</sup> suggest that there is a secondary site for vitamin D<sub>3</sub> binding distinct from the calyx.

In the present study, we located the secondary vitamin D<sub>3</sub> binding site of LG, which has been a controversy among many researchers, using bioinformatic analysis to narrow the region of potential binding sites for crystallographic verification. We first utilized well-known programs (ActiveSite\_Search Insight II and Q-SiteFinder) to predict the ligand-binding site in search of a possible location for vitamin D binding with the geometric or energetic criteria. The Insight II<sup>27</sup> is based on the size of surface cavities of a given protein without a specified ligand; it searches the location and extent of the pocket according to the geometric criteria. The Q-SiteFinder,<sup>28</sup> however, defines a binding pocket only by energy calculations using a methyl probe for van der Waals interactions with a given protein. We next used a more accurate docking program, GEMDOCK, which was developed in our laboratories,<sup>29</sup> to dock a specific ligand with a given protein based on a nonbiased search for their interac-

tions. GEMDOCK is specifically designed for a flexible ligand that may best fit into possible binding sites. Under this condition the docked ligand conformations are generated. All three programs require an established 3D structure of a given protein. We show that Insight II and Q-SiteFinder predicted three and six major potential regions, respectively, available for any nondefined ligand binding on LG. Docking using GEMDOCK predicted six possible sites for vitamin D<sub>3</sub> binding. Following the analyses of Insight II, Q-SiteFinder, and GEMDOCK cross-docking, we identified that there were two potential secondary sites for vitamin D binding located near the C-terminal  $\alpha$ -helical region. This led us to study the crystal structure of LG–vitamin D<sub>3</sub> complex to further identify the secondary vitamin D binding site, if any.

Furthermore, we cocrystallized the LG–vitamin D<sub>3</sub> complex which was prepared at pH 7 with a vitamin D<sub>3</sub>/LG ratio of 2 according to the previous crystallographic study.<sup>20</sup> A search for an extra electron density for vitamin D<sub>3</sub> around potential secondary binding sites was based on the predicted data obtained from bioinformatic analysis. We found a weak extra electron density that was located near the C-terminal  $\alpha$ -helical region. With respect to cocrystallization, the maximum occupancy of the ligand should provide a better opportunity in growing high-quality crystals of the ligand–protein complex. In general, the affinity, solubility, and concentrations of added hydrophobic ligands would influence the ligand occupancy at equilibrium. For 90% occupancy, the amount of added ligands must be greater than the amount of protein so that the free ligands at equilibrium are not depleted.<sup>30</sup> In this work, we reported a rationally designed approach for preparing the complex of LG and vitamin D<sub>3</sub> at various pH and vitamin D<sub>3</sub>/LG ratios to optimize the occupancy of vitamin D<sub>3</sub> and improve the electron density of the secondary binding site. Finally, we identified an exosite for vitamin D binding to be located near the  $\alpha$ -helix and  $\beta$ -strand I of LG using a crystal prepared at pH 8 with a vitamin D<sub>3</sub>/LG ratio of 3:1. The biological significance of the revealed exosite for vitamin D binding in milk LG was also discussed.

## 2. Experimental Section

**2.1. Materials.** LG was purified from fresh raw milk using 40% saturated ammonium-sulfate, followed by a G-150 column chromatography of the supernatant as described previously.<sup>4</sup> Vitamin D<sub>3</sub> (cholecalciferol) was purchased from Sigma (St. Louis, MO).

**2.2. Predicting Possible Binding Site by ActiveSite\_Search Insight II and Q-SiteFinder.** To identify the possible binding sites, the ActiveSite\_Search Insight II<sup>27</sup> and Q-SiteFinder<sup>28</sup> software were

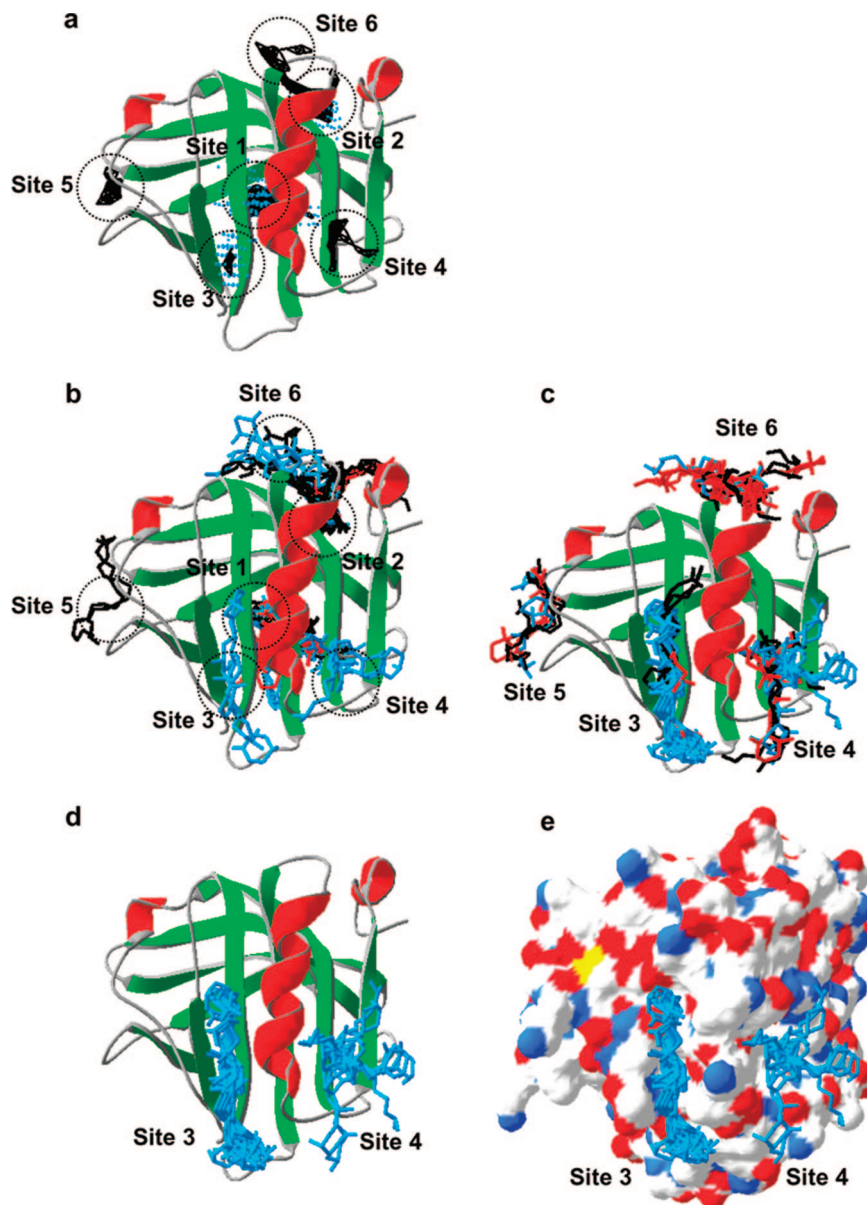


**Figure 2.** Prediction of potential binding pockets of LG using Insight II, Q-SiteFinder, and GEMDOCK. (a) Binding pockets of LG predicted by Insight II (color in blue) and Q-SiteFinder (in black). There are three and six major binding sites predicted by Insight II or Q-SiteFinder, respectively, for any nondefined ligand. (b) There are total six potential binding sites for retinol, palmitic acid, and vitamin D<sub>3</sub> (red, black, and blue) in LG following the GEMDOCK docking. LG structure in 3D used was based on LG-retinol complex (PDB code: 1GX8). Retinol and palmitic acid are able to dock exactly into the calyx (site 1), but not to the other sites except for palmitic acid interacting with site 2. The probability of vitamin D<sub>3</sub> fitting into the calyx is about 50% (see Table 1). It indicates that the calyx is a superior binding site for vitamin D. (c) Cross-docking of retinol, palmitic acid, and vitamin D<sub>3</sub> into the cavity of LG with sites 1 and 2 blocked. The docked orientation of the vitamin D<sub>3</sub> in sites 3 and 4 are distinctly different from retinol and palmitic acid. (d) Comparison of the docked orientation of vitamin D<sub>3</sub> between sites 3 and 4. The docked conformation of vitamin D<sub>3</sub> binding in site 3 seems to be more stable than in site 4. (e) The electrostatic surface model of LG depicting the positively charged (in blue), negatively charged (in red), and hydrophobic (white) side chains, in which the hydrophobic surface of site 4 seems to be large relative to that of site 3.

**Table 3. Percentage Probability of Different Ligands Docking into Possible Sites of LG**

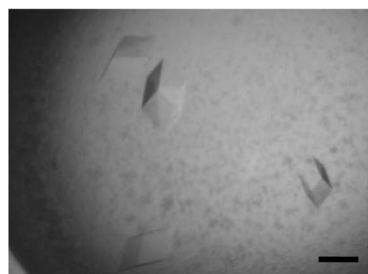
conditions	docking ligands into 1GX8					
	docking search on whole protein			docking search on other parts of protein		
fitness (ratio)	retinol	palmitic acid	vitamin D <sub>3</sub>	retinol	palmitic acid	vitamin D <sub>3</sub>
Site 1 (calyx)	-86.3 (93%)	-75.7 (43%)	-87.2 (50%)			
Site 2	-86.4 (6%)	-77.6 (46%)	-88.4 (20%)			
Site 3			-85.4 (6%)	-76.2 (3%)	-69.7 (10%)	-83.9 (40%)
Site 4			-82.4 (6%)	-73.3 (10%)	-69.4 (16%)	-81.2 (20%)
Site 5		-76.1 (6%)	-75.4 (3%)	-72.9 (6%)	-67.7 (10%)	-80.1 (3%)
Site 6			-83.4 (3%)	-77.2 (43%)	-72.5 (13%)	-87.0 (3%)

used, and the prediction was performed according to the standard protocol. For ActiveSite\_Search Insight II, we used the size within 50

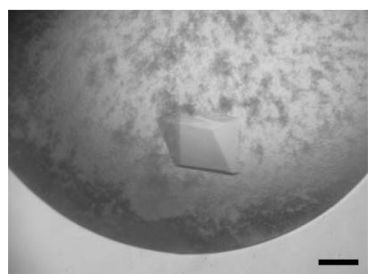
Å as a cutoff site for the smallest cavity (in grid points). For Q-SiteFinder, the parameters for identified protein residues involved



pH 8.0, D<sub>3</sub>/LG ratio 1  
Resolution 2.1 Å  
 $R_{\text{sym}}$ : 4%



pH 8.0, D<sub>3</sub>/LG ratio 2  
Resolution 2.2 Å  
 $R_{\text{sym}}$ : 5%



pH 8.0, D<sub>3</sub>/LG ratio 3  
Resolution 2.1 Å  
 $R_{\text{sym}}$ : 5.5%

**Figure 3.** Typical example of LG–vitamin D<sub>3</sub> crystals prepared with various vitamin D<sub>3</sub>/LG ratios at pH 8. Crystals of LG–vitamin D<sub>3</sub> complexes were grown using a hanging-drop vapor-diffusion method. Complex crystals of rhombohedral shape prepared at vitamin D<sub>3</sub>/LG ratios of 1, 2, or 3 appeared at day 11, 10, or 6 with 2.1, 2.2, or 2.1 Å resolution diffraction were observed, respectively. The crystals grew slowly to a dimension of 0.2–0.4 mm in 18 days. Each bar represents 0.2 mm.

in the van der Waals interactions with the methyl probe, 5.0 Å was used. The coordinates of possible sites predicted by Insight II and Q-SiteFinder were saved in PDB format and depicted using the Swiss-Pdb Viewer program.<sup>31</sup>

**2.3. Docking Analysis between Ligands and LG by GEMDOCK.** We extrapolated the 3D structure of retinol (PDB ID 1GX8, LG-retinol complex), palmitic acid (1GXA, LG-palmitic acid complex), and vitamin D<sub>3</sub> (modified from 25(OH)-vitamin D<sub>3</sub>; 1MZ9, cartilage oligomeric matrix protein–vitamin D<sub>3</sub>) from the Protein Data Bank (PDB). Energy minimization of these three compounds was performed using a SYBYL program package. An established 3D structure of LG (1GX8) was used as the target for cross-docking. Since GEMDOCK is able to search the whole protein for exploring the binding site of a given ligand, we presumed those atoms near the charged surface and hydrophobic areas of LG were the potential binding sites for vitamin D<sub>3</sub>. The predicted area(s) was then compared with the established binding pocket (calyx) for palmitic acid and retinol. Following the removal of all structured water molecules in LG molecule, GEMDOCK search was then conducted according to the procedures previously described.<sup>29</sup> Using an empirical energy function

which consists of the electrostatic, steric, and hydrogen bonding potentials for docking, GEMDOCK<sup>29</sup> seemed to be more accurate than some conventional approaches, such as GOLD and FlexX, based on a diverse data set of 100 protein–ligand complexes proposed by Jones et al.<sup>32</sup> The accuracy of GEMDOCK was demonstrated when screening the ligand database for antagonist and agonist ligands of the estrogen receptor (ER).<sup>33</sup>

In this work, we used an empirical scoring function to estimate interaction energies between LG and ligands. The parameters used in the flexible docking included the initial step size ( $\sigma = 0.8$  and  $\psi = 0.2$ ), family competition length ( $L = 2$ ), population size ( $N = 1000$ ), and recombination probability ( $p_c = 0.3$ ). For each docked ligand, optimization was stopped when either the convergence was below a certain threshold value or the iterations exceeded the maximal preset value of 80. Therefore, GEMDOCK produced 3600 solutions in one generation and terminated when it exhausted to 324 000 solutions for each docked ligand.

**2.4. Crystallization.** Purified LG was concentrated to 20 mg/mL in 20 mM acetate (pH 4), cacodylate (pH 6), HEPES (pH 7), or Tris buffer (pH 8). Vitamin D<sub>3</sub> stock solution prepared as 50 mM in 100% ethanol was added to LG solution to give a molar ratio of 3:1, 2:1, or 1:1 with a final ethanol concentration less than 7% and incubation for three hours at 37 °C. Crystallization of the LG–vitamin D<sub>3</sub> complex was achieved using the hanging-drop vapor-diffusion method at 18 °C with 2  $\mu$ L hanging drops containing equal amounts of LG–vitamin D<sub>3</sub> complex and a reservoir solution (0.1 M HEPES containing 1.4 M trisodium citrate dehydrate, pH 7.5).

**2.5. Crystallographic Data Collection and Processing.** The crystals were mounted on a Cryoloop (0.1–0.2 mm), dipped briefly in 20% glycerol as a cryoprotectant solution, and frozen in liquid nitrogen. X-ray diffraction data at 2.1–2.2 Å resolution were collected at 110 K using synchrotron radiation on the Taiwan contracted beamlines BL12B2 at SPring-8 (Harima, Japan) and BL13B at NSRRC (Hsinchu, Taiwan). The data were indexed and processed using a *HKL2000* program.<sup>34</sup>

### 3. Results and Discussion

Although a secondary vitamin D binding site of LG has been proposed from some physicochemical experiments,<sup>23–25,35,36</sup> its existence and location have remained elusive and controversial. Several studies have clearly demonstrated that the binding stoichiometry between retinol or palmitic acid and LG is 1 where the central calyx of LG is responsible for retinol and palmitic acid binding,<sup>21–23</sup> but whether the binding of vitamin D to LG is 1 or 2 remains uncertain. Wang et al. proposed that LG possesses two potential binding sites for vitamin D: one is in the calyx formed by a  $\beta$ -barrel and the other is near an external hydrophobic pocket between the  $\alpha$ -helix and the  $\beta$ -barrel.<sup>24,25</sup> In the previous study, we first showed that the relative binding of vitamin D to LG was 56% of the maximal binding at a vitamin D<sub>3</sub>/LG ratio of 1:1 and the binding stoichiometry of vitamin D<sub>3</sub> to LG was 2:1 relative to that 1:1 of retinol or palmitic acid verified using extrinsic fluorescence emission, fluorescence enhancement and quenching methods (Table 1).<sup>26</sup> Our previous data tended to support the view that LG comprises two vitamin D binding sites. Second, we monitored the vitamin D<sub>3</sub> binding of LG by utilizing a unique structural change property of LG at various pH to further substantiate the “two site hypothesis”. The EF loop of LG is known to act as a gate over the calyx;<sup>15</sup> at pH values lower than 6 the loop is in a “closed” position. Of remarkable interest, LG still retained about 30% of the maximal binding for vitamin D<sub>3</sub> at pH below the transition (2–6) (Table 1).<sup>26</sup> It suggested that there might be another vitamin D binding site that is independent of pH. Our previous study has shown that thermally denatured LG (heated 100 °C for 5 min) is unable to bind to retinol and palmitic acid owing to the deterioration of the calyx.<sup>7</sup> We tested the hypothesis whether the “secondary binding site” for vitamin D (if any) still existed after heating. Since LG is a molten globule with a



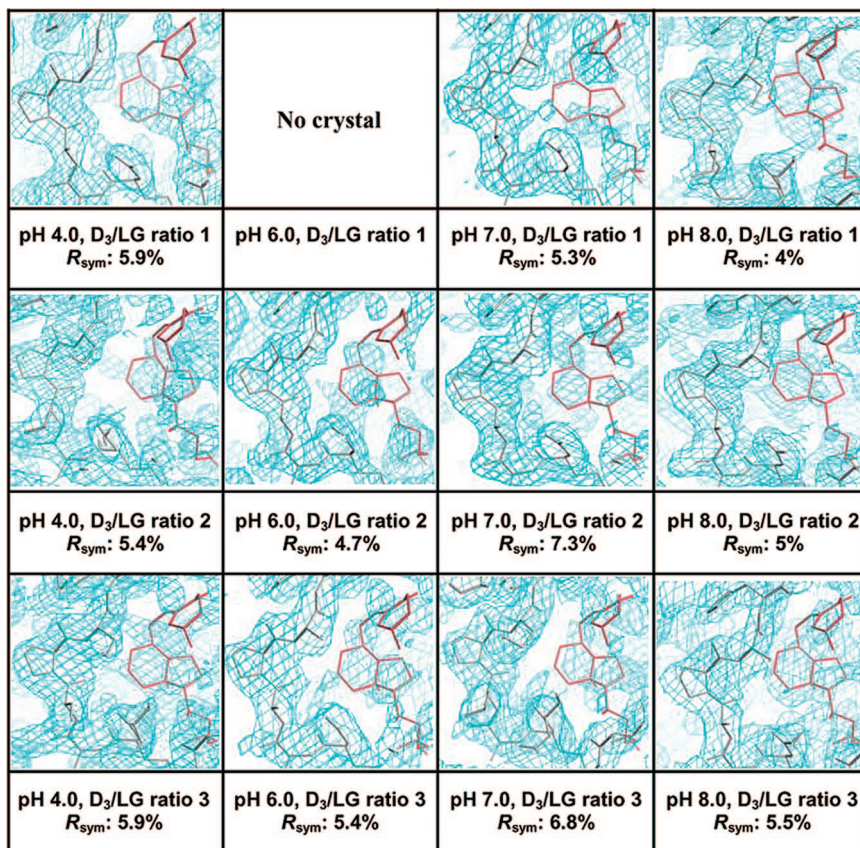


**Figure 4.** Initial electron densities map around the exosite of LG–vitamin D<sub>3</sub> complex prepared at indicated conditions. The  $|2F_{\text{obs}} - F_{\text{calc}}|$  electron density maps generated by the initial LG model with omitted vitamin D<sub>3</sub> show that the electron density (in cyan) of vitamin D<sub>3</sub> molecule (in red) in the exosite is more visible when the complex was prepared at pH 8 with a vitamin D<sub>3</sub>/LG ratio of 3:1. The images were generated using the program O.<sup>46</sup>

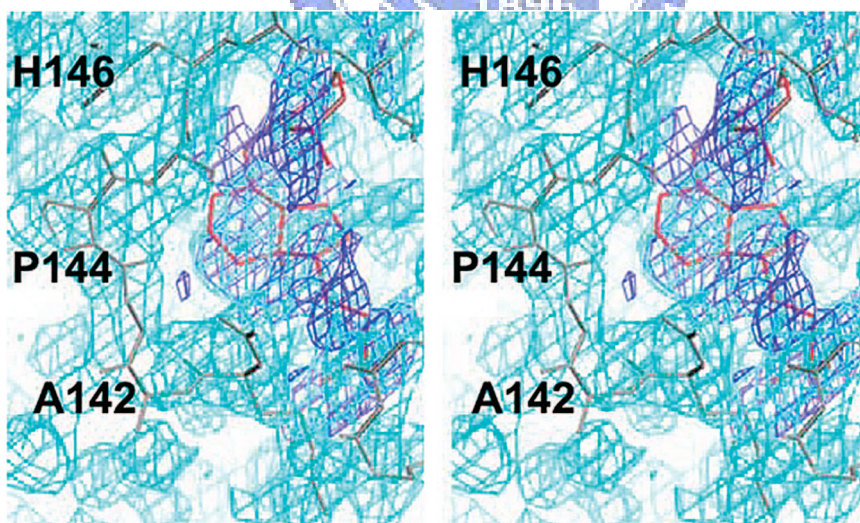


**Figure 5.** The electron density maps around the exosite of LG–vitamin D<sub>3</sub> complex prepared at pH 8 with an initial vitamin D<sub>3</sub>/LG ratio of 3:1 in stereoview. The  $|F_{\text{obs}} - F_{\text{calc}}|$  (in blue) and  $|2F_{\text{obs}} - F_{\text{calc}}|$  (in cyan) electron density maps generated by the initial LG model with vitamin D<sub>3</sub> omitted show that the electron density of the vitamin D<sub>3</sub> molecule (in red) in the exosite is clearly visible.

heating transition between 70 and 80 °C,<sup>5,7</sup> we monitored the vitamin D<sub>3</sub> binding with LG preheated at different temperatures including one that could denature the calyx structure. Interestingly, it showed a dramatic and sharp decrease in retinol, palmitic acid, and vitamin D<sub>3</sub> binding near the LG transition temperature. At the temperature above 80 °C, it almost completely abolished the retinol and palmitic acid binding, while still retaining 40% of the vitamin D<sub>3</sub> binding even at 100 °C

heating for 16 min (Table 1).<sup>26</sup> To confirm it further, we monitored the binding of heated LG (100 °C for 16 min) with various amounts of vitamin D<sub>3</sub>, and a stoichiometry of 1:1 was observed between heat-denatured LG and vitamin D<sub>3</sub> using the same fluorescence quenching analysis.<sup>26</sup> Taking the previous pH and thermal experiments together (Table 1), we concluded that a thermally stable site (defined as an exosite) beyond the calyx exists for vitamin D<sub>3</sub> binding. In the present study, we

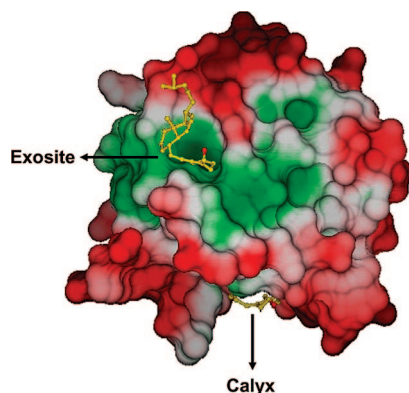


**Figure 6.** Binding characteristics of vitamin D<sub>3</sub> in the exosite of LG. The surface model of vitamin D<sub>3</sub> interacting LG with the hydrophobic (green) or hydrophilic region (red) of LG is displayed. The data reveal that the exosite of LG provides the hydrophobic force to bind vitamin D<sub>3</sub> stably. Notably, the 3-OH group (red) of vitamin D<sub>3</sub> sticks out from the pocket.

located the secondary vitamin D<sub>3</sub> binding site of LG using bioinformatic analysis to narrow the region of potential binding sites, the search of extra electron density around the potential binding sites of the cocrystal prepared on previous crystallographic study,<sup>20</sup> and a rationally designed crystallographic approach for obtaining cocrystals with sufficient quality and ligand occupancy.

**3.1. Structural Analysis of the Binding Pockets of LG Using Insight II and Q-SiteFinder.** We attempted to identify the regions of LG that might be available for the interaction with any nondefined molecules using well-known programs (Insight II<sup>27</sup> and Q-SiteFinder<sup>28</sup>), which are based on the size of the binding pocket and the binding energy between the methyl group and the pocket of a given protein, respectively, for prediction of a ligand binding site. The former and latter predicted that there were 3 and 10 possible “binding sites” for any ligand, respectively. Table 2 and Figure 2a show the ranking and the location of six major predicted sites. Essentially both programs predicted that site **1** is exactly located at the calyx with the ranking superior to any others. This site is also known for all the vitamin D, retinol, and palmitic acid binding. Location of other predicted sites **2** (among C-terminal loop,  $\beta$ -strands C and D), **3** (among the pocket C-terminal  $\alpha$ -helix,  $\beta$ -strands F, G, H, and A), **4** (at the side  $\alpha$ -helix and  $\beta$ -strands I), **5** (near loop H), and **6** (between CD and DE loops) is depicted in Figure 2a.

**3.2. Docking Analysis of the Interaction between LG and Retinol or Palmitic acid Using GEMDOCK.** Because both Insight II and Q-SiteFinder are not able to perform the specific interaction between an assigned ligand and a given binding site, we next used a more accurate docking program, GEMDOCK,<sup>29</sup> for molecular docking to search for a possible number of vitamin D binding sites and to further assess the interaction of a specific ligand with each site. GEMDOCK appeared to be more accurate than comparative approaches, such as GOLD and FlexX, on a diverse data set of 100 protein–ligand complexes<sup>32</sup> for docking and two cross-docking experimental sets.<sup>29</sup> The screening accuracies of GEMDOCK were also better than GOLD, FlexX, and DOCK on screening the ligand database for antagonist and agonist ligands of estrogen receptor (ER).<sup>33</sup> GEMDOCK is a better docking tool for assessing the interaction of a specific ligand with each site of LG. We generated 30 docked conformations of each retinol or palmitic acid with whole LG. Based on the docking protocol,<sup>29</sup> we considered that

a correct binding-mode was reproducible when the root-mean-square deviation (rmsd) between the best energy-scored conformation and crystal coordinates was less than 2 Å.<sup>32</sup> In order to meet this criterion, we then evaluated the feasibility of GEMDOCK by cross-docking retinol and palmitic acid into the calyx or site 1 of LG (PDB code: 1GX8), known to be an established site for the binding of retinol or palmitic acid. Our data reveal that these two ligands could be docked exactly into the calyx with a rmsd less than 2.0 Å. The average fitness of docked energy of retinol and palmitic acid was  $-86.3$  and  $-75.7$  kcal/mol (Table 3), respectively. Following the analyses of all the docking data, we found that none of the other sites 2–6 were fitted by either retinol or palmitic acid ( $<10\%$  probability), except for palmitic acid interacting with site 2 (46% of total 30-docked conformations) (Table 3). For example, none of the docked conformations of retinol and palmitic acid could fit into sites 3, 4, 5, and 6. This result is almost consistent with the current knowledge that the calyx (site 1) is the major pocket for interacting with these two ligands. It is thus feasible to use a similar strategy for studying the interaction between vitamin D<sub>3</sub> and LG.

**3.3. Docking Analysis of the Interaction between LG and Vitamin D<sub>3</sub> Using GEMDOCK.** Each docked conformation of vitamin D<sub>3</sub> ( $n = 30$ ) obtained from GEMDOCK was then evaluated for a possible vitamin D binding ability. Table 2 shows that vitamin D<sub>3</sub> could fit into the calyx with about 50% of the probability. Interestingly, the docked energy of vitamin D<sub>3</sub> into the calyx site 1 was similar to that of retinol. The result suggests that GEMDOCK is suitable in conducting interactions between vitamin D<sub>3</sub> and LG. It also pointed out site 2 (Figure 2b) as a possible second binding site for palmitic acid (46%) and vitamin D<sub>3</sub> (20%). However, since the binding stoichiometry between palmitic acid and LG is 1 (Table 1) and the calyx is the only available binding site for palmitic acid,<sup>21</sup> we ruled out site 2 as a particular site for palmitic acid binding. This site is located among the C-terminal loop,  $\beta$ -strand C, and  $\beta$ -strand D. Since  $\beta$ -strand D is thermally unstable,<sup>7</sup> it is not consistent to the proposed secondary vitamin D binding site that is supposed to be thermally stable in nature (Table 1). Site 2 is thus unlikely for vitamin D interaction.

In order to search for a potential secondary vitamin D<sub>3</sub> binding site location, we blocked sites 1 and 2 with the reason mentioned above and then performed GEMDOCK, while using retinol and palmitic acid as a “negative control”. Table 3 shows that, under this condition, sites 3 and 4 possessed high probability for vitamin D<sub>3</sub> interaction (40 and 20%) relative to retinol and palmitic acid. The other domains (sites 5 and 6) were considered nonsignificant due to the low probability ( $<3\%$ ). Notably, the docked orientation of the vitamin D<sub>3</sub> in sites 3 and 4 was distinctly different from that of other ligands (Figure 2c). Figure 2d tempted to suggest that the docked orientation of vitamin D<sub>3</sub> in site 3 is more stable (with a low rmsd) than that in site 4 due to its large pocket size that could stabilize ligand docking. On the other hand, the hydrophobicity of site 4 is high relative to site 3 based on the electrostatic potential surface model between LG and docked vitamin D<sub>3</sub> conformation (Figure 2e). The prediction of site 4 being involved in vitamin D<sub>3</sub> interaction is consistent with ranking predicted by Q-SiteFinder which is based on van der Waals interaction (Table 2). Taken together, sites 3 and 4 are the potential candidates for the secondary vitamin D binding site and thus led us to localize it via a high-quality LG–vitamin D<sub>3</sub> crystal. We searched for an extra density around C-terminal  $\alpha$ -helix (sites 3 and 4) of LG–vitamin D<sub>3</sub> complex which was prepared at pH 7 with a vitamin D<sub>3</sub>/LG



ratio of 2 according to the previous crystallographic study.<sup>20</sup> We found a weak extra electron density located near the C-terminal  $\alpha$ -helical region. Later, we used a rationally designed crystallography experiment for improving electron density of vitamin D<sub>3</sub> of the secondary binding site. In the bioinformatic prediction of the secondary vitamin D<sub>3</sub> binding site, we excluded false-positive site 2 on the previous biochemical findings. It was confirmed that there is no extra density around site 2 in the crystal structure of LG–vitamin D complex that was prepared using the previous condition. For this reason, bioinformatic prediction excluded site 2 as a potential candidate for the secondary vitamin D binding site based on the previous biochemical findings that is proper for this study.

**3.4. Crystallization and Diffraction of LG–vitamin D<sub>3</sub> Complex Prepared at Various pH and Vitamin D<sub>3</sub>/LG Ratios.** In any event, starting the cocrystallization experiment with maximum ligand occupancy should provide a better opportunity in growing high-quality ligand–protein crystals. The affinity and concentrations of added ligands, as well as ligand solubility, would influence the occupancy of ligands at equilibrium. For 90% occupancy, the amount of added ligands must be greater than the amount of protein so that free ligands at equilibrium is not depleted to less than about  $10 \times K_d$ .<sup>30</sup> In practice, ratios of ligands to a given protein up to 10:1 or more are commonly used, but large excesses should be avoided owing to the possibility of ligand binding to nonspecific sites. In the case of a weak binding affinity, the concentrations of ligands (or ligand solubility) may have to be 10 mM or higher in order to observe crystallographic occupancy.<sup>37,38</sup> We suspect that the lower occupancy of vitamin D<sub>2</sub> might explain an early study in which no electron density was found beyond the calyx using the crystal structure of LG–vitamin D<sub>2</sub> complex.<sup>10</sup> To optimize the binding and occupancy of vitamin D<sub>3</sub> to LG, we prepared this complex at various pH values ranging from 4 to 8 with a vitamin D<sub>3</sub>/LG ratio ranging from 1 to 3. Cocrystallization was conducted using the hanging-drop vapor-diffusion method in the same reservoir solution. Although the complexes were prepared at various pH, all were crystallized in the same bottom reservoir at pH 7.5. It is difficult to assess the true effect of pH on maximizing ligand occupancy, but one can prepare a LG–vitamin D<sub>3</sub> complex with the maximal ligand binding for cocrystallization, and avoid precipitation of water-insoluble vitamin D<sub>3</sub> during preparation of the LG–vitamin D<sub>3</sub> complex. The LG–vitamin D<sub>3</sub> complex crystals of rhombohedral shape appeared in 6–11 days and continued to grow slowly to a dimension of 0.2–0.4 mm in 18 days (Figure 3). In general, crystal could form except for the condition when prepared at pH 6 with a vitamin D<sub>3</sub>/LG ratio of 1. Crystals grew in larger quantity when the complex was prepared at pH 8 with a vitamin D<sub>3</sub>/LG ratio of 3 (data not shown). Although some precipitation was observed while the ratio of vitamin D<sub>3</sub>/LG increased, this was probably due to an excess of water-insoluble vitamin D<sub>3</sub>. Analysis of the diffraction pattern indicated that the crystals exhibited trigonal symmetry and systematic absences suggested that the space group was  $P3_221$ , with unit-cell parameters  $a = b = 53.78 \text{ \AA}$  and  $c = 111.57 \text{ \AA}$ .

**3.5. Initial Electron Density for Secondary Vitamin D<sub>3</sub> Binding Site.** The structures of the LG–vitamin D<sub>3</sub> complexes prepared in various conditions were determined by molecular replacement<sup>39</sup> as implemented in *CNS v1.1*<sup>40</sup> using the crystal structure of bovine LG (PDB code 2BLG)<sup>15</sup> as a search model. The LG molecule was located in the asymmetric unit after the rotation and translation function searches. The initial electron density maps of complexes prepared at various

conditions were generated from the molecular-replacement phase. One elongated extra electron density in the calyx was clearly visible. We then searched the extra electron density around the  $\alpha$ -helix, which was predicted by bioinformatic programs, to explore the existence and location of the exosite. We found one extra electron density located near the  $\alpha$ -helix and  $\beta$ -strand I as “site 4” which was predicted by bioinformatic programs (Figure 4). Interestingly, the electron densities around the exosite of LG–vitamin D<sub>3</sub> crystals prepared at pH 8 were the best defined (Figure 4). Figure 4 reveals the greater the vitamin D<sub>3</sub>/LG ratio prepared for crystallization at pH 8 the more visible electron densities were around the exosite. The result indicates that the occupancy of vitamin D<sub>3</sub> in complexes is an essential requirement for exploring the location of a secondary vitamin D binding site. Stereo-views of the  $|F_{\text{obs}} - F_{\text{calc}}|$  and  $2|F_{\text{obs}} - F_{\text{calc}}|$  electron density maps of LG–vitamin D<sub>3</sub> complex prepared at pH 8 with a vitamin D<sub>3</sub>/LG ratio 3:1 were generated by the initial model with omitted vitamin D<sub>3</sub> (Figure 5). The electron densities around vitamin D<sub>3</sub> in the exosite were all more visible in the  $|F_{\text{obs}} - F_{\text{calc}}|$  and  $2|F_{\text{obs}} - F_{\text{calc}}|$  electron density maps (Figure 5). This result supported the notion that the secondary vitamin D binding site exists and is located between  $\alpha$ -helix and  $\beta$ -strand I. The final refined structure determined using the LG–vitamin D<sub>3</sub> complex prepared at pH 8 with a vitamin D<sub>3</sub>/LG ratio of 3:1 was given in detail and discussed elsewhere.<sup>26</sup> The surface model of the LG–vitamin D<sub>3</sub> complex reveals that vitamin D<sub>3</sub> almost perpendicularly inserts into the calyx cavity, while the other vitamin D<sub>3</sub> is located near the carboxyl terminus of LG (residues 136–149 including part of the  $\alpha$ -helix and  $\beta$ -strand I) (Figure 6). It shows the exosite containing most hydrophobic residues fitted parallel with one vitamin D<sub>3</sub> molecule (Figure 6).

In the present study, with bioinformatic analysis we were able to suggest two sites (sites 3 and 4) around the C-terminal  $\alpha$ -helix as potential binding sites on LG. Subsequently, we searched for an extra density around the C-terminal  $\alpha$ -helix (sites 3 and 4) in the electron density map of the cocrystal prepared in a previous crystallographic study.<sup>20</sup> A weak electron density around site 4 (located between  $\alpha$ -helix and  $\beta$ -strand I) of LG–vitamin D<sub>3</sub> complex was found. The rationally designed crystallographic approach resulted in obtaining cocrystals with sufficient quality and ligand occupancy so as to allow experimental validation of the second vitamin D<sub>3</sub> binding site on LG. We believe that our strategy is useful for others in the search for a ligand-binding site on a given protein.

**3.6. Biological Significance.** Recent studies indicate that increased plasma vitamin D<sub>3</sub> concentrations are associated with decreased incidence of cancer<sup>41</sup> and osteoporotic fractures.<sup>42</sup> Vitamin D is found in only a few foods, such as fish oil, liver, milk, and eggs. As the level of vitamin D in bovine milk has been reported to be low, dairy products are fortified with vitamin D<sub>3</sub> to a level of about  $0.35 \mu\text{M}$  in many sophisticated food industries.<sup>43</sup> Therefore, the vitamin D-fortified milk is a major source for vitamin D in the diet. Because intact LG is acid resistant with a superpermeability to cross the epithelium cells of the gastrointestinal tract via a receptor mediated process,<sup>44</sup> this unique property of LG is worthy of consideration for transport of vitamin D in milk. There are two advantages for the presence of an exosite for vitamin D<sub>3</sub> binding. First, the central calyx of LG is primarily occupied by the fatty acids in milk.<sup>45</sup> Second, many dairy products are currently processed under excessive heat treatment for the purpose of sterilization. The presence of a

thermally stable exosite may provide another route for transporting vitamin D.

#### 4. Conclusion

We concluded that there is a heat-resistant exosite beyond the calyx responsible for vitamin D<sub>3</sub> binding in a previous binding study. GEMDOCK is a helpful tool to localize and search for an extra density map around a possible secondary vitamin D binding site. Both pH and the initial ratio of vitamin D<sub>3</sub>/LG are crucial to optimize the occupancy and enhance the electron density of vitamin D<sub>3</sub> in the complex for rational-designed crystallization. This strategy may be useful for future identification of a ligand-binding site in a given protein.

**Acknowledgment.** We are grateful to Dr. Yuch-Cheng Jean and the supporting staff for technical assistance and the discussion of the synchrotron radiation X-ray data collected at BL13B1 of NSRRC, Taiwan, and Dr. Jeyaraman Jeyakanthan at BL12B2 of SPring-8, Japan. We also thank Mr. James Lee for the critical editing. This work was supported in part by the National Science Council NSC 92-2313-B-009-002, 93-2313-B009-002, 94-2313-B-009-001 & 95-2313-B-009-001 to S. J. T. Mao and NSC 94-2321-B-213-001, 95-2321-B-213-001-M and the National Synchrotron Radiation Research Center 944RSB02 & 954RSB02 to C.-J. Chen, Taiwan, ROC.

#### References

- (1) Hambling, S. G.; MacAlpine, A. S.; Sawyer, L. In *Advanced Dairy Chemistry*; Fox, P. F. Eds.; Elsevier: Amsterdam, 1992; pp 141–190.
- (2) Qi, X. L.; Brownlow, S.; Holt, C.; Sellers, P. Thermal denaturation of beta-lactoglobulin: effect of protein concentration at pH 6.75 and 8.05. *Biochim. Biophys. Acta* **1995**, *1248*, 43–49.
- (3) Sawyer, L.; Kontopidis, G. The core lipocalin, bovine beta-lactoglobulin. *Biochim. Biophys. Acta* **2000**, *1482*, 136–148.
- (4) Chen, W. L.; Huang, M. T.; Liu, H. C.; Li, C. W.; Mao, S. J. T. Distinction between dry and raw milk using monoclonal antibodies prepared against dry milk proteins. *J. Dairy Sci.* **2004**, *87*, 2720–2729.
- (5) Chen, W. L.; Huang, M. T.; Liau, C. Y.; Ho, J. C.; Hong, K. C.; Mao, S. J. T.  $\beta$ -Lactoglobulin is a thermal marker in processed milk as studied by electrophoresis and circular dichroic spectra. *J. Dairy Sci.* **2005**, *88*, 1618–1630.
- (6) Chen, W. L.; Liu, W. T.; Yang, M. C.; Hwang, M. T.; Tsao, J. H.; Mao, S. J. T. A novel conformation-dependent monoclonal antibody specific to the native structure of beta-lactoglobulin and its application. *J. Dairy Sci.* **2006**, *89*, 912–921.
- (7) Song, C. Y.; Chen, W. L.; Yang, M. C.; Huang, J. P.; Mao, S. J. T. Epitope mapping of a monoclonal antibody specific to bovine dry milk: involvement of residues 66–76 of strand D in thermal denatured beta-lactoglobulin. *J. Biol. Chem.* **2005**, *280*, 3574–3582.
- (8) Nagaoka, S.; Futamura, Y.; Miwa, K.; Awano, T.; Yamauchi, K.; Kanamaru, Y.; Tadashi, K.; Kuwata, T. Identification of novel hypocholesterolemic peptides derived from bovine milk beta-lactoglobulin. *Biochem. Biophys. Res. Commun.* **2001**, *281*, 11–17.
- (9) Zsila, F.; Bikadi, Z.; Simonyi, M. Retinoic acid binding properties of the lipocalin member beta-lactoglobulin studied by circular dichroism, electronic absorption spectroscopy and molecular modeling methods. *Biochem. Pharmacol.* **2002**, *64*, 1651–1660.
- (10) Kontopidis, G.; Holt, C.; Sawyer, L. Invited review: beta-lactoglobulin: binding properties, structure, and function. *J. Dairy Sci.* **2004**, *87*, 785–796.
- (11) Salvi, A.; Carrupt, P.; Tillement, J.; Testa, B. Structural damage to proteins caused by free radicals: assessment, protection by antioxidants, and influence of protein binding. *Biochem. Pharmacol.* **2001**, *61*, 1237–1242.
- (12) Chevalier, F.; Chobert, J. M.; Genot, C.; Haertle, T. Scavenging of free radicals, antimicrobial, and cytotoxic activities of the Maillard reaction products of beta-lactoglobulin glycosylated with several sugars. *J. Agric. Food Chem.* **2001**, *49*, 5031–5038.
- (13) Marshall, K. Therapeutic applications of whey protein. *Altern. Med. Rev.* **2004**, *9*, 136–156.
- (14) Liu, H. C.; Chen, W. L.; Mao, S. J. T. Antioxidant nature of bovine milk beta-lactoglobulin. *J. Dairy Sci.* **2007**, *90*, 547–555.
- (15) Qin, B. Y.; Bewley, M. C.; Creamer, L. K.; Baker, H. M.; Baker, E. N.; Jameson, G. B. Structural basis of the Tanford transition of bovine beta-lactoglobulin. *Biochemistry* **1998**, *37*, 14014–14023.
- (16) Qin, B. Y.; Bewley, M. C.; Creamer, L. K.; Baker, E. N.; Jameson, G. B. Functional implications of structural differences between variants A and B of bovine beta-lactoglobulin. *Protein Sci.* **1999**, *8*, 75–83.
- (17) Kuwata, K.; Hoshino, M.; Forge, V.; Era, S.; Batt, C. A.; Goto, Y. Solution structure and dynamics of bovine beta-lactoglobulin A. *Protein Sci.* **1999**, *8*, 2541–2545.
- (18) Uhrinova, S.; Smith, M. H.; Jameson, G. B.; Uhrin, D.; Sawyer, L.; Barlow, P. N. Structural changes accompanying pH-induced dissociation of the beta-lactoglobulin dimer. *Biochemistry* **2000**, *39*, 3565–3574.
- (19) Narayan, M.; Berliner, L. J. Fatty acids and retinoids bind independently and simultaneously to beta-lactoglobulin. *Biochemistry* **1997**, *36*, 1906–1911.
- (20) Qin, B. Y.; Creamer, L. K.; Baker, E. N.; Jameson, G. B. 12-Bromododecanoic acid binds inside the calyx of bovine beta-lactoglobulin. *FEBS Lett.* **1998**, *438*, 272–278.
- (21) Wu, S. Y.; Perez, M. D.; Puyol, P.; Sawyer, L. beta-lactoglobulin binds palmitate within its central cavity. *J. Biol. Chem.* **1999**, *274*, 170–174.
- (22) Kontopidis, G.; Holt, C.; Sawyer, L. The ligand-binding site of bovine beta-lactoglobulin: evidence for a function. *J. Mol. Biol.* **2002**, *318*, 1043–1055.
- (23) Wang, Q.; Allen, J. C.; Swaisgood, H. E. Binding of retinoids to beta-lactoglobulin isolated by bioselective adsorption. *J. Dairy Sci.* **1997**, *80*, 1047–1053.
- (24) Wang, Q.; Allen, J. C.; Swaisgood, H. E. Binding of vitamin D and cholesterol to beta-lactoglobulin. *J. Dairy Sci.* **1997**, *80*, 1054–1059.
- (25) Wang, Q.; Allen, J. C.; Swaisgood, H. E. Binding of lipophilic nutrients to beta-lactoglobulin prepared by bioselective adsorption. *J. Dairy Sci.* **1999**, *82*, 257–264.
- (26) Yang, M. C.; Guan, H. H.; Liu, M. Y.; Lin, Y. H.; Yang, J. M.; Chen, W. L.; Chen, C. J.; Mao, S. J. T. Crystal structure of a secondary vitamin D<sub>3</sub> binding site of milk beta-lactoglobulin. *Proteins* **2008**, *71*, 1197–1210.
- (27) Xiao, L.; Cui, X.; Madison, V.; White, R. E.; Cheng, K. C. Insights from a three-dimensional model into ligand binding to constitutive active receptor. *Drug Metab. Dispos.* **2002**, *30*, 951–956.
- (28) Laurie, A. T.; Jackson, R. M. Q-SiteFinder: an energy-based method for the prediction of protein-ligand binding sites. *Bioinformatics* **2005**, *21*, 1908–1916.
- (29) Yang, J. M.; Chen, C. C. GEMDOCK: a generic evolutionary method for molecular docking. *Proteins* **2004**, *55*, 288–304.
- (30) Danley, D. E. Crystallization to obtain protein-ligand complexes for structure-aided drug design. *Acta Crystallogr.* **2006**, *D62*, 569–575.
- (31) Guex, N.; Peitsch, M. C. SWISS-MODEL and the Swiss-PdbViewer: an environment for comparative protein modeling. *Electrophoresis* **1997**, *18*, 2714–2723.
- (32) Jones, G.; Willett, P.; Glen, R. C.; Leach, A. R.; Taylor, R. Development and validation of a genetic algorithm for flexible docking. *J. Mol. Biol.* **1997**, *267*, 727–748.
- (33) Yang, J. M.; Shen, T. W. A pharmacophore-based evolutionary approach for screening selective estrogen receptor modulators. *Proteins* **2005**, *59*, 205–220.
- (34) Otwinowski, Z.; Minor, W. Processing of X-ray diffraction data collected in oscillation mode. *Methods Enzymol.* **1997**, *276*, 307–326.
- (35) Ragona, L.; Fogolari, F.; Zetta, L.; Pérez, D. M.; Puyol, P.; De Kruijff, K.; Löhr, F.; Rüterjans, H.; Molinari, H. Bovine beta-lactoglobulin: interaction studies with palmitic acid. *Protein Sci.* **2000**, *9*, 1347–1356.
- (36) Muresan, S.; van der Bent, A.; de Wolf, F. A. Interaction of beta-lactoglobulin with small hydrophobic ligands as monitored by fluorometry and equilibrium dialysis: nonlinear quenching effects related to protein-protein association. *J. Agric. Food Chem.* **2001**, *49*, 2609–2618.
- (37) Hartshorn, M. J.; Murray, C. W.; Cleasby, A.; Frederickson, M.; Tickle, I. J.; Jhoti, H. Fragment-based lead discovery using X-ray crystallography. *J. Med. Chem.* **2005**, *48*, 403–413.
- (38) Nienaber, V. L.; Richardson, P. L.; Klighofer, V.; Bouska, J. J.; Giranda, V. L.; Greer, J. Discovering novel ligands for macromolecules using X-ray crystallographic screening. *Nat. Biotechnol.* **2000**, *18*, 1105–1108.

- (39) Rossmann, M. G. The molecular replacement method. *Acta Crystallogr.* **1990**, *A46*, 73–82.
- (40) Brunger, A. T.; Adams, P. D.; Clore, G. M.; DeLano, W. L.; Gros, P.; Grosse-Kunstleve, R. W.; Jiang, J. S.; Kuszewski, J.; Nilges, M.; Pannu, N. S.; Read, R. J.; Rice, L. M.; Simonson, T.; Warren, G. L. Crystallography & NMR system: A new software suite for macromolecular structure determination. *Acta Crystallogr.* **1998**, *D54*, 905–921.
- (41) Lappe, J. M.; Travers-Gustafson, D.; Davies, K. M.; Recker, R. R.; Heaney, R. P. Vitamin D and calcium supplementation reduces cancer risk: results of a randomized trial. *Am. J. Clin. Nutr.* **2007**, *85*, 1586–1591.
- (42) Bischoff-Ferrari, H. A.; Willett, W. C.; Wong, J. B.; Giovannucci, E.; Dietrich, T.; Dawson-Hughes, B. Fracture prevention with vitamin D supplementation: a meta-analysis of randomized controlled trials. *JAMA* **2005**, *293*, 2257–2264.
- (43) Holick, M. F.; Shao, Q.; Liu, W. W.; Chen, T. C. The vitamin D content of fortified milk and infant formula. *N. Engl. J. Med.* **1992**, *326*, 1178–1181.
- (44) Fluckinger, M.; Merschak, P.; Hermann, M.; Haertlé, T.; Redl, B. Lipocalin-interacting-membrane-receptor (LIMR) mediates cellular internalization of beta-lactoglobulin. *Biochim. Biophys. Acta* **2008**, *1778*, 342–347.
- (45) Pérez, M. D.; Díaz de Villegas, C.; Sánchez, L.; Aranda, P.; Ena, J. M.; Calvo, M. Interaction of fatty acids with beta-lactoglobulin and albumin from ruminant milk. *J. Biochem.* **1989**, *106*, 1094–1097.
- (46) Jones, T. A.; Zou, J. Y.; Cowan, S. W.; Kjeldgaard, M. Improved methods for building protein models in electron density maps and the location of errors in these models. *Acta Crystallogr.* **1991**, *A47*, 110–119.

CG800697S



# Evidence for $\beta$ -lactoglobulin involvement in vitamin D transport *in vivo* – role of the $\gamma$ -turn (Leu-Pro-Met) of $\beta$ -lactoglobulin in vitamin D binding

Ming Chi Yang<sup>1</sup>, Nai Chi Chen<sup>1</sup>, Chun-Jung Chen<sup>2,3</sup>, Chin Yun Wu<sup>1</sup> and Simon J. T. Mao<sup>1,4</sup>

1 Department and College of Biological Science and Technology, National Chiao Tung University, Taiwan

2 Life Science Group, Research Division, National Synchrotron Radiation Research Center, Taiwan

3 Department of Physics, National Tsing Hua University, Taiwan

4 Department of Biotechnology and Bioinformatics, Asia University, Taichung, Taiwan

## Keywords

$\beta$ -lactoglobulin; monoclonal antibody; site-directed mutagenesis; vitamin D binding; vitamin D transport and uptake

## Correspondence

S. J. T. Mao, Department of Biological Science and Technology, College of Biological Science and Technology, National Chiao Tung University, 75 Po-Ai Street, Hsinchu 30050, Taiwan  
Fax: +886 3 572 9288  
Tel: +886 3 571 2121 (ext. 56948)  
E-mail: mao1010@ms7.hinet.net

(Received 9 December 2008, revised 3 February 2009, accepted 6 February 2009)

doi:10.1111/j.1742-4658.2009.06953.x

$\beta$ -lactoglobulin (LG) is a major bovine milk protein, containing a central calyx and a second exosite beyond the calyx to bind vitamin D; however, the biological function of LG in transporting vitamin D remains elusive. Crystallographic findings from our previous study showed the exosite to be located at the pocket between the  $\alpha$ -helix and  $\beta$ -strand I. In the present study, using site-directed mutagenesis, we demonstrate that residues Leu143, Pro144 and Met145 in the  $\gamma$ -turn loop play a crucial role in the binding. Further evidence is provided by the ability of vitamin D<sub>3</sub> to block the binding of a specific mAb in the  $\gamma$ -turn loop. Using the mouse ( $n = 95$ ) as an animal model, we initially demonstrated that LG is a major fraction of milk proteins responsible for uptake of vitamin D. Most interestingly, dosing mice with LG supplemented with vitamin D<sub>3</sub> revealed that native LG containing two binding sites gave a saturated concentration of plasma 25-hydroxyvitamin D at a dose ratio of 2 : 1 (vitamin D<sub>3</sub>/LG), whereas heated LG containing one exosite (lacking a central calyx) gave a ratio of 1 : 1. We have demonstrated for the first time that LG has a functional advantage in the transport of vitamin D, indicating that supplementing milk with vitamin D effectively enhances its uptake.

Bovine  $\beta$ -lactoglobulin (LG) is a major whey protein that constitutes 10–15% of the total proteins in bovine milk [1]. Since the 1960s, the thermally unstable and molten globule nature of LG has stimulated extensive research into its physical and biochemical properties [2–10]. The crystal structure of LG, which is well established [11,12], has been used mostly as a benchmark to predict the secondary structure of a given protein with a known amino acid sequence [13]. As shown in Fig. 1A, the protein has predominantly a  $\beta$ -sheet conformation containing nine antiparallel  $\beta$ -strands from A to I. Topographically,  $\beta$ -strands A–D form one surface of the barrel (calyx), and  $\beta$ -strands E–H form the other [14–16]. The calyx has a remarkable ability to

bind hydrophobic molecules such as retinol, fatty acids, and vitamin D [17–20]. According to a crystallographic structure of the LG–vitamin D<sub>3</sub> complex (Fig. 1B) [9,10], the  $\alpha$ -helical region with three turns linking with  $\beta$ -strand I on the surface is involved in binding vitamin D at the secondary exosite. The conformational changes of LG upon heating are rapid and extensive above the transition temperature ( $\sim 70$  °C), at which  $\beta$ -strand D of the calyx participates in the unfolding during thermal denaturation [6]. As a result, thermal treatment diminishes the calyx binding site for palmitate or retinol, but does not affect the exosite for vitamin D binding [6,9,10]. In our previous study, we proposed that this exosite contains a unique inverse

## Abbreviations

LG,  $\beta$ -lactoglobulin; rLG, recombinant  $\beta$ -lactoglobulin; SD, standard deviation.



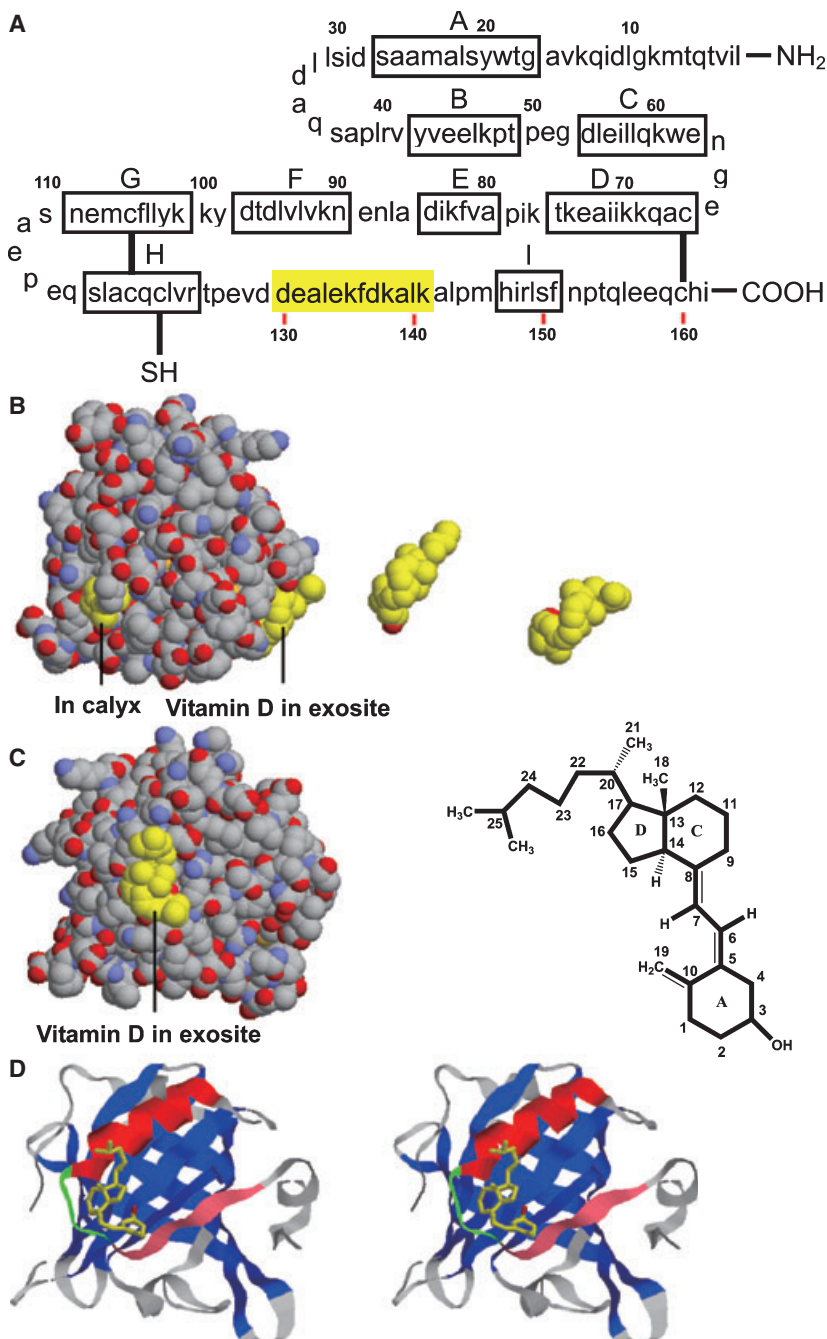


**Fig. 1.** Amino acid sequence of LG and crystal structure of the LG–vitamin D<sub>3</sub> complex. (A) LG comprises 162 amino acids with nine  $\beta$ -sheet strands (A–I). The  $\alpha$ -helix with three turns is located between residues 130 and 141 (yellow). (B) Space-filling drawing of the LG–vitamin D<sub>3</sub> complex at 2.4 Å resolution. Vitamin D<sub>3</sub> (carbon yellow and oxygen red) and LG are drawn on the basis of our previously refined model [9,10], with one vitamin D<sub>3</sub> molecule penetrating inside the calyx (left) and the other lying on the surface pocket at the C-terminus (residues 136–149) (right). (C) Front view of vitamin D<sub>3</sub> binding to the exosite and chemical structure of vitamin D<sub>3</sub>. (D) The 3D ribbon model of the LG–vitamin D<sub>3</sub> complex shows that the exosite combines an  $\alpha$ -helix (red) and  $\beta$ -strand I (pink) with a  $\gamma$ -turn loop (green). (A) and (B) are reproduced from our previous study [9], with permission of the publisher.

$\gamma$ -turn loop (residues 143–145 or Leu-Pro-Met), located between the  $\alpha$ -helix and  $\beta$ -strand I, that is essential in forming a pocket to bind vitamin D [9].

In the present study, we expressed recombinant LG (rLG) in *Escherichia coli*, and used site-directed mutagenesis to produce a set of mutants to test the hypothesis that this  $\gamma$ -turn plays an essential role in the interaction between LG and vitamin D. We further tested this hypothesis using a mAb specific for this  $\gamma$ -turn region (selected from a battery containing

900 mAbs) as a probe, and then determined whether vitamin D might interfere with the binding between LG and the mAb. In addition, although the binding of vitamin D to milk LG is well known [9,10,14,21,22], whether it enhances the transport of vitamin D of milk is still unproven.

We have demonstrated for the first time that LG is a fraction responsible for the uptake of vitamin D<sub>3</sub> from milk, using the mouse ( $n = 95$ ) as an animal model. Most interestingly, we showed that native LG



containing both the calyx and exosite had an efficacy in vitamin D<sub>3</sub> uptake almost twice that of heated LG containing a single exosite. Our study therefore provides new insights concerning the value of supplementing dairy products with vitamin D.

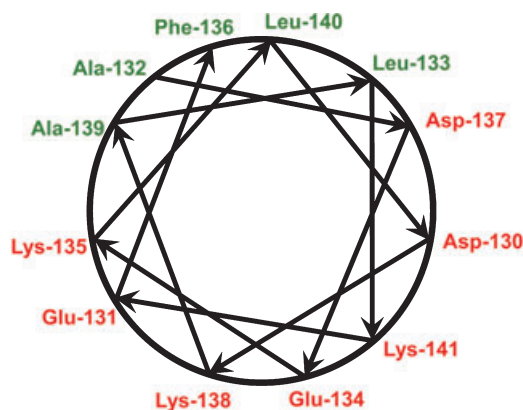
## Results

### Overall crystal structure of the LG–vitamin D<sub>3</sub> complex

Our space-filling drawing of the LG–vitamin D<sub>3</sub> complex at 2.4 Å resolution reveals two domains in which vitamin D<sub>3</sub> is bound (Fig. 1B). One vitamin D<sub>3</sub> molecule inserts almost perpendicularly into the calyx cavity with the 3-OH near the outside similar to that of retinol binding; the other binds to the exosite near the C-terminus of LG (residues 136–149), including a  $\gamma$ -turn loop (residues 143–145) by combining part of the  $\alpha$ -helix and  $\beta$ -strand I (Fig. 1C,D). [Correction added on 18 March 2009 after first online publica-

tion: in the preceding sentence, ‘One vitamin D<sub>3</sub> molecule inserts almost perpendicularly into the calyx cavity with the 3-OH near the outside similar to that of retinol binding;’ has been inserted.] Uniquely, the  $\alpha$ -helix in the exosite is totally amphipathic, as pointed out previously [23], with one face totally comprising charged amino acid residues, and another face totally comprising hydrophobic residues (Fig. 2A). The A-ring and the aliphatic tail of vitamin D<sub>3</sub> (following the C/D-rings) interact with  $\beta$ -strand I and the  $\alpha$ -helix of LG, respectively (Fig. 1D). The crystal structure of the LG–vitamin D<sub>3</sub> complex shows clearly that the conformation of vitamin D<sub>3</sub> differs significantly between the two binding sites (Fig. 1B). This fact explains why fatty acid and retinol are unable to bind at the secondary exosite. In the first phase of the present study, we tested the hypothesis that a  $\gamma$ -turn loop is essential to allow a stable interaction between vitamin D and the exosite (Fig. 1D) [9], using LG mutants produced from *E. coli*.

#### A Amphipathic $\alpha$ -helix in residues 130–141



#### B Electron density map around the exosite containing the $\gamma$ -turn loop

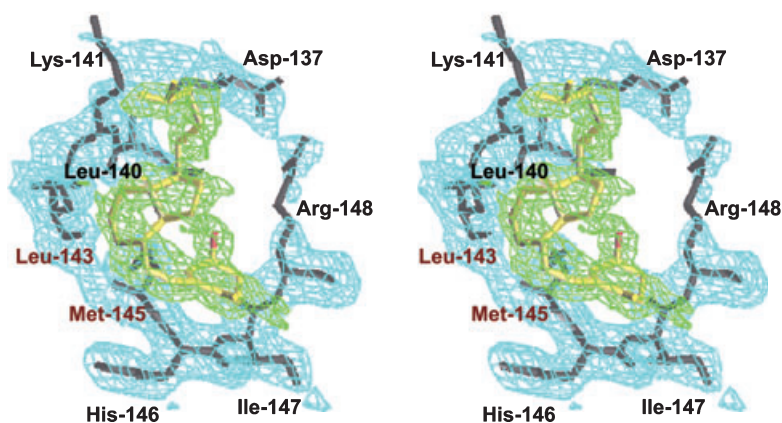


**Fig. 2.** Amphipathic  $\alpha$ -helix of LG and its interaction with vitamin D<sub>3</sub>. (A) Unique amphipathic  $\alpha$ -helix of LG. (B) Final refined model with the  $2|F_{\text{obs}} - F_{\text{calc}}|$  electron density showing that the bulk of the density is sufficient to cover the vitamin D<sub>3</sub> in the exosite. The figures are reproduced from our previous study [9], with permission of the publisher.

### Expression, purification and western blot of rLG and its mutants

Figure 3A shows that each rLG or mutant was abundantly expressed, with the average expression levels being approximately 30% of that of total lysate proteins. As each mutant contains a 6 $\times$  His-tag, the molecular mass ( $\sim$  19.7 kDa) was slightly greater than that (18.4 kDa) of native LG. Each purified recombinant protein showed  $\sim$  95% homogeneity in reducing SDS/PAGE, and this was verified with a western blot using a LG-specific mAb (4D11) [6] (Fig. 3B).

### Vitamin D<sub>3</sub> binding to LG and rLG

To determine whether rLG was capable of interacting with vitamin D in a manner similar to that of native LG, we monitored the quenching of Trp fluorescence for the binding according to an established method [6,9,10,21,22]. Figure 4A and Table 1 show that maximal vitamin D<sub>3</sub> binding to native LG was achieved at a ratio of 2 : 1, but that the binding to rLG remained at a ratio of 1 : 1. The expressed rLG hence incompletely mimics the native LG structure with a loss of one vitamin D binding site or partial loss for both sites. Because palmitate and retinol bind to only the central calyx, not to the exosite [18], we used each of these two ligands as a 'marker' to monitor whether they still interact with rLG. The results revealed that neither palmitate nor retinol interact with rLG, as

judged by the absence of Trp fluorescence changes (Table 1), indicating that the correct conformation of the central calyx was not present in rLG.

Figure 4A shows, however, that the exosite seems to be unaltered in rLG, as the binding ratio for vitamin D<sub>3</sub> remained at 1 : 1. Because heat treatment results in a loss of the central calyx but retention of the exosite [6,9,10], we used heated LG (100 °C for 16 min) as a probe to compare its vitamin D<sub>3</sub> binding to rLG. The binding of heated LG attained a ratio of 1 : 1, similar to previous findings [9,10]. Interestingly, the ratios of vitamin D<sub>3</sub> binding to either heated LG or rLG were almost indistinguishable, and heat had no effect on rLG (Fig. 4A, left panel). The affinities of heated LG, heated rLG and rLG for vitamin D<sub>3</sub> were also similar (Fig. 4A, right panel). The number of vitamin D<sub>3</sub>-binding sites predicted with a Cogan plot and the apparent dissociation constant calculated from the slope (Fig. 4A, right panel) are listed in Table 1. The binding affinity of native LG (containing two binding sites) was about 5 nM ( $K_d^{app} = 4.7 \pm 0.37$  nM), which appears to be seven times that of rLG (containing exosite only) ( $K_d^{app} = 33.1 \pm 3.62$  nM).

Because the  $\beta$ -structure of LG is required to maintain the calyx [6,9], we expected its structure to be altered in rLG. From analysis of the CD spectra, we verified the change of the typical  $\beta$ -structure in rLG according to a leftward shift of a symmetric dip at 215 nm characteristic of native LG (Fig. 5A). Heat produced essentially no additional structural change in rLG. There was a minor difference in the CD spectra between heated LG and rLG, which might be due to the presence of the His-tag in the rLG or to different disulfide linkages, described below. Notably, addition of vitamin D<sub>3</sub> to all LG species did not alter the overall CD spectra (data not shown). To confirm the loss of  $\beta$ -structure in expressed rLG, we used a  $\beta$ -structure-dependent specific LG monoclonal antibody (4H11E8) [8] to show that it recognized only native LG, not rLG, on a native gel western blot (Fig. 5B).

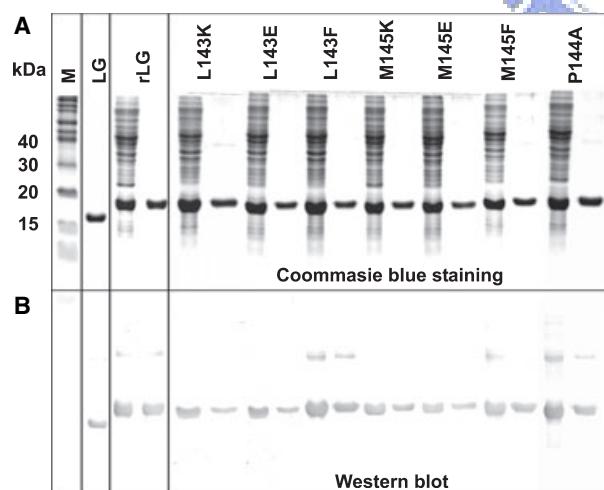


**Fig. 3.** Expression and purification of recombinant LG and its mutants from *E. coli*. (A) SDS/PAGE (in the presence of mercaptoethanol) of native LG isolated from milk, cell lysate (paired left), and isolated rLG (paired right). (B) Western blot of cell lysate and isolated rLG mutants using a LG-specific mAb (4D11). M represents a molecular marker.

### Further characterization of rLG using MALDI-TOF and carboxymethylation

Recombinant LG apparently cannot fold to its native state in the *E. coli* expression system, which is a general issue when utilizing a given recombinant protein for the investigation of a structure–function relationship. In our case, the loss of the binding nature of the central calyx in rLG is probably due to the overall change in the  $\beta$ -structure (Fig. 5). Although the exact mechanism involved in such a change remains elusive, we attempted to further investigate whether the disul-

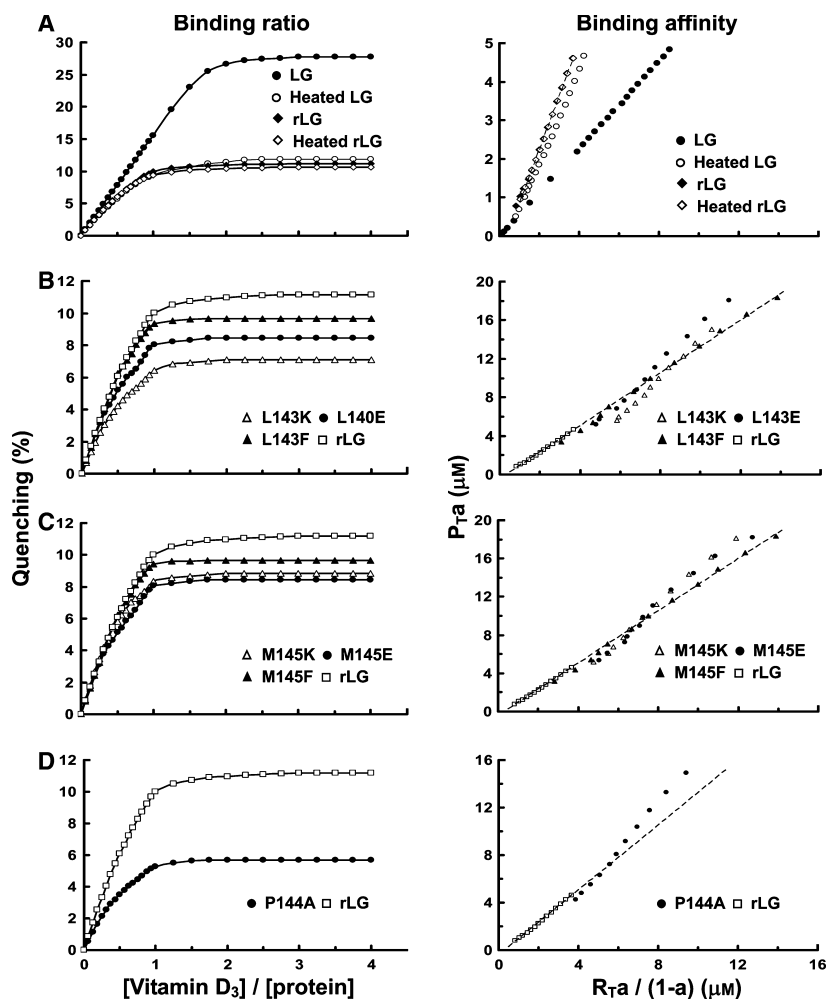


**Fig. 4.** Fluorescence titration curves of native and heated LG, nonheated and heated rLG or rLG mutants with vitamin D<sub>3</sub>. Left panel: titration curve of native LG, heated LG, rLG and heated rLG (A) and mutants (B–D) with vitamin D<sub>3</sub>. Right panel: Cogan plot per titration curve.  $P_T$  = total protein concentration,  $R_T$  = total ligand concentration, and  $a$  = fraction of unoccupied ligand sites on the protein. The dashed line in each right-hand panel represents the titration plot of rLG only, used for reference. Each point represents the mean of triplicate determinations. The average SD was less than 5–8% of the mean.

vide linkages ( $n = 2$  from a total of five Cys residues with one free –SH group at position 121 in native LG) are related. The use of limited trypsin-digested fragments of native, heated and recombinant LG in MALDI-TOF analysis revealed (Fig. 6A–D) that rLG contained two complicated intramolecularly crosslinked fragments, including Trp61–Lys69:Tyr102–Arg124 and Tyr 102–Arg124:Leu149–Ile 162 for Cys66–Cys106, Cys66–Cys119, or Cys66–Cys121, and Cys106–Cys160, Cys119–Cys160, or Cys121–Cys160, respectively, that differed from that of native LG, containing Trp61–Lys69:Leu149–Ile162 for Cys66–Cys160. There was an additional crosslinked fragment in heated LG shown by Trp61–Lys69:Tyr102–Arg124 for Cys66–Cys106, Cys66–Cys119, or Cys66–Cys121.

To elucidate the complicated crosslinked species of rLG (for example, dimerization was seen in both heated and recombinant LG), we irreversibly reduced all linkages by carboxymethylation using iodoacetic acid. Under these conditions, we found that native

LG, heated LG and rLG were able to form monomers with almost the same homogeneity (Fig. 6E). Interestingly, both carboxymethylated rLG and carboxymethylated heated LG had similar binding ratios (1 : 1) and affinities for vitamin D<sub>3</sub> to those without carboxymethylation, whereas carboxymethylated LG also exhibited a 1 : 1 ratio. Further heating of modified proteins did not affect the binding ratios (Table 1). These results indicate that disulfide linkages are essential to maintain the necessary conformation of the central calyx, but are probably not particularly critical for exosite binding. The expressed rLG therefore provided us with a tool in the subsequent mutant tests involving monitoring of a single exosite interaction.

#### Vitamin D<sub>3</sub> binding to rLG mutants of $\gamma$ -turn loop residues 143–145

According to the crystal structure of the LG–vitamin D<sub>3</sub> complex [9], there is a direct interaction

**Table 1.** Apparent dissociation constants and ratios for binding of ligands to native LG and rLG.

Ligand	Protein	Binding ratio calculated from Cogan plot (ligand/LG)	$K_d^{app}$ Apparent dissociation constant ( $10^{-9}$ M)
Vitamin D <sub>3</sub>	Native LG	1.76 ± 0.12	4.7 ± 0.37
	Heated LG	0.84 ± 0.05	45.7 ± 3.12
	rLG	0.73 ± 0.03	33.1 ± 3.62
	Heated rLG	0.72 ± 0.02	38.6 ± 3.56
	Carboxymethylated LG <sup>a</sup>	0.84 ± 0.02	35.2 ± 2.92
	Carboxymethylated heated LG <sup>a</sup>	0.84 ± 0.05	39.2 ± 3.08
	Carboxymethylated rLG <sup>a</sup>	0.79 ± 0.03	32.8 ± 3.61
	Carboxymethylated LG with heat treatment <sup>a</sup>	0.83 ± 0.02	35.2 ± 3.03
	Carboxymethylated heated LG with heat treatment <sup>a</sup>	0.83 ± 0.03	40.0 ± 2.38
	Carboxymethylated rLG with heat treatment <sup>a</sup>	0.78 ± 0.03	33.1 ± 3.41
Retinol	Native LG	0.91 ± 0.09	17.3 ± 1.62
	Heated LG	– <sup>b</sup>	–
	rLG	–	–
	Heated rLG	–	–
	Carboxymethylated LG	–	–
	Carboxymethylated heated LG	–	–
	Carboxymethylated rLG	–	–
	Carboxymethylated LG with heat treatment	–	–
	Carboxymethylated heated LG with heat treatment	–	–
	Carboxymethylated rLG with heat treatment	–	–
Palmitate	Native LG	0.80 ± 0.072	44.0 ± 4.56
	Heated LG	–	–
	rLG	–	–
	Heated rLG	–	–
	Carboxymethylated LG	–	–
	Carboxymethylated heated LG	–	–
	Carboxymethylated rLG	–	–
	Carboxymethylated LG with heat treatment	–	–
	Carboxymethylated heated LG with heat treatment	–	–
	Carboxymethylated rLG with heat treatment	–	–

<sup>a</sup> The titration experiment was conducted as for other proteins, but is not shown in Fig. 4. <sup>b</sup> No fluorescence change or no binding in titration experiments.

between vitamin D<sub>3</sub> and the side chains of Leu143 and Met145 in the  $\gamma$ -turn loop, because the distance between vitamin D<sub>3</sub> and each side chain is < 3.8 Å (Figs 1D and 2B). We replaced each of these two residues with a positively charged Lys, a negatively charged Glu, or a hydrophobic Phe, by site-directed mutagenesis. The effect on the binding to vitamin D<sub>3</sub>, determined by fluorescence quenching, is shown in Fig. 4B (left and right panels) and Table 2. A markedly decreased binding affinity was seen when Leu143 was substituted with Lys or Glu (8.11-fold or 5.84-fold). Interestingly, there was only a slight decrease when it was replaced by a hydrophobic Phe (0.96-fold) (Fig. 4B). A consistent pattern was likewise seen with the M145K, M145E and M145F mutants upon binding vitamin D<sub>3</sub> (Fig. 4C).

Because Pro is typically found in a  $\gamma$ -turn, we tested the importance of Pro144 using the P144A mutant.

Figure 4D and Table 2 show significantly decreased binding of vitamin D<sub>3</sub> (4.6-fold) by the P144A mutant. Table 2 shows that the effects of these residues in the loop region for vitamin D<sub>3</sub> interaction rank overall as Leu143 > Met145 > Pro144.

#### Interference of vitamin D<sub>3</sub> to $\gamma$ -turn specific mAb (1D8F8) binding with LG

To select a mAb that might recognize the  $\gamma$ -turn region, we screened a LG mAb battery ( $n = 900$ ) [5], using a set of mutants as a probe. We found one LG mAb, 1D8F8, that was capable of reacting with the M145K, M145E and M145F mutants, but not with the L143K, L143E and P144A mutants, according to a western blot analysis (Fig. 7A). MAb 1D8F8 is therefore specific for Leu143 and Pro144 located within the  $\gamma$ -turn loop. As Leu143 and Pro144 are located inside

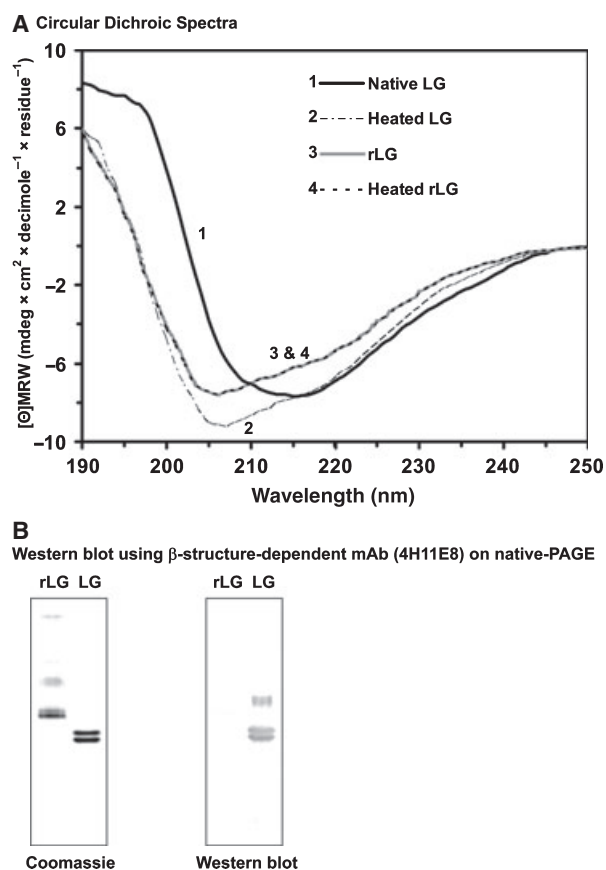


**Fig. 5.** CD and western blot analysis of rLG. (A) Native LG exhibits primarily a typical  $\beta$ -sheet conformation with a symmetrical dip at 215 nm. (B) MAbs (4H11E8) specific for the native  $\beta$ -structure [8]. Western blot was performed using a 15% native PAGE.

the exosite (Fig. 1B,D), the presence of vitamin D<sub>3</sub> in the exosite is expected to interfere with the recognition of mAb 1D8F8, as depicted in our space-filling model (Fig. 7B). As Fig. 7C shows, the binding of vitamin D<sub>3</sub> to the 'exosite' of native LG, heated LG or rLG attenuated the recognition of mAb 1D8F8, according to a dot-blot assay, but, with the use of retinol and palmitate as a control, neither ligand affected the binding of 1D8F8. This result provides additional evidence for the involvement of the  $\gamma$ -turn loop in the binding of vitamin D.

### Biological activity of LG in vitamin D<sub>3</sub> uptake in mice

To investigate whether LG binding to vitamin D can facilitate its uptake in an animal, we used the mouse as a model. We initially fed the animals ( $n = 30$ ) with milk and milk fractions (LG, whey protein, or casein) all fortified with vitamin D<sub>3</sub> (final concentration

100  $\mu$ M) for 3 weeks, and then determined the plasma intake of 25-hydroxyvitamin D (a metabolite of vitamin D). Figure 8A shows that the final mean concentrations of 25-hydroxyvitamin D in mice ( $n = 5$  in each group) fed with raw milk, whey protein (without casein) or LG each supplemented with vitamin D<sub>3</sub> were significantly greater than those without LG (containing no LG) ( $P < 0.001$ ). Casein, which lacks LG appears ineffective in the vitamin D uptake. The levels of 25-hydroxyvitamin D in all tested groups were elevated relative to the naive control without vitamin D<sub>3</sub> ( $P < 0.001$ ).

### Role of the exosite in uptake of vitamin D<sub>3</sub> in mice

To test the hypothesis that the exosite of LG plays a role in the transport of vitamin D, we compared the uptake of vitamin D<sub>3</sub> between native LG (containing a calyx and an exosite) and heated LG (containing only an exosite) as a strategy to evaluate their variation in uptake, if any [6,9]. Mice ( $n = 65$ ) were separated into three major groups: those fed vitamin D<sub>3</sub> as a control (group 1), those fed LG supplemented with vitamin D<sub>3</sub> (group 2), and those fed heated LG supplemented with vitamin D<sub>3</sub> (group 3); mice fed with no vitamin D<sub>3</sub> were included as a baseline. Each subgroup of mice were then divided by increasing dosages of vitamin D<sub>3</sub> according to vitamin D<sub>3</sub>/LG ratios (0.4, 1, 2, and 3), while LG or heated LG was maintained at a constant concentration (250  $\mu$ M). Under these conditions, we expected to see the effect of the dosage of vitamin D<sub>3</sub> on its transport by the exosite. Figure 8B shows a typical dose response in all three major groups supplemented with vitamin D<sub>3</sub>. Among these, the elevation of plasma 25-hydroxyvitamin D was prominent in group 2 (native LG supplemented with vitamin D<sub>3</sub>). There seemed to be no saturation of 25-hydroxyvitamin D with vitamin D<sub>3</sub> at greater dosages in groups 2 and 3. When the values of the control group (group 1 fed vitamin D<sub>3</sub>) were subtracted from those of groups 2 or 3, the levels of 25-hydroxyvitamin D appeared, remarkably, to be saturable (Fig. 8C). The dose-response curves fit exactly the binding ratios of vitamin D<sub>3</sub> versus LG; native LG containing two sites to bind vitamin D<sub>3</sub> hence produces maximal concentrations of plasma 25-hydroxyvitamin D at a dosage ratio of 2 : 1 (vitamin D<sub>3</sub>/LG), whereas heated LG, containing only the exosite, produces maximal concentrations of plasma 25-hydroxyvitamin D at a dosage ratio of 1 : 1. The final increase in plasma 25-hydroxyvitamin D with native LG was almost exactly twice that of heated LG.



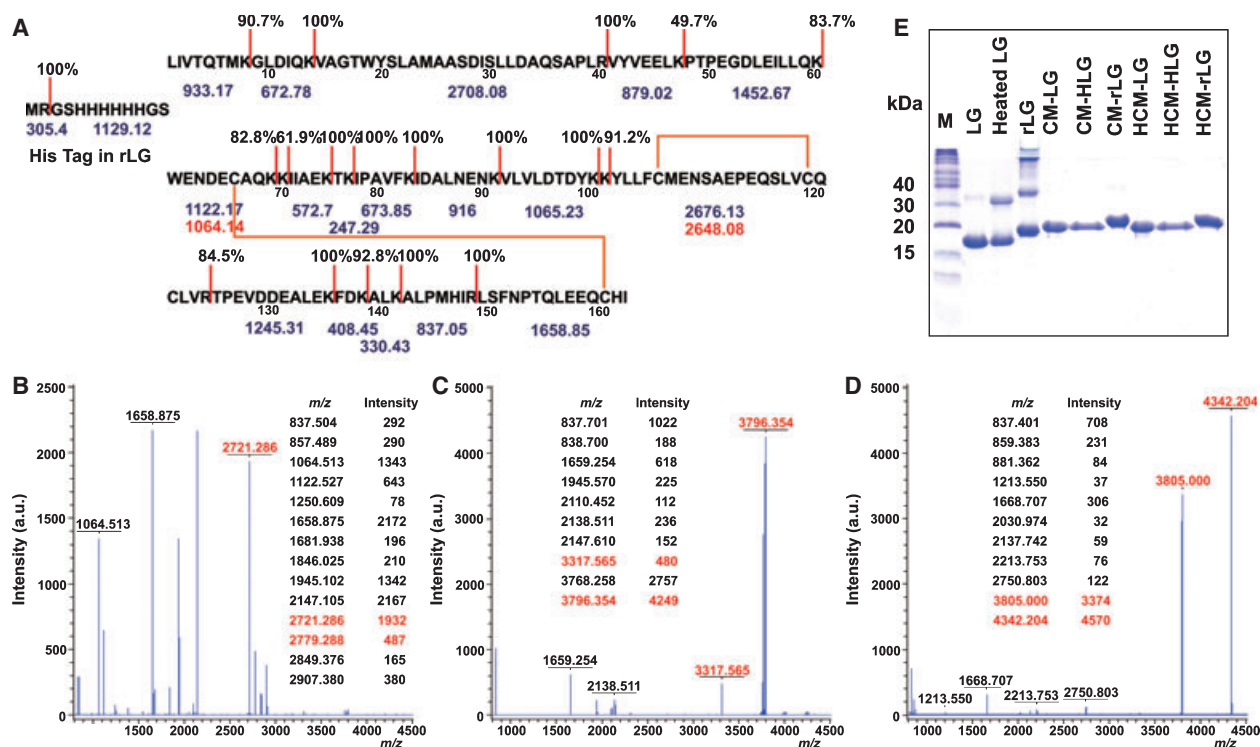


**Fig. 6.** MALDI-TOF MS analysis of trypsin-digested LG and carboxymethylation of LG. (A) Predicted trypsin cleavage sites (red bar, indicating cleavage probability) of LG isoform A obtained using a peptide cutter program (<http://au.expasy.org/tools/peptidecutter/>). The expected masses of peptide fragments (blue) and the disulfide linkages (orange bar) of native LG are depicted. LG isoform A with Asp64 and Val118 and isoform B with Gly64 and Ala118 in fragments 61–69 and 102–124 are shown in red. (B) MALDI-TOF spectrum of trypsin-digested native LG. Two mass spectra showing ions with  $m/z$  2721.286 for isoform B and  $m/z$  2779.288 for isoform A are representative for the fragment Trp61–Lys69:Leu149–Ile162 containing the disulfide linkage Cys66–Cys160. (C) Spectrum of trypsin-digested heated LG. Ions with  $m/z$  3317.565 and  $m/z$  3796.354 represent the dimeric Leu149–Ile162 and Trp61–Lys69:Tyr102–Arg124. (D) Spectrum of trypsin-digested rLG. Ions with  $m/z$  3805.000 and  $m/z$  4342.204 represent Trp61–Lys69:Tyr102–Arg124 and Tyr102–Arg124:Leu149–Ile162. (E) SDS/PAGE in the absence of mercaptoethanol of native LG, heated LG and rLG with or without carboxymethylation. HLG, CM and HCM denote heated LG, and carboxymethylated and heated carboxymethylated proteins, respectively. [Correction added on 18 March 2009 after first online publication: in the preceding sentence, ‘with heat treatment’ has been removed.] The molecular marker (M) is shown.

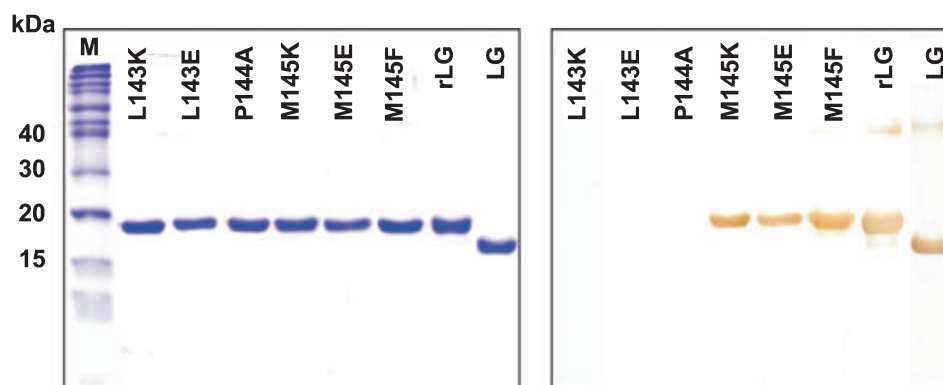
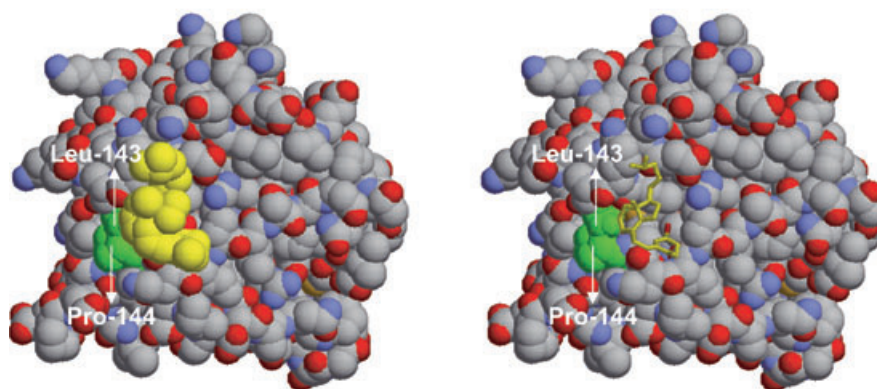
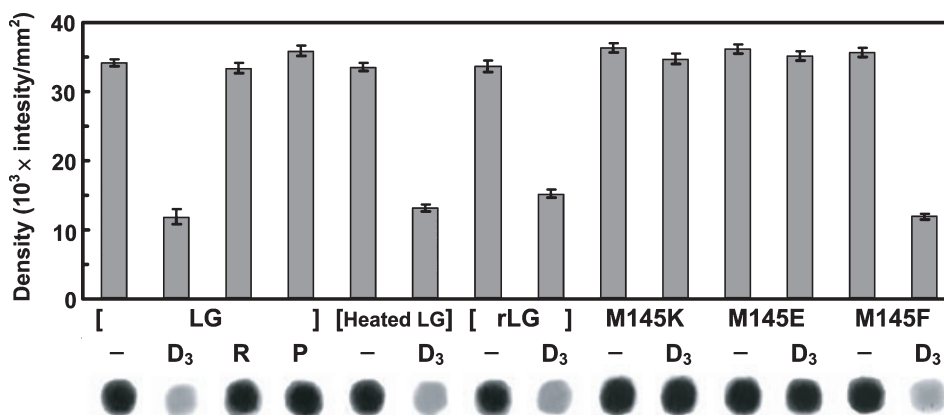
**Table 2.** Apparent dissociation constants and ratios for binding of vitamin D<sub>3</sub> to rLG and its  $\gamma$ -turn loop region mutants.

	Binding ratio calculated from Cogan plot (vitamin D <sub>3</sub> /LG)	$K_d^{app}$ Apparent dissociation constant (10 <sup>-9</sup> M)	Fold decrease in binding affinity
Wild-type	0.73 ± 0.03	33.1 ± 3.62 <sup>a</sup>	
L143K	0.50 ± 0.02	301.1 ± 13.16	8.11
L143E	0.50 ± 0.02	226.3 ± 9.83	5.84
L143F	0.70 ± 0.02	64.8 ± 3.91	0.96
P144A	0.50 ± 0.02	185.3 ± 8.18	4.6
M145K	0.53 ± 0.02	208.6 ± 9.19	5.31
M145E	0.56 ± 0.02	189.8 ± 8.47	4.74
M145F	0.71 ± 0.02	59.7 ± 3.87	0.81

<sup>a</sup>  $P < 0.001$  as compared to mutants. Data represent means of triplicate determinations.

## Discussion

The major concern of this study is that the structure of rLG produced in *E. coli* no longer mimics that of native LG. We demonstrated, using MALDI-TOF analysis, that this phenomenon is due primarily to the mis-crosslinking of five Cys residues present in rLG (Fig. 6). rLG is composed of various dimeric and aggregated forms (Fig. 6E). Interestingly, however, following the irreversible reduction of all disulfide linkages by carboxymethylation, these forms become a homogeneous species similar to carboxymethylated LG. The same is seen with heated LG. We then showed that all carboxymethylated proteins lost a calyx, as they failed to interact with retinol and palmitate, but they still retained the ability to bind vitamin D<sub>3</sub>, with a binding affinity almost identical

**A Mapping of exosite-specific mAb (1D8F8)****B Antigenic epitope of  $\gamma$ -turn specific mAb (1D8F8)****C Effect of vitamin D<sub>3</sub> binding on  $\gamma$ -turn specific mAb (1D8F8)**

**Fig. 7.** Identification and epitope mapping of a  $\gamma$ -turn-specific mAb and the structure–function relationship between the  $\gamma$ -turn loop and vitamin D<sub>3</sub>. (A) Identification of a mAb (1D8F8) specific for a  $\gamma$ -turn loop of LG, utilizing rLG mutants on a western blot. 1D8F8 recognizes native LG, rLG and some rLG mutants, but not mutants L143K, L143E, and P144A, indicating that  $\gamma$ -turn residues 143–144 are located within the epitope. (B) A space-filling model depicting residues 143 and 144 (green). They are within the vitamin D-binding exosite shared with 1D8F8. (C) Effect of vitamin D<sub>3</sub> binding on the immunoreactivity of LG, determined using dot-blot followed by scanning densitometric analysis ( $n = 3$ ). R, P and D<sub>3</sub> represent retinol, palmitate and vitamin D<sub>3</sub>, respectively.

to that of reduced LG or nonreduced rLG (Table 1). These data indicate that disulfide linkages of LG probably do not greatly affect the secondary binding

to vitamin D. The reason for using heated LG in this study was as a control to evaluate exosite binding for rLG, because almost identical binding was found



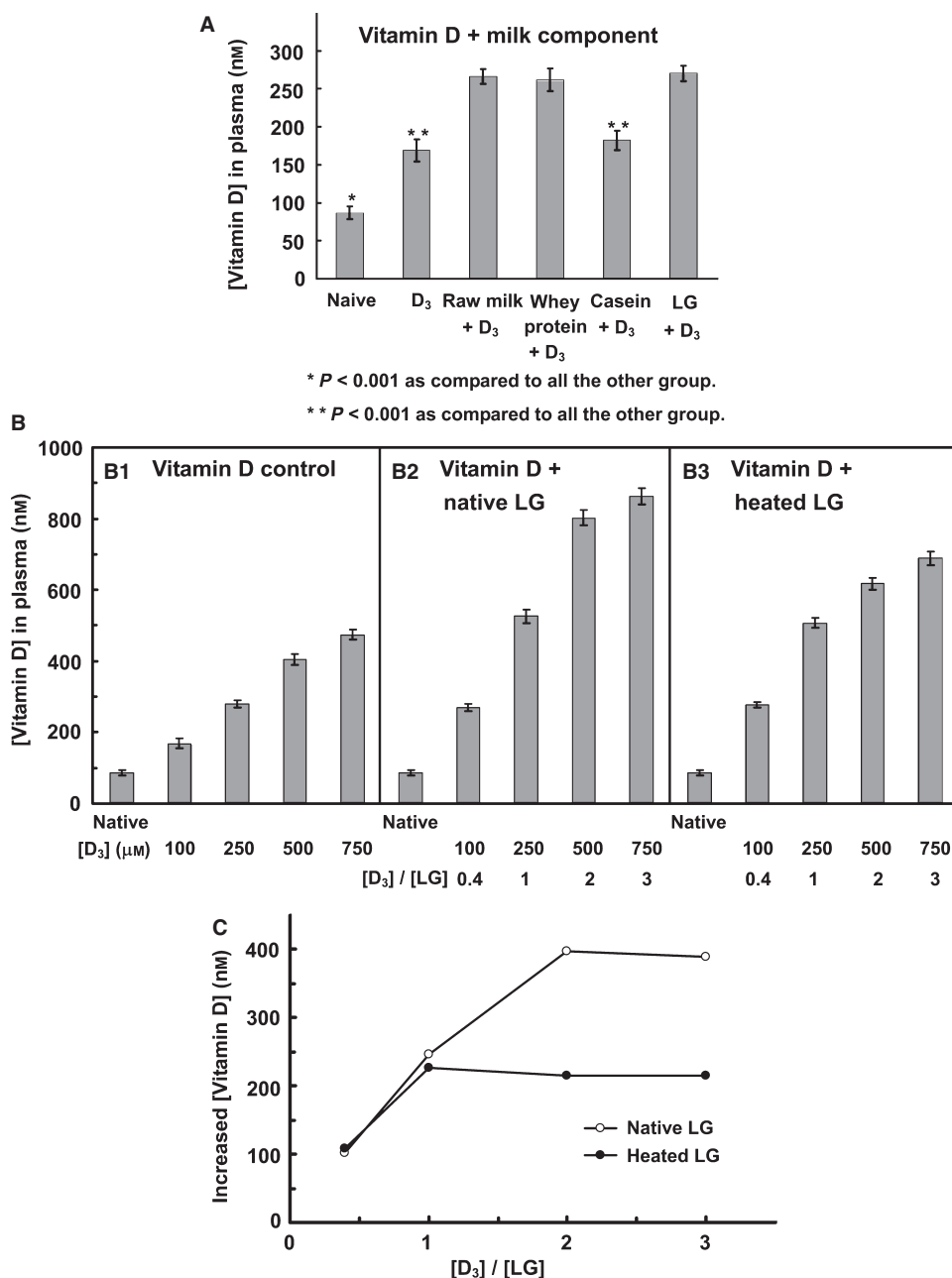


**Fig. 8.** Effect of LG on vitamin D<sub>3</sub> uptake in mice. (A) Concentration of 25-hydroxyvitamin D in plasma of mice fed ( $n = 5$  for each group) with milk or its components supplemented with vitamin D<sub>3</sub> (100  $\mu$ M). (B) Effect of native LG (containing the calyx and exosite) and heated LG (containing only the exosite) on uptake of vitamin D: each subgroup of mice ( $n = 5$ ) was dosed with vitamin D<sub>3</sub> in groups 2 and 3 (0, 100, 250, 500 and 750  $\mu$ M), according to the ratios 0, 0.4, 1, 2, and 3, respectively, of vitamin D<sub>3</sub>/LG; vitamin D<sub>3</sub> alone (group 1) served as a control group. The concentration of LG was kept constant (250  $\mu$ M). (C) Final 'adjusted' uptake of vitamin D after subtracting the values for the vitamin D<sub>3</sub> control group (group 1) from those for the vitamin D<sub>3</sub>-fortified native LG (group 2) or the vitamin D<sub>3</sub>-fortified heated LG group (group 3).

with rLG and heated rLG (Fig. 4A and Table 1). Whether the exosite of rLG maintains the same conformation as that of native LG is currently unknown. An ultimate solution is to obtain the crystal structure

of the rLG–vitamin D complex, including the mutants, but at present we are unable to obtain a rLG–vitamin D crystal, probably because of the heterogeneous structures of rLG. We therefore subsequently used

the rLG mutants as a probe to investigate the importance of the  $\gamma$ -turn loop in vitamin D binding.

Another concern is that two Trp residues – Trp19 and Trp61 – in LG were involved when binding is monitored using fluorescence quenching. Several previous studies suggested that the intrinsic fluorescence of LG is due almost exclusively to Trp19 [24,25]. Trp19 is located at the bottom of the calyx, whereas Trp61 is more accessible to a solvent, and is thus able to make only a minor contribution to fluorescence emission [26]. On the basis of our previous studies [6,9,10], at pH 2–6 or after thermal treatment to switch off the gate of the calyx, we showed that vitamin D<sub>3</sub> interacted with only the exosite (with 35–40% of maximal binding ability), but not retinol and palmitate. The change of fluorescence caused by the binding of the exosite is 35–40% of that of the native LG containing two sites. The binding signal for the exosite is hence also attributed to Trp19, because Trp19 is located slightly away from the exosite. In addition, the fluorescence binding assay was conducted with a control (ethanol) and a blank (*N*-acetyl-L-tryptophanamide), to exclude the effects of a solvent and a ligand, respectively. Despite the small change in the fluorescence, Trp quenching in response to proximate ligand binding has served as a probe to investigate the dynamics of ligand and LG interactions [22].

Regardless of the undesired structural changes in *E. coli*-expressed LG, we provide several observations that might support the idea that the  $\gamma$ -turn loop plays a role in the interaction between the exosite and vitamin D [9]. First, substituting each Leu143 and Met145 with charged amino acids resulted in substantially decreased binding affinity of vitamin D<sub>3</sub> (4.7-fold to 8.1-fold in Table 2), which is consistent with a previous crystallographic report [9] showing the side chains of these two residues to be directly involved in vitamin D binding. It should be noted that these Leu and Met residues are projected into the interior of the protein, such that any mutation to charged residues would be highly disruptive of the structure of this loop; a change in vitamin D binding would therefore be expected. In contrast, such substitution might not greatly change the overall structure of the loop region, as demonstrated by the site-specific mAb 1D8F8 being able to recognize mutants M145K, M145E, and M145F (Fig. 7A). The substitution of centered Pro144 by Ala also significantly attenuated the binding affinity (4.6-fold in Table 2). Because Pro144 has no direct contact with vitamin D<sub>3</sub> [9], we suggest that it might be essential to maintain the conformation of the loop structure. All mutants other than L143F and M145F impaired vitamin D binding. There is a strong inverse correlation ( $r = -0.94$ ) between the apparent dissociation

constants and binding ratios for all mutants (Table 2). The binding ratios calculated from the Cogan plot are near 0.5 (Table 2), but the titration curve (Fig. 4, left panel) revealed that maximal binding was achieved at a ratio of 1 : 1. In general, the Cogan plot might indicate only that an impaired binding ratio might be caused by a markedly decreased binding affinity due to a unique structural change in those mutants. For example, the L143F and M145F mutants still showed a ratio of 0.7. Hence, Phe residues maintain the necessary hydrophobicity, although the overall conformation in this region might undergo some change.

Second, the exosites of rLG, heated LG, carboxymethylated LG, carboxymethylated rLG and carboxymethylated heated LG recognize only vitamin D<sub>3</sub>, and neither palmitate nor retinol. This interaction appears to be ligand-specific and consistent with a previous study, in that there is no second binding site for palmitate and retinol [18]. Third, binding of vitamin D<sub>3</sub> to LG attenuated the recognition of a  $\gamma$ -turn loop-specific mAb (1D8F8) (Fig. 7).

With respect to the animal study, we found almost equal uptake of plasma 25-hydroxyvitamin D for mice dosed with equal concentrations of LG in vitamin D<sub>3</sub>-fortified LG, whey protein (mainly LG and  $\alpha$ -lactalbumin), and raw milk (Fig. 8A). LG is therefore probably the only vehicle that transports vitamin D in milk. Interestingly, the use of LG supplemented with vitamin D<sub>3</sub> at various doses revealed that native LG, comprising two vitamin D-binding sites, produced maximal uptake of plasma vitamin D at a dosage ratio of 2 : 1 (vitamin D<sub>3</sub>/LG), whereas heated LG, possessing only an exosite, produced maximal uptake of plasma vitamin D at a dosage ratio of 1 : 1 (Fig. 8). The final increase in plasma 25-hydroxyvitamin D caused by native LG was almost exactly twice that caused by heated LG. As a single mutation on the  $\gamma$ -turn loop (L143K) resulted in a maximal eight-fold decrease in binding affinity for vitamin D<sub>3</sub>, it would be of interest to investigate the effect of such a mutation on the uptake of vitamin D in animals. This experiment is, however, impracticable at present, because of the limited quantity of rLG isolated in our expression system.

Increased concentrations of vitamin D in plasma have been demonstrated to be associated with a decreased incidence of breast, ovarian, prostate and colorectal cancers [27,28]. Because LG is a fraction that is directly responsible for enhancing the uptake of vitamin D in mice (Fig. 8), there might be two advantages of the presence of an exosite in LG. The first is that the central calyx of LG is thought to be partially occupied by fatty acid in milk [29]; the available

exosite might provide another route to transport vitamin D. Second, at present, the processing of many dairy products involves excessive heat for the purpose of sterilization. The presence of a thermally stable exosite might play a 'bypass' role in maintaining the binding and transport of vitamin D<sub>3</sub>. Such a unique property of LG is worth considering for supplementing vitamin D in dairy products enriched with LG. It is worth mentioning here that mice and humans lack an LG gene [30]; the present finding indicates that vitamin D supplementation in milk (the biochemical event) is therefore essential for general public health. This is well worth following up in species that do express LG.

In summary, this study indicates a potential role of the  $\gamma$ -turn (Leu-Pro-Met) in maintaining the structure of a secondary vitamin D-binding site. The additional mouse experiment provides new insights into the transport role of LG and its supplementation with vitamin D used in dairy products.

## Experimental procedures

### Purification of native LG

LG was purified from raw milk using the supernatant from a saturated ammonium sulfate fraction (40%), followed by chromatography on a G-150 column, as described previously [5].

### Analysis of the crystal structure of the LG–vitamin D<sub>3</sub> complex

The crystal structure of LG in this context is deposited in the Protein Data Bank, code 2GJ5 [9], and the diagram was created with Rasmol [31] and o v7.0 [32].

### Construction of plasmid pQE30–LG

Total RNA was isolated from bovine mammary gland tissue; the cDNA was synthesized from RNA using M-MLV reverse transcriptase (Invitrogen, Carlsbad, CA, USA). The cDNA fragments coding for LG [33] were amplified on proofreading DNA polymerase (Invitrogen) and cloned into the *Bam*HI–*Hind*III sites of an *E. coli* expression vector, pQE30 (Qiagen, Madison, WI, USA). The plasmids were screened in JM109 and expressed in M15 (pREP4) (Qiagen), with the final sequence of pQE30–LG being confirmed by DNA sequencing [34,35].

### Site-directed mutagenesis

Site-directed mutants ( $n = 7$ ) of LG (L143K, L143E, L143F, M145K, M145E, M145F, and P144A) were gener-

ated using oligonucleotides containing the desired mutation with the QuikChange PCR method (Stratagene, La Jolla, CA, USA); the pQE30–LG expression vector served as a template [36], and the nucleotide sequence was confirmed. In addition, DNA nucleotide-sequencing analysis confirmed each inserted cDNA mutant of rLG to be correct.

### Expression and purification of rLG and its mutants

*E. coli* [M15 (pREP4)] with pQE30–LG or its mutants were cultured in LB medium (containing 100  $\mu\text{g}\cdot\text{mL}^{-1}$  ampicillin and 1 mM isopropyl thio- $\beta$ -D-galactoside) at 37 °C for 6 h on a rotary shaker. Cells were harvested at 8000 *g* for 20 min, resuspended in 40 mL of 20 mM Tris/HCl (pH 8.0), sonicated, and then centrifuged at 20 000 *g* for 20 min at 4 °C. The pellet containing inclusion bodies was resuspended in 30 mL of 2 M urea containing 20 mM Tris/HCl, 0.5 M NaCl, and 2% Triton X-100 (pH 8.0), sonicated as above, and then centrifuged at 20 000 *g* for 20 min at 4 °C. The inclusion bodies were then lysed, dissolved in a binding buffer containing 20 mM Tris/HCl, 0.5 M NaCl, 5 mM imidazole, 6 M guanidine-HCl, and 1 mM 2-mercaptoethanol (pH 8.0), and passed through a syringe filter (0.45  $\mu\text{m}$ ). A HiTrap chelating column (GE Healthcare, Uppsala, Sweden) was washed with 0.1 M NiSO<sub>4</sub> and equilibrated with the binding buffer before the cell lysate was loaded as previously described [35]. The column-bound fraction was then treated with a binding buffer containing 6 M urea, and finished with the binding buffer without urea. The recombinant protein was finally eluted with a buffer containing 20 mM Tris/HCl, 0.5 M NaCl, and 250 mM imidazole without 2-mercaptoethanol (pH 8.0). Protein fractions were pooled, desalted on a P-2 column (Bio-Rad laboratories, Hercules, CA, USA), and lyophilized. The protein concentration was determined by the Lowry method [37], using BSA as a standard.

### Gel electrophoresis and immunoblot analysis

SDS/PAGE or native PAGE with 15% polyacrylamide gel was used to characterize rLG and its mutants, using a modified procedure similar to that described previously [7,38]. The samples for SDS/PAGE or native PAGE were mixed with a loading buffer (12 mM Tris/HCl, 0.4% SDS, 5% glycerol, and 0.02% bromophenol blue, pH 6.8) without thermal treatment to ensure the retention of the native structure of LG. For reducing PAGE, mercaptoethanol at a final concentration of 143 mM in the samples was used. Western blot analysis was performed as described previously [6]: the electrotransferred samples were incubated with mAbs (4D11, 4H11E8, or 1D8F8) [5], and developed using 3,3'-di-aminobenzidine containing 0.01% H<sub>2</sub>O<sub>2</sub> [6]. Dot-blot to assess the interaction between vitamin D<sub>3</sub> and

the exosite was performed using the samples of LG or LG–vitamin D<sub>3</sub> complex (ratio 1 : 10) spotted onto the membrane; the final binding was probed with a  $\gamma$ -loop-specific mAb (1D8F8).

### Vitamin D<sub>3</sub> binding to LG, rLG and rLG mutants

The ligand-binding assay for LG was performed with fluorescence emission as previously established [6,9,10,21,22,24,25]. The binding of vitamin D<sub>3</sub> to LG was measured by fluorescence quenching of Trp19 of LG at 332 nm, using excitation at 287 nm. Fluorescence spectra (Cary Eclipse fluorescence spectrophotometer; Varian Inc., Palo Alto, CA, USA) were recorded at 24 °C. For the titration experiment, 5  $\mu$ M native LG, heated LG (preheated at 100 °C for 16 min), rLG or its mutants (in 10 mM phosphate buffer, pH 8.0) was instantly incubated with increased concentrations of vitamin D<sub>3</sub> (0.625–20  $\mu$ M in absolute ethanol). The final concentration of ethanol in the reaction mixture was such that it was < 3% at the end-point of the titration. With this concentration, neither aggregation of LG nor a significant change in fluorescence emission was produced [39,40]. As in previous studies [6,9,10,21,22,25], the titration of LG protein with various concentrations of ethanol (up to 3%) was evaluated and employed as an initial intrinsic fluorescence of LG before the addition of ligands. A solution of *N*-acetyl-L-tryptophanamide (Sigma-Aldrich, St Louis, MO, USA), with an absorbance at 287 nm that was equal to that of the tested protein, was also used as a blank during the ligand titration, according to the method previously established [21,22,25]. The decreased intensity of fluorescence of *N*-acetyl-L-tryptophanamide solution during the titration was thus not due to the interaction between ligand and tryptophanamide, but resulted from the inner filter effect as a consequence of ligand absorbance at 287 nm [41]. The change in fluorescence intensity at 332 nm depended on the amount of protein–ligand complex, allowing the calculation of *a* (the fraction of unoccupied ligand-binding sites), using the equation  $a = (F - F_{\text{sat}})/(F_0 - F_{\text{sat}})$  as previously described [21,22,25]. The data were then transformed to a plot of the Cogan equation,  $(P_T a = (1/n)[R_T a/(1 - a)] - K_d^{\text{app}}/n)$ , in which  $P_T$  is the total protein concentration,  $n$  is the number of binding sites per molecule,  $R_T$  is the total ligand concentration, and  $K_d^{\text{app}}$  is the apparent dissociation constant [42].

### CD

For CD measurement, 0.5 mg·mL<sup>-1</sup> of native or heated LG (100 °C for 16 min), rLG or its mutants (in 20 mM phosphate buffer, pH 7.0) was added to a cuvette of 1.0 mm path length [9,38]. The CD spectra were recorded 20 times on a Jasco-J715 spectropolarimeter (Jasco, Tokyo, Japan) at 24 °C over the range from 200 to 250 nm at a scan speed of 20 nm·min<sup>-1</sup>.

### MALDI-TOF MS analysis of trypsin-digested LG

For trypsin treatment, 100  $\mu$ g of LG, heated LG or rLG in 50  $\mu$ L of NaCl/P<sub>i</sub> containing 0.02 M phosphate and 0.12 M NaCl (pH 7.4) was incubated with 1  $\mu$ L of trypsin (0.5 mg·mL<sup>-1</sup>) at 37 °C for 16 h. The reaction was terminated by adding 1 mM phenylmethanesulfonyl fluoride. The trypsinized samples were then concentrated using C18 Zip-Tips and eluted with 50% acetonitrile/0.1% trifluoroacetic acid following the manufacturer's (Millipore, Billerica, MA, USA) standard protocol. MALDI-TOF MS was performed using a Microflex MALDI-TOF LRF20 mass spectrometer (Bruker Daltonics, Billerica, MA, USA). The Zip-Tips-purified peptide digests were spotted with an  $\alpha$ -cyano-4-hydroxycinnamic acid matrix and run in reflectron positive-ion mode at an accelerating voltage of 25 kV.

### Carboxymethylation of LG

For carboxymethylation [6,8,38], 5 mg of LG, heated LG or rLG was first dissolved in 2 mL of 0.1 M Tris/HCl buffer (pH 8.6), containing 6 M ultrapure urea and 0.02 M dithiothreitol. Following flushing with nitrogen for 2 h, 20 mg of iodoacetic acid was added to the reaction mixture, while the pH was maintained at 8.6 by the addition of 0.1 M NaOH; and incubation was performed for another 3 h. Finally, carboxymethylated LG, carboxymethylated heated LG and carboxymethylated rLG were desalted on a Bio-Gel P2 column, eluted with 0.05 M ammonium bicarbonate, and lyophilized.

### Animal experiments

Female BALB/c mice (4 weeks old,  $n = 95$ , obtained from the National Animal Center, National Science Council of Taiwan) were kept in an animal room (12 h light cycle, 21 °C) and fed with a standard diet; housing and management were according to guidelines established and approved by the National Science Council of Taiwan. In an initial test using milk fortified with vitamin D<sub>3</sub> and fortified milk components, mice ( $n = 30$ ) with body mass  $17.56 \pm 1.28$  g [mean  $\pm$  standard deviation (SD)] were randomly divided into six groups ( $n = 5$ ). Vitamin D<sub>3</sub> (100  $\mu$ M) was emulsified with raw milk, whey protein (milk without casein), casein (reconstituted to the milk volume), LG (250  $\mu$ M, approximately equivalent to the concentration in milk) or distilled water in a feeding bottle (*ad libitum*), and mice were fed with this for 3 weeks. Each mouse drank  $\sim 3$ –3.5 mL·day<sup>-1</sup> on average. The mean body mass of each group increased by 8% in general, and there was no significant difference among the groups at the end of the test. For the experimental dosing with vitamin D<sub>3</sub>, mice ( $n = 65$ , with body mass  $17.73 \pm 1.17$  g, mean  $\pm$  SD) were divided into three major groups: group 1 (vitamin D<sub>3</sub>), group 2 (vitamin D<sub>3</sub> plus native LG), and



group 3 (vitamin D<sub>3</sub> plus heated LG). The experiment was designed to investigate the relationship between the vitamin D-binding sites of LG and the uptake of vitamin D. LG serving as a vehicle was kept at a constant concentration (250  $\mu$ M) during the feeding period. Group 1 ( $n = 20$ ) without LG was dosed with only vitamin D<sub>3</sub>, as a control. All groups were given varied dosages: 100, 250, 500 or 750  $\mu$ M vitamin D<sub>3</sub> according to vitamin D<sub>3</sub>/LG ratios of 0.4, 1, 2, or 3, respectively. Group 2 ( $n = 20$ ) and group 3 ( $n = 20$ ) were provided with native LG (containing two binding sites) and heated LG (containing one binding site), respectively. As well as these three groups, one naive group given no vitamin D<sub>3</sub> and LG was included ( $n = 5$ ). Preparation of the vitamin D<sub>3</sub> supplement and the protocol (3 weeks) were as described above. Analysis of 25-hydroxy-vitamin D in mouse plasma was conducted with a kit (25-Hydroxy Vitamin D Direct EIA; IDS Diagnostics, Fountain Hills, AZ, USA), according to the manufacturer's instructions.

## Acknowledgements

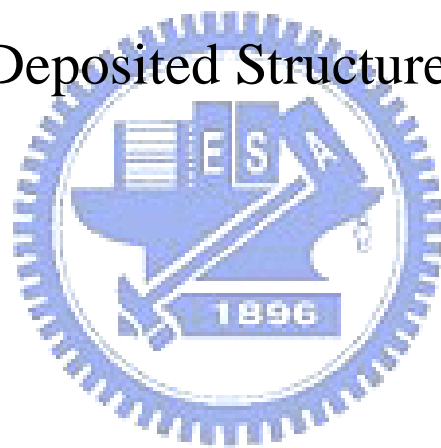
This work was supported by National Science Council (NSC) grants 92-2313-B-009-002, 93-2313-B-009-002, 94-2313-B-009-001, 95-2313-B-009-001, and 97-2313-B-009-001-MY2 (S. J. T. Mao), and NSC 94-2321-B-213-001, 95-2321-B-213-001-M (NSC), 963RSB02, and 973RSB02 (National Synchrotron Radiation Research Center) (C.-J. Chen).

## References

- Hambling SG, MacAlpine AS & Sawyer L (1992) Beta-lactoglobulin. In *Advanced Dairy Chemistry I* (Fox PF, eds), pp. 141–190. Elsevier, Amsterdam.
- Sawyer L & Kontopidis G (2000) The core lipocalin, bovine beta-lactoglobulin. *Biochim Biophys Acta* **1482**, 136–148.
- Marshall K (2004) Therapeutic applications of whey protein. *Altern Med Rev* **9**, 136–156.
- Sava N, Van der Plancken I, Claeys W & Hendrickx M (2005) The kinetics of heat-induced structural changes of beta-lactoglobulin. *J Dairy Sci* **88**, 1646–1653.
- Chen WL, Huang MT, Liu HC, Li CW & Mao SJT (2004) Distinction between dry and raw milk using monoclonal antibodies prepared against dry milk proteins. *J Dairy Sci* **87**, 2720–2729.
- Song CY, Chen WL, Yang MC, Huang JP & Mao SJT (2005) Epitope mapping of a monoclonal antibody specific to bovine dry milk: involvement of residues 66–76 of strand D in thermal denatured beta-lactoglobulin. *J Biol Chem* **280**, 3574–3582.
- Chen WL, Hwang MT, Liao CY, Ho JC, Hong KC & Mao SJT (2005)  $\beta$ -Lactoglobulin is a thermal marker in processed milk as studied by electrophoresis and circular dichroic spectra. *J Dairy Sci* **88**, 1618–1630.
- Chen WL, Liu WT, Yang MC, Hwang MT, Tsao JH & Mao SJT (2006) A novel conformation-dependent monoclonal antibody specific to the native structure of beta-lactoglobulin and its application. *J Dairy Sci* **89**, 912–921.
- Yang MC, Guan HH, Liu MY, Lin YH, Yang JM, Chen WL, Chen CJ & Mao SJT (2008) Crystal structure of a secondary vitamin D<sub>3</sub> binding site of milk beta-lactoglobulin. *Proteins* **71**, 1197–1210.
- Yang MC, Guan HH, Yang JM, Ko CN, Liu MY, Lin YH, Huang YC, Chen CJ & Mao SJT (2008) Rational design for crystallization of  $\beta$ -lactoglobulin and vitamin D<sub>3</sub> complex: revealing a secondary binding site. *Cryst Growth Des* **8**, 4268–4276.
- Qin BY, Bewley MC, Creamer LK, Baker EN & Jameson GB (1999) Functional implications of structural differences between variants A and B of bovine beta-lactoglobulin. *Protein Sci* **8**, 75–83.
- Greene LH, Hamada D, Eyles SJ & Brew K (2003) Conserved signature proposed for folding in the lipocalin superfamily. *FEBS Lett* **553**, 39–44.
- Lüthy R, Bowie JU & Eisenberg D (1992) Assessment of protein models with three-dimensional profiles. *Nature* **356**, 83–85.
- Kontopidis G, Holt C & Sawyer L (2004) Invited review: beta-lactoglobulin: binding properties, structure, and function. *J Dairy Sci* **87**, 785–796.
- Adams JJ, Anderson BF, Norris GE, Creamer LK & Jameson GB (2006) Structure of bovine beta-lactoglobulin (variant A) at very low ionic strength. *J Struct Biol* **154**, 246–254.
- Bello M, Pérez-Hernández G, Fernández-Velasco DA, Arreguin-Espinosa R & García-Hernández E (2008) Energetics of protein homodimerization: effects of water sequestering on the formation of beta-lactoglobulin dimer. *Proteins* **70**, 1475–1487.
- Wu SY, Perez MD, Puyol P & Sawyer L (1999) Beta-lactoglobulin binds palmitate within its central cavity. *J Biol Chem* **274**, 170–174.
- Kontopidis G, Holt C & Sawyer L (2002) The ligand-binding site of bovine beta-lactoglobulin: evidence for a function? *J Mol Biol* **318**, 1043–1055.
- Considine T, Singh H, Patel HA & Creamer LK (2005) Influence of binding of sodium dodecyl sulfate, all-trans-retinol, and 8-anilino-1-naphthalenesulfonate on the high-pressure-induced unfolding and aggregation of beta-lactoglobulin B. *J Agric Food Chem* **53**, 8010–8018.
- Konuma T, Sakurai K & Goto Y (2007) Promiscuous binding of ligands by beta-lactoglobulin involves hydrophobic interactions and plasticity. *J Mol Biol* **368**, 209–218.

- 21 Wang Q, Allen JC & Swaisgood HE (1999) Binding of lipophilic nutrients to beta-lactoglobulin prepared by bioselective adsorption. *J Dairy Sci* **82**, 257–264.
- 22 Wang Q, Allen JC & Swaisgood HE (1997) Binding of vitamin D and cholesterol to beta-lactoglobulin. *J Dairy Sci* **80**, 1054–1059.
- 23 Kuwata K, Shastry R, Cheng H, Hoshino M, Batt CA, Goto Y & Roder H (2001) Structural and kinetic characterization of early folding events in  $\beta$ -lactoglobulin. *Nat Struct Biol* **8**, 151–155.
- 24 Cho Y, Batt CA & Sawyer L (1994) Probing the retinol-binding site of bovine beta-lactoglobulin. *J Biol Chem* **269**, 11102–11107.
- 25 Wang Q, Allen JC & Swaisgood HE (1997) Binding of retinoids to beta-lactoglobulin isolated by bioselective adsorption. *J Dairy Sci* **80**, 1047–1053.
- 26 Brownlow S, Morais Cabral JH, Cooper R, Flower DR, Yewdall SJ, Polikarpov I, North AC & Sawyer L (1997) Bovine beta-lactoglobulin at 1.8 Å resolution – still an enigmatic lipocalin. *Structure* **5**, 481–495.
- 27 Vieth R (2001) Vitamin D nutrition and its potential health benefits for bone, cancer and other conditions. *J Nutr Environ Med* **11**, 275–291.
- 28 Lappe JM, Travers-Gustafson D, Davies KM, Recker RR & Heaney RP (2007) Vitamin D and calcium supplementation reduces cancer risk: results of a randomized trial. *Am J Clin Nutr* **85**, 1586–1591.
- 29 Pérez MD, Díaz de Villegas C, Sánchez L, Aranda P, Ena JM & Calvo M (1989) Interaction of fatty acids with beta-lactoglobulin and albumin from ruminant milk. *J Biochem* **106**, 1094–1097.
- 30 Simons JP, McClenaghan M & Clark AJ (1987) Alteration of the quality of milk by expression of sheep beta-lactoglobulin in transgenic mice. *Nature* **328**, 530–532.
- 31 Sayle RA & Milner-White EJ (1995) RASMOL: biomolecular graphics for all. *Trends Biochem Sci* **20**, 374–376.
- 32 Jones TA, Zou JY, Cowan SW & Kjeldgaard M (1991) Improved methods for building protein models in electron density maps and the location of errors in these models. *Acta Crystallogr A* **47**, 110–119.
- 33 Jamieson AC, Vandeyar MA, Kang YC, Kinsella JE & Batt CA (1987) Cloning and nucleotide sequence of the bovine beta-lactoglobulin gene. *Gene* **61**, 85–90.
- 34 Lai IH, Tsai TI, Lin HH, Lai WY & Mao SJT (2007) Cloning and expression of human haptoglobin subunits in *Escherichia coli*: delineation of a major antioxidant domain. *Protein Expr Purif* **52**, 356–362.
- 35 Lai IH, Lin KY, Larsson M, Yang MC, Shiao CH, Liao MH & Mao SJT (2008) A unique tetrameric structure of deer plasma haptoglobin – an evolutionary advantage in the Hp 2-2 phenotype with homogeneous structure. *FEBS J* **275**, 981–993.
- 36 Ju M, Stevens L, Leadbitter E & Wray D (2003) The roles of N- and C-terminal determinants in the activation of the Kv2.1 potassium channel. *J Biol Chem* **278**, 12769–12778.
- 37 Lowry OH, Rosebrough NJ, Farr AL & Randall RJ (1951) Protein measurement with the Folin phenol reagent. *J Biol Chem* **193**, 265–275.
- 38 Tseng CF, Lin CC, Huang HY, Liu HC & Mao SJT (2004) Antioxidant role of human haptoglobin. *Proteomics* **4**, 2221–2228.
- 39 Dufour E & Haertlé T (1990) Alcohol-induced changes of beta-lactoglobulin retinol-binding stoichiometry. *Protein Eng* **4**, 185–190.
- 40 Dufour E, Genot C & Haertlé T (1994) beta-Lactoglobulin binding properties during its folding changes studied by fluorescence spectroscopy. *Biochim Biophys Acta* **1205**, 105–112.
- 41 Dufour E & Haertlé T (1991) Binding of retinoids and beta-carotene to beta-lactoglobulin. Influence of protein modifications. *Biochim Biophys Acta* **1079**, 316–320.
- 42 Cogan U, Kopelman M, Mokady S & Shinitzky M (1976) Binding affinities of retinol and related compounds to retinol binding proteins. *Eur J Biochem* **65**, 71–78.

# Deposited Structure







# Structure Summary MMDB

[HOME](#) | [SEARCH](#) | [SITE MAP](#)
[Entrez](#)
[Structure](#)
[Protein](#)
[CDD](#)
[PubMed](#)
[Taxonomy](#)
[PubChem](#)
[Help](#)
[Cn3D](#)

**MMDB ID:** 58939

**PDB ID:** 2GJ5

 PDB or MMDB ID

**Description** Crystal Structure Of A Secondary Vitamin D3 Binding Site Of Milk Beta-Lactoglobulin.

**Deposition:** Yang M-C, Guan H-H, Liu M-Y, Yang J-M, Chen W-L, Chen C-J, Mao S-J, 2006/3/30

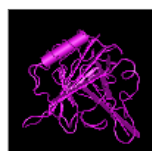
**Taxonomy:** *Bos taurus*

**Related Structure:** VAST

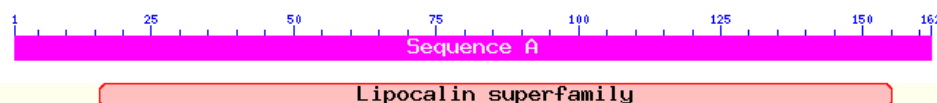

**Tasks:**  **Drawing:** 



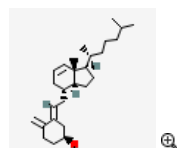
Molecular components in the MMDB structure are listed below and may include macromolecular chains, 3D domains, protein classifications (domain families), and ligands, as available. Mouse over each icon for more information on the component. [?](#)



**Protein**  
**Domain Families**  
Superfamilies



**Ligand**



VD3

2 occurrences

### Citing MMDB:

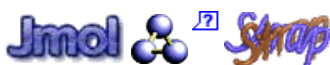
[Wang Y, Address KJ, Chen J, Geer LY, He J, He S, Lu S, Madej T, Marchler-Bauer A, Thiessen PA, Zhang N, Bryant SH. "MMDB: annotating protein sequences with Entrez's 3D-structure database". \*Nucleic Acids Res.\* 2007 Jan; 35\(Database issue\): D298-300.](#)

[Chen J, Anderson JB, DeWeese-Scott C, Fedorova ND, Geer LY, He S, Hurwitz DI, Jackson JD, Jacobs AR, Lanczycki CJ, Liebert CA, Liu C, Madej T, Marchler-Bauer A, Marchler GH, Mazumder R, Nikolskaya AN, Rao BS, Panchenko AR, Shoemaker BA, Simonyan V, Song JS, Thiessen PA, Vasudevan S, Wang Y, Yamashita RA, Yin JJ, Bryant SH. "MMDB: Entrez's 3D-structure database". \*Nucleic Acids Res.\* 2003 Jan; 31\(1\): 474-7.](#)

[Disclaimer](#) | [Privacy statement](#) | [Accessibility](#)



Go to PDB code:



Contents

- Description**
- [Header details](#)
- [Header records](#)
- [References](#)
- [PROCHECK](#)
- Protein chain**
- [A 161 a.a.](#)
- Ligands**
- [VD3 x2](#)
- Waters x38**

Tools

- [Image Generation](#)
- [AstexViewer™@MSD-EBI](#)
- [Run PROCHECK](#)
- [Clefs Calculation](#)

[Top page](#) [Protein](#) [Ligands](#) [Clefs](#) [Links](#)

Transport protein

PDB-id **2gj5**

**PDB id:** 2gj5

**Name:** Transport protein

**Title:** Crystal structure of a secondary vitamin d3 binding site of milk beta-lactoglobulin

**Structure:** Beta-lactoglobulin. Chain: a. Synonym: beta-Ig, allergen bos d 5

**Source:** Bos taurus. Bovine

**UniProt:** [P02754](#) (LACB\_BOVIN) [S&S](#) [Pfam](#)

Seq: Lipocalin 178 a.a.

Struc: 161 a.a.

**Key:** family PfamA domain Secondary structure

**Resolution:** 2.40Å

**R-factor:** 0.236

**R-free:** 0.298

**Authors:** M.-C.Yang,H.-H.Guan,M.-Y.Liu,J.-M.Yang,W.-L.Chen,C.-J.Chen, S.-J.Mao

**Key ref:** m.-c.yang et al. crystal structure of beta-lactoglobulin and vitamin d complex. *TO BE PUBLISHED*, .

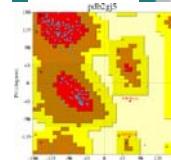
**Date:** 30-Mar-06

**Release date:** 02-Oct-07

Quick links

- [RCSB](#)
- [MSD](#)
- [SRS](#)
- [MMDB](#)
- [JenaLib](#)
- [OCA](#)
- [Proteopedia](#)
- [CATH](#)
- [SCOP](#)
- [FSSP](#)
- [HSSP](#)
- [PDBSWS](#)
- [PQS](#)
- [ProSAT](#)
- [Whatcheck](#)
- [EDS](#)

Procheck



Clefs



Surface



CONTACT US | FEEDBACK | HELP | PRINT

 PDB ID or keyword  Author  [Site Search](#) | [Advanced Search](#)
[Home](#) [Search](#) [Structure](#)[Help](#) [Structure Summary](#) [Sequence Details](#) [Biology & Chemistry](#) [Materials & Methods](#) [Geometry](#) [External Links](#)

- [2GJ5](#)
- [Download Files](#)
- [FASTA Sequence](#)
- [Display Files](#)
- [Display Molecule](#)
- [Structural Reports](#)
- [External Links](#)
- [Structure Analysis](#)
- [Help](#)



To view **sequence details** of this structure click on the *Sequence Details* tab above the summary page.

**2gj5**DOI [10.2210/pdb2gj5/pdb](https://doi.org/10.2210/pdb2gj5/pdb)

Red - Derived Information

**Title** Crystal structure of a secondary vitamin D3 binding site of milk beta-lactoglobulin

**Authors** Yang, M.-C., Guan, H.-H., Liu, M.-Y., Yang, J.-M., Chen, W.-L., Chen, C.-J., Mao, S.-J.

**Primary Citation** Yang, M.-C., Guan, H.-H., Liu, M.-Y., Yang, J.-M., Chen, W.-L., Chen, C.-J., Mao, S.-J. Crystal Structure of Beta-Lactoglobulin and Vitamin D Complex. *To be Published*

**History** Deposition 2006-03-30 Release 2007-10-02

**Experimental Method** Type X-RAY DIFFRACTION [Data](#) [EDS]

**Parameters**

Resolution [Å]	R-Value	R-Free	Space Group
2.40	0.241 (obs.)	0.298	P 3 <sub>2</sub> 2 1

**Unit Cell**

Length [Å]	a	b	c	Angles [°]
	53.78	53.78	111.58	alpha 90.00 beta 90.00 gamma 120.00

## Images and Visualization

&lt;&lt; Biological Molecule &gt;&gt;

Display Options [?](#)

- [KiNG](#)
- [Jmol](#)
- [WebMol](#)
- [MBT SimpleViewer\\*](#)
- [MBT Protein Workshop](#)
- [QuickPDB](#)
- [All Images](#)

\* Capable of displaying biological molecules.

**Molecular Description Asymmetric Unit** Polymer: 1 Molecule: Beta-lactoglobulin Chains: A

Structure Weight: 19070.59

Classification [Transport Protein](#)

## Source

Polymer: 1 Scientific Name: **Bos taurus** Common Name: **Bovine** Bovine

## Ligand Chemical Component

Identifier Name	Formula	Ligand Expo	Drug Similarity	Hapten Similarity	Ligand Structure	Ligand Interaction
VD3	C <sub>27</sub> H <sub>44</sub> O					
(1S,3Z)-3-[(2E)-2-[(1R,3AR,7AS)-7A-METHYL-1-[(2R)-6-METHYLHEPTAN-2-YL]-2,3,3A,5,6,7-HEXAHYDRO-1H-INDEN-4-YLIDENE]ETHYLIDENE]-4-METHYLIDENE-CYCLOHEXAN-1-OL						

## CATH Classification (version v3.2.0)

Domain	Class	Architecture	Topology	Homology
2gj5A00	Mainly Beta	Beta Barrel	Lipocalin	

## PFAM Classification

Chain	PFAM Accession	PFAM ID	Description	Type	Clan ID
A	PF00061	Lipocalin	Lipocalin / cytosolic fatty-acid binding protein family	Domain	

## GO Terms

Polymer	Molecular Function	Biological Process	Cellular Component
Beta-lactoglobulin (2GJ5:A)	<ul style="list-style-type: none"> <li>• transporter activity</li> <li>• binding</li> <li>• retinol binding</li> </ul>	<ul style="list-style-type: none"> <li>• transport</li> </ul>	<ul style="list-style-type: none"> <li>• extracellular region</li> </ul>

**Sequence:Structure Details** [\[help\]](#)

2GJ5

The sequence display provides a graphical representation of the UniProt, PDB - ATOM and PDB - SEQRES sequences. Different 3rd party annotations can be graphically mapped on the sequence and displayed in the Jmol viewer.

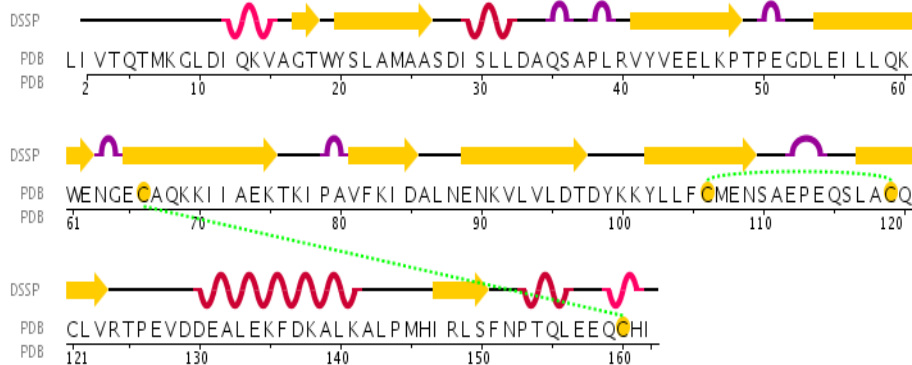
The structure **2GJ5** has in total **1** chains. Out of these **1** are sequence-unique.

Currently viewing **unique chains** only. [\[show all chains\]](#) [\[show 3D in Jmol\]](#)

**Chain A** (polymer 1) [\[help\]](#) [\[fasta\]](#) [\[text/markup\]](#)

<b>Description</b>	Beta-lactoglobulin
<b>Chain Type</b>	polypeptide(L)
<b>UniProt reference</b>	<a href="#">P02754</a>
<b>Length</b>	162 residues
<b>CATH domain assignment</b> <a href="#">[hide]</a> <a href="#">[reference]</a>	2g5A00 : 161 residues <input checked="" type="checkbox"/>
<b>DSSP secondary structure</b> <a href="#">[hide]</a> <a href="#">[reference]</a>	16% helical (5 helices; 27 residues) 43% beta sheet (10 strands; 70 residues)
<b>More annotations</b>	

Currently displayed: SEQRES sequence. [\[display external \(UniProt/PIR\) sequence\]](#)

**Sequence Details****Preferences****Jmol - 3D parameters**

show Jmol  fixed Jmol position

Jmol width  Jmol height

**Page parameters**

Sequence to view  Label residue ids by

Font size  Residues per row

**References****CATH domain assignment reference**

Pearl F.M., Bennett C.F., Bray J.E., Harrison A.P., Martin N., Shepherd A., Sillitoe I., Thornton J., Orengo C.A.  
The CATH database: an extended protein family resource for structural and functional genomics.  
Nucleic Acids Res 2003 Jan

PMID: 12520050 [PubMed](#)

**DSSP secondary structure reference**

Kabsch W., Sander C.  
Dictionary of protein secondary structure: pattern recognition of hydrogen-bonded and geometrical features.  
Biopolymers 1983 Dec

PMID: 6667333 [PubMed](#)



A MEMBER OF THE PDB

MyPDB: [Login](#) | [Register](#)

## An Information Portal to Biological Macromolecular Structures

As of [Tuesday Mar 10, 2009](#) there are 56366 Structures | [PDB Statistics](#)

[CONTACT US](#) | [FEEDBACK](#) | [HELP](#) | [PRINT](#)

PDB ID or keyword  Author

[Site Search](#)

| [Advanced Search](#)

[Home](#) [Search](#) **Structure**

[Help](#) [Structure Summary](#) [Sequence Details](#) **Biology & Chemistry**

[Materials & Methods](#)

[Geometry](#) [External Links](#)

### Biology and Chemistry Report

2GJ5

#### Structure Details

##### Structure Keywords

**Keywords Text**

TRANSPORT PROTEIN  
beta-lactoglobulin, vitamin D3,  
TRANSPORT PROTEIN

##### Polymeric Molecules

###### Chain A

<b>Description</b>	Beta-lactoglobulin
<b>Nonstandard Linkage</b>	no
<b>Nonstandard Monomers</b>	no
<b>Polymer Type</b>	polypeptide(L)
<b>Formula Weight</b>	18301.3
<b>Source Method</b>	nat
<b>Entity Name</b>	Beta-LG, Allergen Bos d 5

##### Ligands and Prosthetic Groups

ID	Name	Chemical Formula	Weight	Ligand Structure
(1s 3z) 3 [(2e) 2 [(1r 3ar 7as) 7a				
Methyl 1 [(2r) 6 Methylheptan 2				
VD3 Y ] 2 3 3a 5 6 7 Hexahydro 1h	C <sub>27</sub> H <sub>44</sub> O	384.64	<a href="#">View</a>	
Inden 4 Ylidene]ethylidene] 4				
Methylidene Cyclohexan 1 Ol				

#### Protein Details

##### UniProt Information

Chain	SWS/UNP ID	SWS/UNP Accession(s)
A	LACB_BOVIN	<a href="#">P02754</a>

- 2GJ5
- ▶ [Download Files](#)
- [FASTA Sequence](#)
- ▶ [Display Files](#)
- ▶ [Display Molecule](#)
- [Structural Reports](#)
- [External Links](#)
- ▶ [Structure Analysis](#)
- ▶ [Help](#)








To view the **3D structure** click on one of the viewers under the image.


**Keywords and Names****Chain RCSB Name UNIPROT UNIPROT Keywords (s) Name**

A Beta-lactoglobulin n/a 3D-structure , Allergen , Direct protein sequencing , Milk protein , Polymorphism , Retinol-binding , Secreted , Signal , Transport

**GO Terms****C: Cellular Location****F: Molecular Function****P: Biological Process****Chain A**

GO ID	Ontology	GO Term	Definition
5215 	F	Transporter Activity	Enables the Directed Movement of Substances (such As Macromolecules Small Molecules Ions) Into Out of Within or Between Cells.
5488 	F	Binding	The Selective Often Stoichiometric Interaction of a Molecule with One or More Specific Sites On Another Molecule.
5576 	C	Extracellular Region	The Space External to the Outermost Structure of a Cell. For Cells Without External Protective or External Encapsulating Structures This Refers to Space Outside of the Plasma Membrane. This Term Covers the Host Cell Environment Outside an Intracellular Parasite.
6810 	P	Transport	The Directed Movement of Substances (such As Macromolecules Small Molecules Ions) Into Out of Within or Between Cells or Within a Multicellular Organism.
19841 	F	Retinol Binding	Interacting Selectively with Retinol Vitamin A1 2 6 6 Trimethyl 1 (9' Hydroxy 3' 7' Dimethylnona 1' 3' 5' 7' Tetraenyl)cyclohex 1 Ene One of the Three Components That Makes Up Vitamin A. Retinol Is an Intermediate in the Vision Cycle and It Also Plays a Role in Growth and Differentiation.

**PFAM Functional Domains****Chain A**

PFAM PF00061   
 Accession  
 PFAM ID Lipocalin  
 Residues 16-157  
 Type Domain  
 Description Lipocalin / Cytosolic Fatty Acid Binding Protein

Family

**Gene Details****Natural Source, Chain A****Common Name**

Bovine

**Scientific Name**

Bos taurus

**Genome Information**

<b>Chromosome</b>	<b>Locus</b>	<b>Gene ID</b>	<b>Gene Name</b>	<b>Symbol</b>
11	11q28	280838	lactoglobulin, beta	LGB

**Publication Details****Literature Network** iHOP: 280838 GeneRIF: 280838 ;

© RCSB Protein Data Bank





A MEMBER OF THE PDB

MyPDB: [Login](#) | [Register](#)

## An Information Portal to Biological Macromolecular Structures

As of [Tuesday Mar 10, 2009](#) there are 56366 Structures | [PDB Statistics](#)

[CONTACT US](#) | [FEEDBACK](#) | [HELP](#) | [PRINT](#)

PDB ID or keyword  Author

[Site Search](#) | [Advanced Search](#)

[Home](#) [Search](#) [Structure](#)

[Help](#) [Structure Summary](#) [Sequence Details](#) [Biology & Chemistry](#)

[Materials & Methods](#) [Geometry](#) [External Links](#)



■ [2GJ5](#)

▶ [Download Files](#)

■ [FASTA Sequence](#)

▶ [Display Files](#)

▶ [Display Molecule](#)

■ [Structural Reports](#)

■ [External Links](#)

▶ [Structure Analysis](#)

▶ [Help](#)



To view **sequence details** of this structure click on the *Sequence Details* tab above the summary page.

### X-RAY Materials and Methods Report

2GJ5

#### Crystallization

##### Crystallization Experiments

**Method** VAPOR DIFFUSION, HANGING DROP  
**pH** 7.5  
**Temperature** 293.0  
**Details** 0.1M HEPES, 1.4M tri-sodium citrate dehydrate, pH 7.5, VAPOR DIFFUSION, HANGING DROP, temperature 293K

#### Crystal Data

##### Unit Cell

<b>Length a (Å)</b>	53.78	<b>Angle Alpha (°)</b>	90.00
<b>Length b (Å)</b>	53.78	<b>Angle Beta (°)</b>	90.00
<b>Length c (Å)</b>	111.58	<b>Angle Gamma (°)</b>	120.00

##### Space Group

**Space Group Name** P 3<sub>1</sub> 2 1

#### Diffraction

##### Diffraction Detector

**Detector** CCD  
**Type** ADSC QUANTUM 4  
**Details** n/a  
**Collection Date** 2005-11-21

##### Diffraction Radiation

**Monochromator** Si 111 channel  
**Diffraction Protocol** SINGLE WAVELENGTH  
**Wavelength** n/a  
**Wavelength List** n/a

**Diffraction Source**

<b>Source</b>	SYNCHROTRON
<b>Type</b>	SPRING-8 BEAMLINER BL12B2
<b>Site</b>	SPRING-8
<b>Beamline</b>	BL12B2

**Data****Reflection Details**

<b>Observed Criterion Sigma (F)</b>	0.0
<b>Observed Criterion Sigma (I)</b>	0.0
<b>Resolution(High)</b>	2.10
<b>Resolution(Low)</b>	15.00
<b>Number Reflections(All)</b>	7671
<b>Number Reflections (Observed)</b>	7671
<b>Percent Possible (Observed)</b>	n/a
<b>R Merge I (Observed)</b>	n/a
<b>Net I Over Average Sigma (I)</b>	n/a
<b>B(Isotropic) From Wilson Plot</b>	n/a
<b>Redundancy</b>	n/a

**High Resolution Shell Details**

<b>Resolution (High)</b>	2.10
<b>Resolution(Low)</b>	2.18
<b>Percent Possible (All)</b>	85.9
<b>R Merge I (Observed)</b>	n/a
<b>Mean I Over Sigma (Observed)</b>	n/a
<b>R-Sym I (Observed)</b>	n/a
<b>Redundancy</b>	n/a
<b>Number Unique Reflections(All)</b>	n/a

**Refinement****Refinement Statistics**

<b>Structure Solution Method</b>	MOLECULAR REPLACEMENT
<b>Resolution(High)</b>	2.40
<b>Resolution(Low)</b>	15.00
<b>Cut-off Sigma(I)</b>	n/a
<b>Cut-off Sigma(F)</b>	3.0
<b>Number of Reflections(all)</b>	n/a
<b>Number of Reflections (Observed)</b>	7191
<b>Number of Reflections(R-</b>	

Free)	551
Percent Reflections (Observed)	n/a
R-Factor(All)	0.25
R-Factor(Observed)	0.24
R-Work	0.24
R-Free	0.30
R-Free Selection Details	Random

### Temperature Factor Modeling

Isotropic Thermal Model	n/a
Mean Isotropic B Value	n/a
Anisotropic B[1][1]	n/a
Anisotropic B[1][2]	n/a
Anisotropic B[1][3]	n/a
Anisotropic B[2][2]	n/a
Anisotropic B[2][3]	n/a
Anisotropic B[3][3]	n/a

### RMS Deviations

Parameter Type	Deviation from Ideal
x_angle_deg	1.283
x_bond_d	0.0070

### Number of Non-Hydrogen Atoms Used in Refinement

Protein Atoms	1272
Nucleic Acid Atoms	0
Heterogen Atoms	56
Solvent Atoms	38

### Software and Computing

#### Computing

Data Collection	n/a
Data Reduction	n/a
Data Reduction (intensity integration)	ADSC
Data Reduction (data scaling)	HKL-2000
Structure Solution	CNS
Structure Refinement	CNS 1.1

#### Software

Classification	Name	Version
refinement	CNS	1.1
model building	CNS	n/a
data reduction	HKL-2000	n/a
data collection	ADSC	n/a

[CONTACT US](#) | [FEEDBACK](#) | [HELP](#) | [PRINT](#) PDB ID or keyword  Author  
[Home](#) [Search](#) [Structure](#)[Help](#) [Structure Summary](#) [Sequence Details](#) [Biology & Chemistry](#) [Materials & Methods](#)[Geometry](#) [External Links](#)

## Structure Variance Analysis Results

2GJ5

- Click on specific 'Bond Type' to get graphical distribution of values
- Click on 'Tot Num' to get table of values
- Click on 'Minimum' and 'Maximum' to get all values for that residue
- The color code is based on FDS (fold deviation score): defined as a multiple of the standard deviation for a specific reference value.

&lt;0.5    1.0    2.0    3.0    4.0    5.0    &gt;5.0

## Bond Length

Bond Type	Chain Id	Tot Num	Cal Ave	Cal StdDev	Std Val	Std StdDev	Minimum	Maximum
C-N	A	152	1.33	0.003	1.329	0.014	1.32	1.34
C-N(P)	A	8	1.34	0.005	1.341	0.016	1.33	1.35
C-O	A	161	1.23	0.005	1.231	0.02	1.22	1.25
CA-C	A	157	1.53	0.007	1.525	0.021	1.50	1.54
CA-C (G)	A	4	1.52	0.003	1.516	0.018	1.51	1.52
CA-CB	A	115	1.53	0.005	1.53	0.02	1.52	1.54
CA-CB (A)	A	15	1.52	0.008	1.521	0.033	1.51	1.54
CA-CB (I,T,V)	A	27	1.55	0.012	1.54	0.027	1.51	1.57
N-CA	A	149	1.46	0.006	1.458	0.019	1.44	1.47
N-CA (G)	A	4	1.45	0.002	1.451	0.016	1.45	1.45
N-CA (P)	A	8	1.47	0.002	1.466	0.015	1.47	1.47

Save Bond Length Summary in:  CSV (Excel) Format

&lt;0.5    1.0    2.0    3.0    4.0    5.0    &gt;5.0

## Bond Angle

Bond Angle	Chain Id	Tot Num	Cal Ave	Cal StdDev	Std Val	Std StdDev	Minimum	Maximum
C-N-CA	A	148	121.70	1.058	121.7	1.8	119.23	124.74
C-N-CA (G)	A	4	120.81	0.642	120.6	1.7	120.19	121.89
C-N-CA (P)	A	8	123.30	3.025	122.6	5.0	119.56	130.07
CA-C-N	A	148	116.19	0.769	116.2	2.0	114.21	118.41
CA-C-N (G)	A	4	115.99	1.421	116.4	2.1	113.76	117.69

2GJ5

- Download Files
- FASTA Sequence
- Display Files
- Display Molecule
- Structural Reports
- External Links
- Structure Analysis
  - Geometry
    - RCSB Graphics
    - RCSB Tables
    - MolProbity Ramachandran Plot
- Help



To view the **3D structure** click on one of the viewers under the image.

CA-C-N (P)	A	8	116.24	1.228	116.9	1.5	114.56	117.81
CA-C-O	A	157	120.82	0.506	120.8	1.7	118.20	122.13
CA-C-O (G)	A	4	120.81	1.005	120.8	2.1	119.94	122.41
CB-CA-C	A	115	109.86	1.208	110.1	1.9	106.81	113.04
CB-CA-C(A)	A	15	110.19	0.444	110.5	1.5	109.56	110.96
CB-CA-C(I,T,V)	A	27	109.18	1.235	109.1	2.2	106.96	111.25
N-CA-C	A	149	110.93	2.817	111.2	2.8	103.05	117.98
N-CA-C (G)	A	4	116.03	3.229	112.5	2.9	110.97	119.87
N-CA-C (P)	A	8	112.85	3.565	111.8	2.5	107.85	117.88
N-CA-CB	A	107	110.16	0.773	110.5	1.7	107.70	112.48
N-CA-CB(A)	A	15	109.93	0.514	110.4	1.5	109.44	111.34
N-CA-CB (I,T,V)	A	27	111.27	0.892	111.5	1.7	108.83	113.09
N-CA-CB(P)	A	8	102.92	0.227	103.0	1.1	102.44	103.28
O-C-N	A	152	122.97	0.504	123.0	1.6	121.42	124.41
O-C-N (P)	A	8	122.85	0.728	122.0	1.4	121.91	123.91

Save Bond Angle Summary in:  CSV (Excel) Format[Save Report](#)

&lt;0.5      1.0      2.0      3.0      4.0      5.0      &gt;5.0

**Dihedral Angle**

Dihedral Angle	Chain Id	Tot Num	Cal Ave	Cal StdDev	Std Val	Std StdDev	Minimum	Maximum
Chi1 g(+)	A	72	-65.07	12.954	-66.7	15.0	-101.30	-30.70
Chi1 g(-)	A	30	53.58	17.582	64.1	15.7	12.90	80.20
Chi1 trans	A	40	185.47	17.703	183.6	16.8	141.60	234.10
Omega	A	160	180.98	14.238	180	5.8	176.20	359.90
Phi	A	126	-99.34	49.483	-65.3	11.9	-175.10	108.70
Phi helix	A	27	-56.42	35.179	-65.3	11.9	-123.60	53.30
Phi(P)	A	7	-63.94	14.411	-65.4	11.2	-82.80	-44.10
Psi	A	129	84.70	90.080	-39.4	11.3	-178.90	177.40
Psi helix	A	27	-21.88	40.628	-39.4	11.3	-54.00	146.20
Psi(G)	A	4	-27.08	76.674	-39.4	11.3	-157.00	32.90

Save Dihedral Angle Summary in:  CSV (Excel) Format[Save Report](#)

© RCSB Protein Data Bank